Physics Lib.

JUN 19 1929

VOLUME 33 SECOND SERIES NUMBER 6

THE PHYSICAL REVIEW

A JOURNAL OF EXPERIMENTAL AND THEORETICAL PHYSICS

CONDUCTED BY

THE

AMERICAN PHYSICAL SOCIETY

BOARD OF EDITORS

Managing Editor John T. Tate, University of Minnesota, Minneapolis
G. Breit, P. W. Bridgman, L. G. McKeehan; I. S. Bowen, R. S. Mulliken,
H. D. Smyth; E. U. Condon, C. J. Davisson, F. K. Richtmyer

JUNE, 1929

Change of Frequency of X-Rays Scattered by Bound Electrons - - Dana P. Mitchell 871
Effect of Chemical Combination on the Absorption of X-Rays at Wave-lengths on Each Side of the K Discontinuity - - - - - - - - - C. L. Cottrell 879
Diffraction of X-Rays in Liquids: Benzene, Cyclohexane and Certain of their Derivatives - - - - - - - - - - - - G. W. Stewart 889
Report on Notation for Atomic Spectra - - - - - - - - - H. N. Russell, A. G. Shenstone and Louis A. Turner 909
The Second Spark Spectrum of Sulphur, S III - - - - - - - - - S. B. Ingram 907
Spectral Relations between Certain Iso-electronic Systems and Sequences, Part III; Ti I, V II, Cr III, Mn IV, and Fe V - - - - - - - - - H. E. White 914
Some Peculiar Hydrogen Bands - - - - - - - - Charles J. Brasefield 925
Diatomic Molecules According to the Wave Mechanics I. Electronic Levels of the Hydrogen Molecular Ion - - - - - Philip M. Morse and E. C. G. Stueckelberg 932
The Near Infra-Red Absorption Spectra of Calcite and Strontianite - - E. K. Plyler 948
Combination Bands in the Infra-Red Spectra of CCl_4 and $SiCl_4$ - - - H. H. Marvin 952
The Interaction of Electron and Positive Ion Space Charges in Cathode Sheaths - - - - - - - - - - Irving Langmuir 954
Note on Oscillations in Ionized Gases - - - - Lewi Tonks and Irving Langmuir 990
The Photoelectric and Thermionic Properties of Molybdenum - - - Miles J. Martin 991
The Rectification of Radio Signals by a Thermionic Tube Containing Alkali Metal Vapor - - - - - - - - - K. H. Kingdon and E. E. Charlton 998
Paths of Charged Particles in Electric and Magnetic Fields - - - - - - - - - W. Bartky and A. J. Dempster 1019
On Time-Lags in Fluorescence and in the Kerr and Faraday Effects - - - E. Gaviola 1023
Dependence of Ultra-Violet Reflection of Silver on Plastic Deformation - - - - - - - - - Henry Margenau 1035
Comets and Terrestrial Magnetic Storms - - - H. B. Maris and E. O. Hulburt 1046
Sound Radiation from a System of Vibrating Circular Diaphragms - - - - - - - - - Irving Wolff and Louis Malter 1061
Book Reviews - - - - - - - - - - - - - 1066

PROCEEDINGS OF THE AMERICAN PHYSICAL SOCIETY

Washington Meeting, April 18–20, 1929. Minutes and Abstracts 1–135, Author Index - - 1067
Index to Volume 33 - - - - - - - - - - - - 1104

PUBLISHED FOR THE AMERICAN PHYSICAL SOCIETY
[illegible] MINNEAPOLIS, MINN.

Second Series *June, 1929* *Vol. 33, No. 6*

THE

PHYSICAL REVIEW

CHANGE OF FREQUENCY OF X-RAYS SCATTERED BY BOUND ELECTRONS

By Dana P. Mitchell

Abstract

This is a report of the detailed investigation which followed the discovery of "fine structure in scattered x-rays" reported in April, 1928. Molybdenum $K\alpha_1$ x-rays were scattered at about 90° by graphite, aluminum and beryllium. Lines from graphite were shifted 0.0013, 0.0023 and 0.0113A to the long wave-length side of Mo $K\alpha_1$. From aluminum the shifts were 0.0023, 0.0055 and 0.069A to the long wave side of Mo $K\alpha_1$. From beryllium the shifts were 0.0048A to the long wave-length side and 0.00065A to the short wave-length side of Mo $K\alpha_1$. Graphite shifts for scattering angles of 42° and 147° were the same as for 90°. This and all curve widths establish the fact that the scattering electrons were ejected with zero kinetic energy. Hence the energy relation is $h\nu^1 = h\nu \pm Ve$. From this the *critical potentials;* 32, 57 and 279 volts are obtained for carbon; 57, 136 and 1550 volts for aluminum; 16 and 119 volts for beryllium.

Introduction

SINCE the first spectroscopic investigation of the change of frequency of scattered x-rays[1] there has always appeared an "unmodified" line as well as the "modified" or "Compton" line. This unmodified line has been so called because within the experimental error it has in each case appeared in the same position as that of the initial rays being scattered. However, in photographic spectra the resolution was in the best case[2] just enough to resolve the $K\alpha_1$ and $K\alpha_2$ lines of molybdenum, and in the ionization spectra even this resolution seems to have been unobtainable.

The chief obstacle to better resolution has been that when sufficiently narrow slits were used either singly or in multiple[3] the energy was diminished below the limit of practical measurement. Investigation of possible fine structure of this line was therefore impractical until the development of the two-crystal x-ray spectrometer by Davis and Purks.[4] With this instrument the heretofore unobtainable, very high, resolution, independent of the width

[1] A. H. Compton, Phys. Rev. **21,** 715 and **22,** 409 (1923).

[2] Ross's Spectrum of Mo*K* series scattered at 55° by paraffin, shown before the A. A. A. S. and Am. Phys. Soc. in December 1923.

[3] W. Soller, Phys. Rev. **23,** 292 (1924).

[4] Bergen Davis and Harris Purks, Proc. Nat. Acad. **13,** 419 (1927).

of slits used, is obtained. This property which permits the use of wide slits without diminution of resolution is invaluable in the investigation of the spectra of such weak radiations as scattered x-rays.

As an illustration of this increase in resolution of scattered x-rays, the author's ionization, wave-length curves[5] obtained by means of a Soller slit[3] and single crystal are 0.014A wide at half maximum while those obtained with the "two-crystal method" are but 0.0006A wide.

In the former the $K\alpha_1\alpha_2$ x-rays of molybdenum give a single broad "rocking curve" and are not resolved, but in the latter Mo $K\alpha_1\alpha_2$ appear as two narrow rocking curves that are widely separated from each other.

The experimental work of this paper is the detailed investigation which followed the discovery of "fine structure in scattered x-rays" (on March 9, 1928) that was reported to the American Physical Society[6] during its April meeting that year, and later described in detail.[7]

Apparatus Details

In each experiment the scatterer was placed between two molybdenum anodes, (1) the anodes being in separate cylindrical tubes or (2) in a single bulb containing the scatterer. (See Fig. 1)

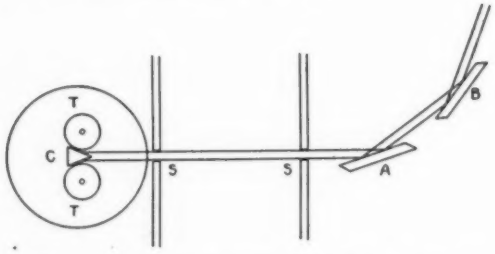

Fig. 1. Diagram of apparatus. *T*, *T*, x-ray tube anodes; *C*, scattering element; *S*, *S*, slits; *A*, collimating crystal; *B*, analyzing crystal.

The scattering investigated was in each case that of Mo $K\alpha_1$ x-rays. Scatterers used were in the order given, graphite, aluminum, and beryllium.

The following may also be of interest:–

Crystals: A previously tested cleaved pair of calcite (Ice-land spar).
Reflection order: First order on each crystal.
Slit width: 2.5 to 3 mm. (Note: this has nothing to do with curve width.)
Slit height: about 2 cm.
Tube power: constant d. c. Maximum potential 42 Kv. Maximum current 85 m.a.
Note: Even with wide slits the very low power of the scattered x-rays is still the chief obstacle to the analysis of these rays.
Electrometer sensitivity: about 2500 mm per volt at one meter.
Ionization system capacity: about 50 cm.
Note: Difficulty here is ratio of ionization produced by x-rays to variable ionization from uncontrolled sources.

[5] Never published. Similar curves were published by A. H. Compton and Y. H. Woo, Proc. Nat. Acad. **10**, 271 (1924).

[6] Mitchell and Davis, Phys. Rev. **31**, 1119 (June, 1928).

[7] Bergen Davis and D. P. Mitchell, Phys. Rev. **32**, 331, (1928).

Experimental Results

Carbon: With a graphite wedge placed so that the right section of the spectrometer slits was equally divided by its edge, the Mo $K\alpha_1$ x-rays scattered at about 90° were analyzed.

A typical spectrum is shown in Fig. 2.

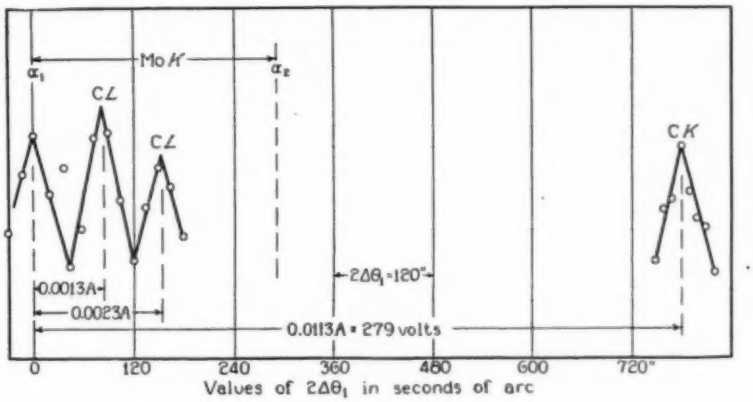

Fig. 2. Typical spectrum of Mo $K\alpha_1$ scattered by bound electrons in graphite.

From such spectra the following data are obtained.

Observed line	$2\Delta\theta_1$	$\Delta\lambda$
Mo $K\alpha_1$	0	0
1st shifted	90″	0.0013A
2nd shifted	158″	0.0023
3rd shifted	780″	0.0113

These values of $2\Delta\theta_1$ are probably not more accurate than $\pm 10''$ which is equivalent to ± 0.00015A.

The half maximum width of each of these rocking curves is about $2\Delta\theta_1 = 40''$ or 0.0006A. In connection with these widths it is well to note that the divergence of the radiation incident on the scatterer was in some cases nearly 90° and yet the curves were of the same width herein noted.

Spectra of radiation scattered by graphite at about 42° and 147° with a divergence of only 5° show similar displacement and curve widths. These latter spectra are less satisfactory because less energy was obtainable.

Aluminum: A typical spectrum of Mo $K\alpha_1$ x-rays scattered by a wedge of aluminum placed as described above, is shown in Fig. 3.

Such spectra yield the following displacements:

Observed line	$2\Delta\theta_1$	$\Delta\lambda$
1st shifted	160″	0.0023A
2nd shifted	380″	0.0055
3rd shifted	($2\theta_1 = 14°44'$)	0.069

The first two values of $2\Delta\theta_1$ are probably not more accurate than $\pm 15''$ or ± 0.0002A and the third about $\pm 2'$ or ± 0.002A. The half maximum width of these lines appears to be a little greater than those from graphite but not more than 50″ or 0.0007A. All spectra of scattering by aluminum

were for about 90° scattering angle and about 45° divergence of the incident radiation

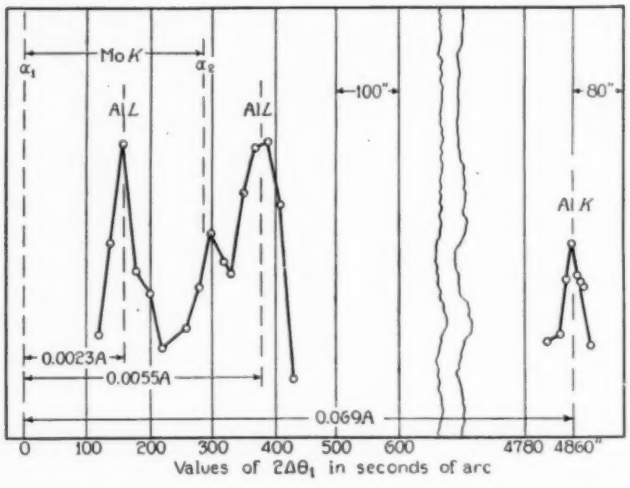

Fig. 3. Typical spectrum of Mo $K\alpha_1$ scattered by bound electrons in aluminum.

Beryllium: The spectrum of Mo $K\alpha_1$ x-rays scattered at about 105° by a block of beryllium is shown in Fig. 4. The average displacements are:

Observed line	$2\Delta\theta_1$	$\Delta\lambda$
1st shifted	−45″	−0.00065A
2nd shifted	334″	0.0048

The first displacement is probably good to ±10″ or 0.00015A and the second to ±15″ or 0.0002A. The half maximum width of the first is not

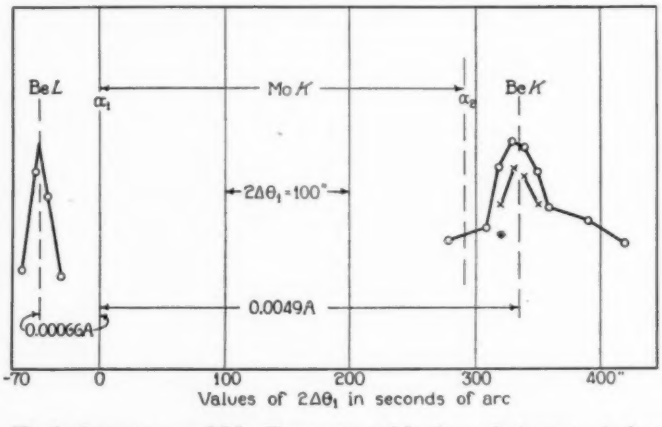

Fig. 4. Typical spectrum of Mo $K\alpha_1$ scattered by bound electrons in beryllium.

over 30″ and the second about 35″ or an average of 0.0005A. The most notable thing in the case of beryllium is that $2\Delta\theta_1$ and $\Delta\lambda$ for the first shifted line are negative. This will be discussed later.

Discussion

The effect of binding on the change of wave-length of x-rays scattered by bound electrons has been discussed at length by A. H. Compton[8] and G. E. M. Jauncey.[9] Both reached the conclusion that when the scattering electron is ejected, the shift in wave-length will probably be

$$\Delta\lambda=\lambda^2/(\lambda_s-\lambda)+(h/mc)\ \text{vers}\ \phi \tag{1}$$

where λ_s is the critical absorption wave-length for the stationary state from which the bound electron was ejected, and ϕ is the angle between incident and scattered quanta. The first term in this expression represents the shift due to the loss of enough energy to release the bound electron; and the second term, the shift due to loss of kinetic energy and momentum given to the *now* free electron.

In these experiments ϕ was about 90° so the second term in Eq. (1) would be about 0.024A for *all* scattering elements, yet nearly all of the *observed* shifts are much less than this. It would therefore appear that the scattering electron must have zero kinetic energy after ejection.

In this case the energy relation is simply

$$h\nu'=h\nu-Ve \tag{2}$$

where V is the critical potential and the shift will be

$$\Delta\lambda=\lambda^2/(\lambda_s-\lambda) \tag{3}$$

If we substitute Thibaud's[10] value of λ_s for K energy level of carbon in Eq. (3) we have

$$\Delta\lambda=0.708^2/(43.5-0.708)=0.0117A.$$

This may be compared with the corresponding value for carbon here observed $\Delta\lambda=0.0113$A.

Likewise using Fricke's[11] value $\lambda_s=7.947$ for K energy level of aluminum we have

$$\Delta\lambda=0.708^2/(7.947-0.708)=0.069\text{A}.$$

This is identical with $\Delta\lambda=0.069$A here observed.

The agreement is so good it seems necessary to conclude that the K *electrons are ejected with zero final kinetic energy.*

Such agreement is however not the only basis for this conclusion. If the x-ray quantum incident on the scattering electron imparted kinetic energy to that electron, momentum would also be imparted. The amount of this kinetic energy would depend upon the momentum and hence upon the relative direction of the scattered and the incident x-ray quanta. That is,

[8] A. H. Compton, Phys. Rev. **24**, 168 (1924); also X-rays and Electrons (D. Van Nostrand).

[9] G. E. M. Jauncey, Phys. Rev. **25**, 314 and 723 (1925).

[10] J. Thibaud, Compte Rendus **186**, 308 (1928).

[11] H. Fricke, Phys. Rev. **16**, 202 (1920).

$\Delta\lambda$ would depend upon the angle ϕ of scattering. Observations at different angles of scattering by graphite showed $\Delta\lambda$ to be independent of angle. That $\Delta\lambda$ is independent of scattering angle for graphite, aluminum and beryllium is also shown by the extremely narrow rocking curves obtained in all cases; curves of practically the same width as the initial Mo $K\alpha_1$. Variation of $\Delta\lambda$ with angle is incompatible with such narrow curves for in most cases the divergence of the incident radiation was so great that if $\Delta\lambda$ did vary with scattering angle, the resulting scattered radiation would be a band of many different wave-lengths, the rocking curve for which would be very wide. This important conclusion was pointed out by Davis and Mitchell[7] in the previous paper.

Beryllium; an unusual case. The change in frequency (Ve/h) of x-rays scattered by the outer electrons of beryllium is opposite in sign to that indicated by Eq. (2).

Instead of the scattering electron being ejected from a "bound" position and absorbing energy Ve from the energy $h\nu$ of the quantum being scattered, it appears that the scattering electron was free or nearly free and in scattering it (the electron) moved into a state (L level) of less energy and in so doing *added* its loss of energy to the quantum being scattered, i.e. in this case $h\nu' = h\nu + Ve$.

It is also remarkable that the *loss* of energy (Eq. 2) observed in the case of carbon and aluminum was not observed in the case of beryllium. Further investigations may disclose both kinds of energy transfers. The question of probability of "kind" is however a very interesting one that is as yet unanswered.

Raman and Krishnan[12] and others have observed both kinds of scattering of optical quanta by molecules and here also the explanation is incomplete

Critical Potentials

Since it is established that the only change in the energy of the x-ray quantum being scattered in these experiments is equivalent to the energy necessary to eject the scattering electron, we may write

$$h\nu' = h\nu \pm Ve \tag{4}$$

and compute the critical potentials indicated by this equation. These critical potentials computed from the observed data are shown in Table I.

Table I. *Critical potentials.*

Scatterer and (Z)	Critical potentials in volts		
	Outer levels		K
Be (4)	16 ± 4		119 ± 5
C (6)	32 ± 5	57 ± 5	279 ± 5
Al (13)	57 ± 5	136 ± 5	1550 ± 40

[12] C. V. Raman and K. S. Krishnan, Indian Jl. of Phys. Mar. 31 and July 31, (1928).

K electrons. Table II was prepared to facilitate comparison of these values for K energy levels with those of other observers. The agreement is well within the experimental error.

TABLE II. *Comparison of K critical potentials with those of other observers.*

Reference	Be ($Z=4$)		C ($Z=6$)		Al ($Z=13$)	
	V	ν/R	V	ν/R	V	ν/R
Table I	119 v.	8.8	279 v.	20.7	1550 v.	114.7
Bul. Nat. Res. C.[13]	121	9.0	288	21.3	1570	115.9
McLennan and Clark[14]	104	7.7				
Kurth[15]			283	20.9		
Thibaud[10]			284	21.		
Fricke[11]					1550	114.7

Outer electrons. The critical potentials here obtained for the outer electrons do not agree so well with earlier determinations. There are however significant differences between values deduced from wave-length measurements in the extreme ultra-violet spectra of gases and those determined by means of the photoelectric action of the emitted radiation from solids.

In Table III are shown a number of these earlier determinations together with those from this investigation. The latter were placed in the first row of this table in order to provide a convenient means of comparison

TABLE III. *Critical potentials of outer electrons.*

Reference	Be (4)	C (6)		Al (13)	
Table I	16 v.	32 v.	57 v.	57 v.	136 v.
Mean values from		11.2			
Bul. Nat. Res. C.[13]	8	34		67	128
Horton Andrews				66	107
and Davies[16]				42	
Hughes[17]		34.5			
Kurth[15]		32.9		37.9	123
McLennan	16				
and Clark[14]	20.3		74		
Millikan	9.5	11.3	45.5		
and Bowen[18]	18.1	24.3	64.2		

That the observed values do not agree with those from the Bulletin of the National Research Council[13] is not surprising since most of those are for the gaseous state. The outer electrons are known to be most effected when gas atoms are brought into close proximity of the solid state. The critical potentials should increase although possibly not so much as here indicated.

The heat of formation is insufficient to account for these differences between gaseous and solid state. The maximum probable value for the heat

[13] Bull. Nat. Res. Council No. 48 (1924).
[14] McLennan and Clark, Proc. Roy. Soc. (A)102 (1923).
[15] E. H. Kurth, Phys. Rev. 17, p. 528 and 18, p. 461 (1921).
[16] F. Horton, U. Andrews and A. C. Davies, Phil. Mag. 46, 721 (1923).
[17] A. L. Hughes, Phil. Mag. 43, 145 (1922).
[18] R. A. Millikan and I. S. Bowen, Phil. Mag. **4**, 561 (1927).

of formation of graphite, 250 kilo-calories per mole, is about 10 equivalent volts. Obviously this is not enough to account for the lack of agreement of the critical potentials here observed and those found for gases.

The agreement of the determinations from solids is in general more satisfactory. The probable precision of this investigation indicates that the outer electrons' critical potentials in Table I are the most accurate yet obtained for these solids.

Multiple Ionization

In this investigation of scattered radiation the scattering substance was radiated with a great abundance of general radiation from about 0.3A upwards. This fact suggests that possibly a majority of the scattering atoms were already partially ionized. In this case the observed critical potentials might be expected to be somewhat greater than those observed for stripped atoms by Millikan and Bowen.[18] Such agreement however is not very good even though the lack of a line in the scattered spectra corresponding to initial ionization in gases be explained by assuming that such ionization was produced by the general radiation, or that the valence electron lost its identity in the solid.

An alternative speculation is that for some unexpected reason two or more electrons are removed by one quantum from one atom, as a single act. In this case the data from enhanced spectra indicate the values here observed are too small.

After the foregoing considerations it seems that attempts to explain these discrepancies on the assumption of multiple ionization are fruitless until additional and more precise data are available.

Conclusion

In conclusion I would recall attention to the observed data set forth (Experimental Results) which fully establish the existence of *the change of frequency of x-rays scattered by bound electrons that are ejected with zero final kinetic energy.*

For his keen interest and assistance in this work and for many privileges in his laboratory, I wish to express my appreciation to Professor Bergen Davis.

Columbia University,
New York, N. Y.
March 4, 1929.

Note added in proof: In view of Ehrenberg's (Zeits. f. Physik **53,** 234, 1929) failure to observe the change in wave-length of Mo x-rays scattered from Acheson graphite and his suggestion that my results were due to uranium impurity it should be pointed out that since obtaining these results on Acheson graphite I have verified them by observing the x-rays scattered from a piece of pure carbon supplied by the General Electric Company.

EFFECT OF CHEMICAL COMBINATION ON THE ABSORPTION OF X-RAYS AT WAVE-LENGTHS ON EACH SIDE OF THE K DISCONTINUITY

By C. L. Cottrell.

Abstract

The difference in the absorption of x-rays by iodine in the free state as compared to that of iodine in the chemically combined state, was investigated for wave-length bands on each side of the *K* absorption limit of this element. The method used was the double ionization chamber method, with the x-ray bands obtained by voltage control and filters. The results indicate that on the long wave-length side of the *K* limit, the absorption coefficient of the chemically free iodine atom is about 0.3 percent greater than that of the combined atom, while on the short wave-length side of the *K* limit, the reverse is indicated with a difference of about 0.5 percent. Silver was also investigated, but from the few measurements obtained, the absorption coefficient of the chemically free silver atom as reduced from AgCl by sunlight, seems to be greater than that of the combined silver atom in the AgCl before reduction, for wave-length bands on each side of the *K* limit of silver.

I. Introduction

IN VIEW of recent work done by W. B. Morehouse[1] which showed an apparent effect of chemical combinations on the absorption of x-rays, it was thought of interest to continue work on this problem to ascertain what effect x-rays of wave-lengths in the region of the *K* absorption limit might show. Accordingly one of the chemical reactions used by Morehouse was selected and data were obtained for bands of wave-lengths on each side of the *K* limit of iodine. This reaction may be represented as follows:

$$I_2+Na_2S_2O_3\rightarrow 2NaI+Na_2S_4O_6$$

in which the I_2 was in alcohol solution and the $Na_2S_2O_3$ in an aqueous solution, as described later.

The method used was essentially the same as that used by Morehouse; i.e., the absorption of two solutions placed in an x-ray beam was measured, after which the solutions were allowed to react chemically and the absorption after reaction was measured. The densities before and after reaction were also measured and taken into consideration in calculating the effect. The separation of the x-rays into groups on each side of the *K* discontinuity was accomplished by voltage control and filters. A preliminary attempt was made to use crystals to obtain homogeneous beams but this was abandoned after it was shown that the effect sought was less than the experimental error involved in this method.

[1] W. V. Morehouse, Phys. Rev. **29**, 765 (1927).

In addition to the iodine reaction, another reaction was used, in which the reduction of AgCl was accomplished by light without disturbing the absorbing materials in the path of the x-ray beam.

II. Experimental Procedure

Figure 1 shows a plan of the general features of the apparatus used. There was little difference between the general method employed in making observations and that used by Becker,[2] Read,[3] and Morehouse.[1] The two ionizations chambers C and C' received x-ray beams 1 and 2 which passed through slits S and S' respectively. There was impressed across the two chambers a potential of 540 volts with its mid-point grounded so that when the separate ionization currents were equal they neutralized each other and there was no deflection of the electrometer needle. This was connected, as

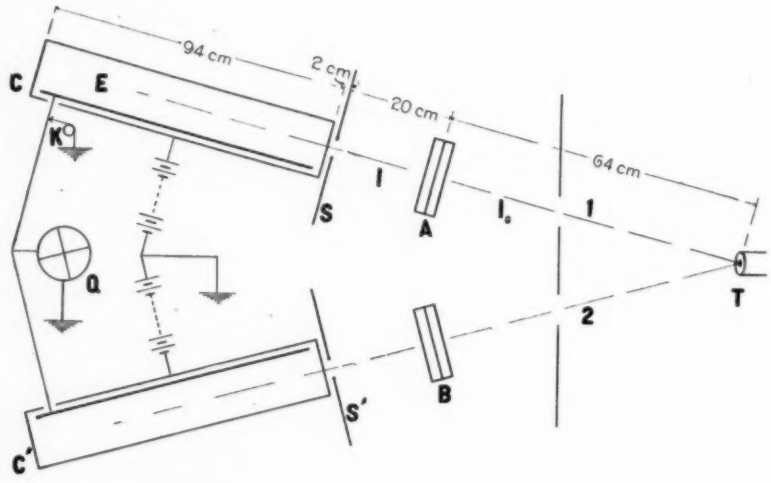

Fig. 1. General plan of apparatus.

shown, to the collecting rods of the ionization chambers. The chambers were filled with methyl bromide to increase their absorption of the x-rays in the usual manner. Amber was used for insulating the collecting rods and quartz for insulating the wire connecting the rods to the quadrant electrometer Q. The electrometer was of the Compton type and was used at a sensitivity of 5000 to 7000 mm/volt.

The slit S was adjusted for a reading by noting when the electrometer needle showed the same drift with x-rays entering the chambers as when they were not. This zero drift could not entirely be eliminated but it was thought that by the above method true settings were obtained despite this drift.

In the path 1 of the x-ray beam was placed a two-compartment cell A, the walls of which were made of 0.16 cm bakelite and washed with melted

[2] J. Becker, Phys. Rev. **20**, 134 (1922).
[3] H. Read, Phys. Rev. **27**, 373 (1926).

paraffin. Each compartment was 1 cm thick. A similar cell B was placed in path 2. The cells were placed far enough from the slits to make the amount of scattered radiation that passed through the slits from the cells, small compared to the transmitted beam itself.

The beams on entering the ionization chambers were limited only by the slits S and S' and the size of the focal spot on the target, so that the energy passing through the slit was proportional to the area of the slit, or for a constant length slit, to the slit width. This was measured by means of a micrometer screw and could be read to 0.0001 inch. The maximum size of the slit bounded a beam which, at the rear of the ionization chamber, subtended an area of about 2×3 cm, the edges of which were well away from the side walls of the chamber.

A lead screen confined the x-rays to the general direction of the two beams. The tube was placed so that the target was symmetrically situated with respect to each beam; i.e., the tube was placed so that each beam made the same angle with the face of the target.

The general procedure in making observations was as follows:—the tube was put in operation and then the density of each separate solution was measured by means of a Westphal balance, while the tube was reaching steady operation. The first balance was obtained with nothing in either path and this was repeated at the end of the run as a check measurement on the apparatus. Then cell B containing the solutions was placed in beam 2, empty cell A was introduced into beam 1, and S was adjusted to make a balance, i. e. to re-establish the initial electrometer drift. This reading of slit S is called S_0 in what follows. Cell A was then filled with the two separate solutions, the iodine solution being placed in the compartment nearest the slit in all cases as it was thought this would help to make the results more comparable. Also, cell A was always used in beam 1. With the filled cell in beam 1, a balance was made and repeated several times. This slit width is called S_1. Then cell A was removed from the path of the x-rays and the cell's contents were poured into a beaker to react, after which the mixed solution was put into the cell and the cell replaced in the x-ray beam. A balance was again made and repeated several times and this slit width is called S_2. Now as a third condition, cell B was removed and its solutions allowed to react and then replaced, when another balance was obtained. This latter condition may be considered the equivalent of that represented by S_1 and as such was used in calculating the results. Finally the densities of the mixed solutions in each cell were measured.

The iodine reaction:

$$I_2+N_2S_2O_3\rightarrow 2NaI+Na_2S_4O_6$$

changed the iodine from the free state in which it was in a 70 percent alcohol solution (12.7 gm I to 1000 cc of 70 percent alcohol) to the combined state with sodium (NaI) still in solution; the reaction of the I-alcohol solution with an equal amount of sodium thiosulfate solution (25 gm $[Na_2S_2O_3+5H_2O]$ to 1000 cc H_2O) being complete. 160 cc of each solution were used in each cell.

In addition to the iodine reaction with the solutions in bakelite cells, silver chloride was used in the form of an emulsion on paper as supplied by the Eastman Kodak Company under the trade name of "Solio" paper. This paper was cut into sheets 5×7 cm in size and these placed back to back in pairs in slots cut in the walls of a light tight box so that between pairs was a space of about 1 cm. Each box contained twenty sheets of "Solio". When the lid of the box was opened, light could be directed at an angle upon the sensitive surfaces of the "Solio" thus causing a darkening of the emulsion, or a reduction of the silver chloride, until the paper became quite dark, or as it customarily appears when used for making photographic "proofs". Exposure to x-rays apparently does not effect the emulsion within a time period of several hours. The face of the box was covered by a thin glass plate sealed on with paraffin, and the open ends of the box were sealed over with two layers of black paper, while all cracks and openings were well coated over with shellac, so that after the "Solio" sheets had been placed in the box they were hermetically sealed within it. This was done to prevent any liberation of chlorine that was not held in the gelatine of the emulsion, from the path of the x-rays, and also to prevent any change due to humidity variation. Two such boxes were used, one in each beam, and slit widths S_1 (papers in each box, unexposed), S_2 (papers in box in beam 1, exposed), and S'_1 (papers in each box, exposed) were observed. To produce blackening, sunlight was used and directed to the surface of the "Solio" by means of a heliostat and suitably placed mirrors so that the boxes were not disturbed in the x-ray beams during the entire run.

Filtered beams of x-rays were obtained uuder the following conditions:

Case (a): Cu filter 0.050 cm thick; tube voltage 60 k.v.$_{eff}$; mean wave-length = 0.24A.

Case (b): Cu filter 0.033 cm thick; tube voltage 49 k.v.$_{eff}$; mean wave-length = 0.30A.

Case (c): Al filter 0.74 cm thick; tube voltage 44 k.v.$_{eff}$; mean wave-length = 0.34A.

Case (d): No filter; tube voltage 22 k.v.$_{eff}$; Mo target; K lines of Mo most prominent; mean wave-length = 0.70A.

The effective mean wave-length of each of the filtered bands of x-rays was approximately determined by finding the effective mass absorption coefficient of a particular thickness of Al for the several bands, and then referring to Richtmyer's tables[4] to find the wave-length that corresponded to the coefficient so obtained. This wave-length was considered the effective wave-length of the filtered band.

As a check on this determination, curves were plotted for each band by extrapolating the curves of Behnken[5] and applying the absorption data of Richtmyer's tables for each filter. These distribution curves showed peaks somewhat less in wave-length than the wave-lengths obtained as the effec-

[4] F. K. Richtmyer, Phys. Rev. **18**, 13 (1921).

[5] Behnken, Zeits. f. Physik **3**, 48 (1920).

tive mean wave-lengths by the first method. However, this shift is to be expected since the longer wave-lengths are relatively more absorbed in the ionization chamber, and, since the effect of the Al plate is to harden the rays that enter one chamber, a too large value of the absorption coefficient is obtained; and thus the mean effective wave-length will be somewhat larger for the absorption method than for the graphical method. However, the agreement is fairly close and is as shown in Table I.

TABLE I. *Comparison of Al plate method with the graphical method.*

Case	Mean effective wave-length of x-ray band	
	By Al plate method	By graphical method
a	0.24A	0.23A
b	0.30	0.275
c	0.34	0.30

The plotted distribution curves were compared, with apparent consistancy, to those given by Mertz[6] in his use of filtered bands of x-rays. These curves showed a width of about 60 percent of the peak wave-length when measured between the wave-lengths of half the energy value of the peak wave-length.

In case (a) values were obtained by using for the first pair of trials a water-cooled Mo target tube, but for the other trials a W target tube was used. This latter tube was also used for cases (b) and (c).

APPENDIX TO PROCEDURE

An attempt was made to carry out the foregoing general procedure by using beams of homogeneous x-rays as obtained by use of rock-salt crystals, one being placed in each beam about midway between the cell and the tube target.

Crystals 7 cm long were used and no limitation was put on the beam other than that determined by the size of the crystal face. At the small angles of incidence desired this produced a reflected beam less than 1 mm wide and as homogeneous as necessary for this work; i.e. the difference in wave-length between the rays reflected by the extreme outside edges of the crystal was about 0.06A. After the set-up had been calibrated for wave-length, angle of crystal setting and ionization chamber position, it was found that the highest accuracy obtainable was about 0.3 percent in slit width settings. This may have been due to the small energy present in the beam, although a particular setting seemed definite enough in itself and not difficult to make, but once made would not remain a balanced setting for more than a few seconds. A shift of the focal spot would cause a relative difference in the energy of the two beams by producing a relative change in the wave-lengths of the two beams since the beams hit the crystals at slightly different relative angles than before the focal spot shifted. This difficulty might be somewhat overcome by having both ionization chambers in practically the same direction as by having them side by side or one above the other, and by using two adjacent crystals mounted for this arrangement.

Also, if the x-ray energy available were sufficient to permit a fixed slit or pin hole to be placed in front of the target, the angle of incidence of the beam on the crystal face would be fixed, thus eliminating variation of the direction of the reflected beam or relative change in energy in the beams because of changed wave-length. This latter variation might be minimized by using a tube voltage so that the maximum of the energy distribution curve occurs at the desired wave-length. For this present work so high a tube voltage was not available.

[6] P. Mertz, Phys. Rev. **28**, 891 (1926).

III. Discussion of Formulae

Referring to the Fig. 1 let I_0 represent intensity of the x-ray beam 1 before reaching cell A, and let I be the intensity of the beam after passing through the cell A and incident on slit S. Also let E be the ionization current in chamber C. E is proportional to S, the slit width, and to I, the intensity of the incident beam; i.e., in arbitrary units, $E=SI$.

Now $I=I_0e^{-\alpha x}$ where e is the base of the natural logarithms; α is the absorption coefficient, defined in the usual way; and x is the thickness of the absorbing layer. If we let $\alpha x=\mu$, which may be called the absorption *constant* (to distinguish it from α, the absorption coefficient) we have

$$I=I_0e^{-\mu}. \tag{1}$$

In this case μ includes the absorption *constants* of all the absorbing media making up the cell and its contents, or $\mu=\mu_1+\mu_2\cdots$. To put μ in terms of the atomic absorption coefficient, let $\mu=\tau nx$, where τ is the apparent absorption coefficient per atom; n is the number of atoms per cc; and x is the thickness of the absorbing layer as above defined. Then letting $nx=N$, the total number of atoms in the path of the beam of unit cross section area, we have: $\mu=\tau N$; and from (1):—

$$I=I_0e^{-\tau N}. \tag{2}$$

In the particular measurements made first with the empty cell A in beam 1 and with cell B plus solutions in beam 2,

$$E=S_0I=S_0I_0e^{-\tau_cN_c} \tag{3}$$

where (τ_cN_c) is the absorption constant for the cell walls alone, and S_0 is the observed slit width.

Then with the separate solutions in cell A in beam 1, and cell B plus solutions as before in beam 2,

$$E=S_1I_0e^{-\tau_cN_c-\tau_1N_1} \tag{4}$$

where τ_1 is the apparent average atomic absorption coefficient; N_1 is the number of these so-called average atoms of solution in the path of the beam per sq. cm; and S_1 is the observed slit width. This summing of the absorption constants of the different absorbers in the beam was proved to be justifiable in Morehouse's paper[1] above referred to.

Since the ionization current in chamber C' is the same for the condition represented by equation (3) and for that represented by equation (4) (except for variation in the tube itself which should effect each beam in the same proportion), we can combine (3) and (4).

$$S_0I_0e^{-\tau_cN_c}=S_1I_0e^{-\tau_cN_c-\tau_1N_1}$$

or

$$S_0=S_1e^{-\tau_1N_1}. \tag{5}$$

Similarly in the case of the mixed solutions:

$$S_0 = S_2 e^{-\tau_2 N_2} \tag{6}$$

where τ_2 is the apparent average atomic absorption coefficient for the mixed solution; N_2 is the number of these average atoms in the path of the beam, per sq. cm; and S_2 is the observed slit width.

Expressing equation (5) in logarithmic form

$$\log (S_0/S_1) = -\tau_1 N_1$$

or

$$\tau_1 = -(1/N_1) \log (S_0/S_1)$$

and

$$\tau_2 = -(1/N_2) \log (S_0/S_2).$$

Let

$$\tau_1 - \tau_2 = \Delta\tau = -(1/N_1) \log (S_0/S_1) + (1/N_2) \log (S_0/S_2)$$

and

$$\frac{\Delta\tau}{\tau} = \frac{(1/N_2) \log (S_0/S_2) - (1/N_1) \log (S_0/S_1)}{(1/N_1) \log (S_0/S_1)}$$

or

$$\frac{\Delta\tau}{\tau} = \frac{N_1(\log S_0 - \log S_2)}{N_2(\log S_0 - \log S_1)} - 1.$$

If we assume that N is proportional, in each case, to the average density, then $N_1/N_2 = \rho_1/\rho_2$ where ρ represents the density of the solutions. This assumption seems valid since no new kinds of atoms are introduced into the path of the beam between measuring the absorption of the separate solutions and that of the mixed solution. Therefore the equation

$$\frac{\Delta\tau}{\tau} = \frac{\rho_1}{\rho_2} \frac{(\log S_0 - \log S_2)}{(\log S_0 - \log S_1)} - 1 \tag{7}$$

gives the fractional change in the atomic absorption coefficient due to the chemical reaction. This formula was used in computing from the data, the effect shown in the results.

IV. Results for Iodine

The results obtained from the observed data are given in the Table II. In this table the first column of figures refers to the trial number of each run; the second column gives the values in percent of the relative change in the average atomic absorption coefficient of iodine for a filtered band of x-rays of mean wave-length equal to 0.24A, as previously described in section II for case (a); the remaining columns present the values obtained for other cases in the same way, using different filtered bands of x-rays of mean wave-lengths as indicated and as also previously described under section II.

The positive values of the percent change in the atomic absorption coefficient mean that τ for the combined iodine atom is greater than τ for the free iodine atom.

TABLE II.

Trial	Case *a* $\lambda_m=0.24$A	Case *b* $\lambda_m=0.30$A	Case *c* $\lambda_m=0.34$A	Case *d* $\lambda_m=0.70$A
1	+0.47%	+0.09%	+0.15%	−0.34%
2	+0.52	+0.29	+0.72	−0.28
3	+0.45	+0.27	+0.25	−0.33
4	+1.09	+0.91	+0.74	−0.30
5	+0.48	+0.27		
6	+0.77	+0.39		
Av.	+0.63	+0.37	+0.47	−0.31 (−0.36)*
Av. deviation of the mean	±0.08	±0.08	±0.13	±0.01

* This value was obtained by Morehouse for about the same band of x-rays, viz. with a Mo target at 21 k.v. eff, and no filter.

V. RESULTS FOR SILVER

The results of measurements on the change in absorption of Ag, by reducing the Ag from AgCl photochemically, are rather uncertain and hardly more than an indication that there is a change. In this case the slit width is the only measurement that need be considered, since density changes do not enter, as these can occur only in the direction of the beam and so do not change the total number of atoms traversed by the x-rays. In terms of slit width, the results are:

Case a	*Case d*
$\Delta S/S=\Delta\tau/\tau=-0.16$ percent	-0.23 percent

$$\therefore \tau(\text{free Ag}) > \tau(\text{combined Ag})$$

VI. SOURCES OF ERROR

The results are affected by errors due to the change in total absorption being measured instead of that due to the iodine or silver alone. In the case of the iodine reaction, Morehouse[1] has shown that the absorption of iodine is about nine times that by sulphur, the only other element that changes its valence is this reaction; and therefore the observed effect may be considered mainly due to the iodine. However, Stobbe and Schmitt,[7] and more recently Batley,[8] have shown spectroscopically that iodine in alcohol solution tends to form hydrogen triiodide or other periodides, which may involve from several percent to one hundred percent of the iodine in the solution, depending upon the time and other factors. But if this occurs there would still be an effective change in valence of a large proportion of the iodine upon the formation of NaI in the reaction here used. The variation shown in the results may be due in part to this uncertainty as to the true state of the iodine in the alcohol solution. In the case of the silver reaction, all other elements in the path of the x-rays are of low atomic number and hence their change in absorption must be a small fraction of the whole change, since comparable amounts of Ag and those light elements take part in the change.

[7] Stobbe and Schmitt, Z. wiss. Phot. **20**, 57 (1920).
[8] A. Batley, Faraday Soc. Trans. **24**, 438 (1928).

The scattering should be nearly the same before reaction as after, except for the small difference made by the change in density; but since the scattering is only a fraction of the whole apparent absorption, any changes in this should be a correspondingly small fraction of the total change observed.

Unsteadiness of the tube operation and ionization chambers was the main cause of erratic readings and the comparatively low accuracy of the results. The tube was operated on an a.c. transformer and was self rectifying. The source of a.c. was a motor generator run by a d.c. generator which in turn was operated by an a.c. motor run by the power from the university generating plant. However, the a.c. voltage applied to the tube transformer had to be constantly regulated by a manually controlled series resistance to keep its variations within 0.5 percent.

In part of the work a water cooled Mo target tube was used and with this it was noted that the rate of flow of water made a slight difference in tube current. Change in tube current and consequent change in x-ray energy in the emitted beam should have affected each beam equally and therefore should have made no difference in the slit setting for a balance. This, however, was not strictly true due probably to slight dissymmetry between the two ionization chambers. Also apparently one ionization chamber continually became relatively less absorbing with respect to the other chamber, thus causing the balancing slit width to gradually become narrower with time, due possibly to unequal activity of the methyl bromide in the two chambers. Differential temperature changes between the two chambers were minimized by connecting the chambers with a rubber tube, and by covering each chamber with about 7 cm thickness of cotton waste.

Errors in the slit width readings were less than 0.004 percent and back lash in the micrometer screw was accounted for by always approaching a balance setting from the same direction.

Measurement of density was made by the Westphal balance and was in itself to an accuracy of 0.01 percent but after the solutions reacted, due to the heat of reaction the temperature of the mixture rose several degrees and slowly returned to that of the room. Too long a wait between the slit readings for the separate solutions and the mixed solution could not be permitted because of tube and ionization chamber variation, and so readings were made on the warmer mixed solution, and an effort made to measure its density at the temperature at which it had been used. Evaporation of the lighter solvent (alcohol) during the slit measurement would also introduce error into the density measurement made somewhat later. This total density measurement error might be as large as 0.05 percent.

Error might also be incurred by relative changes in the cell widths. This was the first serious error encountered and it was found that a variation of 15 percent in slit width was produced in five hours time by simply filling one cell with the solution and letting it stand in position in the x-ray beam for that length of time. Apparently the iodine or the alcohol or the combination attacks the bakelite and causes warping. Other materials were then sought but nothing with sufficiently low absorption in the desired region of

x-ray wave-lengths and that would withstand the iodine solution, could be found, so melted paraffin was poured into the bakelite cells and then immediately poured out, leaving a thin coating on the inside surface of the cell. This appeared to prevent any effects of the solution on the cell walls.

These errors together made the results certain to no greater accuracy than 0.08 percent.

Acknowledgment is made with pleasure to Professor F. K. Richtmyer, who suggested this problem, and to Dr. Warren Nicolas, for their helpful interest and criticism.

ROCKEFELLER HALL,
ITHACA, NEW YORK,
March 14, 1929.

DIFFRACTION OF X-RAYS IN LIQUIDS: BENZENE, CYCLOHEXANE AND CERTAIN OF THEIR DERIVATIVES

By G. W. Stewart

Abstract

An examination by the x-ray diffraction ionization method was made of benzene, toluene, *o*-, *m*- and *p*-xylene, mesitylene, ethyl benzene and isopropyl benzene; cyclohexane, methyl cyclohexane, *o*-, *m* and *p*-dimethyl cyclohexane; phenol, aniline, cyclohexanol and cyclohexanone; 2-hydroxy-1,3-dimethyl benzene and three isomers, *o*-, *m*- and *p*-toluidine, and *o*-, *m*- and *p*-cresyl methyl ether. The diffraction peaks are taken to be caused by the semi-orderly space arrangement of the molecules in the liquid, or cybotactic condition, and the distances of separation of the planes containing diffraction centers are computed by Braggs' diffraction law. Both assumptions have been previously proved justifiable.

Structure and dimensions of benzene and cyclohexane rings.—The structure of the benzene and cyclohexane rings are shown to be distinctly flat, having a thickness of 4.70A.u. and 5.10A.u. respectively. The proof of the flatness rests upon the effect of substitutions and the relative prominence of diffraction peaks. The general dimension in a plane perpendicular to the thickness is indicated by a diameter of approximately 6A.u., as indicated by an area of 31.4(A.u.)^2 for benzene and 35.2(A.u.)^2 for cyclohexane. These dimensions of the rings are based upon direct measurements and are limited in reliability only by the correctness of the theory of the x-ray measurements. The evidence is preponderately in favor of the maintenance of the general shape of the benzene and cyclohexane rings as units of structure. The similarity of the thickness to the diameter of *n*-paraffin and *n*-alcohol and monobasic *n*-fatty acids chains indicates the general correctness of the ring conception.

Effect of substituents on the thickness of the rings.—It is shown that the thicknesses of the benzene and cyclohexane "rings" depend upon the relative positions of the substituents. Four ortho, meta and para series, one with derivatives of cyclohexane and three with derivatives of benzene, show that the para substitutions give distinctly the least "thickness" of ring and that usually the meta gives less thickness than the ortho position. In a case of three substituents, variations caused by position were distinctly noticeable.

Other effects of substituents on the diffraction patterns.—Six compounds having the substituent OH, with one a cyclohexane derivative, were found to show "double" molecules produced by the juxtaposition of the two OH groups. None of the others showed this type of orientation. This evidence was obtained by a second semi-orderly arrangement of molecules with diffraction centers in planes separated by a distance of the magnitude of two molecular lengths. Ten compounds gave also an additional set of planes, caused more importantly by the positions than by the nature of the substituents. Of these ten, three, the hydroxy-dimethyl benzenes, showed the three sets of planes; namely, one corresponding to the thickness of the ring, one to an arrangement in a perpendicular direction caused by the substituents, and one in a third direction perpendicular to the other two sets and corresponding to the double molecule of the polar groups.

The above conclusions are in harmony with current investigations from other viewpoints and strengthen the theory of semi-orderly and temporary space arrangements of the molecules in a liquid, or the cybotactic condition.

IN THIS continuation of contributions to the study of x-ray diffraction in liquids,[1] evidence is given concerning two important subjects; namely, the structure of the molecules and the physical nature of a liquid. The experiments described give the effective thicknesses of the so-called rings of benzene and cyclohexane, the changes in these thicknesses with substitutions, and certain information concerning the orientation of molecules in the liquid state. The self-consistency of the results and the agreement with other lines of evidence assist in further verification of the group arrangement or cybotactic theory of the liquid state.

X-ray diffraction measurements in one or more of the liquids here used have been made by at least one of the authors cited in the accompanying foot note.[2] Inasmuch as the function of this paper is not to establish the accuracy of measured values but rather to make comparisons among the results here presented, the results of these earlier experiments will not be detailed. Nevertheless, it should be stated that no serious or inexplicable disagreements exist.

Results. The apparatus and procedure is precisely that in the earlier papers from this laboratory. The Mo $K\alpha$ doublet is the x-radiation used. The compounds fall into the following groups: benzene, toluene, *o*-,*m*- and *p*-xylene, mesitylene, ethyl benzene and isoprophyl benzene; cyclohexane, methylcyclohexane, *o*-*m*-and *p*-dimethylcyclohexane, phenol, aniline, cyclohexanol, cyclohexanone, 2-hydroxy-1,3-dimethyl benzene, 2-hydroxy-1,4-dimethyl benzene, 4-hydroxy-1,2-dimethyl benzene, 4-hydroxy-1,3-dimethyl benzene, *o*-,*m*- and *p*-toluidine, *o*-,*m*- and *p*-cresyl methyl ether.[3] Five of these compounds are in the solid state at room temperature. Observations on them were made at a temperature a few degrees above their respective melting points, the higher temperatures being obtained by a hot air blast. All other measurements were made at room temperature. The relative intensity of the diffracted ray as a function of the angle of diffraction is shown

[1] Stewart and Morrow, Phys. Rev. **30**, 232 (1927); Stewart and Skinner, Phys. Rev. **31**, 1 (1928); Stewart, Phys. Rev. **31**, 174 (1928) and **32**, 153 (1928).

[2] Articles recording measurements on one or more of the compounds used,

1. Debye and Scherrer, Nachr. Kgl. Ges. Wiss. Gëtting (1916); 1.
2. Hewlett, Phys. Rev. **20**, p. 688 (1922); 1, 6.
3. Keesom and Smedt, Proc. Amster. Acad. **25**, p. 118 (1922) and **26**, p. 112 (1923); 1.
4. Wyckoff, Am. Jl. Sci. p. 455 (1923); 15.
5. Eastman, Am. Chem. Soc. Jl. **46**, p. 917 (1924); 1.
6. Herzog and Janke, Zeits. f. Physik **45**, p. 194 (1927); 24.
7. Raman and Sogani, Nature, Apr. 23 (1927); 9.
8. Sogani, Ind. Jl. Phys. Vol. I, Pt. IV, p. 357 (1927); 1, 9, 14, 15; Ind. Jl. Phys. Vol. II, Pt. I, p. 97 (1927); 2, 3, 4, 5, 6, 7.
9. Katz, Zeits. f. Physik **45**, p. 97 (1928); 1, 2, 7, 14, 15, 16.
10. Krishnamurti, Ind. Jl. Phys. Vol. II, Pt. III, p. 355 (1928); 22, 23, 24. Vol. IV, Pt. IV, p. 104 (1928); 1, 9, 14, 15.

There are 27 compounds listed in Table I. The numbers following each of the above references refer to the serial number of the compound as listed in Table I.

[3] These compounds were all obtained from the Eastman Kodak Company, with the exception of the dimethyl cyclohexane which were supplied by R. E. Marker of Yonkers, N.Y.

for these groups in Figs. 1, 2, 3 and 4. The proportionality of relative intensity to ionization currents is assumed to be sufficiently accurate. The computed data, assuming Bragg's diffraction law, are shown in Table I.

Theory. The theory adopted and fully justified elsewhere[4] is that the peaks found in the curves are caused by the orientation of the molecules with diffraction centers in approximately parallel planes and in large enough groups to give a noticeable diffraction effect. These groups are neither permanent in constitution nor perfect in form. The nearest approach to a quantitative theory of the diffraction is to be found in that of a powdered crystal. The separa-

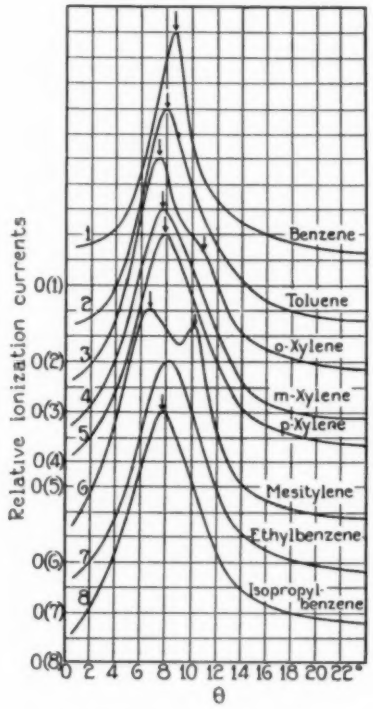

Fig. 1. Relative intensity diffraction curves of benzene derivatives.

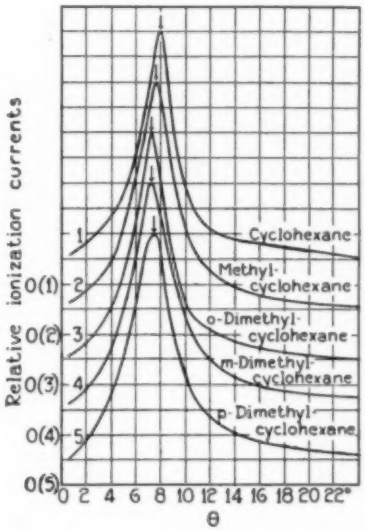

Fig. 2. Relative intensity diffraction curves of cyclohexane derivatives.

tion of the approximate planes in which the diffraction centers lie is obtained by Bragg's law, $\lambda = 2d \sin \theta/2$, wherein θ is the angle of deviation on the spectrometer. The computed values of d are in the fourth column of Table I.

Thickness of rings. It will be noticed that the most important diffraction peak has an angular position which is common to all, though with the value of angle changing significantly. It corresponds to a distance between diffraction centers arranged in parallel planes. The corresponding orientation of the molecules is caused by molecular forces and these, it might be assumed, would

[4] Stewart, Phys. Rev. **32**, 558 (1928).

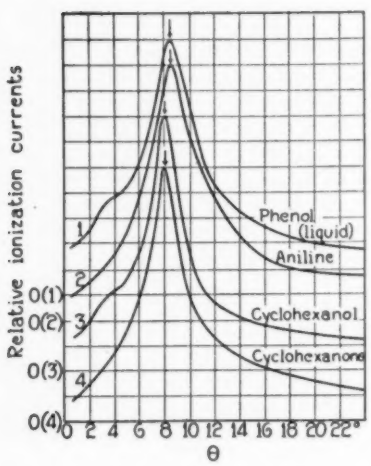

Fig. 3. Relative intensity diffraction curves of derivatives of benzene and cyclohexane

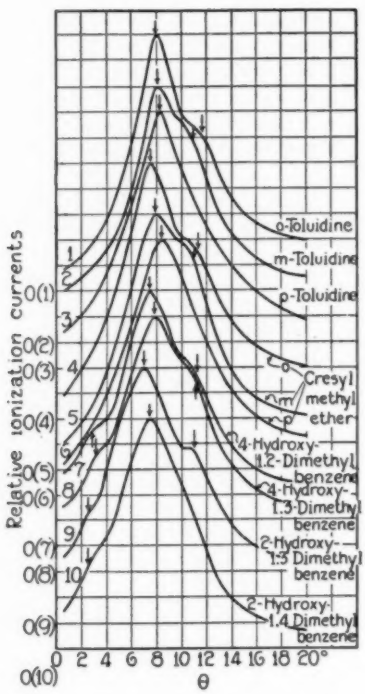

Fig. 4. Relative intensity diffraction curves of benzene derivatives.

TABLE I. *Data computed from the diffraction of x-rays in various liquids.*

No.	Name	Ring and Substitutions *B*(benzene) *C*(cyclohexane)	Spacings of Diffraction centers in 10^{-8} cm	Width of peak
1	Benzene	*B*	4.70	2.3°
2	Toluene	*B*: CH_3	5.06	3.6°
3	*o*-Xylene	*B*: 2(CH_3) at 1,2	5.51 3.72	3.8° —
4	*m*- "	*B*: 2(CH_3) at 1, 3	5.35	4.8°
5	*p*- "	*B*: 2(CH_3) at 1, 4	5.17	4.5°
6	Mesitylene	*B*: 3(CH_3) at 1, 3, 5	6.13 4.00	4.2° —
7	Ethyl benzene	*B*: C_2H_5	4.99	4.5°
8	Isopropyl benzene	*B*: $CH(CH_3)_2$	5.35	4.5°
9	Cyclohexane	*C*	5.10	1.8°
10	Methylcyclohexane	*C*: CH_3	5.35	2.4°
11	*o*-Dimethyl cyclohexane	*C*: 2(CH_3) at 1, 2	5.62	2.0°
12	*m*- " "	*C*: 2(CH_3) at 1, 3	5.64	2.3°
13	*p*- " "	*C*: 2(CH_3) at 1, 4	5.49	2.7°
14	Phenol (liquid)	*B*: OH	4.77 11.79	3.1° —
15	Aniline	*B*: NH_2	4.75	2.9°
16	Cyclohexanol	*C*: OH	5.04 11.80	1.9° —
17	Cyclohexanone	*C*: O	5.04	2.0°

be most effective in that orientation which may loosely and descriptively be said to be caused by the shape of the molecule. If the benzene and cyclohexane molecules are somewhat flat, the most prominent orientation would be in parallel planes in which the "flat" disks may be said to lie. The distance of separation of these planes may then be called the "thickness" of a molecule. Evidence in these experiments will presently be adduced, showing that there is a decided flatness of both the benzene and cyclohexane rings. This distance of separation or the thickness of the molecules is, as shown in Table I, 4.70A.u. for benzene and 5.10A* for cyclohexane.

TABLE II.

No.	Name	Ring and Substitutions *B*(benzene)*C* (cyclohexane)	Spacings of Diffraction centers in 10^{-8} cm	Width of peak
18	2-Hydroxy-1,3-dimethyl benzene	*B*: OH at 2 $2CH_3$ at 1, 3	11. 3.7 5.84	5.0°
19	2-Hydroxy-1,4-dimethyl benzene	*B*: OH at 2 $2CH_3$ at 1, 4	11. 5.51	5.1°
20	4-Hydroxy-1,2-dimethyl benzene	*B*: OH at 4 $2CH_3$ at 1, 2	13.9 3.65 5.46	5.0°
21	4-Hydroxy-1,3-dimethyl benzene	*B*: OH at 4 $2CH_3$ at 1, 3	13.1 3.68 5.20	5.5°
22	*o*-Toluidine	*B*: CH_3 at 1 NH_2 at 2	5.12 3.5	3.2°
23	*m*- "	*B*: CH_3 at 1 NH_2 at 3	5.07 3.46	4.5°
24	*p*- "	*B*: CH_3 at 1 NH_2 at 4	4.96	4.4°
25	*o*-Cresyl methyl ether	*B*: CH_3 at 1 OCH_3 at 2	5.50 3.6	4.2°
26	*m*- " " "	*B*: CH_3 at 1 OCH_3 at 3	5.21 3.76	5.0°
27	*p*- " " "	*B*: CH_3 at 1 OCH_3 at 4	4.86	4.8°

Flatness of benzene and cyclohexane molecules. Table I shows that a substitution of OH for H (phenol) in benzene gives an increase in thickness of only 0.07A, and of NH_2 for H (Aniline), only 0.05A. Similarly with the saturated ring of cyclohexane, the substitution of OH for H (cyclohexanol) increases the thickness −0.06A and the substitution of O for H_2 (cyclohexanone), −0.06A. All these differences are within possible errors in experi-

* For simplicity, "A" will hereinafter be used for A.u.

ment, caused not only by apparatus but by lack of purity of the compounds. Hence these simple substitutions may be said to alter the thickness little or none at all. This could scarcely be the case were the rings spherical in shape, for then the increase in our separation of planes would be a sensible fraction of an atomic diameter. If the rings are distinctly flat, the substitutions may extend chiefly in the plane of the ring.

The substitution of CH_3 for H in benzene and in cyclohexane does make an increase in thickness, 0.36A (toluene) and 0.25A (methyl cyclohexane). The substitution of an ethyl (ethyl benzene) causes an increase of 0.29A. The substitution of $CH(CH_3)_2$ for an H in benzene (isopropyl benzene) makes an alteration of 0.65A. But these details are in harmony with the view that the ring is noticeably flat, for, although these substitutions do increase the thickness by an appreciable fraction of an atomic diameter which may be regarded as 1-2A, yet the increase is an even smaller fraction of the diameter of the substituted group. All of these substitutions, then seem to give distinct evidence favoring the flatness of the benzene and cyclohexane rings.

Other evidence for the flatness of the benzene ring is found in the measurements of electric moments by two independent investigators, Smythe and Morgan[5] and Williams.[6] It may be well to note also, in this connection that Adam,[7] in experiments with monomolecular liquid films, has determined the cross-section perpendicular to the plane of the benzene ring to be 24 $(A)^2$. This is in fair agreement with our value of 4.7A for the thickness, for then the other dimension in this cross-section would be 5.1A. To summarize, then, our measurements clearly would not lead to the conclusion that all the C and H atoms are in the "same plane", for a distance of 5A is perhaps three times an atomic diameter. A conservative statement is that the ring is markedly flat.

Thickness as dependent upon the position of the substituted group in the ring. It is interesting to note the differences in thickness caused by a substituted group being moved from the ortho to the meta and then to the para positions. Sogani[8] was the first to notice this effect. He reported upon *o*-,*m*-, and *p*-nitro-toluene, *o*-,*m*-, and *p*-xylene. Krishnamurti[9] measured *o*-,*m*-, and *p*-toluidine, and *o*-and *m*-nitrobenzaldehyde. Herzog and Janke[10] measured *o*- and *m*-chlornitrobenzol.

Our data include four different compounds. The substitution of $2(CH_3)$ in the benzene ring with one of the CH_3 in the three positions, *o*-, *m*- and *p*, xylene, causes increases over the thickness of the ring of 0.81A, 0.65A and 0.47A, respectively. With the cyclohexane ring, similar substitutions, *o*-, *m*- and *p*-dimethylcyclohexane, the increases are 0.52A, 0.54A, and 0.39A, respectively. Using CH_3 and NH_2 in a similar manner, *o*-, *m*- and *p*-tolui-

[5] C. P. Smythe and S. O. Morgan, Jl. Am. Chem. Soc. **49**, 1030 (1927).
[6] Williams, Phys. Zeits. **29**, 683 (1928).
[7] N. K. Adam, Roy. Soc. Proc. **103**, 676 (1923).
[8] Sogani, Ind. Jl. Phys. **II**, 97 (1927).
[9] Krishnamurti, Ind. Jl. Phys. **II**, 355 (1928).
[10] Herzog and Janke, Zeits. f. Physik **45**, 194 (1927).

dine, the increases are 0.42A, 0.37A and 0.26A, respectively. With CH_3 and OCH_3, *o*-, *m*- and *p*-cresyl methyl ether, the increases are 0.80A, 0.51A and 0.16A. In each of the four cases, the para-position shows the least thickness, the meta, the next and the ortho the greatest thickness. The one exception, i.e., 0.54A, is not regarded as such because of the possible error of 0.05A. Moreover, the compounds with NH_2 show the effect more strikingly than the others, the para position causing an increase over the benzene ring thickness of only 0.2A. These substituted groups seem to lie more nearly in the plane of the ring, the farther they are separated from each other.

When three substitutions are made as in the case of the hydroxydimethyl benzenes in Table I, the situation is more complicated, but the decrease of thickness with separation plainly exists.

The above conclusions, if extended to other compounds, are not altogether in accord with those of Sogani, Krishnamurti and Herzog and Janke, referred to at the beginning of this section. The first named author shows in both of his experiments that the para compound has a less separation of planes, for the moment designated as d, than the meta. In the one case with Krishnamurti the para compound has the greatest d of the group. In the cases of the five meta compounds of the above three authors, the meta has a greater d than the ortho. In considering these results it is well to bear in mind that (1) perhaps no generalization can be made for the alteration ortho to meta, (2) there is a chance of error because of the impurity of the liquid, (3) the change in resolving power from one liquid to another coupled with the lack of monochromaticity in the x-ray beam, may produce a shift of the diffraction peak without any change in d whatever. Nevertheless, with but one exception, results of all observers to date agree in giving the para a less value of d than the meta and ortho. Referring to the results of this paper, the accuracy of measurements, the monochromaticity of the radiation, the superiority of the ionization method for the purpose, and the high consistency of results, lead the author to opine that conclusions drawn from the measurements here recorded are worthy of confidence. These conclusions are that in the four series using two substitutions, one with the cyclohexane and three with the benzene rings, the para position of the substitutions give a markedly less thickness than the ortho and meta positions, and the meta less than the ortho. From these data one may not generalize, but he may anticipate either similar results with other derivatives, or else new and interesting effects depending upon the nature of the substituents.

Orientation of polar molecules. In earlier contributions[11] the long spacing found in the alcohols and fatty acids were attributed to the pairing of the molecules. For example, in the alcohols, the two end polar OH groups were adjacent, resulting in the two molecules lying end to end in a line and parallel to other similar double molecules. A similar long spacing is found in the current results for phenol, cyclohexanol, 2-hydroxy-1,3-dimethylbenzene, 2-hydroxy-1,4-dimethylbenzene, 4-hydroxy-1,2-dimethylbenzene, and 4-hy-

[11] Stewart and Morrow, Phys. Rev. **30**, 232 (1927); Morrow, Phys. Rev. **31**, 10 (1928).

droxy 1-3 dimethylbenzene. All of these compounds are polar and the above explanation of the long spacings 10.8A, 10.8A, 11A, 11A, 13.9A and 12.1A proves to be reasonable. For assume the molecules to be grouped like the piling of disks with the flat surfaces lying in planes. By means of the molecular weight, the density and the distance of separation in direction of thickness as shown in Table I, one can readily compute the areas of the cross-section perpendicular to this direction. As an illustration, for benzene this computed area is $31.4 \times (A).^2$ If this cross-section of the molecule may be regarded roughly as hexagonal, and the hexagons are in a plane with sides in contact, then the separation of centers in the plane is 6.01A. Similar computations for the other compounds for which the densities are available, give results of a similar magnitude, e.g., cyclohexane gives 35.2 $(A).^2$ Thus one would expect that with double molecules, the doubling being in the plane of disks, the distance between planes containing diffraction centers would be 12A or more, if these planes are perpendicular to the set containing the disks. But if these sets of planes are not mutually perpendicular, then the distance of separation would be less than about 12A. It is obvious from Table I, that this doubling of molecules is precisely what happens with all the six compounds having an OH substituent. It is also to be noticed that with two of the compounds, 2 hydroxy 1-3 dimethyl benzene and 2 hydroxy 1-4 dimethyl benzene, the double molecules are only faintly in evidence Whether this is caused by a difference in number of double molecules or by differences in the diffraction effect caused by alterations in the arrangement of atomic diffraction centers, has not been examined.

These experiments, together with the preceding contributions from this laboratory show that without the polar OH, there is usually in a group of molecules, only one set of parallel and equidistant planes which can be drawn through diffraction centers. With polar molecules there is at least one other set of parallel planes and these are drawn through the pairs of OH groups. The molecules in the group of polar molecules have, in the six compounds shown in Table I, a well defined arrangement in a second set of planes. The effect of polar groups just noted is precisely that found with alcohols[12] and fatty acids,[13] and the reduction to only one spacing in the absence of the polar quality is found similarly with normal paraffins.[14] Krishnamurti[15] has measured twenty-six organic liquids and concludes that in all cases where the surface tension method (a modified Ramsay-Shields method) indicates association, there is an inner ring prominent in the diffraction halo. He reaches the same conclusion as to double molecules as given above. While the present authors do not agree with his conclusion as to an inner ring in cyclohexane and *p*-toluidine they have no reason to doubt the basis for the general conclusion.

[12] Stewart and Morrow, Phys. Rev. **30**, 232 (1927).

[13] Morrow, Phys. Rev. **31**, 20 (1928).

[14] Stewart, Phys. Rev. **32**, 153 (1928).

[15] Krishnamurti, Ind. Jl. Phys. Vol. **II**, 491 (1928).

Additional spacings. There are yet to be discussed the second distances of separation of planes in the cases of *o*-xylene, mesitylene, *o*- and *m*-toluidine, and *o*- and *m*-cresyl methyl ether. And also the corresponding third separation in 2-hydroxy-1,3-dimethyl benzene, 2-hydroxy-1,4-dimethyl benzene, 4-hydroxy-1,2-dimethylbenzene and 4-hydroxy-1,3-dimethyl benzene. The most direct explanation is that, in the first group, we are dealing with a second set of planes, and in the second group with a third set, separated by a distance of from 3.5A to 4A. If the molecules were so piled that there would be not only the first set (giving the 4.7A separation) but also another set of planes perpendicular thereto, then the separation of the second set would be a molecular dimension. But instead of this perpendicularity there may be a displacement of the molecules lying in one of the planes of the first set relative to an adjacent parallel plane, so the molecules no longer lie immediately "above" and "below" the molecules adjacent in planes. Moreover, this relative displacement may be less than a molecular dimension. Thus we may readily secure this separation of planes of the order of 3.5 to 4.0A. One may be tempted to identify this value 3.5 to 4.0A as the thickness of the rings, but the reasons that 4.7A is the thickness of a benzene ring and the smallest molecular dimension in the liquid state are as follows. (1) The corresponding peak is not only the most prominent, but also the only peak in the case of benzene. (2) The evidence given in sections, "Thickness of rings" and "Flatness of benzene and cyclohexane molecules" substantiates this view. (3) The corresponding peak is the most prominent one in all our measurements. (4) There is a corresponding peak, giving approximately the same separation in the case of the *n*-alcohols and *n*-paraffins. This gives additional confidence rather than evidence. (5) The shape of the molecule, if decidedly unsymmetrical, would, through the action of molecular forces, probably be the most potent factor in producing a semi-orderly arrangement of the molecules. For the most prominent peak would be due to the most prominent asymmetry. These reasons are emphasized because Krishnamurti[16] has found this small separation of the order of 3.5A to 4A in a number of compounds and interprets it as the thickness of the benzene ring and its derivatives. His chief reason is based on the shape of the ring as found in solid form. This additional peak at the larger angles has also been found by Sogani[8] and Herzog and Jancke,[10] but without any interpretation.

Shape of the benzene ring. Bragg,[17] Caspari,[18] Morse[19] and Mack[20] are virtually in agreement that the benzene ring in the solid state has a thickness not greater than about 3A. But this conclusion is an interpretation based on the crystalline arrangement of C in the diamond and as Caspari states, the atomic arrangement thus proposed is by no means certain. On the other hand, the measurements in this paper are direct and are limited as to re-

[16] Krishnamurti, Ind. Jl. Phys. **III,** 225 (1928).
[17] Bragg, Proc. Phys. Soc. Lond. **34,** 33 (1921).
[18] Caspari, Phil. Mag. **26,** 1276 (1927).
[19] Morse, Proc. Nat. Acad. **13,** 789 (1927).
[20] Mack, J. Amer. Chem. Soc. **47,** 468 (1925).

liability only by the validity of the method of measurement. The accumulation of evidence favors the theory of the author as to the cybotactic condition, and hence it is believed that the application of Bragg's law is justified and the measurements are worthy of confidence. The thickness of the rings as 4.7A and 5.1A may occasion some surprise, but the comparison of crystal measurements in diamond and graphite seems to restore confidence. This distance between two successive layers in the diamond is 2.05A, whereas in graphite it has been increased to 3.40.[21] This accounts for the slippage of planes in and the lubricating qualities of graphite. If the arrangement of carbon atoms in benzene and cyclohexane is in puckered planes, somewhat analogous to the arrangements in these planes in diamond, then one might reasonably expect that the separations of molecules in a liquid would be greater than 3.40A, when measured between diffracting centers. There is relatively less difference between our value of 4.7A in benzene and 3.4A in graphite than there is between 3.4A in graphite and 2.05A in diamond. Moreover, in the molecule of benzene we have in addition to the C atoms, the six H atoms. Thus, the value of 4.7A, seems a reasonable one.[22]

Our experiments give no evidence as to the detail of the shape of the benzene ring. If one conceived of liquid benzene as consisting of closely packed hexagons, then, using the value of density, these hexagons would have the same dimensions perpendicular to thickness as given by the above named crystal workers; namely, 6.0A, the distance betweeen opposite sides and 7.1A the diagonal distance. The positive evidence of the experiments can give only the result that the area of the benzene ring in a plane perpendicular to the thickness is, as indicated above, approximately 31.4 (A),^{2} and of the cyclohexane ring approximately 35.2 (A).^{2} The evidence of the double molecules in the polar compounds is compatible with the dimensions just stated. But it is well to bear in mind that the entire group of experiments emphasizes the correctness of assuming the benzene and cyclohexane rings to maintain fairly well their general shape when substitutions are made. Thus these rings may be treated as units and not as aggregates changing in a marked manner with each substitution. This is in accord with Bragg's assumption in dealing with organic compounds in the crystalline state and is of fundamental importance to the chemist.

Comparison of measurements. There is little or nothing to be gained by a comparison of the spacings reported in this paper with those obtained by other workers. There are differences in the method, theirs being photographic and ours, the ionization method. Again there is a difference in monochromaticity of the x-rays. There are also differences in the purity of the liquids. Moreover, at the present stage, we should be chiefly concerned with a comparison of results taken with one equipment.

[21] W. H. and W. L. Bragg, X-rays and Crystal Structure (1924), p. 231.

[22] Kathleen Lonsdale has just concluded [Proc. Roy. Soc. A. 792, p. 494, (1929)] that in the (solid) benzene ring, the carbons all lie in the same plane, or at least within 0.1A of the (0.01) cleavage plane.

General conclusion. The detailed conclusions are presented in the abstract of the article. Here they may be stated in a more general form. The observations are in harmony with present views of chemical structure in the flatness of the rings and in the effect of substituents in altering the thickness and in the variation caused by the position of the substituents. But very importantly, it shows that the treatment of the benzene and cyclohexane as units of structure is justified. The increased orientaion caused by double molecules in the case of an OH substituent in both the benzene and cyclohexane rings and caused by more than one substituent and their relative positions in the benzene ring, are shown. The thickness of the benzene ring in the liquid state is 4.7A, and of the cyclohexane ring is 5.1A. The cross-section of the former is about 31.4 $(A)^2$ and of the latter 35.2 $(A)^2$. All the experiments add to the general conclusion that the interpretation of the distance found by Bragg's law as the separation of molecular diffraction centers and the corresponding demonstration of the cybotactic condition of the molecules in the liquid state, are worthy of full confidence.

The author acknowledges with much appreciation the splendid skill of Mr. H. A. Zahl, research assistant, who is responsible for all the measurements herein recorded, and the cordial cooperation of Professors L. C. Raiford and J. N. Pearce of the Department of Chemistry.

PHYSICS LABORATORY,
UNIVERSITY OF IOWA,
March 20, 1929.

REPORT ON NOTATION FOR ATOMIC SPECTRA*

By H. N. Russell, A. G. Shenstone and Louis A. Turner

AT AN informal meeting of spectroscopists at Washington in April, 1928, the writers of this report were requested to draw up a scheme for the clarification of spectroscopic notation. After much discussion and correspondence with spectroscopists both in this country and abroad we are able to present the following recommendations.

The analysis of a spectrum can be of three different types. (1) A multiplet, or in many cases a level, analysis. This includes the determination of the types of terms (S, P, D, etc.), the multiplicities, and the inner quantum numbers of the individual levels when possible. (2) A configuration analysis. The description of the electron configuration with which the spectroscopic terms are to be correlated as given by Hund in his book. (3) A series analysis. The identification of series of terms and finding of their limits. A complete notation must be capable of adequately expressing the results of all three types of analysis whether complete or only partial.

Multiplet Analysis

The proposed system of notation for a multiplet analysis is nearly the same as that which is now in general use. The type of term is denoted by the letters S, P, D, etc., to correspond to the quantum number L of Hund's theory.

Letter:	S	P	D	F	G	H	I	K	L	M	N	O	Q	R	T	U	V	W	X	Y	Z
L:	0	1	2	3	4	5	6	7	8	9	10	11	12	13	14	15	16	17	18	19	20

In the case of the rare earths it appears that there may occur terms of type Z. The multiplicity is denoted by a superscript at the left, ^{1}, ^{2}, etc. for singlet, doublet, etc., terms. The inner quantum number is used as a subscript at the right, $_0$, $_1$, $_2$, etc., for odd multiplicities, and $_{\frac{1}{2}}$, $_{\frac{3}{2}}$, etc. or $_{\frac{1}{2}}$, $_{1\frac{1}{2}}$, $_{2\frac{1}{2}}$, etc., for even multiplicities. The latter form is recommended because of its typographical advantages.

In all spectra the terms may be divided into two groups, even and odd, such that the terms of one group do not combine with one another (except for "forbidden" lines) but only with those of the other group. At present these groups are distinguished by the use of primes or bars (e.g., P', $\overline{P}$) as follows.

Even terms:	S	P'	D	F'	etc.
Odd terms:	S'	P	D'	F	etc.

It is now proposed to leave all even terms unmarked and to denote all odd terms by the superscript ° (the symbol for degrees) at the right. The above terms would be written

Even terms:	S	P	D	F	G
Odd terms:	S°	P°	D°	F°	G°

There are two reasons for this suggested change.

* A limited number of reprints of this article are for sale by the Editor for thirty cents each in U. S. postage stamps.

(1) The distinction between odd and even terms has a physical basis. (The rules for determining whether a term is odd or even will be discussed below.)

(2) An unclassified level (type of term unknown) is shown to be odd or even by its combinations and can be so designated. This is not possible with the old notation.

It is suggested that, following a fairly general custom, unclassified levels be denoted by arabic numbers to which the indices for multiplicity, inner quantum number, etc., can be added when known (e.g. $^4 23_{1\frac{1}{2}}^{\circ}$). It is recommended that when such a number has once been assigned to a given level in a particular spectrum, it should not be changed until the level is classified. The number released by such a classification of a level should never be used for any other level in that spectrum.

The final result of a multiplet analysis should be expressed in two tables. First, a table giving all the energy levels, classified and unclassified, with the notation for each. In order to facilitate work by other investigators it is recommended that the odd terms be printed in heavy-faced type or in italics in this table. At least five different methods of arranging a table of terms may be found in the literature. We recommend that in this main table the individual levels be tabulated in order beginning with the lowest, irrespective of the extent to which the components of multiple terms may be intermingled. The placing together of those levels which are regarded by the author as being components of a multiple term introduces an element of individual and, perhaps, fallible judgment. It is to be avoided both for that reason and also because it obscures the overlapping of terms which may be of great theoretical importance. The typical term tables given below illustrate these points, and indicate a simple way of giving the necessary information concerning components of terms and the intervals between them. The second table should be a list of all the classified lines in the order of frequency giving for each the wave-length, wave-number, intensity, temperature-class when known, and origin, i.e., the combination between levels of the first table (the level of lower energy to be given first). For the sake of brevity it is recommended that one use as simple a notation as possible for differentiation of terms of the same type. This is usually done by prefixing lower case letters a^3D, b^3D, etc. It is not essential that the same system for assigning these letters should be used for all spectra but it *is very important* that a detailed explanation of the system should accompany every such table. It is recommended that the lowest terms and higher ones of the same type, multiplicity and parity, should be lettered a, b, c, etc., beginning with the lowest. The terms of the opposite parity of the same type and multiplicity should be labelled z, y, x, etc., beginning with the lowest. In this way all the resonance lines will be designated as $a(\ )-z(\ )$. By this scheme, lines of similar physical nature will have a similar designation. In accordance with this idea it is suggested that the letters a, b, c, d be reserved for low metastable terms and that the high terms should uniformly begin with e. It follows from the Hund theory that the number of low terms of the same character which

TABLE I. *Term table for Ag II (Part of)*

	Level			Intervals (Higher J's first)		
$5d^3S_1$	86405.0					
$5d^3G_5$	87496.6	*				
$5d^3G_4$	87509.2	*				
$5d^3P_2$	87596.3	·	*			
$5d^3P_1$	87599.8	·	*			
$5d^3D_3$	88041.1	·	·	*		
$5d^3F_3$	88320.6	·	·	·	*	
$5d^3D_2$	88353.1	·	·	*	·	
$5d^1S_0$	88356.9?	·	·	·	·	
$5d^3F_4$	88437.9	·	·	·	*	
$5d^1P_1$	91592.1	·	·	·	·	
$5d^3G_3$	92082.4	*	·	·	·	
$5d^3D_1$	92336.6		·	*	·	
$5d^1G_4$	92346.6		·		·	
$5d^1D_2$	92620.0		·		·	
$5d^3F_2$	92985.0		·		*	
$5d^1F_3$	93027.9		·			
$5d^3P_0$	93904.5?	*				

^3P	3.5	6304.7?
^3D	312.0	3983.5
^3F	−117.3	4664.4
^3G	12.6	4573.2

TABLE II. *Quartet term table for Cl III.*

A	B	C	Level	
aS	$a^4S^\circ_{1\frac{1}{2}}$	$3p^4S^\circ_{1\frac{1}{2}}$	*321936.*	
bP_1	$z^4P_{\frac{1}{2}}$	$z^4P_{\frac{1}{2}}$	222461.	*
bP_2	$z^4P_{1\frac{1}{2}}$	$z^4P_{1\frac{1}{2}}$	222806.	*
bP_3	$z^4P_{2\frac{1}{2}}$	$z^4P_{2\frac{1}{2}}$	223416.	*
$4kP_1$	$y^4P_{\frac{1}{2}}$	$4s^4P_{\frac{1}{2}}$	148200.	*
$4kP_2$	$y^4P_{1\frac{1}{2}}$	$4s^4P_{1\frac{1}{2}}$	147842.2	*
$4kP_3$	$y^4P_{2\frac{1}{2}}$	$4s^4P_{2\frac{1}{2}}$	147322.1	*
$4mD_1$	$e^4D^\circ_{\frac{1}{2}}$	$4p^4D^\circ_{\frac{1}{2}}$	*120862.6*	*
$4mD_2$	$e^4D^\circ_{1\frac{1}{2}}$	$4p^4D^\circ_{1\frac{1}{2}}$	*120604.0*	*
$4mD_3$	$e^4D^\circ_{2\frac{1}{2}}$	$4p^4D^\circ_{2\frac{1}{2}}$	*120170.9*	*
$4mD_4$	$e^4D^\circ_{3\frac{1}{2}}$	$4p^4D^\circ_{3\frac{1}{2}}$	*119568.4*	*
$4mP_1$	$e^4P^\circ_{\frac{1}{2}}$	$4p^4P^\circ_{\frac{1}{2}}$	*117914.4*	*
$4mP_2$	$e^4P^\circ_{1\frac{1}{2}}$	$4p^4P^\circ_{1\frac{1}{2}}$	*117812.0*	*
$4mP_3$	$e^4P^\circ_{2\frac{1}{2}}$	$4p^4P^\circ_{2\frac{1}{2}}$	*117394.8*	*
$4mS$	$e^4S^\circ_{1\frac{1}{2}}$	$4p^4S^\circ_{1\frac{1}{2}}$	*115997.3*	
$4nD_2$	$z^4D_{1\frac{1}{2}}$	$3d^4D_{1\frac{1}{2}}$	80363.6	*
$4nD_3$	$z^4D_{2\frac{1}{2}}$	$3d^4D_{2\frac{1}{2}}$	80250.9	*
$4nD_4$	$z^4D_{3\frac{1}{2}}$	$3d^4D_{3\frac{1}{2}}$	79889.8	*
$5kP_1$	$x^4P_{\frac{1}{2}}$	$5s^4P_{\frac{1}{2}}$	76984.5	*
$5kP_2$	$x^4P_{1\frac{1}{2}}$	$5s^4P_{1\frac{1}{2}}$	76543.6	*
$5kP_3$	$x^4P_{2\frac{1}{2}}$	$5s^4P_{2\frac{1}{2}}$	75798.8	*

Explanation of symbols

A	C	Configuration
a	$3p$	$3s^23p^3$
b	z	$3s3p^4$
$4k$	$4s$	$3s^23p^24s$
m	$4p$	$3s^23p^24p$
n	$3d$	$3s^23p^23d$
$5k$	$5s$	$3s^23p^25s$

Column A. Bowen's notation. (Phys. Rev. **31**, 34, 1928).

Column B. *Notation which would be used if the configurations were unknown or if the table were for a complicated spectrum.*

Column C. A simple abbreviated electron configuration notation which would be logical in this case.

Both A and C require an explanatory table in *every* paper in which they are used.

are observable is never likely to exceed four, though five is theoretically possible in a few cases. The use of Greek letters or other notations may be found convenient by authors under special circumstances. But we would emphasize again the desirability that a clear explanation of such an individual notation should be published in *every* paper in which it appears.

Tables I and II are given as illustrations.

Configuration Analysis

Following Hund, the individual electrons in an atom may be defined by two quantum numbers, "azimuthal" and "total." The former is expressed by use of the letters s, p, d, etc., the latter numerically in specific cases or by n in general. The following table gives the values of these quantities.

Table III. *Designation of quantum numbers.*

Literal designation	Azimuthal quantum number l	k (Bohr)	
s	0	1	The total quantum number
p	1	2	is equal to or greater than
d	2	3	$l+1$, i.e., 1, 2, 3, · · · for s
f	3	4	electrons, 2, 3, 4, · · · for p
g	4	5	electrons, etc.
h	5	6	
etc.			

An electron is characterized, for instance, as a $6p$ electron, 6 being the total quantum number, the letter p implying an l value of 1. It will be noticed that $4p$, $5s$, $3d$, etc., electrons are exactly equivalent to Bohr's 4_2, 5_1, 3_3, etc. electrons. The spin of the electron need not be specified in describing configurations. The number of electrons of a given type in an atom may be expressed by an exponent (e.g., $3d^5$). For a complete description of the relation between electronic configuration and spectroscopic terms reference should be made to Hund's book. In this connection, we recommend the use of the lower case letters n, l, s, j, m for the quantum numbers of an electron, and the capital letters L, S, J, M to designate the quantum numbers of a term (or level) of an atom, either ionized or neutral. The symbol "N" is not included because the total quantum numbers of electrons do not combine to give a resultant.

A complete specification of atomic structure in terms of electronic configuration would include all the inner electrons, e.g., for Fe in its normal state $1s^22s^22p^63s^23p^63d^64s^2$. For ordinary spectroscopic purposes only those electrons "outside" an inert gas shell need be considered. A complete np^6 group, and all the groups which are normally completed earlier in the periodic table, can be neglected. Thus the notation for the normal state of Fe becomes $3d^64s^2$. The nd^{10} groups can be ignored from Ga, In, and Tl onward, and it is

probable that the rare earth group $4f^{14}$ can be ignored for atoms beyond Hf or Ta.

An example of the notation for a level and the configuration from which it arises is $3d^6\ 4s^2\ {}^5D_4$, which represents the normal state of the iron atom. $2s^2\ 2p^3\ {}^4S^\circ_{1\frac{1}{2}}$ represents the low level of O II. For brevity, the total quantum numbers may be omitted when their values are the lowest which the particular sort of electron can have if not belonging to already completed shells. For example, $4s$, $4p$, $3d$, $4f$ in spectra from K I to Zn I and Ca II to Ga II, etc., are the s, p, d, and f electrons of lowest quantum numbers not belonging to completed groups. The $3p^6$ group is completed and the $3s^2$ and all the groups of smaller n have been previously completed, leaving $4s$, $4p$, $3d$, $4f$ still to be added. These last can therefore be represented by s, p, d and f respectively.

The normal state of Fe I would thus be designated as $d^6s^2\ {}^5D_4$, that of O II as $s^2p^3\ {}^4S^\circ_{1\frac{1}{2}}$. For Ge I, in which the electron groups $3d^{10}$ and $4s^2$ may be regarded as completed the electrons to be represented by the letters alone would be the $5s$, $4p$, $4d$, and $4f$ electrons: and so on.

Odd terms arise from the configurations for which the sum of the l values for all electrons is odd, even terms from configurations for which the l sum is even. Since the l sum for completed groups is always even, only outer uncompleted groups need be considered. Even (odd) terms are those in which the number of p and f electrons together is even (odd). In the parts of the periodic table where s and d groups are being completed the lowest terms of all the atoms are even. Where p groups are being completed (and also in the rare earth f-group) the lowest terms are alternately odd and even. Except in the rare earth group the only spectra for which the normal state corresponds to an odd term are B I, N I, F I and C II, O II, Ne II etc. and the homologous spectra in later periods.

Permitted transitions are those in which the l of one electron changes by one unit, (and the l of another electron by 0 or 2 units, if two electrons change) so that all such transitions are between even and odd terms.

Series Analysis

Series of terms arise from configurations in which one electron, keeping the same value of l, has successively higher values of n, the total quantum number. A configuration such as $3d\ 4s4p$ theoretically belongs therefore to three different series in which either the d, the s, or the p electron takes higher total quantum numbers. In practice this complication is rare as there is almost always one electron which is more easily detached than the others, and is therefore the one to take the higher quantum numbers and give the series. An electron whose total quantum number is higher than those of the electrons discussed in the last section may always be regarded as the most easily detached, as may also one belonging to a group which is not represented in the configurations giving the low terms of the spectrum.

The limiting configuration (i.e., the one obtained by the removal of the electron which takes successively higher values of n to give the series)

usually gives multiple terms. Each separate level of these terms is the limit of certain sets of the individual levels of the multiple terms converging to the limit. It is suggested that the following notation be used to indicate such series and their limits. The configuration of the limit is to be represented as above, followed in parentheses by the notation for the particular type of term which is the limit for the series under consideration, then by the "running" electron, then by the notation for the term (or particular level) given by the whole configuration. For instance, $s^2p^5(^2P^\circ)ns\,^3P^\circ$ represents the series of $^3P^\circ$ terms of Ne which converge to the $^2P^\circ$ limit, $s^2p^5(^2P^\circ_{1\frac{1}{2}})ns\,^3P^\circ_2$ represents the series of $^3P^\circ_2$ levels of those $^3P^\circ$ terms which converge to the component $^2P^\circ_{1\frac{1}{2}}$ of Ne II as limit. In this particularly simple case the use of the notation for the limit would be of little value except for extreme explicitness. In more complicated cases, however, some such notation is necessary to avoid ambiguity. For instance, the s^2p^3 configuration of O II gives $^4S^\circ$, $^2D^\circ$ and $^2P^\circ$ terms. If we add to this one np electron to get terms of O I the $^4S^\circ$ term gives ^5P and ^3P, the $^2D^\circ$ gives ^3P, ^3D, ^3F, ^1P, ^1D, ^1F and the $^2P^\circ$ gives ^3S, ^3P, ^3D, ^1S, ^1P, ^1D terms. Thus, theoretically, the $s^2p^3\,np$ configuration gives three ^3P terms, two ^3D terms, two ^1P terms and two ^1D terms. For distinguishing between them it is most convenient to use the notation suggested above. The three ^3P terms would be written $s^2p^3(^4S^\circ)np\ ^3P$, $s^2p^3(^2D^\circ)np\ ^3P$, and $s^2p^3(^2P^\circ)np\ ^2P$.

The notation described is applicable to all cases where the running electron is unlike any other in the atom. But if no such singular electron exists, the Pauli exclusion principle must be applied to the electron groups and the number of terms is reduced. A discussion of the question of whether the terms due to such a structure can be considered as series members (i.e. whether $d^{10}\ ^1S_0$ is the first series member of the $d^9md\ ^1S_0$ sequence) is beyond the purpose of this report. As far as notation is concerned two types of configuration must be considered. The first type is one in which the atom contains, outside the rare gas shell, a single group of two or more p or d or f electrons, with or without an s^2 group in addition. The terms arising from such configurations need no limit designation since the electron configuration defines them unambiguously, e.g., $d^9s^2\ ^2D$, $d^2\ ^2F$, $p^2s^2\ ^3P$, $p^5\ ^2P^\circ$ etc. The second type of configuration mentioned above is one which contains more than one group of two or more p or d or f electrons, e.g., $p^2d^2s^2$, p^3d^2, $d^4f^2s^2$. The method of dealing with such cases may be best explained by an example taken from Ti I. The configuration is $3d^24p^2$ from which there arise a great number of terms including several repetitions of the same multiplicity and name (i.e. five ^3D terms, six ^3P, etc.) which must be differentiated in the notation. The description of such sets of terms requires the specification of the term arising from the configuration d^2 and the term from the configuration p^2 which were involved in the production of the final result, i.e., we must state the terms which would result if either the p^2 or d^2 groups were removed from the atom. For instance the ^3D terms would be

$$d^2(^3F)p^2(^3P)^3D$$
$$d^2(^3P)p^2(^3P)^3D$$
$$d^2(^1D)p^2(^3P)^3D$$
$$d^2(^3F)p^2(^1D)^3D$$
$$d^2(^3P)p^2(^1D)^3D$$

It is interesting and explanatory to notice that terms of this kind belong to sequences of the type $3d^24p^2$, $3d^25p^2$, etc., which would carry an atom through two ionizations at once. Such sequences are not known to exist; but, since these first terms do exist, it is necessary to have the notation to deal with them.

The notation here suggested appears to be as simple as any that will give an adequate statement of the known relations in a complex spectrum. Indeed, it is insufficient to take into account certain complexities which are anticipated in the rare earths and even in some of the simpler spectra. These complexities arise from the fact that two or more terms of identical multiplicity and name may result from the same restricted electron configuration (e.g. two ^2D terms from d^3). But, as such terms have not as yet been found, they will not be considered here further.

When a satisfactory configuration analysis has been made, a full specification of the electrons and limits for each term should be given at least once. In many cases, perhaps in most, considerable abbreviation may be practical. In the simpler spectra, in fact, it is possible to abbreviate to such an extent that the electron structure may be used throughout a paper without becoming too cumbersome for reading or for printing. But it is emphasized that no paper should contain such abbreviations without a table giving the complete notation for which they are substituted.

It is obviously out of the question to use the complete notation in the analysis of a complex spectrum, especially in the extensive term and wavelength tables. In such cases it is recommended that, when the electron configurations are known, two additional tables be included in the paper; one giving against the arbitrary designations, such as a ^3D, the specifications of the electron configurations as outlined above; and a second table giving the electron configurations in some structural order and the terms of the spectrum arising from them.

We should like to take this opportunity to thank our critics for their helpfulness in calling out attention to points which we had neglected and in suggesting different and more acceptable methods than those we originally proposed for dealing with some of these matters. The following physicists have contributed to the discussion of this subject either in conversation or by correspondence: E. Back, I. S. Bowen, Keivin Burns, M. A. Catalan, K. K. Darrow, T. L. de Bruin, A. Fowler, R. C. Gibbs, S. Goudsmit, W. Grotrian, F. Hund, C. C. Kiess, R. De L. Kronig, O. Laporte, A. B. McLay, J. E. Mack, W. F. Meggers, F. Paschen, W. Pauli, A. E. Ruark, A. Sommerfeld, J. T. Tate, H. C. Urey, H. E. White.

PRINCETON UNIVERSITY,
February 25, 1929.

THE SECOND SPARK SPECTRUM OF SULPHUR, S III

By S. B. Ingram*

Abstract

Analysis of the sulphur III spectrum.—With experimental data previously obtained the spectrum of sulphur III is analyzed. Most of the triplet terms predicted by the Hund theory are found and the strongest lines in both the visible and extreme ultra-violet regions are classified. The ground term $3s^2 3p^2\ ^3P_0$ gives the ionization potential as 34.9 ± 0.4 volts. Complete term tables and a list of classified lines are given. The term $3s^2 3p \cdot 4s\ ^3P$ is anomalous, having a total separation of 450 while the p doublet of the ion is 950. The interval ratio of this term is 10 to 1, instead of the 2 to 1 give by Landé's rule. Combinations of this term with the ground term in the extreme ultra-violet are unusually weak.

IN A preceding paper[1] the spectrum of singly ionized sulphur was analyzed. With the same data it has been possible to classify most of the strong lines in the spectrum of the doubly ionized atom. Recently Gilles[2,3] has published a classification of most of the strong lines of the sulphur III spectrum in the visible and ordinary ultra-violet regions. Except for a few minor points our work is in agreement but as there are several very irregular features in the spectrum it seems worth while to repeat that part of the work which overlaps, particularly as, in these two analyses, two entirely different sets of experimental data were used. In addition to the identifications published by Gilles this paper includes a number of new terms. Most of these new identifications were made possible by the investigation of the extreme ultra-violet part of the spectrum.

The experimental work is described in the paper to which reference has been made.[1] Above 2000A two sets of data were employed. The strongest lines were photographed with a 7-meter concave grating in a Rowland mounting. The wave-lengths of the lines measured by this method are probably accurate to 0.02A. As only a few lines appeared on the plates below 3000A the spectrum in the ultra-violet was photographed with a Hilger quartz spectrograph E2. The wave-lengths determined by this instrument may be in error by 0.1 or 0.2A. The extreme ultra-violet spectrum was measured with a vacuum spectrograph with a grating of 1 meter radius. The probable error in these measurements is about 0.03A.

Term Values

The spectrum of sulphur III is built up on the sulphur IV ion which has for its ground configuration[4] a ^2P term with a separation of 950. Addition of another electron gives a singlet system and a triplet system. All the

* National Research Fellow.

[1] Ingram, Phys. Rev. **32**, 172 (1928).

[2] Gilles, Comptes Rendus **188**, 63 (1929).

[3] Gilles, Comptes Rendus **188**, 320 (1929).

[4] Millikan and Bowen, Phys. Rev. **25**, 600 (1925).

identifications so far made belong to the latter. Table I gives the terms expected according to the Hund theory. Terms which have been found are printed in bold face in the table.

TABLE I. *Predicted terms of S III.* Terms in bold face have been identified.

Electron Configuration	Prefix		Terms	
$3s^2 3p^2$	a		^3P	$^1D\ ^1S$
$3s3p^3$	b	^5S	$^3S\ ^3P\ ^3D$	$^1P\ ^1D$
$3s^2 3p \cdot 3d$	$3d$		$^3P\ ^3D\ ^3F$	$^1P\ ^1D\ ^1F$
$3s^2 3p \cdot 4s$	$4s$		^3P	^1P
$3s^2 3p \cdot 4p$	$4p$		$^3S\ ^3P\ ^3D$	$^1S\ ^1P\ ^1D$
$3s^2 3p \cdot 4d$	$4d$		$^3P\ ^3D\ ^3F$	$^1P\ ^1D\ ^1F$
$3s^2 3p \cdot 4f$	$4f$		$^3D\ ^3F\ ^3G$	$^1D\ ^1F\ ^1G$
$3s^2 3p \cdot 5s$	$5s$		^3P	^1P

TABLE II. *Term values of S III.*

	$3s^2 3p^2$			$3s^2 3p \cdot 4p$	
a^3P_0	282752		$4p^3D_1$	112976.05	
		300			297.30
a^3P_1	282452		$4p^3D_2$	112678.75	
		535			581.71
a^3P_2	281917		$4p^3D_3$	112097.04	
	$3s3p^3$		$4p^3P_0$	110114.68	
					154.50
b^3D_1	198729		$4p^3P_1$	109960.18	
		28			405.88
b^3D_2	198701		$4p^3P_2$	109554.30	
		51			
b^3D_3	198650		$4p^3S_1$	108709.76	
b^3P_0	[183978]not resolved from P_1			$3s^2 3p \cdot 3d$	
		-6			
b^3P_1	183984		$3d^3D_1$	135195.60	
		-19			140.69
b^3P_2	184003		$3d^3D_2$	135054.91	
					53.39
b^3S_1	144686		$3d^3D_3$	135001.52	
	$3s^2 3p \cdot 4s$		$3d^3P_0$	139650.11	
					20.20
$4s^3P_0$	136049.72		$3d^3P_1$	139629.91	
		40.24			7.82
$4s^3P_1$	136009.48		$3d^3P_2$	139622.09	
		409.48			
$4s^3P_2$	135600.00			$3s^2 3p \cdot 4d$	
	$3s^2 3p \cdot 5s$		$4d^3F_2$	78167.11	
					491.86
$5s^3P_0$	72972.6		$4d^3F_3$	77675.25	
		152.7			489.92
$5s^3P_1$	72819.9		$4d^3F_4$	77185.33	
		771.5			
$5s^3P_2$	72048.4		$4d^3D_1$	76207.13	
					132.74
			$4d^3D_2$	76074.39	
					239.36
			$4d^3D_3$	75835.03	
			Term combining with a^3P		
			x	145905	

Gilles, in his paper, gives the value of the $4s^3P_2$ term as 135,600 which value has apparently been determined by means of a Rydberg formula from the two terms $4s^3P_2$ and $5s^3P_2$. According to Hund's theory of convergence to limits these terms go to the $^2P_{3/2}$ limit and hence Gilles' values are probably about 1000 too great when referred to the most stable state of S IV. However as the absolute values of the terms may be in error by an amount as great as this Gilles' value of $4s^3P_2$ has been adopted and the other terms evaluated on this basis.

Table II gives a complete list of term values. The P_1 and P_0 terms which I have assigned to the $s^2p.5s$ configuration Gilles has assigned to $s^2p.4d$.

TABLE III. *Classified lines of S III in the visible and ordinary ultra-violet regions.*

Int.	λ I.A. Air	ν	Triplets	Int.	λ I.A.Air	ν	Triplets
*R*0	4527.96	22078.83	$3dD_2-4pD_1$*	*Q*4	3234.17	30911.0	$3dP_2-4pS_1$
*R*0	4499.29	22219.52	$3dD_1-4pD_1$*	*Q*3	3233.24	30919.8	$3dP_1-4pS_1$
*R*2	4478.48	22322.76	$3dD_3-4pD_2$*	*Q*3	3231.10	30940.3	$3dP_0-4pS_1$
*R*1	4467.83	22375.97	$3dD_2-4pD_2$*	*Q*3	3185.16	31386.5	$4pP_2-4dF_3$
*R*4	4439.88	22516.83	$3dD_1-4pD_2$*	*Q*3	3136.00	31878.6	$4pP_2-4dF_3$
*R*2	4418.87	22623.89	$4sP_2-4pD_1$*	*Q*6	2985.98	33480.1	$4pP_2-4dD_2$*
*R*5	4364.74	22904.46	$3dD_3-4pD_3$*	*R*4	2964.80	33719.27	$4pP_2-4dD_3$*
*R*7	4361.54	22921.26	$4sP_2-4pD_2$*	*R*0	2961.83	33753.08	$4pP_1-4dD_1$*
*R*5	4354.57	22957.95	$3dD_2-4pD_3$*	*R*3	2950.23	33885.79	$4pP_1-4dD_2$*
*R*5	4340.29	23033.48	$4sP_1-4pD_1$*	*R*2	2948.34	33907.51	$4pP_0-4dD_1$*
*R*7	4332.72	23073.73	$4sP_0-4pD_1$*	*Q*6	2904.31	34421.5	$4pD_3-4dF_3$
*R*8	4284.99	23330.73	$4sP_1-4pD_2$*	*R*0	2896.71	34511.83	$4pD_2-4dF_2$
*R*10	4253.59	23502.96	$4sP_2-4pD_3$*	*R*2	2872.00	34808.75	$4pD_1-4dF_2$
*R*5	3985.97	25080.92	$3dD_1-4pP_0$*	*R*5	2863.53	34911.71	$4pD_3-4dF_4$
*R*7	3983.76	25094.84	$3dD_2-4pP_1$*	*R*4	2856.02	35003.50	$4pD_2-4dF_3$
*R*4	3961.55	25235.53	$3dD_1-4pP_1$*	*Q*4	2797.39	35737.1	$4pS_1-5sP_0$*
*R*9	3928.59	25447.25	$3dD_3-4pP_2$*	*Q*6	2785.49	35889.8	$4pS_1-5sP_1$
*R*0	3920.37	25500.60	$3dD_2-4pP_2$*	*Q*1	2778.82	35975.9	bS_1-4pS_1?
*R*4	3860.64	25895.13	$4sP_1-4pP_0$*	*Q*5	2775.25	36022.2	$4pD_3-4dD_2$*
*R*8	3838.32	26045.70	$4sP_2-4pP_2$*	*Q*8	2756.89	36262.1	$4pD_3-4dD_3$*
*R*5	3837.79	26049.30	$4sP_1-4pP_1$*	*Q*5	2741.01	36472.1	$4pD_2-4dD_1$*
*R*5	3831.87	26089.54	$4sP_0-4pP_1$*	*Q*7	2731.10	36604.4	$4pD_2-4dD_2$*
*R*6	3794.70	26345.09	$3dD_2-4pS_1$*	*Q*7	2726.82	36661.9	$4pS_1-5sP_2$*
*R*5	3778.91	26455.17	$4sP_1-4pP_2$*	*Q*5	2721.40	36734.9	$4pP_2-5sP_1$*
*R*1	3774.54	26485.80	$3dD_1-4pS_1$*	*Q*7	2718.88	36769.0	$4pD_1-4dD_1$*
*R*3	3750.74	26653.86	$3dP_1-4pD_1$*	*Q*2	2713.28	36844.8	$4pD_2-4dD_3$*
*R*5	3747.90	26674.05	$3dP_0-4pD_1$*	*Q*2	2709.03	36902.6	$4pD_1-4dD_2$*
*R*7	3717.77	26890.23	$4sP_2-4pS_1$*	*Q*5	2702.76	36988.3	$4pP_1-5sP_0$*
*R*2	3710.44	26943.34	$3dP_2-4pD_2$*	*Q*5	2691.68	37140.5	$4pP_1-5sP_1$*
*R*6	3709.37	26951.12	$3dP_1-4pD_2$*	*Q*4	2680.47	37295.8	$4pP_0-5sP_1$*
*R*5	3662.00	27299.73	$4sP_1-4pS_1$*	*Q*7	2665.40	37506.7	$4pP_2-5sP_2$*
*R*3	3656.61	27339.97	$4sP_0-4pS_1$*	*Q*4	2636.88	37912.3	$4pP_1-5sP_2$*
*R*6	3632.03	27524.99	$3dP_2-4pD_3$*	*Q*7	2508.15	39858.1	$4pD_2-5sP_1$*
*R*4	3387.12	29515.16	$3dP_1-4pP_0$*	*Q*6	2499.08	40002.7	$4pD_1-5sP_0$*
*R*4	3370.37	29661.84	$3dP_2-4pP_1$*	*Q*6	2496.24	40048.1	$4pD_3-5sP_2$*
*R*3	3369.47	29669.76	$3dP_1-4pP_1$*	*Q*5	2489.59	40155.2	$4pD_1-5sP_1$*
*R*4	3367.18	29689.94	$3dP_0-4pP_1$*	*Q*5	2460.50	40629.9	$4pD_2-5sP_2$*
*R*6	3324.85	30067.92	$3dP_2-4pP_2$*	*Q*1	2442.62	40927.3	$4pD_1-5sP_2$*
*R*4	3323.99	30075.70	$3dP_1-4pP_2$*				

* Identified by Gilles.

The P_2P_0 separation of the $s^2p.5s$ term should be slightly less than 950, the doublet separation of the ion, and the separation of the P_2P_0 terms here found is 924. This, together with the fact that the members of the multiplets

follow the intensity rules nicely, supports the present assignment. In addition to these terms Gilles has found two others, P_2 which he assigns to $s^2p.4d$ and P_1 which he assigns to $s^2p.5s$. Each of these terms is identified on the basis of only two combinations and as the values of the terms, calculated from these combinations, differ by rather more than would be expected from the accuracy of the data they have been omitted from the table.

The ground term, $3s^23p^2\ {}^3P_0$, has a value of 282,752. This gives an ionization potential for the sulphur III ion of 34.9 volts. As the absolute values of the terms are uncertain to the extent of several thousand units this value may be in error by 0.3 or 0.4 volts. Gilles[3] has suggested that the PP' group at 850A which Bowen and Millikan[5] have assigned to S V may be a^3P-4s^3P of S III, since one of the P' separations is very near to the $4s^3P_2P_1$ separation. The present data in the extreme ultra-violet, however, show that this reassignment is not necessary. Furthermore the group at 850A, $3s3p^3P-3p^2\ {}^3P$, is in an iso-electronic sequence and is given additional support by the closeness with which it follows the irregular doublet law.

Classified Lines

Tables III and IV give a complete list of the classified lines in S III. Many of the combinations among the high terms have been identified by

Table IV. *Classified lines of S III in the extreme ultra-violet region.*

Int.	λ I.A. Vac.	ν	Triplets	Int.	λI.A. Vac	ν	Triplets
0	1390.67	71907.7	bP_2-4pD_3	2	735.24	136011	aP_2-x
0	1343.53	74430.7	bP_1-4pP_2	2	732.36	136546	aP_1-x
0	1343.25	74446.3	bP_2-4pP_2	0	730.74	136848	aP_0-x
0	1328.52	75271.5	bP_1-4pS_1, bP_0-4pS_1	3	728.69	137233	aP_2-bS_1
				3	725.86	137767	aP_1-bS_1
0	1328.12	75294.5	bP_2-4pS_1	3	724.29	138067	aP_0-bS_1
0	1202.10	83187.7	aP_2-bD_1	(masked by 702 O III)			aP_2-3dP_2, aP_2-3dP_1
2	1201.71	83214.9	aP_2-bD_2				
4	1200.97	83266.2	aP_2-bD_3	3	700.29	142798	aP_1-3dP_0
3	1194.40	83724.0	aP_1-bD_1	3	700.15	142827	aP_1-3dP_1, aP_1-3dP_2
4	1194.02	83750.9	aP_1-bD_2				
2	1190.17	84021.8	aP_0-bD_1	2	698.73	143118	aP_0-3dP_1
0	1166.13	85753.9	bD_1-4pD_1	0	685.35	145911	aP_2-4sP_1
1	1162.52	86020.0	bD_2-4pD_2	1	683.47	146312	aP_2-4sP_2
2	1155.34	86554.8	bD_3-4pD_3	0	683.07	146398	aP_1-4sP_0
1	1126.85	88743.1	bD_2-4pP_1	1	681.50	146735	aP_0-4sP_1, aP_2-3dD_1
0	1126.48	88772.1	bD_1-4pP_1				
2	1122.42	89093.2	bD_3-4pP_2				aP_1-4sP_2, aP_2-3dD_2
2	1021.32	97912.7	aP_2-bP_2	2	680.95	146853	
1	1021.10	97933.6	aP_2-bP_1	2	680.69	146910	aP_2-3dD_3
1	1015.76	98448.1	aP_1-bP_2	2	679.11	147252	aP_1-3dD_1
2	1015.51	98472.9	aP_1-bP_1, aP_1-bP_0	2	678.46	147392	aP_1-3dD_2
				2	677.75	147548	aP_0-3dD_1
3	1012.49	98766.7	aP_0-bP_1	0	485.22	206092	aP_2-4dD_2
				0	484.58	206365	aP_1-4dD_2

Gilles and these have been marked with an asterisk (*). The stronger lines, which have been measured on the large Rowland grating, are dis-

[5] Bowen and Millikan, Phys. Rev. **25**, 591 (1925).

tinguished by a capital *R* placed in the column of the intensities, and the frequencies of these lines are given to two decimals. The weaker lines, which were obtained only on the quartz spectrograph, are marked with a capital *Q*, and the frequencies given to one decimal. All such lines are to be considered as weaker than the *R O* lines and this fact must be borne in mind when intensities are being compared.

The line 3860.64 was previously classified as belonging to the sulphur II spectrum. Lines are predicted from the term values in S II and S III at 3860.61 and 3860.69, respectively, too close to be resolved, so that this line is doubtless a blend.

The line 2665.40 is identified as $4p^3P_2-5s^3P_2$. Bowen and Millikan[5] have identified this line as $4s^3S_1-4p^3P_0$ of S V and have used it to fix the $4p^3P_0$ level. As no other combinations with this level were observed the present identification may throw some doubt on the $4p^3P_0$ term of S V. The present assignment is very certain since five other combinations confirm it.

Discussion

There are several very irregular features in this spectrum. The principal ones of these are connected with the $3s^23p.4s^3P$ term. Goudsmit[6] has developed the theory of multiplet separations. In this theory certain Γ values are defined which represent the energy differences between the various levels and the center of gravity of the multiple term. Also a Γ sum rule is formulated which states that "the sum of all Γ values belonging to a definite value of j is independent of the coupling." Now when we add an *s* electron to an ion in a ^2P state we get four levels, one with $j=2$, two with $j=1$, and one with $j=0$, and it follows from the Γ sum rule, as Goudsmit states in his paper, that "the separation of the *s* levels with $j=2$ and $j=0$ is exactly constant through the whole series of levels, and equal to the *p* doublet of the ion."* This condition should hold quite independently of the type of coupling between the electrons. The remarkable accuracy with which it usually holds is well illustrated by the case of the *s* levels in neon as has been pointed out by Goudsmit and Back.[7] Table V *A* illustrates this case. In Table V *B* are collected all the data which are available on the total separations of the s^3P terms of the spectra iso-electronic with S III, together with the doublet separations of the corresponding ions. It is at once obvious that the $4s^3P$ term of S III is anomalous, the separation being about one half of that which would be expected. The second term of the series appears to be perfectly regular.

This calls to mind a somewhat analogous case in the spectrum of N I. The ground state of the N II ion is a ^3P term of total separation 132.[8] Addition of an *s* electron gives a series of ^4P terms and a series of ^2P terms of which several members are known through the recent work of Compton

[6] Goudsmit, Phys. Rev. **31**, 946 (1928).

* Actually the screening effect of the added *s* electron may cause this total separation to be somewhat smaller. This is clearly illustrated by the data in Table V.

[7] Goudsmit and Back, Zeits. f. Physik **40**, 530 (1927).

[8] Bowen, Phys. Rev. **29**, 231 (1927).

and Boyce.[9] The theory of Goudsmit and Humphreys[10] predicts for this case, ^4P terms with total separation 117, and ^2P terms with separation 88. The comparison of the calculated and observed values is shown in Table V *C*. Here, again, the first member of the series, the $3s^4P$ term shows a marked deviation.

It should be remarked however that there is an essential difference between this case and that occurring in S III. In the N I case we have one level with $j=5/2$ and two with $j=1/2$, and the Γ sum rule may not be applied to predict the total separation of the ^4P term. Hence this separation is not independent of the coupling and it is only justified to apply the theory

TABLE V.

A. *Difference of levels with $j=2$ and $j=0$ in Neon I.*

Configuration	$j=2-j=0$	Configuration	$j=2-j=0$
$3s$	776.80	$9s$	780.73
$4s$	—	$10s$	779.95
$5s$	778.16	$11s$	780.16
$6s$	781.34	—	—
$7s$	780.13		
$8s$	780.98	Ne II $^2P_{3/2,}-^2P_{1/2,}$	782 ± 3

B. *Total separation of s^3P terms.*

Terms	Si I	P II	S III	Cl IV
$4s^3P_0-4s^3P_2$	275	527	450	1446
$5s^3P_0-5s^3P_2$	283	546	924	—
—	—	—	—	—
$^2P_{1/2,}-^2P_{3/2,}$ in ion	287	560	950	1495

C. *Total separation of s^4P and s^2P terms in N I.*

Terms	Obs.	Calc.	Terms	Obs.	Calc.
$3s^4P_{1/2}-3s^4P_{5/2}$	81	117	$3s^2P_{1/2}-3s^2P_{3/2}$	83	88
$4s^4P_{1/2}-4s^4P_{5/2}$	118	117	$4s^2P_{1/2}-4s^2P_{3/2}$	83	88
$5s^4P_{1/2}-5s^4P_{5/2}$	114	117	$5s^2P_{1/2}-5s^2P_{3/2}$	76	88
$6s^4P_{1/2}-6s^4P_{5/2}$	117	117			

in case that the electrons are coupled according to the Russell-Saunders scheme. In S III however we have only one level with $j=2$ and one with $j=0$, and hence the total separation should be quite independent of the type of coupling.

Not only is the total separation of the $4s^3P$ term irregular, but the interval ratio is 409:40 or about 10 to 1 instead of the normal 2 to 1. A further abnormality occurs in the weakness of the combinations of this term with the ground term a^3P. Ordinarily, in other light elements, these lines are among the strongest in the whole extreme ultra-violet spectrum. A glance at the classified lines in Table IV shows, however, that they are here com-

[9] Compton and Boyce, Phys. Rev. **33**, 145 (1929).

[10] Goudsmit and Humphreys, Phys. Rev. **31**, 960 (1928).

paratively weak. The combination of a^3P with $4s^3P$ falls between those with $3d^3P$ and $3d^3D$ and is much weaker than either of the other multiplets.

It is, perhaps, worth remarking that the line $4s^3P_2-4p^3P_1$ is either entirely missing or else very weak. Gilles gives the line 3899.27 this designation but as it lies about 0.2A from the predicted position the identification is doubtful. In any case the intensity is only 1 on my scale while the other lines of the multiplet range from 4 to 8.

Bowen [11, 12] has identified the combinations of a^3P with $3d^3D$ and $3d^3P$ in P II and Cl IV which are iso-electronic with S III. Table VI gives the wave-numbers of the strongest lines of these multiplets. These should follow the irregular doublet law and the fact that the deviations are very large may indicate that some of the identifications need revision. The terms $3d^3D$ and $3d^3P$ seem quite certain in S III since they combine not only with a^3P but also with $4p^3S$, ^3P and ^3D.

TABLE VI. *Irregular doublets.*

Terms	P II		S III		Cl IV
$a^3P_2-3d^3D_3$	103726		146910		165401
		43184		18491	
$a^3P_2-3d^3P_2$	109823		142290		180735
		32467		38445	

In conclusion I wish to acknowledge the use of certain unpublished data of Dr. I. S. Bowen and to express my thanks to Dr. S. A. Goudsmit and Dr. O. Laporte for their helpful discussion. The experimental part of this work and a large part of the analysis were done at the California Institute of Technology and the remainder has been completed at the Univeristy of Michigan while the writer has been under appointment as a National Research Fellow.

DEPARTMENT OF PHYSICS,
UNIVERSITY OF MICHIGAN,
March, 1929.

Noted added to proof, April 24, 1929.—Considering the irregularity of the $4s^3P$ term it seems wise to add a few words giving the reasons for the indentification. These reasons are briefly as follows: (1) The position in the spectrum at which the multiplets involving the $4s^3P$ term should fall can be predicted from the iso-electronic spectrum of P II and also by analogy with the spectra of other elements in this part of the periodic table. The observed term agrees with these predictions to within about 1000 wave-numbers. (2) The three levels assigned to this term are undoubtedly real as can readily be seen from the number of combinations they give with $4p^3(SPD)$ and a^3P. There are no other levels to be expected in this region according to the Hund theory except those from the $s^3p\cdot 3d$ configuration. Of these ^3P and ^3D are found and ^3F could not possibly give the combinations given by the levels in question. By exclusion, therefore, the levels are assigned to $4s^3P$. (3) The $4s^3P$ level should combine with $4p^3(SPD)$ to give some of the strongest multiplets in the whole spectrum while among the unidentified lines are only three of intensity greater than 4. The multiplets involving $4s^3P$ are much stronger than this as can be seen from Table III.

[11] Bowen, Phys. Rev. **29**, 510 (1927).
[12] Bowen, Phys. Rev. **31**, 34 (1928).

SPECTRAL RELATIONS BETWEEN CERTAIN ISO-ELECTRONIC SYSTEMS AND SEQUENCES, PART III; Ti I, V II, Cr III, Mn IV, AND Fe V

By H. E. White

Abstract

Spectral relations between the iso-electronic systems, Ti I, V II, Cr III, Mn IV, and Fe V.—The removal of, one valence electron from neutral vanadium, two valence electrons from neutral chromium, three valence electrons from neutral manganese, and four valence electrons from neutral iron forms with neutral titanium the five iso-electronic systems Ti I, V II, Cr III, Mn IV, and Fe V.

The irregular doublet law.—The irregular doublet law, wherever applicable, proves to be a powerful method of attack in attempting to analyze the spectra arising from ionized atoms. In this report for the electron transition $3d^34p$ to $3d^34s$ about forty lines, and for the electron transition $3d^34d$ to $3d^34p$ about twelve lines, have been traced through the first three elements Ti I, V II and Cr III. In the first electron transition the multiplet $^5F'-{}^5G'$ has been traced as far as Fe V.

Term separations, The Landé interval rule, and Hund's rule.—The systematic increase in term separations is given for the $^5F'$ and $^5G'$ terms arising from the electron configurations $3d^3\ 4s$ and $3d^3\ 4p$ respectively. For these same terms the Landé interval rule is found to be in general agreement with observed separations. Hund's rule for relative term positions is followed for the terms thus far identified.

Energy levels and the Moseley law.—A new type of energy level Moseley diagram for Ti I to Fe V is compared with a similar diagram for the three sequences starting respectively with Sc I, Ca I, and K I. These four diagrams together with a similar diagram for V I, V II, V III, V IV, and V V are found to be almost identical. The constancy in the values of $\Delta\lambda$ between the diagonal lines of certain multiplets is traced through the first five elements of each of the four iso-electronic sequences starting with Ti I, Ca I, Sc I and K I.

THE neutral atoms of titanium, vanadium, chromium, manganese, and iron contain four valence electrons, $3d^24s^2$, five valence electrons, $3d^34s^2$, six valence electrons, $3d^54s$, seven valence electrons, $3d^54s^2$, and eight valence electrons, $3d^64s^2$, respectively. The removal of one of these electrons from vanadium, two from chromium, three from manganese, and four from iron, forms with neutral titanium the five iso-electronic systems Ti I, V II, Cr III, Mn IV, and Fe V.

Neutral titanium, Ti I. Identifications of singlet, triplet, and quintet terms and multiplets in the spectra of neutral titanium have been made by several investigators.[1] The most complete analysis, however, has been given by Russell[2] in which he has classified some 1400 lines involving about 364 energy levels.

Singly ionized vanadium, V II. The identification of a number of terms and multiplets in the first spark spectrum of vanadium, V II, has been

[1] Kiess and Kiess, Proc. of Wash. Acad. Sci. **13**, 270 (1923); Jour. Opt. Soc. Amer. **8**, 607 (1924). Gieseler and Grotrian, Zeits. f. Physik **25**, 342 (1924).

[2] Russell, Astrophys. J. **66**, 347–438 (1927).

made by Meggers.[3] Most of these terms arise from the three lowest electron configurations in the singly ionized atom, $3d^4$, $3d^3 4s$, and $3d^3 4p$.

In a previous report on the sequence of iso-electronic systems Sc I to Mn V[4] the quartet multiplet $^4F' - {}^4G'$ $(3d^2 4s - 3d^2 4p)$, following very closely the irregular doublet law, was found to be displaced to higher frequencies by approximately 12,000 cm^{-1} in going from one element to the next, (Fig. 7[4] in the previous report). It was also found that the quartet multiplet $^4G' - {}^4H'$ $(3d^2 4p - 3d^2 4d)$ was displaced to higher frequencies by approximately 20,000 cm^{-1} in going from one element to the next. In the sequence of iso-electronic systems starting with Ti I the multiplet $^5F' - {}^5G'(3d^3 4s - 3d^3 4p)$ in going from Ti I to V II has been displaced to higher frequencies by approximately 12,000 cm^{-1}. By analogy with the preceding sequence it was predicted that the multiplet $^5G' - {}^5H'(3d^3 4p - 3d^3 4d)$ in going from Ti I to V II would be displaced to higher frequencies by some 20,000 cm^{-1}. This prediction is verified by the finding of the multiplet $^5G' - {}^5H'$ in the spark spectrum of vanadium, V II, approximately 20,000 cm^{-1} higher than the corresponding multiplet in Ti I. The wave-lengths, relative intensities, and frequencies of the lines thus identified are given in multiplet form in Table XVI. The term values given in the table have been computed from the lowest term in the spectrum $^5D_0(3d^4)$ taken as zero.[3]

TABLE XVI. *Singly ionized vanadium, V II.*
$^5G' - {}^5H'$ $(3d^3 4p - 3d^3 4d)$

		$^5G_6'$ 290 35483.3	$^5G_5'$ 247 35192.9	$^5G_4'$ 201 34946.3	$^5G_3'$ 153 34745.5	$^5G_2'$ 34592.5
		100*n* 2664.19				
$^5H_7'$	73018.1	37534.8				
	182.	20*n* 2677.20	90*n* 2656.57			
$^5H_6'$	72835.6	37352.5	37642.6			
	157.	2?*n* 2688.39	20*n* 2667.66	80*n* 2650.24		
$^5H_5'$	72678.8	37197.0	37486.0	37732.4		
	129.		2?*n* 2676.86	20*n* 2659.32	70*n* 2645.21	
$^5H_4'$	72549.7		37357.2	37603.5	37804.2	
	102.			?	20*n* 2652.36	60*n* 2641.74
$^5H_3'$	72446.1			37501.5	37702.3	37853.8

Doubly ionized chromium, Cr III. Applying the irregular doublet law to the spectra of Ti I and V II, Gibbs and White[5] were able to identify the quintet multiplet $^5F' - {}^5G'$ arising from the electron transition $3d^3 4p$ to

[3] Meggers, Zeits. f. Physik **33**, 509 (1925); **39**, 114 (1926).
[4] White, Phys. Rev. **33**, 681 (1929).
[5] Gibbs and White, Proc. Nat. Acad. Sci. **13**, 525 (1927).

$3d^34s$ in doubly ionized chromium, Cr III. With the ${}^5G'_{2,3,4,5,6}(3d^34p)$ term separations thus known the ${}^5G'-{}^5H'(3d^34p-3d^34d)$ multiplet (using again the irregular doublet law) was predicted and identified approximately 20,000 cm^{-1} higher than the corresponding multiplet in V II.

The triad of triplet terms ${}^3D'$, ${}^3F$, ${}^3G'(3d^34p)$ are found to combine strongly with b^3F' of $3d^34s$ and with a ${}^3F'$ and ${}^3G'$ of $3d^4$. The latter electron configuration gives the lowest terms in the spectrum, the ${}^5D_{0,1,2,3,4}$, terms of which have not yet been definitely identified. The relative term values for Cr III are given in Table XVII. Since the lowest terms, ${}^5D(3d^4)$ and intercom-

TABLE XVII. *Term values of doubly ionized chromium, Cr III*

Triplet Terms					Quintet Terms				
Config. (Limit)	Term	Value	Combinations	$(\nu)^{1/2}$	Config. (Limit)	Term	Value	Combinations	$(\nu)^{1/2}$
	a^3F_2'	19000	${}^3D', F$			${}^5F_1'$	50000	${}^5G', {}^5F$	
		56					136		
	a^3F_3'	19056	${}^3G'$			${}^5F_2'$	50136		
$3d^4$		75			$3d^34s$		200		
	a^3F_4'	19131		472		${}^5F_3'$	50336		
$(3d^3)$					$(3d^3)$		263		
$({}^4F')$	${}^3G_3$	21250	${}^3F, {}^3G'$		$({}^4F')$	${}^5F_4'$	50559		
		148					319		
	${}^3G_4$	21398				${}^5F_5'$	50918		438
		146							
	${}^3G_5$	21544		469		${}^5G_2'$	94273	${}^5F'$	
							264		
	b^3F_2'	57194	${}^3D', {}^3F$			${}^5G_3'$	94537		
$3d^34s$		342					347		
	b^3F_3'	57536	${}^3G'$			${}^5G_4'$	94884		
$(3d^3)$		430					425		
${}^4F'$	b^3F_4'	57966		429		${}^5G_5'$	95309		
							504		
	${}^3D_1'$	97621	a^3F', b^3F'		$3d^34p$	${}^5G_6'$	95813		383
		228							
	${}^3D_2'$	97849			$(3d^3)$	${}^5F_1$	97281	${}^5F'$	
		378					147		
	${}^3D_3'$	98227		379	$({}^4F')$	${}^5F_2$	97428		
							200		
	${}^3G_3'$	100384	$a^3F', {}^3G$			${}^5F_3$	97628		
$3d^34p$		259					239		
	${}^3G_4'$	100643	b^3F'			${}^5F_4$	97867		
$(3d^3)$		323					259		
$({}^4F')$	${}^3G_5'$	100966		375		${}^5F_5$	98126		380
	${}^3F_2$	101988	$a^3F', {}^3G$			${}^5H_3'$	152694	${}^5G'$	
		302					184		
	${}^3F_3$	102290	b^3F'			${}^5H_4'$	152878		
		354			$3d^34d$		229		
	${}^3F_4$	102644		373		${}^5H_5'$	153107		
					$(3d^3)$		280		
					$({}^4F')$	${}^5H_6'$	153387		
							323		
						${}^5H_7'$	153710		298

binations between triplet and quintet terms have not been identified with certainty, absolute term values have not been given in the table. For convenience only the $a^3F'_2(3d^4)$ term has been taken to be 19,000 cm^{-1}, and the ${}^5F_1'(3d^34s)$ taken to be 50,000 cm^{-1}, above the ${}^5D_0(3d^4)$ term. The values

of $(\nu)^{1/2}$ given in the fifth and tenth columns of this table are taken with respect to $^4F_5'(3d^3)$ of the once more ionized atom, and were obtained from an extrapolation of a Moseley diagram. The wave-lengths, relative intensities, frequencies and designations of the lines thus far identified in this report on Cr III are given in Table XVIII.

Triply ionized manganese, Mn IV. Extrapolating by means of the irregular doublet law the quintet multiplet $^5F'-{}^5G'(3d^34s-3d^34p)$ was pre-

TABLE XVIII. *Doubly ionized chromium, Cr III*

λ(vac.)	Int.	ν	Designation	Mult. No.	λ(vac.)	Int.	ν	Designation	Mult. No.
2483.79	25	40261.0	$b^3F'_4-{}^3D'_3$	1	2104.05	20	47527.5	$^5F'_4-{}^5F_5$	5
2480.53	22	40313.9	$b^3F'_3-{}^3D'_2$	1	2103.90	20	47530.8	$^5F'_3-{}^5F_4$	5
2473.56	20	40427.5	$b^3F'_2-{}^3D'_1$	1	1735.89	25	57574.2	$^5G'_6-{}^5H'_6$	6
2459.69	6	40655.5	$b^3F'_3-{}^3D'_2$	1	1730.16	20	57798.1	$^5G'_5-{}^5H'_5$	6
2457.54	7	40691.1	$b^3F'_3-{}^3D'_3$	1	1727.19	100	57897.5	$^5G'_6-{}^5H'_7$	6
2343.18	6	42677.1	$b^3F'_4-{}^3G'_4$	2	1724.31	15	57994.2	$^5G'_4-{}^5H'_4$	6
2333.80	4	42848.5	$b^3F'_3-{}^3G'_3$	2	1721.82	90	58078.1	$^5G'_5-{}^5H'_6$	6
2325.60	80	42999.6	$b^3F'_4-{}^3G'_5$	2	1719.51	15	58156.1	$^5G'_3-{}^5H'_3$	6
2319.78	70	43107.5	$b^3F'_3-{}^3G'_4$	2	1717.54	80	58222.8	$^5G'_4-{}^5H'_5$	6
2315.35	60	43190.0	$b^3F'_2-{}^3G'_3$	2	1714.08	70	58340.3	$^5G'_3-{}^5H'_4$	6
2275.99	2	43936.8	$^5F'_3-{}^5G'_2$	3	1711.74	60	58420.1	$^5G'_2-{}^5H'_3$	6
2275.93	2	43938.1	$^5F'_4-{}^5G'_3$	3	1271.90	15	78622.5	$a^3F'_2-{}^3D'_1$	7
2274.47	2	43966.3	$^5F'_5-{}^5G'_4$	3	1269.19	20	78790.4	$a^3F'_3-{}^3D'_2$	7
2265.65	15	44137.4	$^5F'_2-{}^5G'_2$	3	1268.23	tr	78850.0	$a^3F'_2-{}^3D'_2$	7
2262.40	15	44200.8	$^5F'_4-{}^5G'_3$	3	1266.06	tr	78985.1	$^3G_4-{}^3G'_4$	8
2258.70	50	44273.2	$^5F'_1-{}^5G'_2$	3	1264.27	25	79097.1	$a^3F'_4-{}^3D'_3$	7
2258.11	15	44284.8	$^5F'_3-{}^5G'_4$	3	1264.27		79097.1	$^3G_5-{}^3G'_4$	8
2256.17	6	44322.9	$b^3F'_4-{}^3F_3$	4	1263.65	20	79135.8	$^3G_3-{}^3G'_3$	8
2252.70	15	44391.2	$^5F'_5-{}^5G'_5$	3	1263.11	5	79169.6	$a^3F'_3-{}^3D'_2$	7
2252.18	60	44401.4	$^5F'_2-{}^5G'_3$	3	1261.91	30	79244.9	$^3G_4-{}^3G'_4$	8
2249.62	8	44451.9	$b^3F'_3-{}^3F_2$	4	1259.52	8	79395.3	$^3G_3-{}^3G'_4$	8
2244.83	70	44546.8	$^5F'_3-{}^5G'_4$	3	1259.10	40	79421.8	$^3G_5-{}^3G'_5$	8
2238.25	60	44677.6	$b^3F'_4-{}^3F_4$	4	1256.85	2	79564.0	$^3G_4-{}^3G'_5$	8
2236.62	80	44710.4	$^5F'_4-{}^5G'_5$	3	1238.60	40	80736.3	$^3G_3-{}^3F_3$	9
2234.45	50	44754.8	$b^3F'_3-{}^3F_3$	4	1236.23	50	80891.1	$^3G_4-{}^3F_3$	9
2232.46	40	44793.6	$b^3F'_2-{}^3F_2$	4	1233.99	tr	81037.9	$^3G_3-{}^3F_3$	9
2227.40	100	44895.4	$^5F'_5-{}^5G'_6$	3	1233.04	60	81100.3	$^3G_5-{}^3F_4$	9
2217.53	2	45095.3	$b^3F'_2-{}^3F_2$	4	1230.84	tr	81245.3	$^3G_4-{}^3F_4$	9
2216.92	2	45107.6	$b^3F'_3-{}^3F_4$	4	1229.52	10	81332.5	$a^3F'_3-{}^3G'_3$	10
2129.95	2	46949.4	$^5F'_5-{}^5F_4$	5	1228.67	15?	81388.8	$a^3F'_2-{}^3G'_3$	10
2126.37	5	47028.6	$^5F'_4-{}^5F_3$	5	1226.81	8	81512.2	$a^3F'_4-{}^3G'_4$	10
2123.50	5	47092.1	$^5F'_3-{}^5F_2$	5	1225.69	20	81586.7	$a^3F'_3-{}^3G'_4$	10
2121.09	10	47145.6	$^5F'_2-{}^5F_1$	5	1221.97	20	81835.1	$a^3F'_4-{}^3G'_5$	10
2118.27	60	47208.3	$^5F'_5-{}^5F_5$	5	1205.79	2	82933.2	$a^3F'_3-{}^3F_2$	11
2115.60	50	47267.8	$^5F'_4-{}^5F_4$	5	1204.97	30	82989.6	$a^3F'_3-{}^3F_3$	11
2115.00	20	47281.3	$^5F'_1-{}^5F_1$	5	1202.49	8	83160.7	$a^3F'_4-{}^3F_3$	11
2114.50	60	47292.5	$^5F'_3-{}^5F_3$	5	1201.41	40	83235.5	$a^3F'_3-{}^3F_3$	11
2114.50		47292.5	$^5F'_2-{}^5F_2$	5	1200.61	2	83291.0	$a^3F'_2-{}^3F_3$	11
2108.43	10	47428.7	$^5F'_1-{}^5F_2$	5	1197.42	50	83512.8	$a^3F'_4-{}^3F_4$	11
2105.61	15	47492.2	$^5F'_2-{}^5F_3$	5	1196.33	2	83589.0	$a^3F'_3-{}^3F_4$	11

dicted and identified approximately 12,000 cm^{-1} higher than the corresponding multiplet in Cr III. The wave-lengths, relative intensities, and frequencies of the lines thus identified are given in multiplet form in Table XIX. The quintet multiplet $^5G'-{}^5H'(3d^34p-3d^34d)$ for Mn IV, although the frequencies of the radiated lines are quite accurately predictable in the region

of 1200 A.U., has not been definitely identified owing to its low intensity even with long exposures.

TABLE XIX. *Triply ionized manganese, Mn IV.*

$(5F'-{}^5G'(3d^34s-3d^34p)$

		${}^5F_5'$ 475 1375	${}^5F_4'$ 394 900	${}^5F_3'$ 302 506	${}^5F_2'$ 204 204	${}^5F_1'$ 000
		200				
		1742.17				
${}^5G_6'$	58775	57399.7				
	786	90	150			
		1766.36	1751.65			
${}^5G_5'$	57989	56613.6	57089.0			
	661	tr	30	120		
		1787.21	1772.17	1759.87		
${}^5G_4'$	57328	55953.1	56428.0	56822.4		
	535		1	30	100	
			1789.16	1776.62	1767.13	
${}^5G_3'$	56793		55892.1	56286.6	56588.9	
	410			0	10	90
				1789.64	1780.02	1773.57
${}^5G_2'$	56383			55877.2	56179.1	56383.4

Quadruply ionized iron, Fe V. Just as for Cr III and Mn IV the quintet multiplet ${}^5F'-{}^5G'(3d^34s-3d^34p)$ was predicted and identified approximately 12,000 cm^{-1} higher than in the preceding element. The wave-lengths, relative intensities, and frequencies of the lines thus identified are given in multiplet form in Table XX.

TABLE XX. *Quadruply ionized iron, Fe V.*

${}^5F'-{}^5G'(3d^34s-3d^34p)$

		${}^5F_5'$ 669 1953	${}^5F_4'$ 573 1284	${}^5F_3'$ 427 711	${}^5F_2'$ 284 284	${}^5F_1'$ 000
		100				
		1430.51				
${}^5G_6'$	71858	69905.1				
	1152	30	80			
		1454.48	1440.47			
${}^5G_5'$	70706	68753.1	69421.8			
	971	?	10	60		
		1475.32	1460.89	1448.77		
${}^5G_4'$	69735	67781.9	68451.4	69024.1		
	775		?	5	45	
			1477.63	1465.21	1456.11	
${}^5G_3'$	68960		67675.9	68249.6	68676.1	
	585			?	5	30
				1477.91	1468.63	1462.53
${}^5G_2'$	68375			67663.1	68090.7	68374.7

The irregular doublet law. The irregular doublet law, wherever applicable, proves to be the most powerful method of attack in attempting to analyze the spectra arising from ionized atoms. The irregular doublet law is applicable to those radiated lines arising from electron transitions involving no

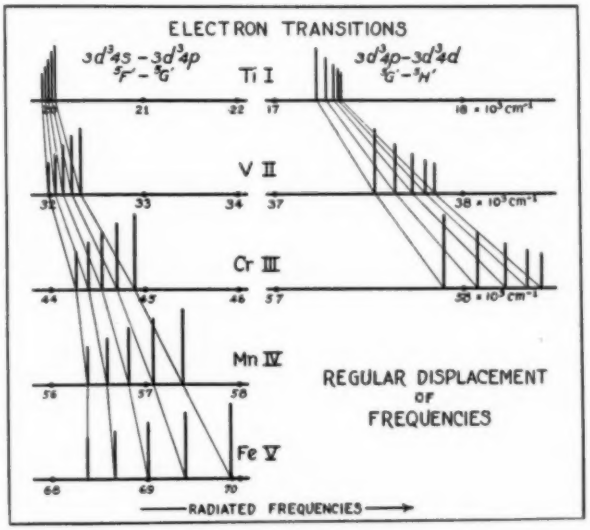

Fig. 8. Irregular doublet law.

change in total quantum number. For sequences of iso-electronic systems involving only one valence electron (i.e. K I, Ca II, Sc III, etc.) an electron transition gives rise to only two or three radiated lines. In the sequence starting with Ti I, however, where four valence electrons are involved and electron transition may give rise to over a hundred radiated lines. In this

TABLE XXI. *Irregular doublet law.*

Atom	$3d^34s-3d^34p$ $^5F_5-{}^5G_6$ $\Delta\nu$	$3d^34s-3d^34p$ $^3F_4-{}^3G_5$ $\Delta\nu$	$3d^34p-3d^34d$ $^5G_6-{}^5G_7$ $\Delta\nu$
Ti I	20068	15973	17224
	12253	14542	20311
V II	32321	30515	37535
	12574	12484	20362
Cr III	44895	42999	57897
	12504	12688	20403
Mn IV	57399	*55687	*78300
	12506	(12880)	(20434)
Fe V	69905	(68567)	(98734)

* Not definitely identified.

report on the latter sequence of iso-electronic systems only a few of the strongest lines have been traced through five elements. For the electron transition $3d^34p$ to $3d^34s$ about forty lines, and for the electron transition $3d^34d$ to $3d^34p$ about twelve lines, have been traced through the first three

elements, Ti I, V II, and Cr III. Examples of the almost linear progression in frequency of these radiated lines may be seen in Table XXI where the lines $^5F_5'-{}^5G_6'$ and $^3F_4'-{}^3G_5'$ are chosen to represent the electron transition $3d^34p$ to $3d^34s$ and the line $^5G_6'-{}^5H_7'$ chosen to represent the electron transition $3d^34d$ to $3d^34p$. This almost linear progression is best brought out graphically as in Fig. 8. Each frequency scale, although the same for each element and corresponding multiplet, has been displaced to the left of the one just preceding it by 12,000 cm^{-1} and 20,000 cm^{-1} for the two electron transitions respectively.

Term separations, the Landé interval rule, and Hund's rule. The systematic increase in term separations in going from one element to the next for one set of terms from each of the two electron configurations $3d^34s$ and $3d^34p$ is shown in Table XXII. In the lower half of the table it is seen that the Landé interval rule for quintet terms is in general in agreement with the observed separations.

TABLE XXII. *Quintet term separations.*

Atom	$3d^34s$ $^5F_1'$	$^5F_2'$	$^5F_3'$	$^5F_4'$ $^5F_5'$	$3d^34p$ $^5G_2'$	$^5G_3'$	$^5G_4'$	$^5G_5'$ $^5G_6'$
Ti I	42	62	82	100	70	93	116	148
V II	82	122	159	194	153	201	246	290
Cr III	136	200	263	319	264	347	425	504
Mn IV	204	302	394	475	410	535	661	786
Fe V	284	427	573	669	585	775	971	1152
Theor.	2.0	3.0	4.0	5.0	3.0	4.0	5.0	6.0
Ti I	2.1	3.1	4.1	5.0	2.8	3.8	4.7	6.0
V II	2.1	3.1	4.1	5.0	3.2	4.2	5.1	6.0
Cr III	2.1	3.1	4.1	5.0	3.1	4.1	5.1	6.0
Mn IV	2.1	3.2	4.2	5.0	3.1	4.1	5.0	6.0
Fe V	2.1	3.2	4.3	5.0	3.0	4.0	5.0	6.0

Hund's rule for relative term positions gives a satisfactory account of the terms thus far identified. All of the terms given in this report are built upon, and therefore have as a limit, the $^4F'(3d^3)$ terms of the once more ionized atoms.

Energy levels and the Moseley law. Combining the data now available for Ti I, and V II, and the data here given for Cr III, Mn IV, and Fe V, the same type of *energy level Moseley diagram* may be drawn for the triplet and quintet terms of these spectra as was drawn for the doublet and quartet terms of the sequence Sc I to Mn V, Fig. 5[6] for the singlet and triplet terms of the sequence Ca I to Cr V, Fig. 4[7] and for the doublet terms of the sequence K I to V V, Fig. 1[7]. This type of diagram is shown in Fig. 9 for all four of the above mentioned sequences.

For each electron configuration shown in the diagram, including the limits, a point has been plotted for the term involving the largest R, L,

[6] White, Phys. Rev. **33**, 672 (1929)
[7] White, Phys. Rev. **33**, 538 (1929).

and J value. Points for all the terms in each configuration would lie within the range covered by the circles. It has been convenient to draw a single line to represent each set of energy levels and a single arrow to represent all of the observed radiated frequencies resulting from jumps between two sets of energy levels. The electron configuration corresponding to each set of four heavy diagonal lines is given below each sequence in the order in which they appear for the last elements. It is apparent from the figure that there is a striking similarity between the separate diagrams for each sequence of iso-electronic systems. The parallelism existing between three of the four heavy diagonal lines for each diagram involve those energy levels between which the transition frequencies have been shown to follow very closely the irregular doublet law. The increased binding of the electron configuration

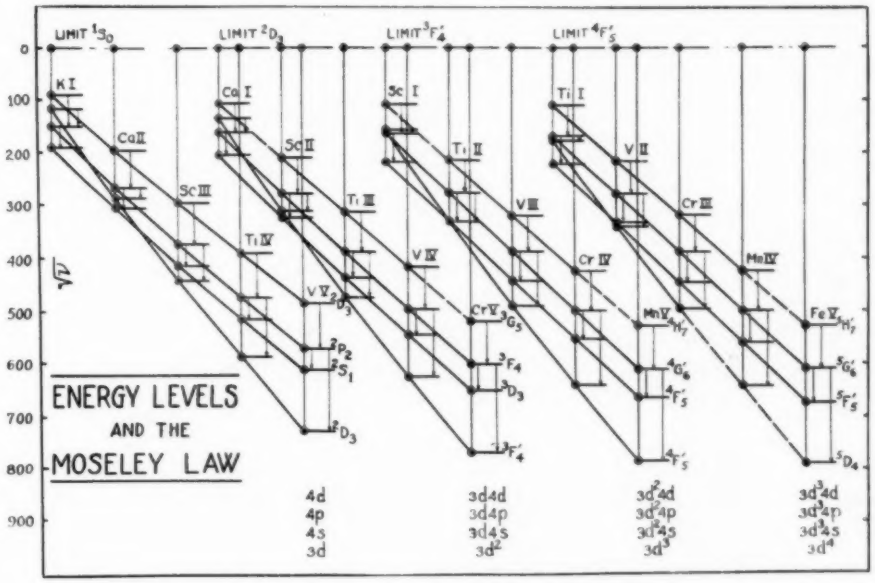

Fig. 9. Regularities between energy levels.

$3d^n$ over the electron configurations $3d^{n-1}4s$, $3d^{n-1}4p$ and $3d^{n-1}4d$ (where $n=1, 2, 3, 4$ for the first, second, third and fourth sequences respectively) appears to be almost identical for each sequence. In going from one sequence to the next (from left to right) the heavy diagonal line $3d^n$ gradually shifts down with respect to the other three parallel diagonals.

A careful examination of the plotted points for, V II in the fourth sequence of Fig. 9, V III in the third sequence, V IV in the second sequence and V V in the first sequence shows that smooth curves can be drawn through certain sets of energy levels. These points for the various stages of ionization of vanadium have been replotted as shown in Fig. 10. Figures similar to that of Fig. 10 have been drawn for Ti I to Ti IV and for Cr I to Cr VI. A comparison of all these diagrams with those of Fig. 9 shows them to be almost identical.

The multiplet structure of $^5F' - {}^5G'(3d^3 4s - 3d^3 4p)$. The characteristic wavelength separations and relative intensities of the diagonal lines in the

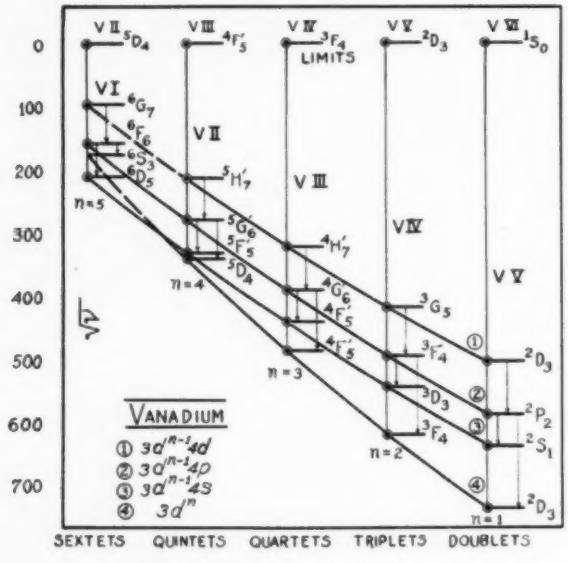

Fig. 10. A new energy level relation.

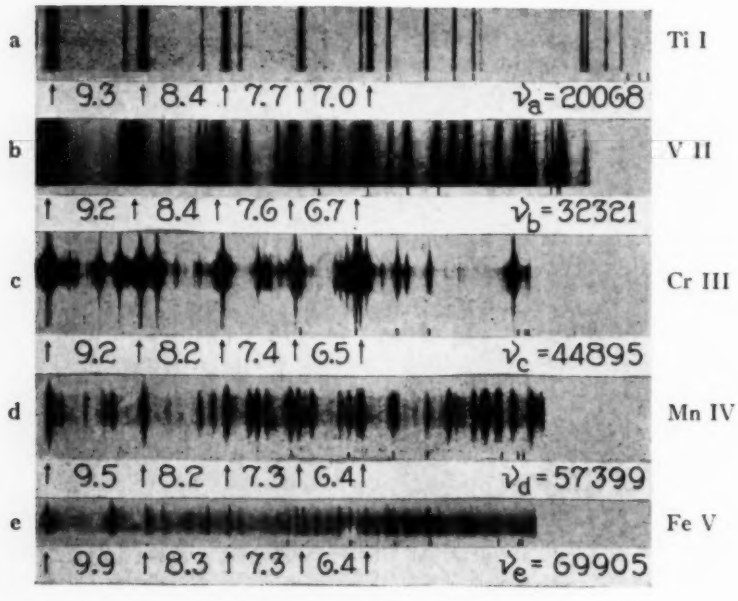

Fig. 11. Quintet multiplets.

$^5F' - {}^5G'(3d^3 4s - 3d^3 4p)$ multiplet for Ti I to Fe V are almost identical. This multiplet is so easily recognized by sight that for Cr III, Mn IV and

Fe V the diagonal lines were identified on the spectrograms before any wave-length determinations were made. Owing to this striking similarity this multiplet, for each of the five elements Ti I, V II, Cr III, Mn IV, and Fe V, has been enlarged from the original plates to exactly the same scale of wave-lengths and reproduced in Fig. 11. It is interesting to note in this figure the different types of spectra present. The first three spectra, the titanium arc spectrum, the vanadium spark spectrum and the chromium vacuum spark spectrum were taken on the same apparatus with the same dispersion and have been enlarged about six times. The last two, spectra of manganese and iron were taken with a vacuum spectrograph and are enlarged about 15 times. The wave-numbers for the strongest line (given at the right and below each multiplet) are the ones given in Column 2, Table XXI, which indicates the almost linear progression of frequency with atomic number, Fig. 8. The constancy of $\Delta\lambda$ between the diagonal lines indicated in Fig. 11 is a characteristic which also appears in the corresponding quartets, triplets, and doublets of the sequences mentioned above starting with Sc I, Ca I, and K I. This constancy in the value of $\Delta\lambda$ for all four sequences is shown in Table XXIII.

TABLE XXIII. *Wave-length separations of diagonal lines.* ($\Delta\lambda$ in A.U.)

Atom	$3d^34s-3d^34p$ $^5F'-{}^5G'$				Atom	$3d^34s-3d^34p$ $^4F'-{}^4G'$		
Ti I	9.3	8.4	7.7	7.0	Sc I	15.0	13.3	11.6
V II	9.2	8.4	7.6	6.7	Ti II	11.8	11.6	11.0
Cr III	9.2	8.2	7.4	6.5	V III	11.4	11.1	10.6
Mn IV	9.5	8.2	7.3	6.4	Cr IV	11.8	11.2	10.8
Fe V	9.9	8.3	7.3	6.4	Mn V	12.4	11.4	11.3

Atom	$3d4s-3d4p$ $^3D-{}^3F$		Atom	$4s-4p$ $^3S-{}^3P$
Ca I	23.5	3.12	K I	34.1
Sc II	16.9	12.0	Ca II	34.8
Ti III	11.8	12.0	Sc III	35.0
V IV	12.4	11.6	Ti IV	35.6
Cr V	12.0	11.5	V V	36.5

The analysis of complex spectra as exemplified by Ti I (the lines of which are nearly all accessible with existing high dispersion apparatus) when extended to Cr III, Mn IV, etc. must rely upon spectrograms taken with relatively small vacuum spectrographs. In working with these complex spectra of atoms in the higher states of ionization one cannot help but feel the need for vacuum spectrograms taken with much higher dispersion and resolving power. Since in the vacuum region the frequencies of lines increase so rapidly in going toward shorter wave-lengths, and since analysis of spectra depends upon the frequency separations, apparatus capable of giving higher disper-

sion and resolving power must be constructed before much progress can be made in identifying high frequency spectral lines.

The author wishes to take this opportunity to express his appreciation and indebtedness to Professor R. C. Gibbs for his valuable advice and criticism in carrying on this investigation as well as those of the two preceding papers under the same general title.

CORNELL UNIVERSITY,
February 25, 1929.

SOME PECULIAR HYDROGEN BANDS

By Charles J. Brasefield*

Abstract

Photographs of the *secondary spectrum of hydrogen* as excited by an electrodeless ring discharge were taken at various pressures in the range 0.08 to 0.001 mm. A number of lines were found to be much more intense at low pressures than at high pressures. The more prominent of these were arranged into a band with P, Q and R branches corresponding to a $\Pi \rightarrow \Sigma$ type electronic transition; this band was assumed to be a $0 \rightarrow 0$ band. The majority of the remaining lines were tentatively arranged into three more bands which appeared to be the $1 \rightarrow 0$, $0 \rightarrow 1$ and $1 \rightarrow 1$ bands corresponding to the same $\Pi \rightarrow \Sigma$ electronic transition. The values of the moments of inertia are $I_0' = 3.8 \times 10^{-40}$, $I_1' = 5.5 \times 10^{-40}$, $I_0'' = 2.0 \times 10^{-40}$ and $I_1'' = 2.3 \times 10^{-40}$. The corresponding values of the nuclear separation "r" are $r_0' = 2.14 \times 10^{-8}$ cm, $r_1' = 2.57 \times 10^{-8}$ cm, $r_0'' = 1.55 \times 10^{-8}$ cm, and $r_1'' = 1.66 \times 10^{-8}$ cm. The emitter of these bands is thought to be either H_2^+ or doubly excited hydrogen.

Introduction

IN THE excitation of a gas by means of an electrodeless discharge, it appears that as the pressure is lowered the spark spectrum of the gas is enhanced relative to the arc spectrum. Thus in exciting argon by means of an electrodeless ring discharge, Wachsmuth and Winawer[1] observed at high pressures only the red argon spectrum while at low pressures, the blue spectrum also appeared. Similarly, in exciting potassium, Foote and Ruark[2] have observed that at high vapor pressures, the arc spectrum alone is observed; but that when the pressure is reduced, the spark lines appear. Even more striking are Balasse's[3] observations on caesium. He found that at low vapor pressures (temperature about 150°), the spectrum contained only spark lines and that when the temperature, and consequently the vapor pressure, was raised, the spark spectrum was replaced progressively by the arc spectrum.

With these facts in mind, the writer set up an electrodeless ring discharge in hydrogen in the hope that a comparison of the intensities of the lines of the secondary spectrum obtained at a very low pressure and at a relatively much higher pressure would indicate which lines of the secondary spectrum, if any, had H_2^+ as an emitter.

Apparatus

The discharge tube was of Pyrex glass, 35 cm long and 4 cm in diameter, with an optical glass window sealed into one end. This end, which was im-

* National Research Fellow.

[1] Wachsmuth and Winawer, Ann. d. Physik **42**, 599 (1913).

[2] Foote and Ruark, Nature **114**, 750 (1924).

[3] G. Balasse, Comptes Rendus **184**, 1002 (1927).

mediately in front of the slit of the spectrograph, was wrapped with 11 turns of 2 mm copper wire. When high frequency currents passed through the coil, the gas inside the tube was excited. At very low pressures, it was found that the gas could be excited more readily if the coil were extended the whole length of the tube to a dead end (about 40 more turns). This dead end seemed to act as a resonating circuit and was apparently self tuned.

The oscillating circuit which was found to be most satisfactory for this work was the ordinary Colpitts circuit, of which the coil around the experimental tube was the inductance. Undamped oscillations were fed into the circuit from a U.X.852 75-watt tube-oscillator, whose plate was connected to a 3000 volt transformer. The high frequency currents which flowed around the experimental tube varied with the gas pressure inside the tube, ranging from 10 amperes at the lowest pressures to 1 ampere at high pressures. The frequency of oscillation used was 10^7 cycles per sec. (30 meters wave-length).

Hydrogen was admitted to one end of the experimental tube by means of a platinum tube, and was pumped out at the other end, thus insuring a continuous flow of pure hydrogen. The platinum tube was 20 cm long, 1 mm in diameter with 0.1 mm walls. It was surrounded by a glass jacket through which commercial hydrogen was flowed. On heating the platinum tube to a dull red heat (about 600°K) by passing a current of about 16 amperes through it, an adequate flow of hydrogen was obtained through the experimental tube. The pressure could be varied either by changing the temperature of the platinum tube or by means of a valve which regulated the rate of pumping. Pressures were measured by a McLeod gauge.

The spectrograph used for photographing the electrodeless discharge was a three prism Steinheil instrument having an opening $f/3.0$ and giving a dispersion of 113A per mm at H_α, 31.3A per mm at H_β and 13.5A per mm at H_γ. Ilford Special Rapid Panchromatic Plates were used for all exposures.

Results

The appearance of the discharge varied greatly according to the pressure. At high pressures (0.08 to 0.01 mm), the discharge was intense pinkish white all along the tube with a tendency to break up into white "eggs" of luminosity as the pressure approached 0.01 mm. As soon as the pressure was lowered below 0.01 mm, these white "eggs" disappeared leaving a hazy bluish-gray luminosity which filled the whole tube. This luminosity, together with a peculiar blue fluorescent band of light on the walls of the tube near the center, persisted down to the lowest pressures (0.0001 mm), getting fainter of course as the pressure was lowered.

In connection with the apparent discontinuity at 0.01 mm pressure, it might be remarked now that the Fulcher bands, which are quite strong at the higher pressures, decrease markedly in intensity below 0.01 mm pressure. Moreover, the mean electronic velocity, which is increasing as the pressure decreases, reaches 30 volts for the first time at 0.01 mm pressure.[4] At first

[4] C. J. Brasefield, Phys. Rev. **31**, 57 (1928).

sight, this would seem to suggest that at 0.01 mm, the spark spectrum of hydrogen was appearing for the first time, together with a simultaneous suppression of the arc spectrum. Unfortunately, a closer examination of the spectrum showed that this was at least not entirely the case.

Photographs of the spectrum were taken at various pressures in the range 0.001 mm to 0.08 mm, lasting from 12 hours in the first case to 1 minute in the second. From these, two plates were chosen, namely an 8 hour exposure at 0.0025 mm and a 1 minute exposure at 0.08 mm, on which the lines of the singlet system at λ4934.2 and λ4631 were approximately equally intense. Microphotometric traces were then made of these plates by means of a Moll self registering microphotometer. The results were rather startling.

They showed that the Fulcher bands in the red and blue had decreased markedly in intensity as the pressure was lowered from 0.08 mm to 0.0025 mm. By referring to Hughes and Lowe's[5] curves on the probability of excitation in hydrogen, we see that this change in intensity can be explained by the increase in mean electronic velocity from approximately 15 volts to a value considerably in excess of 30 volts.[4]

TABLE I.

Line[a]	Wave-length[b] in I.A.	Wave-number (in vacuo)	Intensity[c]	Remarks
		$\Pi\rightarrow\Sigma$ 0→0 $\nu_0=21145$		
$Q(1)$	4732.4	21125	8.7	See footnote (*d*)
$Q(2)$	4738.7	21097	9.7	
$Q(3)$	4745.0	21069	(14.9)	Also $P(2)$ and $R(4)$
$Q(4)$	4759.9	21003	7.8	
$Q(5)$	4774.5	20939	(14.9)	See footnote (*d*)
$P(2)$	4745.0	21069	(14.9)	Also $Q(3)$ and $R(4)$
$P(3)$	4756.4	21018	7.8	
$P(4)$	4770.9	20955	5.9	
$P(5)$	4790.0	20871	14.9	See footnote (*d*)
$R(0)$	4725.8	21154	10.7	Also $R(1)$
$R(1)$	4725.8	21154		Also $R(0)$
$R(2)$	4727.4	21146	9.7	
$R(3)$	4733.2	21121	5.9	
$R(4)$	4745.0	21069	(14.9)	Also $Q(3)$ and $P(2)$

Footnotes:

[a] The number in parenthesis is the j_k value for the final level.

[b] The maximum error in measurement of these lines is estimated at 0.5 A.U. or about 2 wave-numbers. More than half of the lines are not listed in Gale, Monk and Lee's[6] table as is to be expected from the difference in conditions of excitation. No lines due to impurities were detected.

[c] The intensities were computed from the relation $I=\log d/d-h$ where d is the total galvanometer deflection in the absence of a line and h is the height of the peak on the trace corresponding to the line. Those values of intensities appearing in parenthesis are due to two or more lines superimposed.

[d] These lines have been previously assigned by the writer to H_2^{+0}.

[5] A. L. Hughes and P. Lowe, Phys. Rev. **21**, 297 (1923).

[6] H. G. Gale, G. S. Monk and K. O. Lee, Astrophys. J. **67**, 89 (1928).

TABLE I (continued)

Line[a]	Wave-length[b] in I.A.	Wave-number (in vacuo)	Intensity[c]	Remarks
		$\Pi \rightarrow \Sigma$ 1→0 $\nu_0 = 21786$		
$Q(1)$	4593.9	21762	2.6	
$Q(2)$	4600.9	21729	4.4	
$Q(3)$	4613.1	21671	13.6	
$Q(4)$				Masked by λ4628, 4631 of H_2
$Q(5)$	4650.2	21499	14.8	
$P(2)$	4606.3	21704	(3.5)	Also $R(3)$
$P(3)$				Masked by λ4617.5 of H_2
$P(4)$	4639.4	21549	(4.4)	Also $R(5)$
$P(5)$				Masked by λ4661 of H_2
$R(0)$	4588.8	21786		Also $R(1)$ } Also λ4588.7
$R(1)$	4588.8	21786	16.0	Also $R(0)$ } of H_2
$R(2)$	4595.2	21756	5.3	See footnote (*d*)
$R(3)$	4606.3	21704	(3.5)	Also $P(2)$
$R(4)$				Masked by λ4620.8 of H_2
		$\Pi \rightarrow \Sigma$ 0→1 $\nu_0 = 19890$		
$Q(1)$	5030.4	19874	(7.9)	Also $R(3)$
$Q(2)$	5033.8	19860	2.7	
$Q(3)$	5041.6	19829	(9.5)	Also $P(2)$
$Q(4)$	5055.1	19777	(12.9)	Also $P(3)$
$Q(5)$	5063.9	19742	4.1	$0\beta 1Q$ (1) of Richardson
$P(2)$	5041.6	19829	(9.5)	Also $Q(3)$
$P(3)$	5055.1	19777	(12.9)	Also $Q(4)$
$P(4)$	5067.5	19728	7.1	
$P(5)$	5082.2	19671	8.7	
$R(0)$	5025.0	19895	1.3	
$R(1)$	5022.7	19904	1.3	$4\alpha 2$ $Q(2)$ of Richardson
$R(2)$	5021.2	19910	2.0	
$R(3)$	5030.4	19874	(7.9)	Also $Q(1)$
$R(4)$	5036.6	19849	2.7	
		$\Pi \rightarrow \Sigma$ 1→1 $\nu_0 = 20519$		
$Q(1)$	4877.5	20497	(6.8)	Also $R(2)$
$Q(2)$	4882.8	20474	4.4	
$Q(3)$	4895.4	20422	(2.9)	Also $R(4)$
$Q(4)$	4910.8	20357	2.1	See footnote (*d*)
$Q(5)$	4922.5	20309	6.8	
$P(2)$	4889.2	20449	4.4	
$P(3)$	4901.6	20396	7.6	
$P(4)$	4919.1	20323	2.1	$3\alpha 1$ $Q(4)$ of Richardson
$P(5)$				Masked by λ4934, 4939 of H_2
$R(0)$				}
$R(1)$				} Masked by λ4873 of H_2
$R(2)$	4877.5	20497	(6.8)	Also $Q(1)$
$R(3)$	4887.2	20456	2.1	See footnote (*d*)
$R(4)$	4895.4	20422	(2.9)	Also $Q(3)$

A large number of the lines remained approximately constant in intensity. These, of course, included the lines of the singlet system of hydrogen. They also included some lines ascribed by Richardson to the triplet system and a number of unassigned lines.

But most remarkable was the appearance on the low pressure plate of a number of lines which either did not appear at all or else were weak on the high pressure plate. An exhaustive study was made of these lines, with the result that the more prominent lines were arranged into a band with P, Q and R branches. The intensity relations $Q>R>P$ together with the absence of the $P(1)$ line show that this band is of the type $\Pi\rightarrow\Sigma$. This band was assumed to be a $0\rightarrow0$ band. The majority of the remaining lines were tentatively arranged into three more bands, which appeared to be the $1\rightarrow0$, $0\rightarrow1$ and $1\rightarrow1$ bands corresponding to the same $\Pi\rightarrow\Sigma$ electronic transition. Alternating intensities were observed in all branches as is to be expected for hydrogen bands. Transitions to the final (Σ) levels $j_k=1, 3, 5$ are stronger than to the levels $j_k=0, 2, 4$. The four bands are given in Table I.

Discussion

For a $\Pi\rightarrow\Sigma$ band corresponding to Hund's case (b),[7] if the σ-type doubling of the Π state is neglected,[8] we would expect P, Q, and R branches obeying the relations

$$\begin{aligned} F'(j_k+1)-F''(j_k)&=R(j_k)\\ F'(j_k)\quad\ -F''(j_k)&=Q(j_k)\\ F'(j_k-1)-F''(j_k)&=P(j_k)\end{aligned}$$

from which we deduce

$$\begin{aligned} Q(j_k+1)-P(j_k+1)=R(j_k)-Q(j_k)&=F'(j_k+1)-F'(j_k)=\Delta F'(j_k)\\ Q(j_k)-P(j_k+1)=R(j_k)-Q(j_k+1)&=F''(j_k+1)-F''(j_k)=\Delta F''(j_k).\end{aligned}$$

The observed ΔF values as calculated from these combination relations are given in Table II.

It is interesting to notice that in the Π state when $n=0$, $\Delta F'(2)=\Delta F'(3)$ approximately and when $n=1$, $\Delta F'(1)=\Delta F'(2)$ approximately. This irregularity does not appear in the final (Σ) state. Although unusual, it is perhaps not unexpected that such irregularities would occur in such an unstable molecule as H_2^+ or doubly excited H_2.

From the ΔF values, we can calculate approximate values of the moments of inertia of the various states by use of the relation $F(j_k)=B[j_k(j_k+1)-\sigma_k^2]$ where $B=h/8\pi^2Ic$. As shown by the irregularities in the ΔF values, this expression for $F(j_k)$ can of course be only a rough approximation to the true expression. Very approximately, then, for the Π state $I_0=3.8\times10^{-40}$ and $I_1=5.5\times10^{-40}$; for the Σ state $I_0=2.0\times10^{-40}$ and $I_1=2.3\times10^{-40}$. The corresponding values of the nuclear separation "r" are $r_0'=2.14\times10^{-8}$ cm, $r_1'=2.57\times10^{-8}$ cm, $r_0''=1.55\times10^{-8}$ cm and $r_1''=1.66\times10^{-8}$ cm. The intervals between the vibrational levels of the Π and Σ states are 635 and 1260

[7] The spin energy is negligible in H_2 as is shown by the triplet bands of hydrogen. See R. S. Mulliken, Phys. Rev. **30**, 793–4 (1927), especially Ref. 17.

[8] This is justifiable since the $\Delta F'$ values obtained from the $P-Q$ and $Q-R$ combinations agree, within experimental error. See Table II.

TABLE II.

j_k	$Q-P$ (from 0→0 band)	$R-Q$	$Q-P$ (from 0→1 band)	$R-Q$	Average (in wave-numbers)
		$\Delta F'(j_k)$ for Π state $(n=0)$			
0	—	—	—	—	—
1	28*	29*	31*	30*	29.5
2	51*	49	52*	50	50.5
3	48	52*	49*	45*	48.5
4	68	66*	71	72*	69.3
		$\Delta F'(j_k)$ for Π state $(n=1)$			
	(from 1→0 band)		(from 1→1 band)		
0	—	—	—	—	—
1	25*	24*	25	?	24.7
2	?	27	26*	23*	25.3
3	?	33*	34	34*	33.7
4	?	?	?	65*	65
		$\Delta F''(j_k)$ for Σ state $(n=0)$			
	(from 0→0 band)		(from 1→0 band)		
0	—	29*	—	24*	26.5
1	56*	57*	58*	57*	57.0
2	79	77*	?	85	80.3
3	114*	118	122	?	118
4	132	130*	?	?	131
		$\Delta F''(j_k)$ for Σ state $(n=1)$			
	(from 0→1 band)		(from 1→1 band)		
0	—	21*	—	?	21
1	45*	44	48*	?	45.7
2	83*	81*	78	75*	79.3
3	101*	97*	99*	99	99
4	106*	107	?	113*	108.7

* These combinations involve observed lines which have been assigned places in more than one branch of the band.

wave-numbers, respectively. From this we find that $I_0\omega_0 = 2400+$ for the Π state and $I_0\omega_0 = 2500+$ for the Σ state.

We now come to the question as to the emitter of these bands. We have seen that they appear in strength when the mean electronic velocity is well above 30 volts. This would be consistent with the hypothesis that they are due either to H_2^+ or doubly excited hydrogen. The values of I_0 and $I_0\omega_0$ are apparently consistent with either hypothesis. Using an entirely different method of attack,[9] the writer has assigned a number of the lines in the secondary spectrum to H_2^+ as an emitter. Only six of this group of lines appear in the bands here described, within the error of measurement. From this angle, then, there seems to be but little supporting evidence to the hypothesis that these bands are due to H_2^+.

Morse and Stueckelberg have calculated the potential energy curves for the lower states of H_2^+.[10] Insofar as the energy relations are concerned, these curves suggest that the bands here described might arise in transitions from a $4x\pi^2\Pi$ state to either the $3d\sigma$ or the $4f\sigma^2\Sigma$ states of the H_2^+ molecule.

[9] C. J. Brasefield, Proc. Nat. Acad. Sci. **14**, 688 (1928).

[10] Although these curves have as yet not been published, the writer has had the privilege of examining them.

However, the values of the moments of inertia for these states as calculated by them, are very much larger than the I_0' and I_0'' of the bands here described. Thus we conclude that if Morse and Stueckelberg's curves are correct, these bands cannot be due to H_2^+. On the other hand the values of I_0' and I_0'' are too large for the bands to be due to neutral hydrogen with one electron excited. (The largest known value of I_0 for H_2 is 1.42×10^{-40} in $2^1\Sigma$ state).[14] They are not, however, unreasonable values for states of neutral hydrogen in which two electrons are simultaneously excited; and moreover, the conditions of excitation, namely, high electronic velocities, suggest that such a molecule is indeed the emitter.

In addition to the four bands described here, there are a number of other lines which are enhanced at the low pressures. These include a group of nine lines (which suggest a possible band), namely, λλ 5317.9, 5334.3, 5355.9, 5386.2, 5392.3, 5410.2, 5459.9, 5475.7, 5499.6 and three prominent isolated lines, λλ 4802.0, 4651.3, 4404.6. Of these, λ4802.0 and λ4404.6 have been previously assigned by the writer to H_2^+.[9]

There remains a word to be said concerning the continuous spectrum of hydrogen. Ordinarily, the continuous spectrum is intense relative to the secondary spectrum at very high pressures, becoming very weak at the lowest pressures.[11] This phenomenon was confirmed in the present work, for at 0.08 mm pressure, the writer observed no indication of a continuous spectrum. However, at a still lower pressure (0.0025 mm) there seemed to be an indication of a continuous spectrum between H_β and H_γ. In an attempt to obtain a photograph of the spectrum of the discharge at the very lowest pressures, the writer took two 12 hour exposures at 0.0005 mm and 0.0001 mm pressure on Cramer Hi-Speed plates. These plates showed very surprisingly a strong continuous spectrum which completely masked the whole secondary spectrum. It extended from λ5300 to λ4150 with a maximum intensity between λ4800 and λ4500. This continuous spectrum was also observed by Herzberg at extremely low pressures.[12] The probable high concentration of H_2^+ ions at these low pressures suggests that this continuous spectrum is due to the H_2^+ molecule. Just as the ordinary continuous spectrum of hydrogen has been explained[13] by transitions to the low unstable $^3\Sigma$ state of hydrogen, so we can explain this continuous spectrum by transitions to any one or all of the unstable states $2p\pi$, $3d\pi$, $2s\sigma$, or $3p\sigma$ of the H_2^+ molecule.[10] The energies involved in this continuous spectrum are consistent with such an explanation.

In conclusion, the writer wishes to express his sincere appreciation to Professor R. S. Mulliken for the benefits derived from numerous conferences with him.

RYERSON PHYSICAL LABORATORY,
UNIVERSITY OF CHICAGO.
March 4, 1929.

[11] G. Herzberg, Ann. d. Physik **84,** 586, (1927); see there also a list of other references.
[12] G. Herzberg, Ann. d. Physik **84,** 560 (1927).
[13] J. G. Winans and E. C. G. Stueckelberg, Proc. Nat. Acad. Sci. **14,** 867 (1928).
[14] H. H. Hyman and R. T. Birge, Nature **123,** 277 (1929).

DIATOMIC MOLECULES ACCORDING TO THE WAVE MECHANICS I: ELECTRONIC LEVELS OF THE HYDROGEN MOLECULAR ION

By Philip M. Morse and E. C. G. Stueckelberg

Abstract

The electronic energies $W_\rho(n_\eta, n_\phi, n_\xi)$ of the hydrogen molecular ion are calculated by means of the wave mechanics as functions of the nuclear separation $c=2\rho$, for several values of the quantum numbers n_η, n_ϕ and n_ξ. The wave function is separable in the elliptical coordinates $y=(r_1+r_2)/2\rho$, ϕ and $x=(r_1-r_2)/2\rho$. A qualitative idea of the behavior of these energies as ρ changes from infinity to zero is gotten by an investigation of the behavior of the nodal surfaces. The number of these surfaces in any coordinate equals the quantum number in that coordinate. When $\rho=\infty$ the resulting system is that of a hydrogen atom and a separated nucleus, the nodes are paraboloids and planes with quantum numbers n_η, n_ϕ and n_ξ, and the electronic energy is $W_\infty=R/(n_\eta+n_\phi+n_\xi+1)^2$ where R is the lowest energy of the hydrogen atom. When $\rho=0$ the system is that of a helium ion, the nodes are spherically symmetric with quantum numbers n_r, n_ϕ and n_θ, and the electronic energy is $W_0=4R/(n_r+n_\phi+n_\theta+1)^2$. As ρ changes from zero to infinity it is shown that the quantum numbers are related in the manner $n_r\rightarrow n_\eta\rightarrow n_\eta$; $n_\phi\rightarrow n_\phi\rightarrow n_\phi$; $n_\theta\rightarrow n_\xi\rightarrow 2n_\xi$ or $2n_\xi+1$. Therefore $W_0=4R/n_\eta+n_\phi+2n_\xi+1)^2$ or $=4R/(n_\eta+n_\phi+2n_\xi+2)^2$. By this rule it is possible to check the following quantitative calculations. The first order perturbations of the various electronic energies of the first three degenerate levels of the helium ion resulting when $\rho=0$ were calculated; the perturbation being the slight separation of the nuclei ($\rho>0$). The first order perturbations of the various electronic energies of the first two degenerate levels of the hydrogen atom resulting when $\rho=\infty$ were calculated when the perturbation was the diminution of the separation ($\rho<\infty$). The first method is not valid for $\rho>a/2$, where a is the radius of the first Bohr orbit of the hydrogen atom, and the second is not valid for $\rho<3a/2$. The gap between was extrapolated by means of the nodal reasoning above. These electronic energies plus the energy of nuclear repulsion give the molecular potential energies. A calculation of these shows that of the eight curves obtained only three, the $1s\sigma$, $3d\sigma$ and $4f\sigma$ states show minima, and therefore are stable configurations to this order of approximation (the Hund molecular notation is used for the states). The numerical results check with previous calculations and with the data available.

Introduction

IN THE study of the diatomic molecule one of the most important of its properties is the so-called potential energy curve of the nuclei, giving the energy of the electrons plus the energy of repulsion of the nuclei as a function of the nuclear separation. The simplest case, that of two similar nuclei with a single electron in common (represented by the hydrogen molecular ion) must be investigated first, in order that a general idea of the behavior of one electron be obtained before attacking the problem of the more complicated molecule formed by the addition of more electrons.[1-8]

[1] For a general qualitative statement of the problem see the papers of Hund and Mulliken.

[2] F. Hund, Zeits. f. Physik 36, 657 (1926).

It has been shown that the electronic energy (the sum of the electronic potential and kinetic energies) of a diatomic molecule is approximately independent of the rotatory or vibrational velocity of the nuclei, and only dependent on their instantaneous relative separation.[9]

This means that for purposes of calculating this energy the nuclei can be considered as fixed in space at a distance $d=2\rho$ apart. The equation for the wave function of the electron then becomes

$$\nabla^2\Psi+\frac{8\pi^2\mu}{h^2}\left(W_\rho+\frac{e^2Z}{r_1}+\frac{e^2Z}{r_2}\right)\Psi=0$$

where r_1 is the distance from the point in question to the first nucleus and r_2 the distance from the second nucleus. This equation can be separated in elliptical coordinates, $y=(r_1+r_2)/2\rho$, $x=(r_1-r_2)/2\rho$ and ϕ the angle about the nuclear axis.

This means that $\Psi=N\cdot\Phi(\phi)\cdot Y(y)\cdot X(x)$, where N is the normalizing factor. The factor Φ is $e^{im\phi}$, since angle ϕ is a cyclic coordinate, and the equations for the other two factors become

$$\frac{d}{dy}\left[(y^2-1)\frac{dY}{dy}\right]-\frac{m^2Y}{y^2-1}+\frac{8\pi^2\mu\rho^2}{h^2}\left(W_\rho y^2+\frac{2Ze^2}{\rho}y+C\right)Y=0 \qquad (1)$$

$$\frac{d}{dx}\left[(1-x^2)\frac{dX}{dx}\right]-\frac{m^2X}{1-x^2}+\frac{8\pi^2\mu\rho^2}{h^2}(-W_\rho x^2-C)X=0. \qquad (2)$$

The problem presented by these two equations, namely that of finding values of W and C for which X is finite over the range $-1\leqq x\leqq+1$ and Y finite over the range $+1\leqq y\leqq\infty$, has not been solved in general. Burrau[10] found W_ρ as a function of ρ for the lowest allowed level by a numerical integration which is only applicable to this lowest state.

It is possible to determine what form Ψ takes for the two limiting values of ρ, zero and infinity. When $\rho=0$, Ψ is the wave function of the singly ionized helium atom (the united atom)

$$\Psi_0(n,l,m)=N_0(nlm)\cdot e^{im\phi}\cdot\sin^m\theta\cdot P_l^m(\cos\theta)\cdot e^{-r/na_0}\cdot(2r/na_0)^l\cdot L_{n+l}^{2l+1}(2r/na_0) \qquad (3)$$

These quantum numbers bear relation to $n_\phi n_r$ and n the quantum numbers for each coordinate, for $n_\phi=m$, $n_\theta=l-m$, $n=n_r+n_\phi+n_\theta+1$. The relation between the spherical coordinates used above and the general ellip-

[3] F. Hund, Zeits. f. Physik **40**, 742 (1927).
[4] F. Hund, Zeits. f. Physik **42**, 93 (1927).
[5] F. Hund, Zeits. f. Physik **43**, 805 (1927).
[6] F. Hund, Zeits. f. Physik **51**, 759 (1928).
[7] R. S. Mulliken, Phys. Rev. **32**, 186 (1928).
[8] R. S. Mulliken, Phys. Rev. **32**, 761 (1928).
[9] Born and Oppenheimer, Ann. d. Physik **84**, 457 (1927).
[10] Burrau, Kgl. Danske Vid. Selskab. **VII**, 14, (1927).

tical coordinates is that as $\rho\to 0$, $y\to r/\rho$, $x\to\cos\theta$ and ϕ remains ϕ. P_b^a is the generalized Legendre polynomial; $P_b^a(x)=d^aP_b(x)/dx^a$. L_b^a is the generalized Laguerre polynomial; $L_b^a(x)=d^aL_b(x)/dx^a$.[11] The constant $a_0=\frac{1}{4}\hbar^2/(8\pi^2\mu e^2Z_0)=a/2Z_0$, where a is the radius of the first Bohr orbit in hydrogen ($a=5.4\times10^{-9}$ cm). The normalizing factor is

$$N(nlm)=\left(\left(\frac{2}{na_0}\right)^3\cdot\frac{1}{2\pi}\cdot\frac{2l+1}{2}\cdot\frac{(l-m)!}{(l+m)!}\cdot\frac{(n-l-1)!}{2n[(n+l-1)!]^3}\right)^{1/2}.$$

For the hydrogen molecular ion the value of Z_0 will be two, and the allowed energy levels for $\rho=0$ are

$$W_0(n)=-2\pi^2\mu Z_0^2e^4/n^2h^2=4R/n^2$$

where R is the energy of the normal state of the hydrogen atom.

When $\rho=\infty$ the wave function must represent a hydrogen nucleus infinitely separated from a neutral hydrogen atom (the separated atom) and must represent the fact that the electron is as likely to be about nucleus number one as about nucleus number two. If ψ_1 be the wave function for a single separate hydrogen atom at the position of nucleus one, and ψ_2 the same at nucleus two, then the function which must be used in this limiting case is

$$\Psi_\infty=(\psi_1\pm\psi_2)/(2)^{1/2} \tag{4}$$

the possibility of either sign being due to the fact that $\Psi\bar{\Psi}$ and not Ψ, has physical reality, and for $\rho=\infty$ this change in sign makes no change in the value of $\Psi\bar{\Psi}$. Unsöld[12] made the mistake of considering the wave function as entirely about one nucleus when he attacked the problem.

The elliptical coordinates for the general problem become parabolic coordinates $\xi_1=r_1(1+\cos\theta_1)$; $\eta_1=r_1(1-\cos\theta_1)$ about nucleus one, and $\xi_2=r_2(1-\cos\theta_2)$; $\eta_2=r_2(1+\cos\theta_2)$ about nucleus two, with angle ϕ in both cases. In other words, when $\rho\to\infty$ then $y\to1+\eta_1/2\rho$ and $y\to1+\eta_2/2\rho$; $x\to-(1-\xi_1/2\rho)$ and $x\to1-\xi_2/2\rho$.

The wave function of the hydrogen atom in parabolic coordinates for the electron about nucleus one is

$$\psi_1=N_\infty e^{im\phi}\left(\frac{\xi_1\eta_1}{n^2a_\infty^2}\right)^{m/2}\cdot e^{-(\xi_1+\eta_1)/2na_\infty}\cdot L_{k+m}^m\left(\frac{\xi_1}{na_\infty}\right)\cdot L_{n-k-1}^m\left(\frac{\eta_1}{na_\infty}\right) \tag{5}$$

and similarly for ψ_2. Here $a_\infty=a/2Z_\infty$, Z_∞ has half the value of Z_0 for the united atom, and of the quantum numbers $m=n_\phi$, $k=n_\xi$, but otherwise the definitions of the terms are the same. The total quantum number $n=n_\eta+n_\phi+n_\xi+1$ and the normalizing factor

$$N_\infty(nkm)=\left(\frac{4}{2\pi}\,\frac{1}{(na_\infty)^3}\,\frac{2n[(k+m)!]^3[(n-k-1)!]^3}{k!(n-k-m-1)!}\right)^{1/2}$$

[11] For definitions of P_b and L_b see Courant-Hilbert, (Methoden der Mathematischen Physik, Berlin, 1924.) pp. 67 and 77.

[12] A. Unsöld, Zeits. f. Physik **43**, 563 (1927).

and the allowed energy levels are those of the hydrogen atom

$$W_\infty(n\ k\ m) = R/n^2.$$

Therefore the wave function for the hydrogen molecular ion for infinite separation of the nuclei is, when the parabolic coordinates are transformed to elliptical coordinates,

$$\begin{aligned}\Psi_\infty = \frac{N_\infty}{\sqrt{2}} e^{im\phi} \cdot \left[\frac{2\rho(y-1)}{na_\infty}\right]^{m/2} \cdot e^{-\rho y/na_\infty} \cdot L^m_{n-k-1}\left[\frac{2\rho(y-1)}{na_\infty}\right] \cdot \\ \cdot \left\{\left[\frac{2\rho(1+x)}{na_\infty}\right]^{m/2} \cdot e^{-\rho x/na_\infty} \cdot L^m_{k+m}\left[\frac{2\rho(1+x)}{na_\infty}\right]\right. \\ \left. \pm \left[\frac{2\rho(1-x)}{na_\infty}\right]^{m/2} \cdot e^{+\rho x/na_\infty} \cdot L^m_{k+m}\left[\frac{2\rho(1-x)}{na_\infty}\right]\right\}\end{aligned} \tag{6}$$

according to Eq. (4).

Thus the form of the wave function and the value of the energy levels are known for the two limits of ρ. Presumably the wave functions and energy levels will change continuously from one form to the other as ρ changes from ∞ to 0. The curves obtained for the energy levels will represent the electronic energies and, by adding the repulsion energy $Z^2e^2/2\rho$, the potential energy curves will be obtained.

The Oscillatory Properties of Ψ

It is possible to tell qualitatively where these electronic energy curves go (i.e., which states $W_0(n_r n_\phi n_\theta)$ are connected to the states $W_\infty(n_\eta n_\phi n_\xi)$ by continuous curves) by a study of the oscillatory properties of the wave function Ψ for any separation.

It has been shown above that

$$\Psi = N \cdot \Phi(\phi) \cdot Y(y,\rho) \cdot X(x,\rho)$$

where the function $\Phi(\phi)$ is always $e^{im\phi}$ no matter what the value of ρ. The surfaces $Y=0$, $X=0$ and (real part of Φ) $=0$ are called nodal surfaces, and are coordinate surfaces with either ϕ, y or x constant, where Ψ is zero or pure imaginary. As ρ is varied these surfaces change in shape and position but can never change in number, due to the inherent character of the Schroedinger equation.[13] The number of nodes in any coordinate at a finite distance from the nucleus corresponds to the quantum number in that coordinate, and in the case considered the total number of nodes plus one equals the total quantum number n. The meaning of these quantum numbers in terms of a molecular model has been discussed by Mulliken.[7]

The quantum number n_ϕ represents the number of nodal surfaces in ϕ. The number of nodal surfaces in y is called n_η; when $\rho=0$ this becomes n_r, and when $\rho=\infty$ it is n_η. The number of nodal surfaces in x equals n_ξ, and

[13] One of us (P. M. M.) will shortly publish a paper dealing with the general properties of these nodal surfaces, and a proof of the above propositions will be included.

when $\rho=0$ it becomes n_θ. The nodes in ϕ are planes in which lies the nuclear axis, and those in y are ellipsoids with the nuclei as foci. The nodes in x are hyperboloids with the nuclei as foci, and as the nuclear separation increases these last surfaces separate out; if n_x is an even number half of them stay about one nucleus and half about the other and $n_x=2n_\xi$; but if n_x is odd one surface stays midway between the nuclei and when $\rho=\infty$ it is an infinite distance from either nucleus, so that $n_x-1=2n_\xi$. No more than one nodal surface can be an infinite distance from either nucleus, for in this space midway between them the potential energy is greater than W and from the nature of the Schroedinger equation, only one nodal surface can be present in such a region.

Therefore it can be seen that for $\rho=\infty$ a hydrogen atom having the quantum numbers n_η, n_ϕ, and n_ξ and having the energy $W_\infty(n_\eta n_\phi n_\xi)=R/(n_\eta+n_\phi+n_\xi+1)^2$, plus a nucleus, will become a molecule having quantum numbers $n_y=n_\eta$; $n_\phi=n_\phi$ and $n_x=2n_\xi$ or $=2n_\xi+1$ according as there is or is not a nodal plane midway between the nuclei. This molecule will, when $\rho=0$, become a united atom with quantum numbers $n_r=n_\eta$; $n_\phi=n_\phi$ and $n_\theta=2n_\xi$ or $=2n_\xi+1$, having the energy

$$W_0(n_r n_\phi n_\theta)=4R/(n_\eta+n_\phi+2n_\xi+1)^2$$

or

$$=4R/(n_\eta+n_\phi+2n_\xi+2)^2.$$

As ρ changes from infinity to zero W_ρ changes from the above set of values of W_∞ to the corresponding set of pairs of W_0. Thus there is an additional degeneracy in W_∞ due to the possibility of the presence or absence of this central node in x; when this node is absent the electronic state of the molecule is called symmetric, when present the state is called antisymmetric with respect to the nuclei.

As the nuclei are brought together the total quantum number n changes from $(n_\eta+n_\phi+n_\xi+1)$ to $(n_\eta+n_\phi+2n_\xi+1)$ for the symmetric case or to $(n_\eta+n_\phi+2n_\xi+2)$ for the antisymmetric, and therefore n changes in value unless $n_\xi=0$ and the molecule is symmetric. Such an increase in n is called promotion. The maximum promotion possible is a doubling of n and occurs when $n_\eta=n_\phi=0$ and the molecule is antisymmetric. In this case $W_0=W_\infty$.

The energy levels for $0<\rho<\infty$ will be labelled by the new Hund notation,[6] the number indicating the value of $n(=n_y+n_\phi+n_x+1)$ the Roman letter (in the sequence s, p, d, f, g, $\cdots$,) indicating the value of n_x+n_ϕ, and the Greek letter (in the sequence σ, π, δ, ϕ, γ, $\cdots$,) indicating the value of n_ϕ. Thus a $3d\pi$ state is one in which $n=3$, $n_y=0$, $n_\phi=1$, and $n_x=1$. Since n and n_x undergo a change in value for $\rho=\infty$, but n_ϕ does not, the important letter in the label is the Greek one.

The connections between the W_0 and W_∞ labels can thus be calculated by the above formulas and labels can be given each connecting energy curve. It is perhaps well to consider several simple examples of this nodal argument in connecting the W_0 and W_∞ levels. The task is to follow the changes in the nodal surfaces as ρ goes from zero to infinity or vice versa.

The normal state of the united atom, He^+, has no nodal surfaces, and its energy is $4R$. When the nuclei are separated the wave function separates into two portions, each concentrated about a nucleus, and each of the same sign. Therefore when $\rho = \infty$ there will still be no nodal surface and the energy of the system will be that of the normal state of the hydrogen atom, R. This energy curve $4R \rightarrow R$ is labelled the $1s\sigma$ state.

When $n = 2$ for the united atom the energy is R and there are three possibilities for the one nodal surface. It can be in r, in which case the nodal surface is a sphere. Then when $\rho > 0$, $r \rightarrow \rho y$ and the sphere becomes an ellipsoid. When $\rho = \infty$ the ellipsoid becomes two paraboloids, one about each nucleus, and so there is still a nodal surface near each nucleus, and the energy level for the separated atom is the second hydrogen atom level, $R/4$. This state is labelled $2s\sigma$.

If the nodal surface is in ϕ, the surface will still be through each nucleus when $\rho = \infty$, and so this state, called the $2p\pi$, also has an energy going from R to $R/4$.

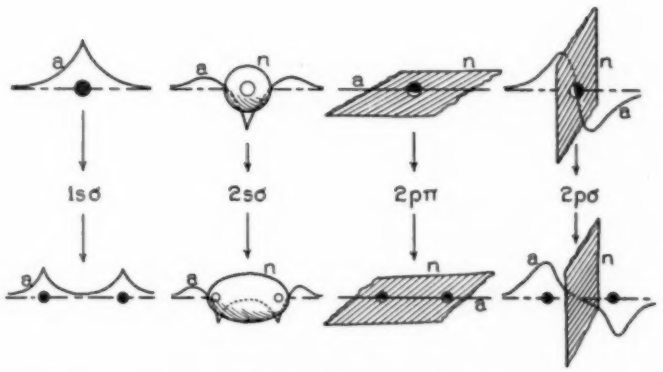

Fig. 1. Behavior of the nodal surfaces. Small circles represent the nuclei, shaded surfaces n the nodal surfaces and curves a the values of ψ along the axis.

If, however, the node is in θ, then when $\rho > 0$, the two nuclei will separate, leaving the nodal plane halfway between them and perpendicular to the nuclear axis. When $\rho = \infty$ this plane will be an infinite distance from either nucleus, and the energy of the system is R, that of a hydrogen atom in the normal state. This state is called the $2p\sigma$ state, and when $\rho = \infty$ it differs from the $1s\sigma$ state only in the fact that the wave function about the two nuclei are of opposite sign. In other words, the $1s\sigma$ state corresponds to the symmetric case and the $2p\sigma$ state to the antisymmetric.

Figure 1 shows these four states and the change in the nodal surfaces. The value of the wave function along the nuclear axis is also given.

The general study above developed will show that the following levels for separated and united atoms must be connected by curves.

It should be noted that states where the Greek and Roman letters are the same are unpromoted states, for a difference between the two letters

would indicate a node in x, and these nodes are the ones which cause promotion. It should also be noted that this scheme differs from that which Hund published at first,[3] but coincides with his latest scheme.[6]

TABLE I

United Atom		Molecule		Separated Atom	
Energy	Quantum No. for He^+ $n\,n_r n_\phi n_\theta$	Quantum No. for H_2^+ $n\,n_\eta n_\phi n_\chi$	State	Quantum No. for H $n\,n_\eta n_\phi n_\xi$	Energy
$4R$	1000	1000	$1s\sigma$	1000	R
R	2001	2001	$2p\sigma$ (promoted)	1000	R
R	2010	2010	$2p\pi$	2010	$R/4$
R	2100	2100	$2s\sigma$	2100	$R/4$
$4R/9$	3101	3101	$3p\sigma$ (promoted)	2100	$R/4$
$4R/9$	3002	3002	$3d\sigma$ (promoted)	2001	$R/4$
$4R/9$	3011	3011	$3d\pi$ (promoted)	2010	$R/4$
$4R/9$	3020	3020	$3d\delta$	3020	$R/9$
$4R/9$	3110	3110	$3p\pi$	3110	$R/9$
$4R/9$	3200	3200	$3s\sigma$	3200	$R/9$
$R/4$	4003	4003	$4f\sigma$ (dbly. prom.)	2001	$R/4$
$R/4$	4102	4102	$4d\sigma$ (promoted)	3101	$R/9$
$R/4$	4201	4201	$4p\sigma$ (promoted)	3200	$R/9$
$R/4$	4012	4012	$4f\pi$ (promoted)	3011	$R/9$
$R/4$	4111	4111	$4d\pi$ (promoted)	3110	$R/9$
$R/4$	4021	4021	$4f\delta$ (promoted)	3020	$R/9$
$R/4$	4030	4030	$4f\phi$	4030	$R/16$
$R/4$	4120	4120	$4d\delta$	4120	$R/16$
$R/4$	4210	4210	$4p\pi$	4210	$R/16$
$R/4$	4300	4300	$4s\sigma$	4300	$R/16$

Any approximate quantitative values obtained for the various energies as functions of ρ must be joined so that they satisfy the requirements of this scheme.

PERTURBATION METHOD I

There are two different methods of obtaining these approximate values. The first is to consider the wave function of the molecule to be that of the united atom, Ψ_0, in the first approximation, and to study the perturbation of the energy levels of the united atom when ρ is made greater than zero. The perturbing energy will be the difference between the potential field due to the united nuclei and the field due to the two nuclei a small distance 2ρ apart. This method will not be valid for large values of ρ, values, say, larger than $a/2$, but it will serve to indicate how the various degenerate levels of the united atom split.

A slightly better approximation is to consider as the unperturbed wave function not the Ψ_0 for the He^+ ion with $Z=2$, but a wave function for an ion with such a Z' that the first order perturbation of the corresponding energy, due to the separation of the nuclei and increase of their joint charge to $2e$, is zero. This has the effect of increasing the spread of the unperturbed wave function, and although this "stretching" is spherically symmetric, it approximates the true wave function better than the "unstretched" function.

The function used is that in Eq. (3) with Z changed to Z' and a_0 to a_0', and Z' left undetermined for the time being.

The theory of perturbations of a degenerate system[14] is that the various perturbations of the energy levels W resulting from one degenerate level $W_0(n)$ are to be found by the equation

$$\begin{vmatrix} (W_{nlm}^{nlm}-W) & W_{nlm}^{nlm'} & W_{nlm}^{nl'm'} & \cdots \\ W_{nlm'}^{nlm} & (W_{nlm'}^{nlm'}-W) & W_{nlm'}^{nl'm'} & \cdots \\ W_{nl'm'}^{nlm} & W_{nl'm'}^{nlm'} & (W_{nl'm'}^{nl'm'}-W) & \cdots \\ \cdot & \cdot & \cdot & \cdots \\ \cdot & \cdot & \cdot & \cdots \end{vmatrix} = 0 \qquad (7)$$

where n is the principal quantum number, and l, l', m and m' are various values of the quantum numbers with respect to which the system is degenerate; and where

$$W_{nl'm'}^{nlm} = \int \Psi_0(nlm) \cdot \bar{\Psi}_0(nl'm') \cdot V_1 dv$$

where dv is the volume element and V_1 is the perturbation of the potential energy. The actual energy $W(nrs)$ of any one of these resultant levels is then $W_0(n)$ plus one of the roots of Eq. (7). If all the non-diagonal terms of the type $W_{n^n l'^l m'^m}$ and $W_{n^n l^{l'} m^{m'}}$, are zero for a particular l and m then the root corresponding will be $W = W_{n^n l^l m^m}$, and r and s can be indentified with the quantum numbers l and m of the unperturbed wave function. Otherwise r and s cannot be identified with l and m, but represent quantum numbers corresponding to a new coordinate system. In other words, if the coordinate system for the perturbed function is in the first approximation equal to the principal coordinate system for the unperturbed function then r and s can be identified with l and m. But if these two coordinate systems are not equal in the first approximation then the two quantum number sets cannot be identified and non-diagonal terms appear in the above determinant. The problem is to choose a coordinate system for the unperturbed function by proper combination of the wave functions such that this determinant is all diagonal, and failing this, to make it have as few non-diagonal terms as possible.

In the case considered, symmetry shows that sperical coordinates are the best ones to use for Ψ_0. The perturbing energy

$$V_1 = (Z'e^2/r) - (Ze^2/2r_1) - (Ze^2/2r_2)$$

Here $Z = 2$ and Z' will be determined later to make the perturbation energy zero. These last terms can be expanded in a series of Legendre polynomials, and

[14] E. Schroedinger, Ann. d. Physik 80, 452 (2926).

$$V_1\begin{cases}=\dfrac{Z'e^2}{r}P_0-\displaystyle\sum_{\alpha=0}^{\infty}\frac{Ze^2\rho^{2\alpha}}{r^{2\alpha+1}}P_{2\alpha}(\cos\theta) & \text{when} \quad r>\rho \\ =\dfrac{Z'e^2}{r}P_0-\displaystyle\sum_{\alpha=0}^{\infty}\frac{Ze^2r^{2\alpha}}{\rho^{2\alpha+1}}P_{2_\infty}(\cos\theta) & \text{when} \quad r<\rho.\end{cases} \tag{8}$$

Using the unperturbed wave function from Eq. (3), the perturbation energy becomes a function of n, l, l' and m, ρ and $a_0'(=a/2Z')$, namely, $W_{n^n l^{l'} m}{}^m$

Since the angle ϕ only enters in the $e^{im\phi}$ factor the above energy cannot be non-diagonal in m and the only non-diagonal terms possible will be those in l as is shown. An application of the recurrence formulas of the type:

$$P_0P_l{}^m=P_l{}^m$$

$$P_2P_l{}^m=\frac{1}{2(2l-1)(2l+1)(2l+3)}[3(2l+3)(l+m)(l+m-1)P_{l-2}^m \tag{9}$$
$$+2(2l+1)(l^2+l-3m^2)P_l{}^m+3(2l-1)(l-m+1)(l-m+2)P_{l+2}^m]$$

etc.

shows that $W_{n^n l^{l'} m}{}^m$ (for $l\neq l'$) is zero unless $l=l'+2s$ where s is an integer. This can only happen when n is 3 or greater and therefore there will be no non-diagonal terms in the first two levels, and but one pair when $n=3$.

The expressions for these energies were calculated for the first three values of n and the exponentials expanded to give a series in $c=d/a=2\rho/a$, the distance between the nuclei in terms of the first Bohr orbit of the hydrogen atom as a unit. For instance

$$W_{100}^{100}=R\left[8e^{-2cZ'/Z}\left(\frac{Z'}{Z}+\frac{1}{c}\right)-(8/c)+8(Z'/Z)^2\right]$$

is expanded into a series in c, and the perturbed energy

$$W(1s\sigma)=R[8g-4g^2-16c^2g^3/3+16c^3g^4/3-16c^4g^5/5+64c^5g^6/45+\cdots]$$

where $g=Z'/Z$. In this lowest state the series converges quite slowly and is not as well adapted for calculation as the actual energy expression. For the higher states, however, the series is a satisfactory approximation of the complicated set of exponentials in the actual expression, and is simpler than it.

The quantity $g(=Z'/Z)$ is adjusted so that $W_{100}^{100}=0$ for a given c. Then the energy $W(1s\sigma)=4Rg^2$ is equal to the perturbed energy for the particular value of c chosen. This method "stretches" the wave function as discussed earlier. However, in the higher states, especially when $n>2$, the difference $1-g$ is very small, and it is then easier and nearly as accurate to set $g=1$ and compute the resulting value of $W_{n^n l^l}{}_m{}^m$ as a function of c, and add it to $W_0(n)=4R$ to obtain the perturbed energy.

The series for the various perturbed energies for the higher states are tabulated in Table II as functions of c.

TABLE II.

$$W(2p\sigma)=R[2g-g^2+2g^3c^2/15-9g^5c^4/140+7g^6c^5/180+\cdots]$$
$$W(2p\pi)=R[2g-g^2-g^3c^2/15+g^5c^4/140-g^6c^5/180+\cdots]$$
$$W(2s\sigma)=R[2g-g^2-2g^3c^2/3+2g^4c^3/3-7g^5c^4/20+11g^6c^5/90+\cdots]$$
$$W(3p\sigma)=R\left\{\frac{4}{9}+\frac{16e^{-2c/3}}{405}[c^2+2c^3/3-22c^4/\ 63+\ 8c^5/567+\cdots]\right\}$$
$$W(3d\pi)=R\left\{\frac{4}{9}+\frac{8e^{-2c/3}}{2835}[c^2+2c^3/3+20c^4/163-\ 4c^5/\ 81+\cdots]\right\}$$
$$W(3d\delta)=R\left\{\frac{4}{9}-\frac{16e^{-2c/3}}{2835}[c^2+2c^3/3+17c^4/\ 81+10c^5/729+\cdots]\right\}$$
$$W(3p\pi)=R\left\{\frac{4}{9}-\frac{8e^{-2c/3}}{405}[c^2+2c^3/3+2\ c^4/\ 21+\ 8c^5/567+\cdots]\right\}$$

The two states having a non-diagonal term are

$$W^{320}_{320}=R\frac{32e^{-2c/3}}{2835}[c^2+2c^3/3+8c^4/9+8c^5/27+\cdots]$$
$$W^{300}_{300}=-R\frac{16e^{-2c/3}}{81}[c^2-c^3/3+c^4/15+0+\cdots]$$
$$W^{320}_{300}=R\frac{8e^{-2c/3}}{225(2)^{1/2}}[19c^2/9-8c^3/27-16c^4/567-4c^5/1601+\cdots].$$

And the resulting energy levels are

$$W(3s\sigma)=4R/9+\frac{(W^{300}_{300}+W^{320}_{320})}{2}+\left[\frac{(W^{300}_{300}-W^{320}_{320})^2}{4}+(W^{320}_{300})^2\right]^{1/2}$$
$$W(3d\sigma)=4R/9+\frac{(W^{300}_{300}+W^{320}_{320})}{2}-\left[\frac{(W^{300}_{300}-W^{320}_{320})^2}{4}+(W^{320}_{300})^2\right]^{1/2}$$

The values of the energies in units of R are given in Table III for five values of c.

TABLE III

State \ c	0	0.25	0.50	0.75	1.00
$1s\sigma$	4.000	3.742	3.318	3.015	2.750
$2p\sigma$	1.000	1.008	1.031	1.065	1.120
$2p\pi$	1.000	.996	.980	.955	.921
$2s\sigma$	1.000	.968	.910	.861	.822
$3p\sigma$	.444	.446	.453	.462	.471
$3d\sigma$	.444	.445	.449	.455	.465
$3d\pi$	.444	.444	.446	.447	.450
$3d\delta$	.444	.444	.443	.441	.439
$3p\pi$	.444	.443	.439	.434	.428
$3s\sigma$	.444	.434	.412	.387	.363

Notice that the sequence of the levels does not agree with that given by Hund[3,6] for small values of nuclear separation. Hund's sequence, however, was obtained by a purely qualitative process, and so is likely to be in error. Furthermore the calculations here have assumed no relativity or spin fine structure separation of the levels in the excited levels in the united atom. This would impose a different sequence of very small energy dif-

ferences for very small values of c; but this sequence would soon be wiped out, for the sequence given above would soon become the predominating one.

Notice also that the energies of all the promoted states are perturbed downward (i.e., these energies become larger numerically) and those of the unpromoted states are perturbed upward.

Perturbation Method II

The second method of obtaining approximate values of the energy as a function of ρ is a modification of the method used by Heitler and London,[15] utilizing the fact that Ψ is known for $\rho=\infty$, and has been given by Eq. (6). It can be assumed that to the first approximation Ψ retains its form as ρ is made "less than" infinity. The change in the energy levels will be due to the slight effect of the distant nucleus on the electron. When the electron is about the first nucleus the perturbing energy is e^2Z_∞/r_2, and when about the second nucleus is e^2Z_∞/r_1. Thus when $\Psi\bar{\Psi}\ V_1dv$ is integrated in the range $-1\leqq x\leqq 0$, V_1 is $-Z_\infty e^2/r_2=-Z_\infty e^2/\rho(y-x)$, and in the range $0\leqq x\leqq+1$ it is $-Z_\infty e^2/r_1=-Z_\infty e^2/\rho(y+x)$.

When $\rho<\infty$ the normalizing factor is no longer N_∞, and the best way to determine it is by actual integration. From Eq. (4), $(N_\rho)^{-2}=\frac{1}{2}\int\psi_1^2dv+\frac{1}{2}\int\psi_2^2dv \pm\int\psi_1\psi_2dv$. But the first terms are equal and so $(N_\rho)^{-2}=\int\psi_1^2dv\pm\int\psi_1\psi_2dv=N_A\pm N_B$, for convenience, where, if $b=\rho/na_\infty$, $u=yb$ and $v=xb$

$$N_A=2\pi(na_\infty)^3\int_1^\infty[2(u-b)]^m\cdot e^{-u}\cdot[L^m_{n-k-1}(2u-2b)]^2\cdot du \cdot\int_{-1}^1(u^2-v^2)\cdot[2(b+v)]^m\cdot e^{-v}\cdot[L^m_{k+m}(2b+2v)]^2dv \tag{10}$$

$$N_B=2\pi(na_\infty)^3\int_1^\infty[2(u-b)]^m\cdot e^{-u}\cdot[L^m_{n-k-1}(2u-2b)]^2\cdot du \cdot\int_{-1}^1(u^2-v^2)[4(b^2-v^2)]^{m/2}\cdot L^m_{k+m}(2b+2v)\cdot L^m_{k+m}(2b-2v)\cdot dv. \tag{11}$$

Similarly the integral

$$V_1dv=V_A\pm V_B=-2\pi e^2Z(na_\infty)^2\int_1^\infty[2(u-b)]^m\cdot e^{-u}\cdot[L^m_{n-k-1}(2u-2b)]^2\cdot du \cdot\int_{-1}^1\{(u-v)\cdot[2(b+v)]^m\cdot e^{-v}\cdot[L^m_{k+m}(2v+2b)]^2 +(u-v)[2(b-v)]^m\cdot e^{+v}\cdot[L^m_{k+m}(2b-2v)]^2 \pm 2(u-v)[4(b^2-v^2)]^{m/2}\cdot L^m_{k+m}(2b+2v)\cdot L^m_{k+m}(2b-2v)\}dv \tag{12}$$

and the perturbed energy is thus

$$W(n,k,m)=W_\infty(n)+V_A/(N_A\pm N_B)\pm V_B/(N_A\pm N_B)$$
$$=W_\infty(n)+A\pm B.$$

[15] Heitler and London, Zeits. f. Physik **44**, 455, (1927).

The plus sign is taken for the symmetric case and the minus for the antisymmetric.

The non-diagonal terms in the energy determinant of Eq. (7) are all zero here, for the wave functions have been so chosen that $\psi_1/(r_2)^{1/2}$ is orthogonal for different values of n, k and m, and the integral of the product of a symmetric and antisymmetric Ψ gives the difference between two equivalent integrals, and is thus also zero.

The perturbed energies $W(n,k,m)$ have been calculated for the states $n=1$ and $n=2$ as functions of c. They are given in Table IV.

TABLE IV

$$W(1s\sigma)=R\left[1+\frac{4}{c}\cdot\frac{2+(c^2+2c+2)e^{-c}}{4+(4c^2/3+4c+4)e^{-c}}\right]$$

$$W(2p\sigma)=R\left[1+\frac{4}{c}\cdot\frac{2-(c^2+2c+2)e^{-c}}{4-(4c^2/3+4c+4)e^{-c}}\right]$$

$$W(2s\sigma)=R\left[\frac{1}{4}+\frac{4-2e^{-c}-2e^{-c/2}+(c^2/4+3c)e^{-c/2}}{(2c+6)-(c+6)e^{-c}+(c^3/12+3c^2/2+7c)e^{-c/2}}\right]$$

$$W(3p\sigma)=R\left[\frac{1}{4}+\frac{4-2e^{-c}-2e^{-c/2}-(c^2/4+3c)e^{-c/2}}{(2c+6)-(c+6)e^{-c}-(c^3/12+3c^2/2+7c)e^{-c/2}}\right]$$

$$W(3d\sigma)=R\left[\frac{1}{4}+\frac{4+(2c+2)e^{-c}-(c^2/2+2c+6)e^{-c/2}+(5c^4/96-c^3/12-3c^2/4+c)e^{-c/2}}{(2c-6)+(c^2+5c+6)e^{-c}+(c^3/60-c^3/4-c^2/2+c)e^{-c/2}}\right]$$

$$W(4f\sigma)=R\left[\frac{1}{4}+\frac{4+(2c+2)e^{-c}-(c^2/2+2c+6)e^{-c/2}-(5c^4/96-c^3/12-3c^2/4+c)e^{-c/2}}{(2c-6)+(c^2+5c+6)e^{-c}-(c^3/60-c^3/4-c^2/2+c)e^{-c/2}}\right]$$

$$W(2p\pi)=R\left[\frac{1}{4}+\frac{1}{2c}\cdot\frac{8-2ce^{-c}-(2c+8)e^{-c/2}+(\pi c^3/8-c^3/6+\pi c^2/8)e^{-c/2}}{2-(c/2+2)e^{-c}+(3\pi c^3/256+\pi c^2/8+3\pi c/8)e^{-c/2}}\right]$$

$$W(3d\pi)=R\left[\frac{1}{4}+\frac{1}{2c}\cdot\frac{8-2ce^{-c}-(2c+8)e^{-c/2}-(\pi c^3/8-c^3/6+\pi c^2/8)e^{-c/2}}{2-(c/2+2)e^{-c}-(3\pi c^3/256+\pi c^2/8+3\pi c/8)e^{-c/2}}\right]$$

The values of these energies in units of R are given for several values of c in Table V.

TABLE V

State \ c	3	4	5	7.5	10	20	∞
$1s\sigma$	1.702	1.516	1.405	1.269	1.200	1.100	1.000
$2p\sigma$	1.454	1.442	1.377	1.260	1.200	1.100	1.000
$2p\pi$	.698	.619	.555	.475	.450	.350	.250
$2s\sigma$	.642	.572	.508	.455	.400	.337	.250
$3p\sigma$	.443	.428	.421	.408	.400	.337	.250
$3d\sigma$	.671	.712	.700	.618	.520	.367	.250
$3d\pi$	.575	.580	.550	.475	.450	.350	.250
$4f\sigma$	.524	.610	.571	.550	.520	.367	.250

The calculations become invalid for small values of c since the wave function in this case is no longer even approximately like that for $c=\infty$. Due to the character of the wave function it should be expected that the calculations for the promoted states will cease to be valid at a larger c than those for the unpromoted states. In no case, however, should it be expected that this perturbation method be valid for c less than 3 or 4. Several curves

when extended to $c=1$ coincided almost exactly with the value of the energy calculated by method I. This was considered fortuitous however, for several other curves gave wide discrepancies at $c=1$.

So the method used was to plot the curves obtained by method I from $c=0$ to $c=1$, and those obtained by method II from $c=3$ to $c=\infty$, and to

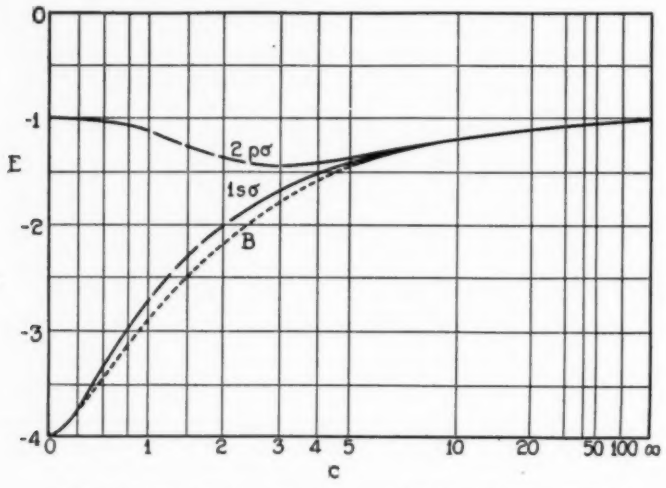

Fig. 2. Electronic energy curves for lowest two states.

fill in the intermediate gaps by a smooth curve. In case of any doubt as to which curve joins which, the nodal reasoning discussed earlier is the criterion used.

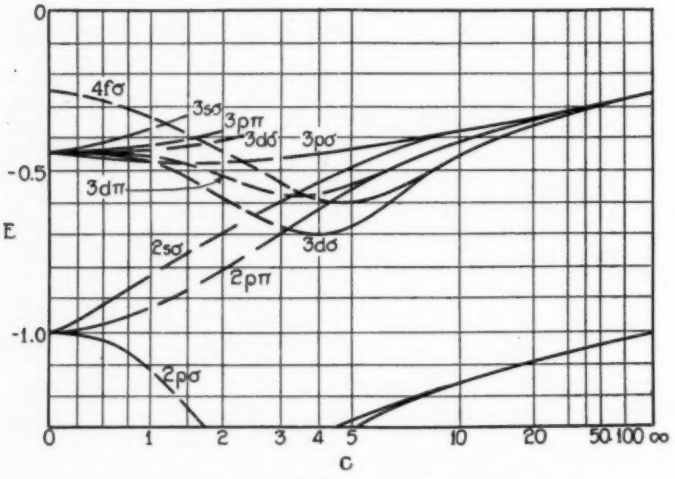

Fig. 3. Electronic energy curves for upper states.

Fig. 2 shows curves for the $1s\sigma$ and $2p\sigma$ states. The abscissa is in terms of $10c/(c+5)$ in order to get the whole range $0 \leqq c \leqq \infty$ in the figure. The ordinate is in terms of R. The solid lines represent the parts of the curves which could be calculated, and the intermediate dashed lines represent the

extrapolated portions. The dotted line below the $1s\sigma$ curve is that calculated by Burrau for this same state and is probably fairly correct throughout the whole range of c. This is the only independent check available for the curves, but the good agreement indicates that the other curves are not far from the actual values.

Fig. 3 shows the curves for the other levels on a magnified energy scale.

These curves are but the electronic energies as functions of c. The potential energy $V(nlm)$ of the molecule is the electronic energy plus the energy of repulsion of the nuclei $E_n = Z_\infty^2 e^2/d$. Potential energy curves for all the various states are shown in Fig. 4.

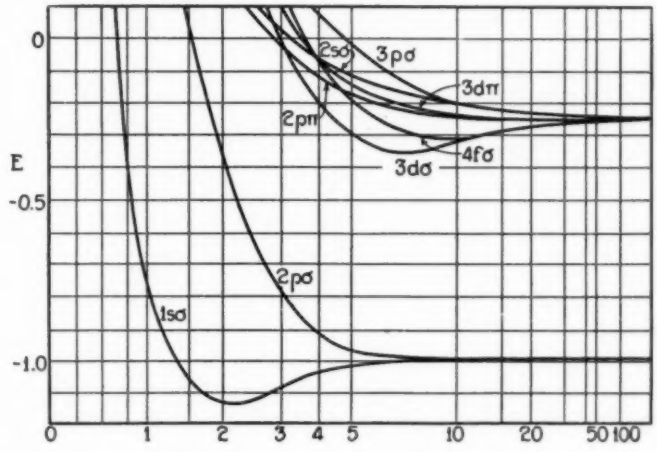

Fig. 4. Potential energy curves.

Only three of these curves show minima, those corresponding to the $1s\sigma$, the $3d\sigma$ and the $4f\sigma$ states. Therefore to this degree of approximation the molecule H_2^+ is only stable in these three states of all the ones considered. The other states, with their curves, cannot be considered as having no meaning however, for transitions from stable to unstable states have been used to explain certain experimental results.[16,17]

The value of V at the minimum point shall be called $V_m(nlm)$, and the value of c at the minimum shall be $c_m(nlm)$. The values of the calculated V_m are

$$V_m(1s\sigma) = 1.142R = 15.49 \text{ volts}$$
$$V_m(3d\sigma) = 0.350R = 4.74 \text{ volts}$$
$$V_m(4f\sigma) = 0.309R = 4.19 \text{ volts}.$$

The energy of dissociation $E_D(nlm)$ is the difference $W_\infty - V_m$, and has the values

$$E_D(1s\sigma) = 0.142R = 1.93 \text{ volts}$$
$$E_D(3d\sigma) = 0.100R = 1.35 \text{ volts}$$
$$E_D(4f\sigma) = 0.059R = 0.80 \text{ volts}.$$

[16] Winans and Stueckelberg, Proc. Nat. Acad. **14**, 867 (1928).
[17] Smyth and Condon, Proc. Nat. Acad. **14**, 871 (1928).

The value for the normal state agrees fairly well with the one experimentally determined value available. This value is the ionization potential of H_2, which is 16.1v.[18] The value given here would be the ionization potential of H, 13.5v, plus the dissociation energy of H_2, 4.3v, minus the difference between W_∞ and the $1s\sigma$ curve at $c=1.6$ (the equilibrium separation of the H_2 normal state), 1.5v, giving a value of 16.3v as ionization potential of H_2 expected from these curves.

The values of c_m are

$$c_m(1s\sigma)=2.1a=1.12\times10^{-8}\text{ cm}$$
$$c_m(3d\sigma)=7.6a=4.10\times10^{-8}\text{ cm}$$
$$c_m(4f\sigma)=9.4a=5.06\times10^{-8}\text{ cm}.$$

These values of c may differ considerably from the correct values, since all three minima fall on the portion of the curve which is least accurately known. It is possible that the true values are all somewhat smaller than those calculated.

There are few experimental data available to check these curves. C. J. Brasefield is at present making measurements on the electronic bands corresponding to these levels, and so an experimental check should be forthcoming shortly.

The results above have been rather surprising, since it has been expected that all unpromoted states have minima and that no promoted state could have a minimum.[7] There has been no theoretical justification for this expectation, however, and the above results show it to be erroneous. For even if the minima for the two promoted states $3d\sigma$ and $4f\sigma$ are not actually as deep as these first approximations indicate, the curves for both these states start downward as c is decreased from infinity, and at $c=20$, where the first approximation should still give fairly accurate results, the energy for these two states is definitely below the value of W_∞; thus showing that they must have a minimum point and a finite c_m. It seems fairly certain that the pair of states $2s\sigma$ and $3p\sigma$ have no minimum, for the energy curves corresponding to these states are above W_∞ for every finite value of c. Thus two promoted states, $3d\sigma$ and $4f\sigma$, have minima, and one unpromoted state, $2s\sigma$, has no minimum.

However the energies for the levels $2p\pi$, $3d\pi$ remain practically equal to W_∞ throughout the range $\infty \geqq c > 10$, and a second approximation may show that these states have slight minima. But these minima, if they exist, will have large values of c_m and small values of E_D, and so will be relatively unstable.

No determination was made of the size of the second or higher orders of approximation, due to the prohibitive difficulty of such calculations. There is no proof that the method of successive approximations used above gives such a rapidly converging series that the first term is sufficient or even in-

[18] E. Franck und P. Jordan, Anregung von Quantensprüngen Hand. d. Phys. XXIII. Springer, Berlin (1926).

dicative, except that in the cases where calculation by other methods and where experimental data were available these first terms checked fairly well.

Work is being carried on by V. Guillemin and C. Zener to obtain these same curves by a completely different method of approximation. It will greatly strengthen belief in the general validity of the wave-mechanical perturbation methods if these new curves check the ones presented above.

Having now obtained the energy curves for one electron, the problem of the many electron diatomic molecule can be attacked next. For instance, the hydrogen molecular electronic energy can be considered as being due to the sum of the individual electronic energies as given above, plus the energy of interaction between the electrons. The writers are calculating a set of curves of this type.

The authors wish to express their appreciation of the aid rendered by Professor E. U. Condon in the preparation of this paper.

PALMER PHYSICAL LABORATORY,
PRINCETON UNIVERSITY,
February, 1929.

THE NEAR INFRA-RED ABSORPTION SPECTRA OF CALCITE AND STRONTIANITE

By E. K. Plyler

Abstract

A study of the near infra-red absorption spectra of calcite and strontianite has been made by using thick specimens. With a specimen 2 cm thick, cut at right angles to the optic axis, bands were observed for calcite at 1.76μ, 1.90μ, 2.00μ and 2.20μ. These bands have the same characteristics as those observed by Schaefer, Bermuth and Matossi in the near infra-red. The second order equations have been applied to the bands observed in this work and to those observed by Schaefer and it was found that series relationships existed between them with only small deviations of the observed from the calculated values. In strontianite a similar set of bands was observed at 1.89μ, 2.01μ and 2.19μ, and they were of the same type as those for calcite. The value of the inactive fundamental was calculated and found to correspond to a band at 9.2μ, which is in good agreement with the value of 8.98μ found theoretically by Nielsen.

Introduction

THE infra-red absorption spectra of several carbonates in crystal form have been measured by different observers.[1,2] Moreover, Schaefer and Schubert[3] have found regions of intense selective reflection at 6.7μ, 11.38μ and 14.16μ in the reflection spectra of calcite which they attributed to the fundamental vibrations of the carbonate ion. The band at 11.38μ was found to be due to a vibration along the optic axis and the bands at 6.7μ and 11.38μ were found to be due to vibrations at right angles to the optic axis. The absorption measurements of Schaefer, Bermuth and Matossi included the region from 2μ to 20μ and it was found that the spectra of the different carbonates studied had almost similar bands, from the standpoint of intensity and location, in the region from 2μ to 7μ. The bands in this region were attributed to the harmonics and the combinations of the fundamental vibrations of the carbonate ion.

From theoretical considerations Kornfeld[4] has shown that the carbonate ion should have three active and one inactive vibration, the inactive vibration corresponding to a band at about 8μ. Certain bands were found which were attributed to a combination including this inactive vibration but fairly large differences were found between the theoretical and calculated values. More recently Nielsen[5] has considered the vibrations of the carbonate ion from a point of view somewhat different from Kornfeld's and has

[1] Schaefer, Bermuth and Matossi, Zeits. f. Physik **39**, 648 (1926).
[2] Rawlins and Rideal, Proc. Roy. Soc. **A116**, 140 (1927).
[3] Schaefer and Schubert, Ann. d. Physik **50**, 283 (1916).
[4] Kornfeld, Zeits. f. Physik **26**, 205 (1924).
[5] Nielsen, Phys. Rev. **32**, 773 (1928).

obtained a value of about 9μ for the inactive fundamental which is in good agreement with the value obtained from observations of Schaefer.

The present work was undertaken in order to extend the bands of the carbonates into the near infra-red and to test the series relationships for this region.

Experimental Procedure

A clear section of calcite 2 cm thick was cut at right angles to the optic axis and was then placed in and out of a beam of radiation so that the relative transmission could be determined for each setting of the prism. A Hilger infra-red spectrometer with a quartz prism was used as the resolving instrument. The instrument was calibrated by means of certain lines and bands in the near infra-red which had been measured by other observers. A steady and intense source of radiation was obtained by sending a current of three amperes from a set of storage batteries through a piece of globar. The detecting system consisted of a linear thermopile connected in series

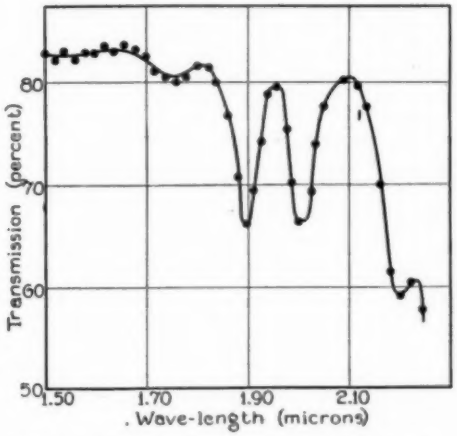

Fig. 1. The absorption spectra of calcite for a section 2 cm thick cut perpendicular to the optic axis.

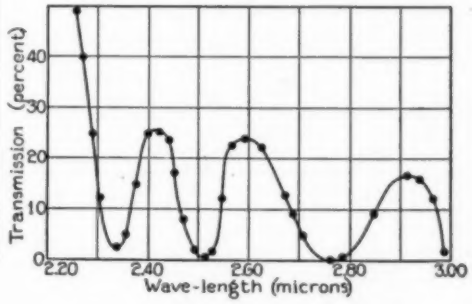

Fig. 2. The absorption spectra of calcite from 2.2μ to 2μ.

with a low resistance galvanometer having sensitivity of 10 mm per microvolt. The thermopile slit included about 0.02μ in the region of 2μ. The telescope and scale were two meters from the galvanometer, the average deflection was 15 cm, and each deflection was estimated to 0.02 cm. When the crystal was in the beam of radiation, the deflections were never smaller than 2 cm. In measuring the absorption of strontianite in the region from 1.5 to 2.5μ a section 6 mm thick cut perpendicular to the optic axis was used.

Results

The absorption spectrum for calcite in the region from 1.70μ to 2.64μ is shown in Fig. 1 and in Fig. 2. The bands at 2.34μ and 2.52μ were observed by Schaefer, Bermuth and Matossi, but those at 1.76μ, 1.90μ, 2.00μ and 2.20μ have not been previously reported. The region from 1.20μ to

1.50μ was also studied but no bands were found. In Fig. 3 the absorption bands of strontianite are shown. These are weaker and the transmission between the bands is not as large as for calcite. There were several cleavage fractures in the specimen and this probably caused the transmission to be less. Also, since the thickness of the crystal was 6 mm as compared with 2 cm for the calcite, a set of bands of less intensity might have been expected.

It has already been stated that all the observed bands for carbonates in the near infra-red are due to vibrations of the carbonate ion. The more intense of these may be identified with the harmonics of the band at about 6.7μ, called ν_1, or with combinations of ν_1 with ν_0, and ν_2 (ν_2 being used to denote the band at 13.78μ and ν_0 the inactive frequency corresponding to a band at 9μ). The three intense bands between the region ν_1 and $2\nu_1$ have been identified with the combinations $\nu_2+\nu_0$, $\nu_1+\nu_2$ and $\nu_1+\nu_0$ by Schaefer, Bermuth and Matossi[1] while those between $2\nu_1$ and $3\nu_1$, correspond to the combinations $\nu_1+\nu_2+\nu_0$, $2\nu_1+\nu_2$ and $2\nu_1+\nu_0$. The bands observed by the writer may be identified with the combinations $2\nu_1+\nu_2+\nu_0$, $3\nu_1+\nu_2$ and $3\nu_1+\nu_0$. Table I gives the observed and calculated positions of the bands together

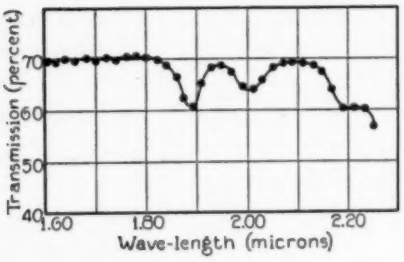

Fig. 3. The absorption spectra of strontianite for a section 6 mm thick.

TABLE I. *Observed and calculated bands of calcite and strontianite.*

Calcite			Strontianite	
Obs.	Cal.	Combination	Obs.	Cal.
1.76μ*	1.77μ	$4\nu_1$		1.80
1.90*	1.87	$3\nu_1+\nu_0$	1.89μ*	1.88
2.00*	2.00	$3\nu_1+\nu_2$	2.01*	2.02
2.20*	2.16	$2\nu_1+\nu_2+\nu_0$	2.19*	2.15
2.34*	2.33	$3\nu_1$	2.34	2.34
2.52*	2.53	$2\nu_1+\nu_0$	2.55	2.53
2.77*	2.78	$2\nu_1+\nu_2$	2.82	2.78
3.10	3.10	$\nu_1+\nu_2+\nu_0$	3.10	3.09
3.47	3.50	$2\nu_1$	3.45	3.45
3.92	3.96	$\nu_1+\nu_0$	3.97	3.94
4.64	4.64	$\nu_1+\nu_2$		
5.55	5.52	$\nu_2+\nu_0$		
	6.92	ν_1		6.75
13.92	13.92	ν_2	14.35	14.35
	9.20	ν_0		9.40

* Bands observed in the present work.

with their identification. The experimental values marked with an asterisk are those which have been found by the present investigation, the remainder for calcite are taken from the work of Schaefer. The calculated values differ from those of Schaefer because the values for ν_2 have been calculated from absorption rather than reflection and because the value of ν_1 has been determined by applying the second order equations to the observed frequencies of the harmonics. In the calculations only the more intense component of a complex band was considered. The bands of strontianite at 1.89μ, 2.01μ and

2.19μ have been observed in the present work and the other bands to 4μ have been observed by Rawlins and Rideal.[5] The fourth overtone of the intense band at 7μ was not observed. The check between the computed and experimental values is very good and it is found that the divergencies which do appear are not incompatible with the form of the second order correction terms.

It is of interest to note that the calculated value of the inactive frequency gives a value of 9.2μ which is in good agreement with the value of 8.98μ obtained theoretically by Nielsen. Taylor[6] has considered the supposition of an inactive fundamental being active in combination as somewhat artificial. However, this objection does not seem valid in view of the experimental and theoretical evidence, and especially since Wood[7] has recently shown that calcite gives a Raman effect line corresponding to a band at 9.19μ.

The calculated values of the two components of the fundamental at 6.7μ obtained from the observed values of the overtones, give values of 6.42μ and 6.92μ for the two maxima. An experimental study has been made of the reflection spectra of calcite in this region in order to see if these maxima were present. A Hilger infra-red spectrometer with a rock-salt prism was used as the resolving instrument. Four maxima were observed at 6.36μ, 6.54μ, 6.62μ and 7.05μ, the two components at 6.54μ and 7.05μ being much more intense. The reflection spectra are shown in Fig. 4 for this region. The writer[8] had previously noted the existence of these bands and at that time an attempt was made to identify the separate maxima with effects produced by the calcium atom. However, both theory and experiment point to the fact that the 7μ band of the carbonates is due to the carbonate ion and that the above interpretation is untenable. While all the bands observed for the carbonates have not been identified with combinations of the fundamental frequencies, yet the near infra-red bands may be arranged in three series which are found to correspond with simple combinations of the fundamentals.

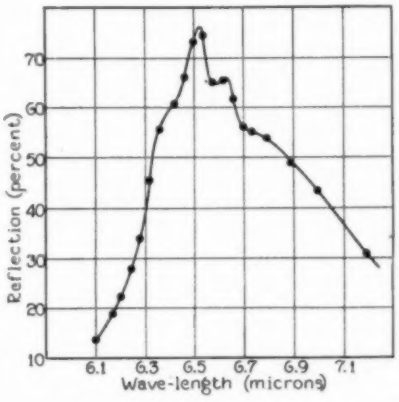

Fig. 4. The reflection spectra of calcite in the region of 7μ.

The writer is indebted to Professor D. M. Dennison for some suggestions made in reference to this work.

UNIVERSITY OF NORTH CAROLINA,
January 30, 1929.

[6] Taylor, Phil. Mag. **6**, 88 (1928).
[7] Wood, Phil. Mag. **6**, 729 (1928).
[8] Plyler, Science **55**, 578 (1927).

COMBINATION BANDS IN THE INFRA-RED SPECTRA OF CCl_4 AND $SiCl_4$

By H. H. Marvin

Abstract

It is assumed that the six Raman bands of CCl_4 found by Pringsheim and Rosen give the fundamental absorption frequencies. Simple combinations of these frequencies by addition account for all of the absorption bands between 1μ and 16μ, except a few very weak bands. The absorption bands of $SiCl_4$ in the same region are accounted for by similar combinations of six fundamental frequencies, four of which are known either as Raman bands or as resonance frequencies in the dispersion formula. The two systems of fundamental frequencies and their combinations are strikingly similar, as one might expect in consequence of the chemical similarity of the compounds.

Introduction

JULIUS[1] examined the absorption spectra of CCl_4 and $SiCl_4$ between 1μ and 10μ and found several bands in each. Coblentz[2] observed the spectrum of CCl_4 to 15μ, and discovered a very strong band, extending from 12.5μ to 13.5μ, which he was unable to analyse. Marvin[3] extended both spectra to 16μ, and studied the dispersion of each liquid in the same region. The strong CCl_4 band which Coblentz had discovered, was resolved into a doublet at 12.73μ and 13.09μ. This doublet was found to cause marked anomalous dispersion. Resonance wave-lengths had to be assumed at 12.64μ and 13.16μ in order to fit a dispersion formula to the data for CCl_4. Resonance bands had to be assumed likewise at 16.60μ and 47.12μ in the case of $SiCl_4$. The band last mentioned might be shifted considerably without spoiling the agreement between the dispersion formula and the data. The other bands are fixed within a few hundredths of a unit.

Pringsheim and Rosen[4] have recently found six bands in the spectrum of CCl_4 by means of the Raman effect. Three of these, at 46.07μ, 31.74μ, and 21.83μ are outside of the range of observations on absorption. The others, at 13.21μ, 12.61μ, and 6.50μ agree, within the limits of experimental error with absorption bands observed by Marvin. These observers have found one Raman band, at 23.47μ in the spectrum of $SiCl_4$.

Results

If we assume that the Raman bands correspond to fundamental modes of vibration in the molecule, we can account for all except the weakest CCl_4 absorption bands as fundamental bands or combination bands. The frequency of each combination band is the sum of two or more fundamental frequencies. The fundamental bands are denoted by the symbols $A, \ldots, F$, and the combination bands by $A+C$, etc., in the first column of Table I.

[1] Julius, Verh. d. Kongh. Akad. d. Wentenschaft, Amsterdam **1**, 1 (1892).
[2] Coblentz, Investigations of Infra-red Spectra Vol. I. (1905)
[3] Marvin, Phys. Rev. **34**, 161 (1912).
[4] Pringsheim and Rosen, Zeits. f. Physik **50**, 741 (1928).

The wave-numbers of bands $A, \ldots, F$, according to Pringsheim and Rosen, and the calculated wave-numbers for the combination bands appear in the second column. The calculated wave-lengths are given in the third column, and the wave-lengths of absorption bands observed by Marvin appear in the fourth column.

Columns five to eight, Table I, contain a similar tabulation for $SiCl_4$ which accounts for all except the weakest absorption bands. Bands B and D are assumed, without experimental evidence of their existence. Band E

TABLE I. *Calculated and observed absorption bands.*

CCl_4				$SiCl_4$			
Combination	Wave-number	Wave-length Calc.	Obs.	Combination	Wave-number	Wave-length Calc.	Obs.
A	217 cm^{-1}	46.07μ	—	A	233 cm^{-1}	42.92μ	—
B	315	31.74	—	B	323	30.96	—
C	458	21.83	—	C	426	23.47	—
$A+C$	675	14.82	14.89μ	D	522	19.16	—
D	757	13.21	13.09	E	600	16.67	—
E	794	12.61	12.73	$A+C$	659	15.17	15.13μ
$A+D$	974	10.27	10.21	$A+D$	755	13.24	13.21
$A+E$	1010	9.90	9.94	$A+E$	833	12.00	12.08
$B+B+C$	1088	9.19	9.13	$B+E$	923	10.83	10.75
$B+E$	1108	9.03		$C+D$	948	10.55	
$C+D$	1215	8.23	8.24	$C+E$	1026	9.75	9.74
$C+E$	1251	7.99	7.99	$D+D$	1044	9.58	9.65
$D+D$(*)	1514	6.60	—	$B+B+C$(*)	1072	9.33	—
F	1539	6.50	6.47	$D+E$	1122	8.91	8.92
$D+E$	1550	6.45	6.41	F	1220	8.20	8.20
$E+F$	2333	4.29	4.31	$E+F$	1820	5.50	5.53

at 16.67μ corresponds to the resonance band at 16.60μ, and A may correspond to the resonance band located, uncertainly, at 47.12μ. Band C is a Raman band, and F is an observed absorption band.

The CCl_4 band at 9.13μ is broad, and the two combinations $B+B+C$ and $B+E$ fall within in it. Combinations $B+E$ and $C+D$ fall within the broad $SiCl_4$ band at 10.75μ. Combination $D+D$, marked (*), in CCl_4 is masked by the band at 6.47μ, but there is a slight bend in the experimental curve at about 6.6μ; it is included in the table because the same combination is identified in $SiCl_4$. Likewise, $B+B+C$, marked (*), is masked in $SiCl_4$, but is indentified in CCl_4.

The band systems of CCl_4 and $SiCl_4$ are strikingly similar, as one might expect because of the chemical similarity of the compounds. Six fundamental bands appear in each system. The wave-lengths of the $SiCl_4$ bands A and B are shorter, and those of bands C, D, E, and F are longer than the wave-lengths of the corresponding CCl_4 bands. The same combinations appear in both systems. Combinations which contain B all correspond to weak absorption bands, but combinations which contain E, but not B, correspond to strong bands.

BRACE LABORATORY OF PHYSICS,
UNIVERSITY OF NEBRASKA,
February 25, 1929.

THE INTERACTION OF ELECTRON AND POSITIVE ION SPACE CHARGES IN CATHODE SHEATHS

By Irving Langmuir

Abstract

Effect of positive ions generated at a plane anode upon the space charge limitation of electron currents from a parallel cathode.—Mathematical analysis shows that single ions emitted with negligible velocity permit 0.378 $(m_p/m_e)^{1/2}$ additional electrons to pass; but with an unlimited supply of ions the electron current approaches a limiting value 1.860 times that which flows when no ions are present, and the electron current is then $(m_p/m_e)^{1/2}$ times the ion current, both currents thus being limited by space charge and the electric field being symmetrically distributed between the electrodes. Single ions introduced into a pure electron discharge at a point 4/9ths of the distance from cathode to anode produce a maximum effect, 0.582 $(m_p/m_e)^{1/2}$, in increasing the electron current. These conditions apply to a cathode emitting a surplus of electrons surrounded by ionized gas. The cathode sheath is then a double layer with an inner negative space charge and an equal outer positive charge, the field being zero at the cathode and at the sheath edge. The electron current is thus limited to $(m_p/m_e)^{1/2}$ times the rate at which ions reach the sheath edge. If ions are generated without initial velocities uniformly throughout the space between two plane electrodes, a parabolic potential distribution results. If the total ion generation exceeds 2.86 times the ion current that could flow from the more positive to the more negative electrode, a potential maximum develops in the space. Electrons produced by ionization are trapped within this region and their accumulation modifies the potential distribution yielding a region (named plasma) in which only weak fields exist and where the space charge is nearly zero. The *potential distribution in the plasma*, given by the Boltzmann equation from the electron temperature and the electron concentrations, *determines the motions of the ions* and thus fixes the rate at which the ions arrive at the cathode sheath. The *anode sheath* is usually also a positive ion sheath, but with anodes of small size a detached double-sheath may exist at the boundary of the anode glow. In discharges from *hot cathodes in gases* where the current is limited by resistance in series with the anode, the electron current is space-charge-limited, being fixed by the rate of arrival of ions at the cathode sheath. Thus the cathode drop is fixed by the necessity of supplying the requisite number of ions to the cathode. The *effect of the initial velocities of the ions and electrons* that enter a double-sheath from the gas is to decrease the electron current by an amount that varies with the voltage drop in the sheath. A nearly complete theory of this effect is worked out for plane electrodes. A detailed study is made of the *potential distribution in the plasma and near the sheath edge* for a particular case and the conclusion is drawn that the velocities of the ions that enter the sheath can be calculated from the electron temperature if the geometry of the source of ionization is given.

Experiments with double sheaths.—With large cathodes coated with barium oxide in low pressure mercury vapor, simultaneous measurements showed that the electron current density was independent of the cathode temperature and was from 140 to 200 times the ion current density, this ratio being independent of the intensity of ionization and of the gas pressure but varying slowly with the voltage drop in the cathode sheath, in good accord with the theory. The observed ratio, however, was about 40 percent of that calculated, this discrepancy being probably due to non-uniformity in the cathode coating. Similar results were obtained with double sheaths

on wire type cathodes, the ratio of the electron current to the ion current through the sheath ranging from 450:1 at high current densities to 2000:1 and more at very low currents, this variation being in agreement with the approximate theory developed for cylindrical sheaths. In these experiments *two cathodes* were used; one at rather large negative voltage to produce any desired intensity of ionization, while from the volt-ampere characteristics of the other cathode the space-charge-limited electron currents were measured. The ion currents were measured either by cooling the test cathode so that it emitted no electrons, or by the use of an auxiliary ion collector.

THE maximum electron current that can flow from a given hot cathode to an anode in high vacuum is limited by the space charge of the electrons.[1] If even a small amount of gas is present and the applied anode voltage is appreciably higher than the ionizing potential, the positive ions formed tend to neutralize the electron space charge and thus allow the current to increase until, with sufficient gas, the current becomes limited only by the electron emission from the cathode as determined by its temperature.

Since in a given electric field the ions move hundreds of times slower than the electrons, the rate at which the ions need to be produced in order to neutralize the space charge is usually less than one percent of the rate at which the electrons flow from the cathode. In formulating a quantitative theory for calculating the increase in electron current produced by a given amount of ionization we meet the difficulty that the ions are produced at different points within the gas and therefore are not all moving with the same velocity. Then, too, the probability of ionization as a function of the electron velocity must be known. The problem thus becomes so complicated that it seems hardly worth while to attempt a general solution.

About 13 years ago the writer derived the equations, given in the present paper, for the space charge problem between parallel planes where the cathode emits a surplus of electrons and the anode emits positive ions without initial velocities. The results, although interesting, did not seem to be applicable directly to experimental conditions and therefore the results were not published. Some years later,[2] however, by the discovery that all caesium atoms which strike a tungsten surface at 1300°K are converted into ions, it became practicable to generate positive ions at the anode in any desired number, and thus obtain the conditions which were assumed in the theory.

Still more recently in a study of gaseous discharges at low pressures[3] it was found that the space charge equations could be applied to the positive ion currents flowing to negatively charged collectors.

If we consider a negatively charged hot collector or in fact any hot cathode in a gas we see that there are present in the positive ion sheath electrons as well as ions. In the present paper it will be shown that the theory which was developed 13 years ago is now applicable to the calculation of the properties of these double sheaths.

[1] Langmuir, Phys. Rev. **2**, 450 (1913); Phys. Zeits. **15**, 348, 516 (1914).

[2] Langmuir and Kingdon, Proc. Royal Soc. **A107**, 61 (1925).

[3] Langmuir and Mott-Smith, Gen. Elec. Rev. **27**, 449, 538, 616, 762, 810 (1924), and Phys. Rev. **28**, 727 (1926).

Jaffe[4] has attempted to develop a theory of the effect of small amounts of gas ionization on currents limited by space charge in gases at low pressures. However, he based his entire treatment upon the inadmissible assumption that as many ions recombine in each element of volume as are produced by ionization within that volume. We now know that even with the high current densities in a mercury vapor arc carrying amperes, recombination of ions in the gas is negligible, compared to the removal of the ions by diffusion to the walls and to the electrodes. Thus the equations which Jaffe derived are not even approximately correct.

Theory of the Effect of Ions on Space Charge Currents Between Parallel Planes

Consider an infinite plane cathode C at zero potential, and a similar parallel plane anode A at the potential V_A and at a distance a from C. Let the cathode emit a surplus of electrons without appreciable initial velocities. There will thus be an infinite concentration of electrons at the cathode surface and the potential gradient will be zero, but a finite electron current, I_0 per unit area, will flow to the anode, this current limited by space charge being given by the equation[1]

$$I_0=\frac{(2)^{1/2}}{9\pi}\left(\frac{e}{m_e}\right)^{1/2}\frac{V_A^{3/2}}{a^2} \tag{1}$$

where e is the charge and m_e the mass of the electrons.

Let us now consider the effect of introducing positive ions without initial velocities, uniformly distributed over a plane B which is at a distance b from C. Between B and C there is thus an ion current I_p per unit area. Because of the partial neutralization of the electron space charge, the electron current from the cathode will increase to a new value, say I_e per unit area. We assume that the ions and electrons do not collide with gas molecules nor with each other and that no appreciable number of ions or electrons is lost by recombination during the passage between the electrodes. Our problem is to determine how the electron current I_e depends on I_p the positive ion emission and on b the location of the source of ions.

Let v_e be the velocity of the electrons at any point P which is at a distance x from the cathode, ρ_e the electron space charge density at P. The corresponding quantities for the positive ions are denoted by the subscript p. The signs of all these quantities will be taken as positive.

Then

$$\rho_e v_e=I_e \qquad \text{and} \qquad \rho_p v_p=I_p \tag{2}$$

and assuming the ions have unit charge

$$\tfrac{1}{2}m_e v_e^2=V_x \qquad \text{and} \qquad \tfrac{1}{2}m_p v_p^2=(V_B-V)e \tag{3}$$

where V is the potential at the point P and V_B the potential at B.

[4] George Jaffe, Ann. d. Physik **63**, 145–174 (1920).

Poisson's equation gives

$$d^2V/dx^2=4\pi(\rho_e-\rho_p) \tag{4}$$

We may eliminate ρ and v by Eqs. (2) and (3) and then after substituting

$$\alpha=(I_p/I_e)(m_p/m_e)^{1/2} \quad \text{and} \quad \phi=V/V_A \tag{5}$$

we obtain

$$\frac{d^2\phi}{dx^2}=2(2)^{1/2}\pi\left(\frac{m_e}{e}\right)^{1/2}\frac{I_e}{V_A{}^{3/2}}[\phi^{-1/2}-\alpha(\phi_B-\phi)^{-1/2}] \tag{6}$$

Combining Eqs. (1) and (6) and substituting

$$\lambda=x/a \tag{7}$$

we have

$$\frac{d^2\phi}{d\lambda^2}=\frac{4}{9}\frac{I_e}{I_0}[\phi^{-1/2}-\alpha(\phi_B-\phi)^{-1/2}] \tag{8}$$

Since the electron current is limited by space charge, we impose the condition $dV/dx=0$ when $x=0$, or in other words

$$d\phi/d\lambda=0 \qquad \text{when} \qquad \lambda=0 \tag{9}$$

Integration of Eq. (8) then gives

$$d\phi/d\lambda=(4/3)(I_e/I_0)^{1/2}[\phi^{1/2}+\alpha\{(\phi_B-\phi)^{1/2}-\phi_B{}^{1/2}\}]^{1/2} \tag{10}$$

Ions Emitted From Anode, $\phi_B=1$

According to Eq. (10) the potential gradient at the surface of the anode, ($\phi=\phi_B=1$), is proportional to $(1-\alpha)^{1/2}$ and so becomes imaginary if $\alpha>1$. When $\alpha=1$ the potential gradient at the anode is zero and the positive ion current as well as the electron current is thus limited by space charge.

It appears, therefore, that even an unlimited supply of positive ions available at the anode is not capable of neutralizing the electron space charge, for the positive ion current cannot become more than a definite fraction of the electron current, this fraction (according to Eq. 5, when $\alpha=1$) being equal to the square root of the ratio of the mass of the electron to that of the ion.

Examination of Eqs. (8) and (10) shows that when $\phi_B=1$ and $\alpha=1$ the equations remain unchanged in form if we substitute $1-\phi$ in place of ϕ. Thus the curve representing the potential distribution between the cathode and anode is symmetrical about its central point ($\lambda=\frac{1}{2}$, $\phi=\frac{1}{2}$). Between the cathode and this central point there is an excess of negative space charge, while from the central point to the anode there is an excess of positive charge.

To calculate the potential distribution we integrate Eq. (10) after placing $\phi_B=1$

$$\lambda=(3/4)(I_0/I_e)^{1/2}\int_0^{\phi}[\phi^{1/2}+\alpha\{(1-\phi)^{1/2}-1\}]^{-1/2}d\phi. \tag{11}$$

The ratio I_e/I_0 is found by observing that $\phi=1$ when $\lambda=1$, thus

$$(I_e/I_0)^{1/2}=(3/4)\int_0^{1}[\phi^{1/2}+\alpha\{(1-\phi)^{1/2}-1\}]^{-1/2}d\phi \tag{12}$$

Table I gives values of λ obtained from Eq. (11) by numerical integration. The values of I_e/I_0 which were used in these calculations as found by Eq. (12) are given for various values of α in the next to last horizontal line of the table.[5]

From the values of I_e/I_0 we see that the electron current increases as more positive ions are emitted from the anode until the positive ion current also becomes limited by space charge. When this occurs the electron current and the positive ion current are each 1.860 times as great as the currents of electrons or ions that could flow (with the same applied potentials) if carriers of the opposite sign were absent.

It is interesting to inquire how large is the effect of single positive ions emitted from the anode, in causing an increased electron flow from the cathode. By differentiating Eq. (12) with respect to α and then placing $\alpha=0$, and $I_e=I_0$ we find in terms of Gamma functions

$$dI_e/d\alpha=[3-3\Gamma(1.25)\Gamma(1.5)/\Gamma(1.75)]I_0=0.378I_0 \tag{13}$$

or by Eq. (5)

$$dI_e/dI_p=0.378(m_p/m_e)^{1/2} \qquad \text{for} \qquad \alpha=0 \tag{14}$$

A similar calculation for the case $\alpha=1$ involves a numerical evaluation of the resulting integral giving

$$dI_e/dI_p=3.455(m_p/m_e)^{1/2} \qquad \text{for} \qquad \alpha=1$$

A plot of I_e/I_0 as function of α from the data of Table I shows that the slope of the curve increases gradually from 0.378 at $\alpha=0$ up to 3.455 at $\alpha=1$. Thus the effectiveness of the ions in raising the electron current increases as the field strength decreases in the region where they originate, but only up to a certain limiting value. Of course when $\alpha=1$ the further increase in the electron current is stopped by the space charge limitation of the ion current.

The square root of the ratio of the masses of the ions and the electrons is 607 for mercury vapor, 271 for argon, and 60.8 for hydrogen, and there-

[5] In carrying out these calculations it was found convenient to replace ϕ by a new variable σ such that $\phi=\sigma^{4/3}$. By so doing the infinite value of the integrand that occurs when $\phi=0$ is avoided. When $\alpha=1$ and $\phi=1$ a similar difficulty still occurs but the value of λ in the range $\phi=\frac{1}{2}$ to 1 can be obtained from those calculated in the range $\phi=0$ to $\frac{1}{2}$ by making use of the fact already noted that in this case λ is symmetrical about the point $\phi=\frac{1}{2}$.

fore each positive ion of these gases liberated at the anode will increase the number of electrons that cross the space by 229, 102 or 23 respectively in the case of a pure electron discharge ($\alpha=0$).

TABLE I. *Potential distribution between plane cathode emitting surplus of electrons and parallel plane anode which emits given numbers of ions. Table of values of* λ, *the fraction of the distance to the anode, at which the potential is a given fraction* ϕ *of the anode potential (zero potential at cathode).*

	$\alpha=(I_p/I_e)\ (m_p/m_e)^{1/2};\ \lambda=x/a$						
ϕ	$\alpha=0$	$\alpha=0.2$	$\alpha=0.4$	$\alpha=0.6$	$\alpha=0.8$	$\alpha=0.9$	$\alpha=1.0$
0	0	0	0	0	0	0	0
0.02	0.0532	0.0513	0.0491	0.0467	0.0438	0.0419	0.0396
0.05	.1057	.1022	.0981	.0934	.0879	.0842	.0798
0.1	.1778	.1723	.1661	.1588	.1498	.1437	.1367
0.2	.2991	.2911	.2823	.2714	.2573	.2477	.2363
0.3	.4054	.3962	.3855	.3721	.3546	.3423	.3274
0.4	.5030	.4932	.4815	.4667	.4467	.4324	.4146
0.5	.5946	.5847	.5731	.5580	.5371	.5218	.5000
0.6	.6817	.6723	.6612	.6461	.6245	.6080	.5854
0.7	.7653	.7570	.7471	.7332	.7123	.6958	.6726
0.8	.8459	.8395	.8314	.8198	.8016	.7861	.7637
0.9	.9240	.9201	.9149	.9074	.8940	.8813	.8633
1.0	1.0000	1.0000	1.0000	1.0000	1.0000	1.0000	1.0000
I_e/I_0	1.0000	1.0839	1.1872	1.3237	1.5186	1.6644	1.8605
a/a_0	1.0000	1.0411	1.0896	1.1505	1.2323	1.2901	1.3640

THE SOURCE OF IONS IS AT A PLANE BETWEEN CATHODE AND ANODE $\phi_B<1$.

Let us consider the effect produced by ions that start from a plane B which lies between C and A. In the region between C and B, Eqs. (6) and (10) are applicable and thus the value of $d\phi/d\lambda$ at B is found by putting $\phi=\phi_B$ in Eq. (10). Equation (6) is applicable also in the region between B and A but here $\alpha=0$ for there is no ion current. Thus by integration we obtain the two equations

$$\left.\begin{aligned} &4(I_e/I_0)^{1/2}\lambda_B=3\phi_B^{3/4}\int_0^1\left[\mu^{1/2}+\alpha\{(1-\mu)^{1/2}-1\}\right]^{-1/2}d\mu \\ \text{and}\quad &4(I_e/I_0)^{1/2}(1-\lambda_B)=3\int_{\phi_B}^1\left[\phi^{1/2}-\alpha\phi_B^{1/2}\right]^{-1/2}d\phi \end{aligned}\right\} \tag{15}$$

The constant of the first integration for the second equation was chosen to make $d\phi/d\lambda$ at $\phi=\phi_B$ the same as for the first equation.

Differentiating Eqs. (15) with respect to α, putting $\alpha=0$, adding the resulting equations and combining with Eq. (5) gives rigorously[6]

$$\frac{dI_e}{dI_p}\left(\frac{m_e}{m_p}\right)^{1/2}=3\phi_B^{1/2}-2.622\phi_B^{3/4}. \tag{16}$$

[6] The coefficient 2.622 is equal to 3 minus the coefficient 0.378 as given in Eq. (14).

This equation, which reduces to Eq. (14) if $\phi_B = 1$, allows us to calculate the number of additional electrons that can flow in a pure electron discharge ($\alpha = 0$) if single positive ions are introduced *at any point* in the space between the electrodes. The values given in Column 3 of Table II were calculated by Eq. (16); the second column represents λ_B the fraction of the distance from cathode to anode at which the ions originate. From Eq. (1) we see that $\lambda_B = \phi_B^{3/4}$.

TABLE II. *The increase in electron current caused by ions originating at various positions between cathode and anode, $\alpha = 0$. Initial velocities neglected.*

ϕ_B	λ_B	$\frac{dI_e}{dI_p}\left(\frac{m_e}{m_p}\right)^{1/2}$
0.00	0.00	0.0
0.001	0.0056	0.080
0.01	0.0316	0.217
0.1	0.177	0.483
0.2	0.300	0.554
0.338	0.444	0.582 max.
0.5	0.595	0.561
0.6	0.683	0.534
0.7	0.765	0.502
0.8	0.846	0.464
0.9	0.925	0.419
1.0	1.000	0.378

The ions have a maximum effect in increasing the electron current when they are introduced at a point which is 4/9 of the distance from cathode to anode. If a trace of gas is present and the voltage is so high that we may assume the probability of ionization per cm of electron path is uniform, we find readily from Eq. (16) (integrating with respect to λ) that the average value of dI_e/dI_p is 0.489 $(m_p/m_e)^{1/2}$.

If the probability of ionization is greater near the end of the path, as in the case of low anode voltages, the coefficient will lie between 0.489 and 0.378.

Low Pressure Discharges With Hot Cathode

Let us consider for a moment the phenomena that are observed as we pass from a pure electron discharge to a discharge at low gas pressure in which there is abundant gas ionization. When the ions originate at the anode or at a definite plane between the electrodes we have been able to follow through the effects produced by even an unlimited supply of ions. But when the ions are produced throughout all or a large part of the space between the electrodes, we have been able to analyze only the effects produced by a very small total number of ions ($\alpha = 0$). To understand the typical characteristics of gas discharges, however, we must devise methods of treating the problem involving a large intensity of ionization throughout a volume. The nature of the problem will best be realized by considering briefly some experimental observations.

Suppose for example, we have a hot tungsten cathode (at zero volts) capable of emitting 50 ma in a bulb containing mercury vapor saturated at room temperature. With an anode at 10 volts the current is limited by electron space charge and is practically the same as in the absence of mercury vapor. Beginning at the ionization voltage (10.4 volts) the current increases with the anode voltage more rapidly than in good vacuum until at a voltage of 15 to 25 volts depending on the vapor pressure, and the geometry of the tube, the current rises abruptly to the saturation value corresponding to the cathode temperature.

In this second state of the discharge practically the whole of the voltage difference from cathode to anode is concentrated in a cathode sheath in which there is a positive ion space charge; the rest of the volume is nearly field-free, the space charge of the positive ions being neutralized by low-velocity or "ultimate electrons" which accumulate in this space until their concentration is hundreds or thousands of times greater than that of the primary electrons from the cathode.

By means of a sufficiently large resistance in series with the anode it is possible to observe points on the negative resistance part of the current voltage curve that lies between the parts corresponding to the two regions we have just considered. In this transition region the current is limited by the electron and ion space charges in a double layer or double sheath on the cathode.

In order to understand the formation of this double sheath, the final neutralization of space charge and the accumulation of the ultimate electrons, we will first consider the following problem.

Potential Distribution and Current Flow Resulting from the Production of Ions Uniformly throughout the Volume Between Two Planes

Consider two parallel plane electrodes A and C separated by the distance a and let V_c be the potential of C taking that of A to be zero. We assume that S ions of charge e are generated per unit time in each unit volume, and for the present will assume that no electrons are generated by this ionization.

We will first consider the case in which there is no maximum potential in the space between A and C. We will take V_c negative so that the ions move towards C. Then the ion current density I at any plane at a distance x from A is

$$I = Sex \tag{17}$$

but this current is composed of ions having widely different velocities depending on the potentials of their points of origin. The space charge ρ at any point at a distance x from A where the potential is V_1 is thus given by the integral $\int(1/v)dI$ where v, the velocity of an ion which originated at a point of potential V, is found from

$$\tfrac{1}{2}m_p v^2=(V-V_1)e \tag{18}$$

Thus

$$\rho=S(em_p/2)^{1/2}\int_0^{x_1}(V-V_1)^{-1/2}dx. \tag{19}$$

The problem is now to find V as a function of x which satisfies this integral equation simultaneously with Poisson's equation. By trial the following is found to be a particular solution

$$V=V_c x^2/a^2 \tag{20}$$

which we may now prove as follows.
Substituting this value of V and the corresponding value of V_1 in Eq. (19) We obtain

$$\rho=\tfrac{1}{2}\pi I_a[m_p/(-2eV_c)]^{1/2} \tag{21}$$

where

$$I_a=S_1 ea \tag{22}$$

is the ion current which reaches C, and S_1 is the particular value of S which corresponds to the potential distribution assumed in Eq. (20).
Differentiation of Eq. (20) gives

$$dV/dx=2V_c x/a^2 \tag{23}$$

and a second differentiation and combination with Poisson's equation gives

$$d^2V/dx^2=2V_c/a^2=-4\pi\rho \tag{24}$$

whence

$$\rho=-V_c/2\pi a^2 \tag{25}$$

We see that both Eqs. (21) and (25) give ρ independent of x or a uniform space charge between the planes. Equating the two expressions for ρ and solving the resulting equation for I_a gives

$$I_a=(2e/m_p)^{1/2}(-V)^{3/2}/\pi^2 a^2. \tag{26}$$

If, as before, I_0 is the current calculated by the ordinary space charge equation, Eq. (1), we see that

$$I_a=(9/\pi)I_0=2.865I_0 \tag{27}$$

We now recognize that the parabolic potential distribution assumed in Eq. (20) is a solution of our problem only when the rate of ionization S has the particular value S_1 given by Eq. (22) and where I_a is given by Eq. (26). Curve 1 in Fig. 1 illustrates this parabolic distribution. It will be noted by Eq. (23) that the potential gradient is zero at A, i.e. at $x=0$.

If $S<S_1$ the potential distribution curve will lie between the straight line 0 and Curve 1 in Fig. 1, but will not be parabolic. On the other hand, if $S>S_1$ it is evident that there will be a potential maximum between A and C and that Eq. (26) can then be applied separately to the two branches of

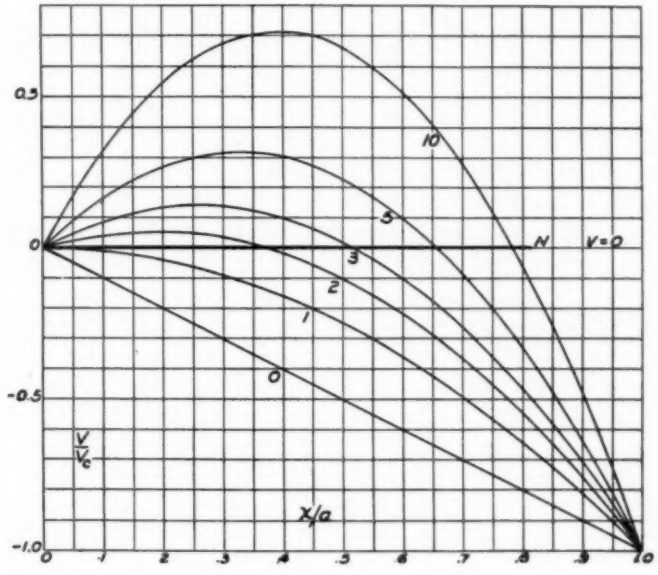

Fig. 1. Potential distributions between plane electrodes when ions are generated uniformly between them.

the curve on the opposite sides of the maximum. The potential distribution curve is thus still a parabola but the origin is no longer at A. The curves marked, 2, 3, 5 and 10 in Fig. 1 have been calculated for values of S equal respectively to 2, 3, 5 and 10 times S_1. The equation of these parabolas is

$$\frac{V}{V_c}=\frac{x}{a}\left[1-\left(\frac{S}{S_1}\right)^{2/3}\left(1-\frac{x}{a}\right)\right]. \tag{28}$$

Effect of the Electrons Generated by Ionization

If the positive ions in the foregoing problem are produced by the ionization of a gas an equal number of electrons will be generated simultaneously. If $S<S_1$ there will be no potential maximum between the electrodes so that these electrons will flow to the electrode A without having appreciable effect on the space charge, for it would take an electron current hundreds of times greater than I_a to neutralize the positive ion space charge due to I_a.

The situation is very different, however, if $S>S_1$ for there is then a tendency to develop a potential maximum as illustrated in Fig. 1. In any region at a potential higher than that of both electrodes the low velocity electrons produced by ionization will accumulate until they nearly neutralize the posi-

tive space charge. The potential of the region which would otherwise be above anode potential (above line ON in Fig. 1) is thus lowered to a value at which the electrons, in virtue of their initial velocities, can just escape to the anode as fast as they are produced. The accumulation of the ultimate or low velocity electrons is greatly favored by the smallness of the field available for drawing away the positive ions. In general there will still be a maximum potential in the space but this usually exceeds the anode potential by not more than a volt or so, and thus the ions flow in nearly equal numbers to anode and cathode, while the electrons go to the anode only. Any calculation of the exact potential distribution must involve some knowledge of the velocity distribution of the electrons and ions.

We see from Fig. 1 that when S/S_1 is as great as 10, the fields at the cathode and anode which are necessary to draw these ion currents, are very large.

These regions of strong field due to space charge which cover the electrodes will be referred to as the *sheaths*. The relatively field-free regions between the sheaths where the positive and negative space charges are nearly balanced will be called the *plasma*. We shall find in general that these two regions are rather distinct and have very different properties. Let us first consider some of the characteristics of the plasma.

Random Currents and Potential Distribution in the Plasma

Experiment has shown[3] that the ultimate electrons in the plasma usually have a velocity distribution corresponding closely with that of Maxwell. Thus we may define the electron velocities in terms of an electron temperature T_e. Through any imaginary plane there is a certain current density I_e of electrons passing from one side to the other and a nearly equal current in the reverse direction, this current being related to n_e the number of electrons per unit volume by the equation

$$n_e=(2\pi m_e/kT_e)^{1/2}I_e/e=4.03\times10^{13}I_e/T_e^{1/2} \tag{29}$$

if I_e is expressed in amperes per cm^2 and n in cm^{-3}, k being the Boltzmann constant 1.372×10^{-16} erg per degree.

The ion velocity distribution is not so easily determined and is far less accurately Maxwellian. Measurements with perforated collectors have shown that the normal components of velocity of the ions that reach the edge of a cathode are roughly that of a Maxwellian distribution[7] corresponding to a temperature T_p which is about half that of the electron, i.e., $T_p=\frac{1}{2}T_e$. In these low pressure discharges the ions probably acquire practically all the kinetic energy they possess from the electric fields within the plasma. The momentum of the electrons is so small that ionizing collisions of electrons with gas molecules cannot impart to the ions appreciable kinetic energy.

[7] Tonks, Mott-Smith and Langmuir, Phys. Rev. **28**, 104 (1926). See pp. 120–123.

All the ions which reach the edge of a cathode sheath pass to the electrodes and thus only half of the ions corresponding to a Maxwellian distribution T_p can be present in the plasma near the sheath edge, so that the directions of the ions can be distributed only over a hemisphere. Thus if I_s is the positive ion current density reaching the sheath edge, and therefore the electrode, we have by analogy with Eq. (29)

$$n_p=\tfrac{1}{2}(2\pi m_p/kT_p)^{1/2}I_s/e=2.02\times10^{13}I_s(m_p/m_eT_p)^{1/2} \tag{29a}$$

The accumulation of ultimate electrons in the plasma will go on until n_e and n_p are very nearly equal and thus from Eqs. (29) and (29a)

$$I_e/I_s=\tfrac{1}{2}(m_pT_e/m_eT_p)^{1/2} \tag{30}$$

or if

$$T_p=\tfrac{1}{2}T_e \tag{30a}$$

$$I_e/I_s=(m_p/2m_e)^{1/2}$$

For mercury vapor this gives

$$I_e=429I_s \tag{30b}$$

The electron current density I_e which enters this equation is practically the same as that in the plasma at a small distance from the sheath edge for since no electron current flows to the collector the electrons are in a state of equilibrium and have a full Maxwellian velocity distribution. The values of n_e and n_p at the sheath edge are thus the same as in the plasma.

To measure I_s we need merely to determine the current density of the ions flowing to a negatively charged plane collector. By then making the collector positive it is frequently possible in a similar way to obtain an *electron current* independent of applied voltage and thus to measure the rate I_e' at which electrons reach the edge of the electron sheath. Although now equilibrium of the electrons is disturbed, so that only half of the full Maxwellian distribution can exist at the sheath edge, we may assume with reasonable accuracy that the observed electron current density I_e' at the sheath edge is the same as that in neighboring regions of the plasma where the distribution has more nearly spherical symmetry. Thus the values of n_e and n_p at the sheath edge are half of those in the interior of the plasma. This non-uniform distribution n_e and n_p is made possible by the fact that the positive ions contain no intrinsic energy by which they could force the electron concentration to become uniform. We can therefore conclude that the measured I_e' is the same as the I_e in Eq. (30b).

Direct measurements[8] of I_e' and I_s in mercury arcs have given for the ratio I_e/I_s the values 405 ± 25 for 14 experiments, 423 ± 30 for 8 experiments

[8] These data are the averages of the values given as I_e/I_p in Tables III, XIII and XV on pages 544, 765 and 769 of Vol. 27 General Electric Rev. Reference 3. At that time the necessity for introducing the factor 1/2 in Eq. (29a) was not realized and therefore it was thought that I_e/I_p should be equal to the square root of the ratio of the masses, viz. 607. The difference between this and the observed value of about 410 was attributed to the possible presence of negative ions.

and 407 ± 15 for 3 other experiments or for the average of all 25 exps. 411 ± 17 which is in good agreement with the value 429 from Eq. (30a).[9] Returning to our consideration of a plasma discharge between parallel plane electrodes we see that, since the current of ultimate electrons flowing to the anode cannot exceed the positive ion current which is simultaneously produced by ionization, there must be an anode sheath with a field sufficient to repel all but this small fraction of the electrons that move towards the anode, but the ions are not repelled.

To obtain clearer conceptions of the typical distribution of ions and electrons in the plasma and of the resulting plasma fields, we may consider, as before, that there is a uniform rate of ionization throughout the plasma and we may neglect for the present the currents carried by primary electrons.

If a is the distance betweeen the anode and cathode sheaths then the current density I_s of ions flowing to each sheath is approximately

$$I_s = \tfrac{1}{2} Sea \tag{31}$$

and to the anode the ultimate electron current density is 2 I_s since no electrons pass to the cathode.

At somewhat higher gas pressures than we have been considering the mean free paths λ_p of the ions may be small compared to a and then the ions and electrons that are formed in the interior of the plasma must move to the sheaths by diffusion. Since the electrons tend to diffuse more rapidly they leave the interior of the plasma positively charged and thus there is a field which aids in moving the ions. The general differential equations for this "ambipolar diffusion" of ions and electrons have been given by Schottky and v. Issendorf.[10] The "ambipolar diffusion coefficient" is

$$D = \frac{M_p M_e k(T_e + T_p)}{(M_p + M_e)e} \tag{32}$$

where M_p and M_e are the mobilities of the ions and electrons (velocity per unit field). The effect of the field produced by the electrons, in accelerating the ions, has been taken into account in this derivation and is represented by the term T_e in the equation.

The current density I of ions (drift current, not random current) at any point in a direction normal to the sheaths is then

$$I = -De(dn/dx) \tag{33}$$

n being the number of ions, or electrons per unit volume. At any point at a distance x from the central plane of the plasma the current will be Sex and therefore from Eq. (33) by integration we find that the ion concentration at x is

$$n = n_M - Sx^2/2D \tag{34}$$

[9] Dr. Tonks is developing the more rigorous theory of the positive ion velocity distribution assuming that the energies are acquired from the plasma fields.

[10] W. Schottky and J. v. Issendorf, Zeits. f. Physik **31**, 163 (1925).

or at the sheath edges where $x=\pm a/2$ we have

$$n_S=n_M-Sa^2/8D. \tag{35}$$

The drift ion current I is zero at the center $x=0$ and increases to I_S at the sheath edge while the random ion current is proportional to n and therefore should decrease from a maximum value I_M at the center to a value $I_M(n_S/n_M)$ at the sheath edge. Although strictly speaking the current at the sheath edge is not a random current for it flows in one directly only we may provisionally[11] identify this calculated value of the random current with the drift current I_S at the sheath edge, so that

$$I_S=I_M(n_S/n_M). \tag{36}$$

The mobility M_p of Eq. (32) is very small compared to M_e and therefore M_e drops out. The ion mobility is

$$M_p=e\lambda_p(2/\pi m_p kT_p)^{1/2} \tag{37}$$

and thus by Eq. (32)

$$D=\lambda_p\left(\frac{2k}{\pi m_p T_p}\right)^{1/2}(T_e+T_p)=3.15\times10^5\lambda_p(T_e+T_p)\left(\frac{m_e}{m_pT_p}\right)^{1/2} \tag{38}$$

if we use c. g. s. units.

Substituting this value of D and the value of S from Eq. (31) in Eq. (34) and combining with Eqs. (36) and (29a)

$$\frac{I_M}{I_S}=\frac{n_M}{n_S}=1+\frac{Sa^2}{8n_SD}=1+\frac{aT_p}{8\lambda_p(T_e+T_p)} \tag{39}$$

or if we put $T_e=2T_p$

$$I_M/I_S=1+a/24\lambda_p. \tag{40}$$

This simple result indicates that the ion concentration will be nearly uniform throughout the plasma if the free path of the ions is large compared to 1/24th of the distance between the electrodes. With mercury vapor at 1 barye pressure and 20°C, λ_p is of the order of 5 cm and therefore if a, the distance between the electrode sheaths, is 5 cm the pressure may be as great as 24 baryes (saturated vapor at 56°C) before the concentration of ions at the center of the plasma becomes twice as great as at the edges.

The potential distribution within the plasma may now be calculated by means of the Boltzmann equation

$$n/n_M=\exp\,[(V-V_M)e/kT_e] \tag{41}$$

[11] Although this assumption is of doubtful accuracy because of the non-Maxwellian character of the ion velocity distribution near the sheath edge, it is far more nearly in accord with the facts than the assumption made by Schottky and Issendorf and others that $n_S=0$ at the sheath edge.

which will be applicable within the plasma since the electron drift currents are negligible compared to the random currents and therefore the conditions will not depart appreciably from those of equilibrium. The difference of potential between the sheath edge and the center of the plasma is thus by Eqs. (41) and (40), since $e/k = 11600$ degrees per volt,

$$V_M - V_S = 1.98 \times 10^{-4} T_e \log_{10} (1 + a/24\lambda_p) \text{ volts}. \quad (42)$$

These fields are ordinarily very weak, for example if $T_e = 10{,}000°$ in a mercury arc at 24 baryes pressure and with $a = 5$ cm we find $V_M - V_S = 0.6$ volts. At a pressure of 240 baryes this voltage difference would be 2.1 volts if T_e remained the same, but actually T_e decreases as the pressure rises so that the potential difference would probably remain approximately constant at about 0.6 volt. Although this field is extremely small compared to that in the sheaths, it must play an essential rôle in gaseous discharges in drawing the positive ions towards the sheath edges. In fact the kinetic energy of the positive ions is probably almost entirely derived from the action of this field.

Anode Sheath

The electron current flowing to the anode is usually dependent on the conditions that exist in other parts of the circuit which supplies the energy for the anode current. For example, it may be fixed by the electron emission from the cathode or by the current that can flow through an external resistance placed in series with the anode. If the anode area is comparable with the cross-section of the plasma the current density I_a of the electron current flowing to the anode is usually far smaller than I_e the electron current density in the plasma near the anode. There will then be a retarding potential V_a (negative anode drop) in the anode sheath whose magnitude can be calculated from the Boltzmann equation which takes the form

$$V_a = 1.98 \times 10^{-4} T_e \log_{10} (I_e/I_a). \quad (43)$$

In cases of low pressure plasma discharges with hot cathodes when no measurements of I_e are available, methods of the following type will usually give I_e with sufficient accuracy to give a fairly reliable value of the anode drop.

Each primary electron from the cathode, in falling through the cathode sheath, acquires a high kinetic energy, which it retains until the energy is dissipated in excitation and ionization of the gas molecules. The glass walls of the tube become so strongly negatively charged that they receive no more electrons than positive ions and thus in ordinary cases only a negligible fraction of the primary electrons are lost to the walls. It has been shown[12] under a wide range of conditions of this kind, that the total number of ions formed per primary electron, which we may call β, is independent of current density, of pressure and of the geometry of the tube, but depends only on the nature

[12] I. Langmuir and H. A. Jones. Phys. Rev. **31**, 357–404 (1928). See particularly pp. 402–3.

of the gas and the energy of the primary electrons. Thus 50 volt electrons in mercury vapor give 1.4 ions per primary electron. Neglecting the relatively small ion currents to the cathode and anode, the primary electron current from the cathode is equal to i_a the electron current to the anode. Thus the total rate of production of ions within the tube is βi_a.

Since recombination in the gas is negligible at low pressures, all these βi_a ions will flow to the electrodes and to the walls of the tube. With envelopes of roughly spherical shape, the ion current density will be fairly uniform over the whole surface. Thus if B is the area of the plasma envelope (sheaths over all electrodes and glass surfaces) find that the positive ion current density I_p is given by

$$I_p = \beta i_a / B. \tag{44}$$

Substituting this value of I_p for I_s in Eq. (30) we can thus calculate I_e, the random electron current density and then Eq. (43) gives the negative anode drop:

$$V_a = 1.98 \times 10^{-4} T_e \log_{10} \left[\frac{A\beta}{2B} \left(\frac{m_p T_e}{m_e T_p} \right)^{1/2} \right] \tag{45}$$

where A is the anode area.

Experiments with discharges from hot cathodes in mercury vapor in spherical and cylindrical bulbs and with anodes of various sizes have demonstrated the general usefulness and reasonable accuracy of this equation.

With large anode area A the anode sheath is thus a positive ion sheath but as A decreases a point is reached where the sheath disappears and is then replaced by an electron sheath, the anode drop becoming positive. When the positive anode drop approaches the ionizing voltage an anode glow appears and with sufficiently high gas pressure the rate of positive ion production becomes so great as to break-down the electron space charge, causing a *second plasma* to develop near the anode. This second plasma usually takes the form of a globular luminous protuberance from the anode. Its interior is a typical plasma with high electrical conductivity; its boundary is a double sheath with an inner positive space charge and an outer negative space charge, the potential drop being of the order of the ionizing potential.

The conditions at this double layer are essentially like those that we postulated in the first section of this paper; the potential gradient vanishes at the inner and outer edges and the potential distribution is determined by the charges of moving ions which acquire their kinetic energy mainly from the field within the double layer.

Cathode Sheaths

An electrode which is at a negative potential with respect to the plasma repels all the ultimate electrons which move towards it, except those that have a sufficient component of energy normal to the surface of the electrode, to enable them to move against the retarding field. The positive ions in the plasma that move towards the electrode are collected by it. The fraction

of the ultimate electrons that penetrate through this positive ion sheath is given by the Boltzmann equation or may be calculated from the ratio I_a/I_e in Eq. (43). Thus if the temperature of the ultimate electrons is 10000° the current density of these electrons which reach the electrode will be only 1/1000th of that in the plasma if the electrode is 5.9 volts negative with respect to the plasma.

If the electrode is 50 volts or more negative with respect to the plasma the sheath will contain no appreciable number of electrons and the positive ions will enter the sheath with energies negligible compared to those they acquire in the sheath itself. Thus the velocity of the ions is given by

$$\tfrac{1}{2}m_p v_p^2 = -Ve$$

and since there is no appreciable field in the plasma itself we will have at the outer edge of the sheath $dV/dx = 0$.

Since these conditions are exactly those that are postulated in the derivation of the ordinary space charge Eq. (1) we may apply this equation to cathode sheaths in gaseous discharges, merely replacing m_e by m_p.

In the usual applications of Eq. (1) the voltage and the distance between the electrodes are known and we wish to calculate the current density that can flow when the current is limited by space charge. In the present case, however, the current density I_p is fixed by conditions within the plasma and since the applied voltage is usually known the equation can be used to calculate only the thickness x of the sheath (a in Eq. (1)). Thus the current density I_p is independent of the applied voltage and x varies in proportion to $V^{3/4}$.

The cathode sheath can usually be seen as a dark space and under favorable conditions its thickness can be measured. In low pressure discharges in mercury vapor the observed sheath thickness agrees well with that calculated by the space charge equations.[13]

Of course, modifications or corrections to this theory may be necessary under special conditions, for example, when the gas pressure is so high that the ions collide with gas molecules within the sheath or when the voltage is so low that the initial velocities of the ions and electrons at the sheath edge can not be neglected.

Sheath on Hot Cathode. Double Sheath.

If the cathode is heated so that it emits electrons these flow out through the positive ion sheath and if this electron current becomes sufficiently great it will neutralize the positive ion space charge in the immediate neighborhood of the cathode. Since the electrons start with negligible velocities from the cathode, the conditions are the same as those postulated when we calculated the effect of ions liberated at the anode upon the electron currents from a hot cathode emitting a surplus of electrons, for example, in our derivation of Eqs. (5), (11) and (12). In the present case, however, it is the

[13] Reference 3, p. 545.

sheath edge, functioning as anode, that emits a surplus of ions (since $dV/dx=0$ at this point) while a limited number of electrons is emitted from the cathode. Thus, in applying our equations to the present problem we need merely interchange the subscripts p and e.

Let us consider the currents of ions and electrons that flow to or from a plane cathode in a plasma having given characteristics, such as I_e, I_p and T_e. Let the cathode, at potential $-V$ with respect to the plasma first be at such low temperature that it emits no electrons. We let a_0 denote the sheath thickness under these conditions, as calculated from the known value of I_p by means of Eq. (1), in which for this purpose we replace I_0 by I_p, V_a by V, m_e by m_p and a by a_0.

Now let the cathode temperature be raised until the current density of the emitted electrons is I_e. To calculate the coefficient α we interchange e and p in Eq. (5) giving

$$\alpha_e=(I_e/I_p)(m_e/m_p)^{1/2} \tag{46}$$

The effect of these electrons in neutralizing the ion space charge cannot cause an increase in I_p for this is fixed by the plasma, but manifests itself by changing the sheath thickness so that this becomes a instead of a_0. In Eq. (12) the ratio I_e/I_0 was calculated on the assumption that the distance between the electrodes was fixed. Evidently for our present problem we must replace I_e in this ratio by I_p and I_0 must be replaced by the positive ion current density that would flow to a cathode of voltage $-V$ if no electrons were emitted and if the sheath thickness were a. This current may be calculated from Eq. (1) by replacing m_e by m_p, and V_a by V. Thus we see that $(I_e/I_0)^{1/2}$ in Eq. (12) must be replaced by a/a_0. The last horizontal line of Table I gives the values of a/a_0 (which are merely the square roots of the numbers in the line above) for various values of α_e. An electron emission for which $\alpha_e=0.2$ would correspond to $I_e=0.2\times 607 I_p=121 I_p$ in a discharge in mercury vapor. The electron current would then be 121 times the positive ion current and yet we see from Table I that this would cause the sheath thickness to increase merely 4.1 percent. The potential distribution functions of Table I are of course applicable to these sheaths on a hot cathode.

As the cathode temperature is raised the electron current density I_e increases and is equal to the electron emission from the cathode until, when α_e becomes equal to unity, the current becomes limited by space charge and a further increase in electron current can not occur. The cathode is then covered by a double layer or double sheath and the ratio of the electron current to the ion current is equal to $(m_p/m_e)^{1/2}$. Even a change in cathode voltage will not cause a change in electron current if the positive ion current I_p remains constant.

These facts are of vital importance in any understanding of discharges from hot cathodes in low pressures of gas. We see that the use of a hot cathode, no matter how high its temperature, does not destroy the cathode drop.

In discharges with a single cathode the intensity of ionization in the plasma depends on the electron current from the cathode and on the cathode drop which gives to these electrons their velocity. Under these conditions, when the total current is restricted by a resistance in series with the anode, and a surplus of electrons is emitted by the cathode, the cathode drop adjusts itself to such a value that I_p in the plasma bears the proper ratio (corresponding to $\alpha=1$) to the electron current that is drawn. For example, with mercury vapor, the cathode drop must be such as to cause an ionization in the plasma that will give a positive ion current equal to 1/607th of the electron current that flows from the cathode.

For very low pressure discharges in which the plasma is very uniform we may calculate the magnitude of the cathode drop and thus learn upon what factors it depends. If C is the effective area of the cathode, then the electron current from it will be CI_e and this will be practically equal to the anode current i_a. Substituting CI_e for i_a in Eq. (44) and then putting for I_e/I_p its value $(m_p/m_e)^{1/2}$ we find

$$\beta=(B/C)(m_e/m_p)^{1/2} \tag{47}$$

where as before, B is the surface of the plasma envelope. The cathode drop will become such as to give to β (which is a function of voltage only) this value. The ratio C/B measures the fraction of the positive ions that are generated that get back to the cathode. The greater this ratio the smaller will be the cathode drop.

At higher gas pressures the intensity of ionization in the plasma will not be uniform but there will be a greater intensity near the cathode; this will greatly decrease the cathode drop. Under the most favorable conditions nearly all the ions formed will pass to the cathode and then β (for mercury vapor) will only need to be 0.0016, a value which will be reached at about 0.1 volt above the ionizing voltage.

Theory of Double-Sheath Considering Initial Velocities

The foregoing theory of the cathode double sheath, simplified by neglecting the effects of the initial velocities of the ions and electrons, has given us a useful picture of the essential character of the phenomena at a hot cathode in gas. We have seen, however, that its main field of application will be to cases involving cathode drops of 10 or 20 volts so that we are not wholly justified in ignoring these initial velocities. Fortunately there is no great difficulty in calculating the ratio I_e/I_p even when these velocities are taken into account.

Let us consider a sheath having parallel plane boundaries or "edges." Any group of electrons or ions entering the sheath with a given velocity distribution will contribute to the space charge at any point P within the sheath the amount $\int(1/v)dI$, where dI denotes the current density, normal to the plane of the sheath, of an elementary group which has the normal component of velocity v. Since with a given initial distribution, both dI

and v are functions solely of the potential at the point P, it follows that the total space charge ρ at any point depends only on the potential at that point.

Multiplying both members of the Poisson equation (for plane case) by dV and integrating we obtain

$$(dV/dx)^2 = -8\pi \int \rho dV + \text{const.} \tag{48}$$

In the case of the double sheath where the electron and ion currents are both limited by space charge, $dV/dx = 0$ at both the inner and outer edges so that we have

$$\int_{V_M}^{V_S} \rho dv = 0 \tag{49}$$

where V_M and V_S are the potentials at these two edges, or more specifically at the places where dV/dx is zero, one of these being at the minimum potential region very close to the cathode and the other S, the outer edge of the sheath.

Later we shall find it necessary to analyze more closely the nature of this sheath edge S, but for the present we will define it as a place where $dV/dx = 0$ and $\rho = 0$ (as in the plasma) so that according to the Poisson equation d^2V/dx^2 is also zero.

Within the sheath there are three groups of carriers to be considered;—the positive ions from the plasma, the ultimate electrons from the plasma and the electrons emitted by the hot cathode. For each of these groups we shall express its space charge in terms of the potential.

1. *Plasma ions.* We have already seen that the velocity distribution at S cannot be Maxwellian and we shall see that it cannot even have hemispherical symmetry. Assuming that the velocities of the ions originate from the weak plasma fields which we now wish to ignore, the velocity must in general be nearly normal to the plane of the sheath. Although the velocities of all the ions cannot be equal, we shall make no great error (especially since the ions are accelerated into the sheath) if we replace the actual distribution by a homogenous swarm of ions moving normal to the plane of the sheath with a kinetic energy corresponding to the potential E_p. If ρ_{pS} is the space charge of these ions at S then their space charge ρ_p at a point of potential V is

$$\rho_p = \rho_{ps} \{ E_p/(V_s - V + E_p) \}^{1/2} \tag{50}$$

We shall wish to calculate the integral of Eq. (49). If we let H_p be the part contributed to this integral by the ions, we have

$$H_p = \int_{V_M}^{V_S} \rho_p dV = 2\rho_{pS} E_p^{1/2} \{ (V_{SM} + E_p)^{1/2} - E_p^{1/2} \} \tag{51}$$

where V_{SM} is the difference of potential between S and M, ie.: $V_S - V_M$.

The space charge ρ_{pS} at the sheath edge can be determined from the positive ion current density I_p flowing to the cathode from the equation

$$\rho_{pS}=I_p(m_p/2E_pe)^{1/2}. \tag{52}$$

2. *Plasma electrons.* We assume that the cathode is sufficiently negative with respect to the plasma so that no appreciable fraction of the ultimate electrons reaches the cathode and thus the velocity distribution of these electrons at S will be a complete Maxwellian distribution corresponding to a temperature T_e and a random electron current density I_{eS}. Then according to the Boltzmann equation the space charge at any point due to these electrons is

$$\rho_e=\rho_{eS}\exp\left\{(V-V_e)/E_e\right\} \tag{53}$$

where E_e is the potential which corresponds to the energy kT_e that is, $E_e=T_e/11600$ volts. The integral H_e is

$$H_e=\int_{V_M}^{V_S}\rho_e dV=E_e\rho_{eS} \tag{54}$$

Finally ρ_{eS} may be expressed in terms of I_e:

$$\rho_{eS}=I_{eS}(2\pi m_e/E_ee)^{1/2} \tag{55}$$

3. *Electrons from cathode.* If the cathode emits more electrons than can flow across the sheath there will be a potential minimum V_M at a short distance from the cathode surface.

If V_c is the potential of the cathode then V_M may be calculated [14] from the equation

$$I_{eM}=I_c\exp\left\{(V_M-V_c)/E_c\right\} \tag{56}$$

where I_c is the current density of the saturation emission from the cathode corresponding to its temperature T_c and I_{eM} is that which gets past the potential minimum and is thus the electron current density passing through the sheath; E_c is the potential corresponding to kT_c, that is $T_c/11600$ volts. The space charge of the electrons at any point in the sheath, between M and S is thus rigorously

$$\rho_c=\rho_{cM}\exp\left\{(V-V_M)/E_c\right\}\operatorname{erf}\left\{(V-V_M)/E_c\right\}^{1/2} \tag{57}$$

where erf denotes the error function defined by

$$\operatorname{erf}(x)=2\pi^{-1/2}\int_x^\infty \exp\,(-y^2)dy$$

When x is greater than about 2 a very close approximation is

$$\exp x^2\operatorname{erf}x=1/\pi^{1/2}(x+1/2x). \tag{58}$$

[14] Eq. (56) and (57) have been derived from equations in a paper by I. Langmuir, Phys. Rev. **21**, 419 (1923).

The quantity E_c is only 0.1 or 0.2 volts and if $V-V_c$ is more than 4 times as great this approximation is justified and Eq. (57) thus becomes

$$\rho_c=\rho_{cM}\{E_c/\pi(V-V_M+E_c)\}^{1/2} \tag{59}$$

Here ρ_{cM} is the space charge density of the emitted electrons at the point of minimum potential.

Integration of Eq. (57) gives rigorously

$$H_c=\int_{V_M}^{V_S}\rho_c dV=E_c[\rho_{cS}-\rho_{cM}+2\rho_{cM}(V_{SM}/\pi E_c)^{1/2}]. \tag{60}$$

Putting $V=V_S$ in Eq. (59) we can express ρ_{cM} in terms of ρ_{cS}. Thus Eq. (60), expanded as a power series in E_c/V_{SM}, becomes

$$H_c=2\rho_{cS}V_{SM}[1-(\pi E_c/4V_{SM})^{1/2}+E_c/V_{SM}\cdots]. \tag{61}$$

The space charge ρ_{cS} expressed as a function of I_{eM} is

$$\rho_{cS}=I_{eM}[m_e/2(V_{SM}+E_c)e]^{1/2} \tag{62}$$

When the current I_M is limited by space charge Eq. (49) can now be used to determine the relation between I_M and I_p. The equation takes the form

$$H_p=H_e+H_c. \tag{63}$$

The values of these quantities from Eqs. (51), (54) and (61) substituted in this equation give a relation between the ρ's and then by means of Eqs. (52), (55) and (62) we find the following relation between the currents

$$\begin{aligned} &I_{eM}[1-(\pi E_c/4V_{SM})^{1/2}+E_c/2V_{SM}] \\ &\quad=I_p(m_p/m_e)^{1/2}[1-(E_p/V_{SM})^{1/2}+E_p/2V_{SM}]-I_{eS}(\pi E_e/V_{SM})^{1/2} \end{aligned} \tag{64}$$

We have defined S as a place where dV/dx is zero. At this region we may also put $\rho=0$, so that

$$\rho_{pS}=\rho_{eS}+\rho_{cS}. \tag{65}$$

Expressing the ρ's in terms of the I's by Eqs. (52), (55) and (62) and using this equation to eliminate I_{eS} we obtain

$$I_{eM}/I_p=(m_p/m_e)^{1/2}\frac{1-(E_p/V_{SM})^{1/2}(1+E_e/2E_p)+E_p/2V_{SM}}{1-(\pi E_c/4V_{SM})^{1/2}-(E_e-E_c)/2V_{SM}}. \tag{66}$$

An examination of this result shows that when $(1/2)E_e<E_p<V_{SM}$ an increase in either E_p or E_e causes a decrease in I_{eM}. Thus the effect of the initial velocities of both the ions and the electrons at the sheath edge is to decrease the electron current that can flow from a hot cathode. As a typical example we may take $E_e=2$ volts (corresponding to $T_e=23000°$), $E_p=1$ volt, $E_c=0.2$ volt. The ratio I_{eM}/I_p instead of being 607 for mercury vapor, will be only 31 percent of this for $V_{SM}=5$ volts, 53 percent for 10 volts and 71 percent for 25 volts.

The Sheath Edge

If the initial velocities of the plasma electrons and ions could be neglected we would be justified in regarding the edge of the sheath as sharp. In our study of the double sheath we must now recognize that the velocities of the ions which are measured by E_p are derived from the weak fields that extend from the sheath a considerable distance into the plasma.

To develop clear conceptions of the relation between the plasma and the sheath we will analyze in some detail a typical although somewhat simplified example. Let us imagine two parallel plane electrodes with a plane between them which acts as a source of ions and electrons, but which is not to be regarded as an electrode. Thus the potential of the source will be determined by space charges and cannot be arbitrarily varied as that of an electrode could be.

If the source emits only ions having no initial velocities, the potential will rise until the ions can flow to the two electrodes in accord with the space charge equation for ions (similar to Eq. (1)). Thus at the source the potential gradient is zero. Without loss of generality we may take the source as the origin both for the potential V and for the distance x and for simplicity may consider phenomena only on one side of the source, i.e. for positive values of x. Let I_p be the positive ion current density that flows from the source in this positive direction.

Now let us introduce electrons having a Maxwellian velocity distribution corresponding to a temperature T_e. We assume that the electrode is at a negative potential sufficient to prevent any appreciable number of electrons from reaching it, and thus the Maxwellian distribution is not disturbed. We assume also that the electrons pass freely through the source in both directions, which is equivalent to assuming that the source is a perfect reflector for electrons. Let I_{e0} be the electron current density passing in one direction through the source (random current). At any point having the potential V the positive ion space charge is

$$\rho_p = I_p(m_p/-2Ve)^{1/2}$$

and the electron charge density according to Eqs. (29), (41) and (53) is

$$\rho_e = I_{e0}(2\pi m_e/E_e e)^{1/2} \exp(V/E_e).$$

We now substitute the total space charge $\rho_p - \rho_e$ into the Poisson equation and then reduce the result to a dimensionless form by introducing the variables η and x_p defined by

$$\left.\begin{aligned} \eta &= -V/E_e \\ I_p &= (1/9\pi)(2e/m_p)^{1/2} E_e^{3/2} x_p^{-2} \end{aligned}\right\} \tag{67}$$

This last equation is similar in form to the space charge Eq. (1). Thus x_p is the positive ion sheath thickness calculated for a collector voltage E_e ignoring the effects of initial velocities. The Poisson equation thus gives

$$d^2\eta/d\lambda^2 = (4/9)[\eta^{-1/2} - 2\pi^{1/2}\alpha_{e0} \exp(-\eta)] \tag{68}$$

where λ is a dimensionless parameter proportional to length defined by $\lambda = x/x_p$ and α_{e0} in accordance with Eq. (46) is

$$\alpha_{e0} = (I_{e0}/I_p)(m_e/m_p)^{1/2}. \tag{69}$$

Multiplication by $d\eta/d\lambda$ and integration gives

$$d\eta/d\lambda = (4/3)\{\eta^{1/2} - \pi^{1/2}\alpha_{e0}[K - \exp(-\eta)]\}^{1/2} \tag{70}$$

where K is a constant of integration. The potential distribution is given by

$$\lambda = (3/4)\int_0^{\eta} \{\eta^{1/2} - \pi^{1/2}\alpha_{e0}[K - \exp(-\eta)]\}^{-1/2} d\eta. \tag{71}$$

For the case that we are now considering where the ions start from the source without initial velocity, we can determine K by the condition $d\eta/d\lambda = 0$ when $\eta = 0$, and find from Eq. (70) that $K = 1$. Let us now consider the nature of this solution to our problem given by Eqs. (70) and (71).

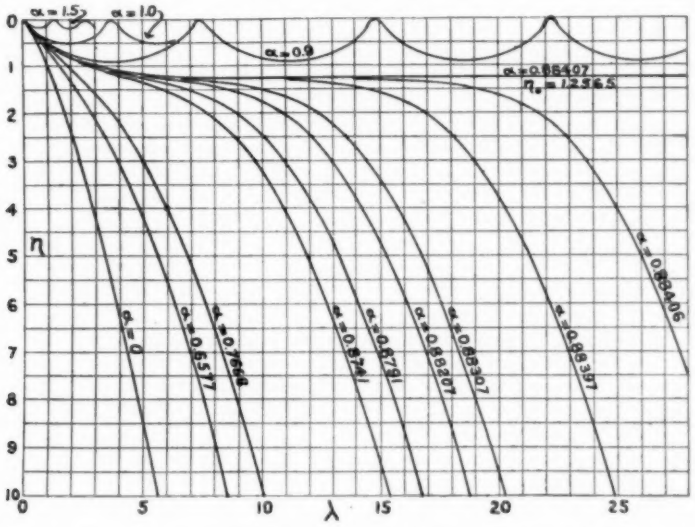

Fig. 2. Effect of electrons of temperature I_e on the potential distribution between planes at one of which ions are generated.

The family of curves shown in Fig. 2 represents the solutions of Eq. (71) for the case $K = 1$ for a series of different values of α_{e0}. By plotting $-\eta$ as ordinate instead of η the curves give directly the potential distribution V as a function of x in terms of E_e and x_p as units. The data for the curves shown in Fig. 2 have been calculated accurately either by numerical quadrature of Eq. (71) or by using some of the equations given below.

If $\alpha_{e0} = 0$, that is, if no electrons are present, Eq. (71) becomes

$$\lambda = \eta^{3/4}$$

which corresponds to the ordinary space charge equation for ions.

For values of α_{e0} small compared to unity, expansion of Eq. (71) gives

$$\lambda=\eta^{3/4}[1+0.3\pi^{1/2}\alpha_{e0}\eta^{1/2}+(9/56)\pi\alpha_{e0}^{2}\eta-\cdots]$$

if η is small, while if $\eta>4$

$$\lambda=\eta^{3/4}+2.66\alpha_{e0}\eta^{1/4}-2.41\alpha_{e0}.$$

Thus the effect of the electrons is to increase λ and decrease the potential gradient.

When α_{e0} is zero there is an infinite positive space charge at $\eta=0$ and elsewhere the charge decreases continuously as η increases. Electrons, when introduced, are confined almost wholly to regions where η is less than 3 or 4. These electrons tend to produce a minimum in the space charge. The condition for the occurrence of such a minimum is that

$$d^{3}\eta/d\lambda^{3}=(2/9)[-\eta^{-3/2}+4\pi^{1/2}\alpha_{e0}\exp(-\eta)]d\eta/d\lambda=0. \tag{72}$$

Before a negative space charge can occur as α_{e0} increases, it is necessary that $d^{2}\eta/d\lambda^{2}$ shall pass through zero. Equating both the third and the second derivatives to zero we find $\eta=0.5$ and $\alpha_{e0}=(\epsilon/2\pi)^{1/2}=0.6577$. The curve obtained with this value is plotted in Fig. 2.

When α_{e0} increases beyond 0.6577 there are two points of inflection between which there is a negative space charge. At the upper one ($\eta<0.5$) the potential gradient $d\eta/d\lambda$ is a maximum while at the lower one it is a minimum. At a certain value of α_{e0} which we shall call α_{e1} the slope at this second inflection becomes zero. We find this value by placing the second members of Eqs. (68) and (70) each equal to zero, thus obtaining

$$\alpha_{e1}=0.88407\ ;\quad \eta_{1}=1.2565.$$

This solution as shown in Fig. 2 is one that gives a region where the space charge and the potential gradient are both zero, conditions which characterize an ideal plasma. We shall return to a consideration of this case later.

When α_{e0} increases beyond α_{e1} the second point of inflection becomes imaginary and the curve no longer dips indefinitely downward but after passing through a minimum rises again to $\eta=0$. Thus for larger values of α_{e0}, η must remain so small that we can replace $1-\exp(-\eta)$ by η and then Eq. (71) after integration gives

$$\lambda=(3/2)\pi^{-3/4}\alpha_{e0}^{-3/2}[\sin^{-1}\nu-\nu(1-\nu^{2})^{1/2}] \tag{73}$$

where

$$\nu=\pi^{1/4}\alpha_{e0}^{1/2}\eta^{1/4}.$$

Thus the potential is a periodic function of the distance λ, the wavelength corresponds to

$$\lambda_{1}=(3/2)\pi^{1/4}\alpha_{e0}^{-3/2}$$

and the minimum potential at $\lambda = 1/2\lambda_1$ corresponds to

$$\eta_{max} = 1/\pi\alpha_{e0}^2.$$

Periodic solutions of this kind are illustrated in Fig. 2 for values of α_{e0} of 0.9, 1.0 and 1.5. These data have been obtained directly from Eq. (71) by quadrature since Eq. (73) is only applicable accurately for still larger values of α_{e0}.

Examination of Fig. 2 shows that when α_{e0} is only slightly less than the critical value $\alpha_{e0} = 0.88407$ the curves show an extended region in which the potential gradient is nearly zero. This clearly corresponds to a plasma. Close to the source of ions at $\lambda = 0$ there is a field which draws the ions outward into the plasma. However, for large enough values of λ, the potential begins to drop again and we thus pass from the plasma into a positive ion sheath. As α_{e0} approaches α_{e1} this descending portion rapidly approaches a limiting form in which the successive curves differ from one another merely in a horizontal displacement. Thus for the limit $\alpha_{e0} = \alpha_{e1}$ the lower part of the curve is like that shown in the curves for $\alpha = 0.88207$, 0.88307, 0.88397 etc. except that it lies at an infinite distance to the right.

To investigate this transition from plasma to sheath we may write Eq. (71)

$$\lambda = (3/4) \int_0^{\eta} f^{-1/2} d\eta \tag{74}$$

where

$$f = \eta^{1/2} - \pi^{1/2}\alpha_{e0}[1 - \exp(-\eta)]. \tag{75}$$

An expansion in the neighborhood of $\eta = \eta_1$ and $\alpha_{e0} = \alpha_{e1}$ gives to 3 terms

$$f = A\Delta\alpha + B\mu\Delta\alpha + C\mu^2$$

where

$$\Delta\alpha = \alpha_{e1} - \alpha_{e0}$$

$$\mu = \eta - \eta_1$$

and $A = 1.2679$, $B = -0.5046$ and $C = 0.13428$.

Substitution of this value of f in Eq. (74) and integration gives

$$\lambda = 0.75C^{-1/2} \log_e [f^{1/2} + C^{1/2}\mu + 0.5BC^{-1/2}\Delta\alpha] + \text{const.}$$

When $\Delta\alpha$ is small this reduces to

$$\Delta\lambda = 4.713 \log_{10} [0.424\mu_2(-\mu_3)/\Delta\alpha] \tag{76}$$

where μ_2 and μ_3 correspond to 2 points η_2 and η_3 that lie on opposite sides of η_1, and $\Delta\lambda$ is the distance between the points η_2 and η_3. It is assumed that μ_2 and $-\mu_3$ are large compared to $\Delta\alpha$.

When η is larger than about 4 the exponential term in Eq. (75) can be neglected in comparison with unity. Integration of Eq. (74) for $\alpha_{e0} = \alpha_{e1}$ then gives

$$\lambda = (\eta^{1/2} + 3.134)(\eta^{1/2} - 1.567)^{1/2} - 4.713 \log_{10} \Delta\alpha - 1.93 \tag{77}$$

the integration constant having been determined from the data of Curve VII in Fig. 2 together with Eq. (76).

Our equations enable us to study the transition between plasma and sheath. Let us consider a typical numerical example. A one ampere arc in a 3 cm diameter tube containing mercury vapor saturated at 30°C gives for a collector flush with the tube wall $I_p = 2 \times 10^{-4}$ amperes per cm², $T_e =$ 21000° and thus $E_e = 1.81$ volts. Then from Eq. (67) we find $x_p = 0.00686$ cm as our unit of length for the sheath measurements ($\lambda = 1$). If a collector is at -25 volts with respect to the ionized gas then at the collector surface $\eta = 1.256 + 25/1.81 = 15.1$. The effective distance between the collector and the source of ions may be taken to be 1 cm so that in Eq. (77) we put $\lambda = 1/0.0068 = 146$, and obtain $\Delta\alpha = 10^{-29}$. From Eq. (76) we see that the plasma field near the sheath falls to 1/10th for an increase in distance from the sheath equal to 0.032 cm (i.e. 4.71×0.0068).

According to the data of Fig. 2 the potential distribution within the sheath is given by

x	0	0.049	0.073	0.089	0.114	0.149
V	25	5.	1.34	0.44	0.080	0.006

where V is the negative voltage at a point whose distance from the collector surface is x cm. If the initial velocities of the ions and electrons could be neglected the total thickness of the 25 volt sheath, calculated by the ordinary space charge equation, like Eq. (67), would be 0.049 cm.

From the foregoing analysis it appears that the motions of the positive ions in the plasma are not to be chosen arbitrarily but are fixed by the electron temperatures and by the geometry of the ion source. With the plane source we have assumed above, we found $\eta_1 = 1.2565$ which means according to the nomenclature of Eq. (66) that $E_p = 1.2565 E_e$.

This particular assumption, however, is of course not directly applicable to experimental conditions. Dr. Tonks has been able to solve the integral equations involved in the problem of potential distribution resulting from a uniform generation of ions throughout the plasma (plane, cylindrical or spherical) and also for the more usual case where the rate of generation at each point is proportional to n_e the concentration of electrons at that point. It is intended to publish these results soon. The way in which the distribution of ion generation in the plasma affects the conditions in the sheath is by altering the average velocity of the ions which enter the sheath. The equations that we derived for the double sheath, such as Eq. (66), are applicable if we choose the proper value for the ratio E_p/E_e. For the case of ion generation proportional to n_e and an infinite plane collector the effective value of this ratio is 0.751 for very high intensity of ionization, decreasing somewhat as the intensity of ionization decreases but probably never falling as low as 0.5 which according to our discussion of Eq. (72) is the limit at which only periodic plasma solutions are possible.

For most experimental conditions we are thus justified in placing $E_p = 0.7 E_e$ in Eq. (66).

Experimental Data on Double Sheaths

In determining the space potential by the hot probe method,[15] the volt-ampere characteristic of a small filament is determined first when the filament is cold and then again when heated to a temperature at which electrons are emitted. Only when the filament is below the space potential do the electrons escape. Thus the voltage at which the two curves separate is the space potential. At lower potentials the difference between corresponding ordinates measures the electron current from the probe.

In using this method in ionized gases it was soon found, when the probe potential was lowered below space potential, that the electron current did not rise abruptly to the saturation emission corresponding to the probe temperature, but often a transition region of several volts was observed. Clearly in this range the current is limited by space charge in spite of the fact that an abundant supply of positive ions is present in the ionized gas. The double sheath theory should apply in such cases.

Experiment 559. Similar limitation of current by space charges in double sheaths is observed in hot cathode tubes containing gas if the current to the anode is lowered below its saturation value by using a large resistance in series with the anode. For example, a spherical bulb 12.5 cm in diameter contained a tungsten filament 1 cm long and 0.18 mm diameter, a disk shaped anode 2.2 cm diameter, and a mica-backed collector 1.1 cm in diameter. The filament was heated to a temperature at which it gave a saturation current of 22.5 ma. The volt-ampere characteristics of the anode were measured when the bulb contained mercury vapor saturated at 20°C, while simultaneous readings were made of the positive ion current flowing to the disk collector, this being kept at -80 volts with respect to the anode. Until the anode potential was raised to about 12 volts above that of the cathode, negative charges on the walls of the tube prevented any appreciable current from flowing. At 15 volts, however, the current rose to about 1 ma and as the voltage was increased to 25 the current increased only slowly to 1.9 ma. Electrons of 25 volts energy have an ionizing power 3.3 times as great as those of 15 volts. This small increase in current in spite of the considerable rise of voltage is probably due to the fact that the sheaths on the walls are relatively thick. As the ion production increases the sheaths become thinner so that the area of the sheath boundary, (which collects the ions that pass to the walls) increases and prevents any large rise of ion concentration. The small ion currents to the collector, ranging from 5 to 8 microamperes, indicate that the sheaths must have been several cm thick.

At voltages above 27 volts the behavior is quite different; as the current is raised from 2 to 22.5 ma the voltage rises slowly from 27 to a sharp maximum 33 at 15 ma and falls to 28 at 22 ma. As saturation is approached the voltage can be raised to 60 or more without increasing the current above 22.5.

In the range of relatively constant voltage (27–33) the collector current rose from 8 to 80 microamperes while the electron current changed from 2

[15] I. Langmuir, J. Franklin Inst. **196**, 754 (1923).

to 22. With such low intensity of ionization the collector currents do not measure accurately the ion current density since the sheath on the collector is many mm thick.

Similarly the diameter of the double sheath on the cathode must have been 10 to 30 times that of the cathode itself. Rough calculations based on the space charge theory of sheaths indicate that the electron current from the cathode, at the higher currents (20 ma) was about 2000 times as great as the positive ion current that flowed to the cathode and at lower currents the ratio may have increased to 4000:1.

In this range the electron current from the cathode is evidently limited by the rate of arrival of positive ions at the cathode sheath. If the total current is fixed by an external resistance, the voltage drop in the sheath adjusts itself to a value which will give just the required number of ions. Since the number of ions formed in the plasma is proportional to the current and increases rapidly with voltage, we have an explanation of the relatively constant voltage.[16]

Tube with Oxide Coated Cylindrical Cathode

Conditions more nearly approaching those of the theory we have developed are to be found in discharges using relatively large oxide coated cathodes. The following data were obtained by F. B. Vogdes. The cathode was a nickel cylinder of 0.63 cm diameter, 2.5 cm length closed at one end and heated by radiation from an inner tungsten helix. The outer cylindrical surface was coated with barium oxide. This cathode was mounted in a well exhausted spherical bulb 10 cm diameter provided with an appendix containing mercury. A collector disk 0.6 cm diameter was placed 2 cm opposite the central part of the cathode, the axis of the cathode lying in the plane of the disk. Shortly after starting to operate the tube (appendix at 12°C) with an anode current of 4 amperes, the arc drop was 50 volts and the current depended greatly on the cathode heating current. Thus the current was limited by the cathode emission. The positive ion current density given by the collector was 14 ma per cm² and the electron temperature T_e was 140000°. The ratio I_e/I_p was thus 57.

After operation for some time, the activity of the cathode suddenly increased, the arc drop fell to 17 volts, and T_e became 38,000. On the following day the characteristics were steady and reproducible and the data given in the accompanying table were taken. The arc current was now independent of the cathode heating current and adjusted to 4 amperes by means of a resistance in series with the anode.

[16] Approximate calculations of the ratio of electron current to ion current for cylindrical sheaths indicate that this ratio should increase from $(m_p/m_e)^{1/2}$ for very thin sheaths up to 2.25 $(m_p/m_e)^{1/2}$ for sheaths of large diameter. However, this theory neglects the fact that for sheaths of large diameter many of the ions may escape from the sheath after describing orbits about the cathode. Thus the ratio i_e/i_p may increase to values much greater than that just given. In the case of mercury vapor, values of this ratio as high as 2000 or 4000 are therefore consistent with the theory.

Appendix Temp.	Pressure baryes	Arc drop	T_e	I_e ma·cm^{-2}	I_p ma·cm^{-2}	I_e/I_p obs.	I_e/I_p cal.	Ratio obs./cal.
19.7°	1.5	16.0	24000	800	5.6	143.	372	0.385
8.8	0.55	20.2	35000	800	6.0	133.	350	0.380

The effect of lowering the vapor pressure of the mercury in a ratio of about 3:1 was to increase the electron temperatures and the arc drop but the ratio of the observed electron to ion currents remained nearly constant at about 140:1. In the last column of the table are given the ratios calculated by the double sheath theory according to Eq. (66) placing $E_p/E_e=0.7$; $E_e=T_e/11600$, $E_c=0.1$ and $V_{SM}=$arc drop$+0.5$.

We see that the small variation of the observed value of I_e/I_p from 143 to 133 is in accord with the effect to be expected from the increased electron temperature. However, the observed ratio is only 38 percent of that given by our theory. Such a difference may probably be explained by a lack of uniformity in the emission from the oxide coated surface.

Experiment 560. In this experiment the intensity of ionization and the voltage drop in the sheath could be varied independently of one another. Two cathodes were used, one to produce the ionization while the volt-ampere characteristics of the second were determined. The spherical bulb having a mercury appendix was of 12.5 cm diameter and contained a cathode K of tungsten wire 0.25 mm diameter wound as an open helix, and an oxide coated cathode C like that used before: a nickel cylinder 2.5 cm long and 0.63 cm diameter heated by an internal tungsten coil. There was also a collector disk B 1.1 cm diameter, backed by mica and a disk shaped anode A 2.2 cm diameter. The collector was so placed in the bulb that primary electrons reflected from the sheath on the bulb were not focussed upon it, for if this precaution is not taken serious errors may sometimes result, especially at low pressures of mercury vapor.

In exhausting the tube all metal electrodes were heated to bright red by high frequency induction and the bulb was baked at about 400°C. During the whole experiment the tube remained connected to a glass condensation pump through a liquid air trap, the readings of a McLeod gauge showing pressures of non-condensible gases less than 10^{-5} barye.

A typical set of data obtained with this tube containing saturated mercury vapor at 20°C is illustrated in Fig. 3. In this case the tungsten cathode K was maintained at -50 volts with respect to the anode (taken as zero potential) and heated to a temperature at which it emitted 60 ma. of electrons. The ionization produced by these 50 volt electrons was such as to give 0.127 ma of ion current to the collector B (kept at -75 volts). This corresponds to $I_p=65\times10^{-6}$ amps. cm^{-2} after correction for the edge effect.[17]

[17] Reference 3, p. 540.

Curve I represents the observed volt-ampere characteristic of the oxide-cathode C when the heating current in the tungsten coil was 5 amperes,—the cathode then being at a temperature too low to emit an appreciable electron current. The rise in current as the voltage approaches zero is due to electrons collected from the plasma. At positive voltages C becomes anode and the current is then limited by the emission from K. By plotting the ratio[18] of the electron currents to C and to the anode A (the sum being approximately 60 ma.) on semi-logarithmic paper against the voltage of C, a straight line was obtained extending over a range of 6 volts, in which the ratio increased 10^4 fold. From the slope of this line, the temperature of the plasma electrons was found to be 8500° which gives $E_c = 0.733$ volt.

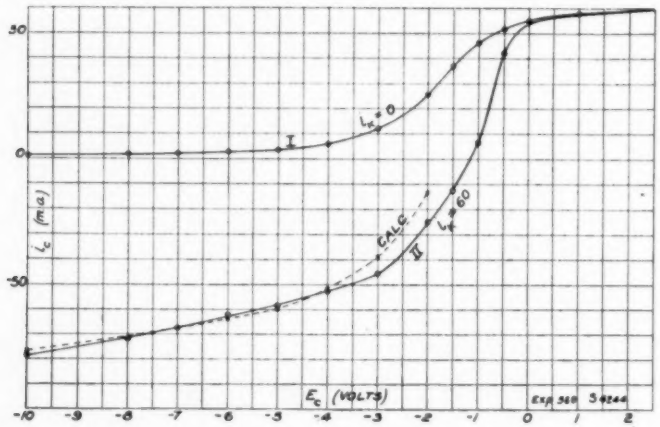

Fig. 3. Volt-ampere characteristics of oxide coated cylindrical cathode; E_c is voltage of the cathode C with respect to the anode A; $E_k = -50$; $i_k = 60$ ma (disregard "$i_k = 0$" on curve I).

When the current through the tungsten coil was raised to 9.5 amperes, the saturation emission from C, calculated by Richardson's equation from measurements of saturation currents at lower temperatures, increased to 2.2 amperes. We see, however, from the observed volt-ampere Curve II, Fig. 3, that the electron currents were less than 80 ma. These currents remained unchanged if the heating current was lowered to 8.0 amperes (calculated emission 180 ma.) but the electron current became saturated at −14 ma. with a heating current of 7.0 amps. Thus the currents of Curve II are limited by space charge.

For positive voltages the two curves coincide since no electrons can escape. The difference between corresponding ordinates for negative voltages thus represents the current of thermionic electrons that leaves the cathode, which we shall call i_e. As the voltage is lowered below 0 volts, a few electrons escape because of their initial velocities which correspond to about $E_c' = 0.1$ volt. The point of inflection at about $E_c = -0.5$ volt thus lies close to the space potential. This would seem to indicate a positive anode drop

[18] Langmuir and Jones, Phys. Rev. **31**, 396 (1928).

of 0.5 volt. However, because of the contact potential of the oxide on the cathode the effective cathode potential is probably a volt or so more positive than indicated by the value of E_c.

The values of i_e obtained by subtracting the ordinates of Curve II from those of Curve I are tabulated in Column 6 of Table III. A corresponding set of data obtained with an ionizing current $i_k = 20$ ma and a heating current of 9.5 amperes for the oxide cathode C is given in Column 3. We see that although these currents are independent of the temperature of C they are nearly proportional to the current from K showing that the electron current is determined by the supply of ions to the cathode.

Let us first examine these data from the point of view of Eq. (66), that is, let us see whether the variation of i_e with E_c can be explained as the effect of the velocities of the plasma electrons and ions. Placing $E_e = 0.733$ volt

TABLE III. *Variation of electron current with cathode potential.*
Mercury vapor sat. at 20° $E_k = -60$ Emission of C 2.2 amps.

1	2	3	4	5	6	7	8
		$i_k = 20$ ma; $I_p = 0.025$ ma cm^{-2}			$i_k = 60$ ma; $I_p = 0.061$ ma cm^{-2}		
E_c	$\frac{I_e}{I_p}$	i_e obs.	i_e cal.	x cm	i_e obs.	i_e cal.	x cm
−3	310	22.4	20.7	0.040	57.7	50.9	0.026
−4	347	23.9	23.7	0.048	58.9	57.8	0.031
−5	375	25.5	26.2	0.056	62.2	63.4	0.036
−6	393	27.0	27.9	0.063	65.2	67.1	0.040
−8	420	31.5	30.9	0.076	73.8	73.5	0.048
−10	437	34.0	33.0	0.087	79.9	78.1	0.056

from the data of Curve I, $E_p = 0.7E_c = 0.513$ volt and $E_c' = 0.1$ volt, we calculate from Eq. (66) the values of the ratio I_e/I_p given in Column 2. Dividing the observed values of i_e by this factor we should obtain the positive ion current to the cathode. However, although I_p in the plasma may be assumed to be independent of E_c (since $-E_c$ is less than the ionizing potential) the positive ion current will vary slightly with E_c because of the changes in the sheath thickness. The fifth and eighth columns give the sheath thickness in cm calculated by the space charge equation making allowance for the initial velocities of the ions.[19] The values of I_p used in these calculations, according to a method which will be described later, were taken to be 0.025 and 0.061 ma cm^{-2} for $i_k = 20$ and 60 ma respectively.

From the diameter of the sheath $(0.635 + 2x)$ the collecting area of the cylindrical sheath was found (length 2.54 cm) and thus a positive ion current density I_p' was calculated from each value of i_e. The averages of these, excluding only those at $E_c = -3$, gave 0.0117 and 0.0299 ma cm^{-2} for $i_k =$ 20 and 60 ma. These multiplied by the sheath areas and the factor I_e/I_p of Column 2, gave the values of i_e (calc.) in Columns 4 and 7. The dotted

[19] Calculated by Eqs. (10) and (11), Reference 3, p. 452. The positive ion "temperature" which enters only as a small correction, was taken to be 5000° and the voltage in the sheath $-E_c$.

curve in Fig. 3 represents the values in Column 7. A comparison of these observed and calculated values (which involve only one empirically determined parameter I_p') shows that the observed variation of i_e with E_c is in satisfactory agreement with Eq. (66) and is thus explained by the velocities of the plasma electrons and ions. Only about 1/4 of the observed variation is due to changes in the sheath thickness.

The slight differences in the shape of the curves obtained from the calculated and the observed values of i_e are probably to be explained;—1. By uncertainties in the contact potentials which would displace the curves horizontally a volt or so;—2. By changes in the distribution of ion currents in in the plasma, resulting from the space charges of the escaping electrons. If the cathode is made more negative than -10 volts ionization is produced by the emitted electrons which may cause considerable departures from the theoretical curve; for this reason we have confined ourselves in this discussion to the region above -10 volts.

Since in deriving Eq. (66) we have assumed that plasma electrons in appreciable numbers are not able to reach the cathode we must not expect this equation to apply when, according to Curve I, any large electron current passes to this electrode. Thus we should not expect agreement between the observed and calculated values of i_e at voltages much higher than -4. We see in fact that considerable differences are observed at -3 volts.

TABLE IV. *Relation between electron and ion currents.*
Hg at 20°C $E_k = -50$ $E_B = -85$ $E_c = -8$
Currents in milliamps.

Hg Temp.	1 i_k	2 i_e	3 i_B	4 I_p	5 i_p	6 x	7 I_p
20°	10	16.7	0.0376	0.0063	0.0923	0.1316	0.0129
	20	28.6	0.0591	0.0168	0.1580	0.0994	0.0237
	30	38.0	0.0765	0.0269	0.2100	0.0854	0.0327
	40	47.9	0.0940	0.0379	0.2646	0.0755	0.0422
	50	57.7	0.1098	0.0484	0.3188	0.0685	0.0517
	60	66.5	0.1270	0.0604	[0.3674]	0.0636	[0.0604]
Exponent		*0.77*	*0.67*	*1.17*	*0.77*		*0.86*
10°	60	63.9	0.117	0.0534	0.328	0.0676	[0.0534]
Exponent		*0.80*	*0.67*		*0.80*		*0.88*

Studies were also made of the variation of i_e with ionizing current i_k, of the relation of i_e to the ion current density I_p and the effect of varying the mercury vapor pressure. For these purposes E_c was kept constant at -8 volts, and, while i_k was varied from 10 to 60 ma measurements were made of i_e and of i_B, the ion current to the collector B, this being at voltages ranging from -70 to -120. The cathode C was heated to a temperature at which it emitted 2.2 amps. Table IV gives data obtained in this way.

Plotting i_e against i_k on double logarithmic paper gives a straight line of slope 0.77 showing that the electron current increases in proportion to the 0.77 power of the ionizing current i_k. The ion current to the collector i_B, plotted similarly gives approximately a straight line of slope 0.67.

Before we can test the proportionality between i_e and i_p, the ion current to the cathode, which is to be expected by our double sheath theory, corrections must be made for the effects of the thickness of the sheaths on C and B. The theory of these edge corrections[17] indicates that $i_B^{1/2}$ should be a linear function of $\nu^{1/2}$, the slope S of this line being

$$S=0.00306g(m_e/m)^{1/4}\text{amp}^{1/2}\text{volt}^{-3/4} \tag{78}$$

where g is a numerical factor approximately equal to unity and which is dependent solely on the geometry of the collector and where

$$\nu=V^{3/2}\{1+0.0247(T/V)^{1/2}\} \tag{79}$$

is the $V^{3/2}$ of the space charge equation multiplied by a correction factor which allows for the effects of the initial velocities of the ions as they enter the sheath. Numerous experiments in which collectors like B have been used for ions in mercury vapor have given $g=0.98$ which corresponds by Eq. (78) to $S=1.21\times10^{-4}$. By this theory, to correct i_B for the edge effects, we subtract $S\nu^{1/2}$ from $i_B^{1/2}$ and thus obtain $i_0^{1/2}$ where i_0 is the corrected current; —that is, the current that would flow if no edge correction were needed. Dividing i_0 by the actual area of the collector gives I_p the ion current density. The figures in Column 4 were obtained in this way. Putting $V=85$ volts, $T=5000$ for the ion temperature, gives $\nu=932$ and $S\nu^{1/2}=3.694\times10^{-3}$ amps$^{1/2}$, so that if i_B is expressed in microamps we subtract 3.694 from $i_B^{1/2}$ to obtain $i_0^{1/2}$, i_0 also being in microamps. Dividing i_0 by 0.95 cm^2, the collector surface, gives I_p.

For the lower currents at least, these values are certainly over-corrected. We realize this if we consider that the sheath thickness for $i_k=10$ ma calculated from the value of I_p in Column 4 is 0.7 cm as compared to a collector diameter of 1.1 cm. We also find by a double logarithmic plot that I_p is proportional to the 1.17 power of i_k, whereas numerous experiments (unpublished) with guard-ring collectors, that need no corrections, have shown that I_p, as observed by a collector mounted not far from the center of a spherical bulb, varies with a power of the ionizing current that ranges from 0.85 to 0.90.[20]

[20] In mercury arcs, (Reference 3, p. 764) I_p varies in proportion to the 1.25 power of the arc current indicating appreciable ionization of excited atoms. Experiments (Langmuir and Jones, Phys. Rev. **31**, 403 (1928)) with ionization by 30–100 volt electrons in which the *total* ion currents were measured using the walls of the cylinder enclosing the discharge as collector have shown that I_p varies with the 1.0 power of the ionizing current even when this varies in a ratio of more than 1:100. The reason for exponents less than unity is undoubtedly to be sought in a variation of the plasma fields which causes the distribution of ions between a central collector and the glass walls to vary with the intensity of the discharge. The fact that the best

Let us see whether the experimental data of Columns 1, 2 and 3 are consistent with the assumption that the electron current from the cathode is proportional to i_p, the ion current that flows to the cathode. The thickness of the double sheath x according to the last line of Table I, is 1.364 times that calculated by the ordinary space charge equation. The current density used for this calculation should be that at a surface half way between the cathode and the outer edge of the sheath, so that the effective area of the cathode sheath is $\pi(0.635+x)$ 2.54 cm². Thus from Eqs. (1) and (79) taking $T=5000$, $V=8$ and expressing i_p in ma we get

$$x^2=0.00212(0.635+x)/i_p. \tag{80}$$

The collecting area for ions, however, is $\pi(0.635+2x)$ 2.54 cm² and therefore

$$i_p=7.98(0.635+2x)I_p. \tag{81}$$

For the highest current, $i_k=60$, we may assume that the value of I_p in Column 4 is approximately correct. With this value of I_p, Eqs. (80) and (81) solved as simultaneous equations, give $x=0.0636$ cm and $i_p=0.3674$ ma. We obtain the other values of i_p in Column 5 by taking them proportional to i_e in Column 2, and from these the sheath thickness x (Column 6) is found by Eq. (80). Equation (81) then enables us to calculate I_p as given in Column 7. These values of I_p give a straight logarithmic plot against i_k of slope 0.86 which agrees with the exponents 0.85 to 0.90 found in the experiments with guard-ring collectors, and therefore our experimental data are consistent with the double sheath theory that requires a proportionality between i_e and i_p.

The ratio i_e/i_p given by these data is 181:1. By Table III at this cathode voltage (−8) we should have the ratio 420:1 so the observed electron current is 0.431 of that calculated, only a little greater than the ratio 0.38 we found from the data supplied by Mr. Vogdes. Undoubtedly part at least of this discrepancy is accounted for by lack of uniformity of the oxide coating and perhaps the lower temperature of the ends of the cathode cylinder.

The last two lines of Table IV give data obtained with mercury vapor saturated at 10° at which the pressure is only 0.40 that at 20°. The exponents were found from logarithmic plots of data with values of i_k ranging from 10 to 60. The ratio i_e/i_p is here 195, somewhat closer to the theoretical value 420.

Filamentary Cathodes

A large number of experiments (Experiment 562–a) have been made with two tungsten cathodes 0.25 mm in diameter, one (K) to produce the ionization of the mercury vapor and the other (C) to give the volt-ampere characteristics. The values of I_p were determined simultaneously using a guard-

---

data (with guard rings) give a straight double logarithmic plot, is entirely inconsistent with recombination of ions and electrons as a cause of the low value of the exponent. Recombination would introduce a term varying with I_p^2 which cannot be reconciled with the observed data.

ring collector. With C cold the positive ion currents i_p to C could be measured as a function of voltage. Then with C hot enough to emit a surplus of electrons the electron current was measured. The ratio i_e/i_p depended on I_p and on the voltage, E_c, but was independent of the pressure of mercury vapor (10 to 20°C) and of the voltage E_k of the ionizing electrons. For $E_c = -10$ volts the following values were obtained.

I_p	i_e/i_p
0.140 ma cm^{-2}	940
0.38	530
0.57	450

A more detailed analysis of the curves obtained in these experiments will be reserved for a subsequent paper.

The writer wishes to express his appreciation of the assistance of Mr. S. P. Sweetser who carried out most of the experiments.

RESEARCH LABORATORY,
GENERAL ELECTRIC COMPANY,
SCHENECTADY, N. Y.,
March 12, 1929.

NOTE ON "OSCILLATIONS IN IONIZED GASES"

By Lewi Tonks and Irving Langmuir

Certain general equations governing plasma-electron oscillations were derived on pages 197 and 198 of the article "Oscillations in Ionized Gases."[1] Only when it was too late to add a note to this article did we realize that certain approximations beyond those specifically mentioned in the paper were involved. The first such approximation occurs in the elimination of $\mathbf{v}$ by taking the time derivative of the third electromagnetic equation. The terms $\dot{n}e\mathbf{v}$ and $ne\dot{\mathbf{v}}$ both appear. For sufficiently small oscillations the former can be neglected since it varies as the square of the oscillation amplitude while the latter is proportional to the first power. Later, a similar situation arises with the occurrence of the term $(4\pi e^2/m)\mathbf{E}\cdot\nabla n$ in passing from Eq. (5B) to (5C). If ∇n arises wholly from the oscillation, this term can be neglected on the same grounds, but if n has a fixed space variation other effects which have not yet been investigated may arise.

[1] Tonks and Langmuir, Phys. Rev. **33**, 195 (1929).

THE PHOTOELECTRIC AND THERMIONIC PROPERTIES OF MOLYBDENUM

By Miles J. Martin

Abstract

The variation of the photoelectric sensitivity of a molybdenum surface during prolonged heat treatment has been studied over a period of 300 hours of intense heating. Thin ribbons of molybdenum were heated to a temperature of 1325°C in a high vacuum and the photocurrents produced by the light from a quartz mercury arc were measured with a quadrant electrometer. The photoelectric sensitivity was found to increase as the heating progressed, finally reaching a limiting value. The increase in sensitivity was accompanied by a shift in the wave-length limit from approximately 2600 A. U. to approximately 3800 A. U.

The photoelectric work function of molybdenum was determined from the characteristic wave-length limit of the heat treated surface after a condition of stability had been attained. The value of the work function so determined was $3.22 \pm .16$ volts.

The thermionic work function of molybdenum was determined for the same specimens. The thermionic emission as a function of temperature was plotted logarithmically according to Richardson's equation. The value of the thermionic work function determined from the slopes of these curves was $3.48 \pm .07$ volts. The photoelectric and thermionic work functions were thus found to agree within 0.26 volts.

The variation of photoelectric sensitivity of molybdenum with temperature was observed. The sensitivity was found to increase with temperature, the variation amounting to approximately 30 percent between room temperature and 1000°C.

Introduction

THIS paper is a brief report of one of a number of experiments now under way in this laboratory upon the general problem of the photoelectric and thermionic characteristics of metals which have been subjected to rigorous heat treatment under extreme vacuum conditions. DuBridge[1] has reported a thorough investigation of the photoelectric and thermionic properties of platinum and Cardwell[2] has recently published an account of the work upon iron. This report deals with the following investigations:

(1) The variation of the photoelectric sensitivity of a molybdenum surface while undergoing prolonged heat treatment.

(2) The determination of the photoelectric work function of the metal from the characteristic long wave-length limit of the heat treated surface.

(3) The determination of the thermionic work function from the slope of the logarithmic graph of Richardson's thermionic equation.

(4) The variation of the photoelectric sensitivity with the temperature of the specimen.

Apparatus

The apparatus was essentially the same as that used by DuBridge[1] and Cardwell.[2] The specimens were prepared from samples of molybdenum

[1] DuBridge, Proc. Nat. Acad. Sci. **12**, 162 (1926; Phys. Rev. **29**, 451 (1927).
[2] Cardwell, Proc. Nat. Acad. Sci. **14**, 439 (1928).

obtained from two different sources.* They were rolled into ribbons 13 cm long by 0.5 cm wide by 0.03 mm thick. After cleaning with alcohol the ribbon was suspended in the form of a loop from two tungsten leads inside a Pyrex tube, thus forming a filament which could be heated to any desired temperature by an electric current. Surrounding the filament was a nickel cylinder in which holes were provided for illuminating the specimen and for viewing with the pyrometer, and which served as a collecting electrode. This nickel cylinder was carefully washed alternately in nitric acid and warm water and then baked in a separate vacuum system before being introduced into the tube. The specimen was illuminated through a quartz window which was attached to the tube by means of a graded quartz-Pyrex joint. The source of ultra-violet light was a Cooper-Hewitt quartz-mercury arc of the vertical type which was enclosed in an asbestos housing. It was operated at a current of 3.5 amperes with 65 volts drop in potential across the arc. This gave a very intense illumination and reduced the maximum variation of light intensity to approximately 3 per cent. Light was focussed upon the specimen by means of a crystalline quartz lens. Pressures in the earlier stages of the process were measured with a McLeod gauge and in later stages with an ionization gauge of the type described by Dushman and Found.[3] The photoelectric currents were measured with a Compton electrometer shunted by a resistance of 10^9 ohms, thus permitting the use of the steady deflection method. In observing the photocurrents produced by the full radiation of the arc a sensitivity of 700 mm per volt was used, while in making determinations of the wave-length limit a sensitivity of 20,000 to 60,000 mm per volt was used. Temperatures in the thermionic work were measured with an optical pyrometer of the disappearing filament type, which had been previously calibrated by observations upon the gold point and the palladium point, intermediate points being determined by sectoring down from the palladium point. Black body temperatures were corrected for the emissivity of molybdenum according to the data of Mendenhall and Forsythe.[4]

Procedure

The entire tube and the ionization gauge were encased in electric furnaces and baked at a temperature of 550°C for over 200 hours. Towards the end of this baking interval the pressure was 10^{-6} mm of Hg with the furnaces hot. Immediately after baking the long wave-length limit and the initial sensitivity of the specimen were observed. The specimen was then heated by a current continuously day and night, frequent observations of the sensitivity being taken as the out-gassing progressed. Finally a stage was reached at which further heat treatment did not change the sensitivity. Observations were then made of the long wave-length limit from which the photoelectric work function was computed. Curves of the thermionic

* Fansteel Products Company and the Elkon Company.

[3] Dushman and Found, Phys. Rev. **23**, 734 (1924).

[4] Mendenhall and Forsythe, Astrophys. Jour. **37**, 380 (1913).

emission were plotted from which the thermionic work function was computed. The variation of photoelectric sensitivity of the out-gassed metal with change of temperature was investigated. A description of the results of these investigations follows.

Results

(1) *The variation of the photoelectric sensitivity with prolonged heat treatment.* Figures 1 and 2 show the results of heat treatment upon two different specimens. Both curves are seen to be of the same general form and bear a strong similarity to the latter part of the curve that Cardwell[2] gives for

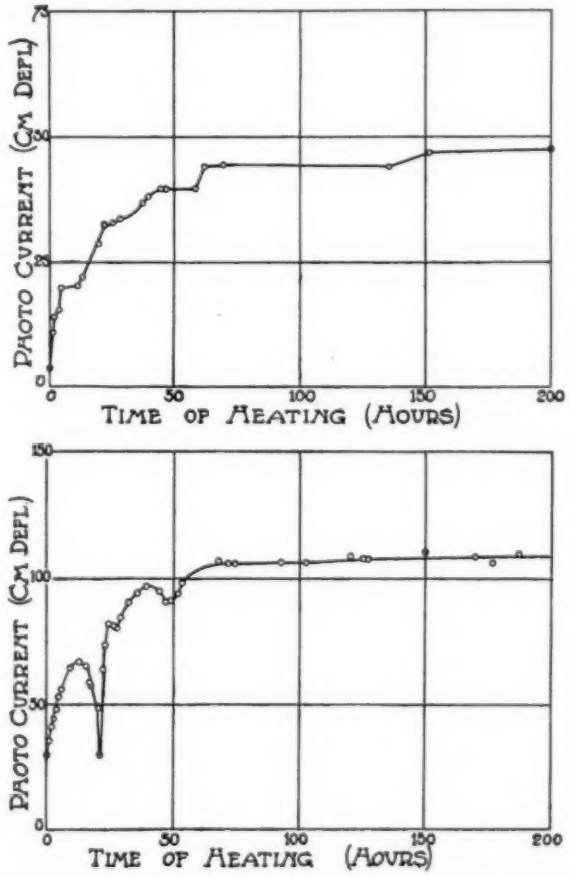

Figs. 1 and 2. Effect of heat treatment on two samples.

iron. The intervals between the observations on the curve of Figure 2 were so short as to indicate variations that would not show up on Figure 1. DuBridge's curve for platinum, although decreasing with time of heating, shows the same sort of variations. He has pointed out the fact that these variations are due to irregularities of pressure that are certain to occur in the initial stages of out-gassing. The curves for molybdenum indicate that the increase in sensitivity takes place in steps, which conforms with Card-

well's[2] findings for iron, and his hypothesis that these steps indicate the effect of additional lines of the spectrum becoming active seems reasonable.

The heating of the molybdenum specimens was begun at a temperature of 850°C and gradually increased to 1325°C at the end of 20 hours. Some of the irregularities of the curve of Figure 2 are due to increases of temperature. The marked decrease in photocurrent at 21 hours (Figure 2) occurred when the temperature was raised and was accompanied by a very great increase of pressure. The temporary decrease in photocurrent was obviously due to the evolution of a large amount of gas, and as the pressure was speedily reduced the photocurrent recovered quickly. At the end of 290 hours (in the case of the specimen represented by Figure 2) which was long after stability of pressure and constancy of photoelectric sensitivity had been reached, the temperature was raised to 1500°C. No appreciable change in sensitivity was observed and the long wave-length limit was the same as it had been found to be previous to this last increase of temperature. This was regarded as evidence that a thorough state of out-gassing had been attained.

At the beginning of this period of heat treatment the pressure was of the order of 10^{-7} mm of Hg as indicated by the ionization gauge. During the first few minutes of heating the pressure went up to about 10^{-5} mm of Hg but was rapidly reduced by subsequent heating. As the out-gassing progressed the pressure with the specimen hot approached the value of the pressure with the specimen cold. The equality of the pressure hot and the pressure cold was adopted as one criterion of complete out-gassing. Final observations were always made at pressures of from 1.0×10^{-8} to 2.0×10^{-8} mm of Hg.

During the out-gassing process "rest tests" were taken at intervals. An observation of the sensitivity was taken as quickly as possible after cutting off the heating current (approximately 30 seconds) and the specimen was allowed to stand without heating while observations of the change of sensitivity with time were taken. It was found that in the earlier stages the sensitivity changed rapidly with time, in some cases falling to half its value in 15 minutes. In the later stages the sensitivity was more stable and fell off much more slowly. Molybdenum was found to be very sensitive to small amounts of gas and a condition was never reached in which several hours standing did not produce a decrease in the sensitivity even though no change could be noted in the first hour or so. In all cases, however, one or two minutes of heating were sufficient to return the specimen to its former sensitivity at the beginning of the rest interval, which indicates that the change in sensitivity is due to a slight surface layer of gas which is readily removed. Figure 3 shows a series of these "rest tests" covering an interval of 15 minutes taken at various stages in the out-gassing process. In this graph the ordinates are merely electrometer deflections. The curves do not therefore appear in sequence, due to changes in sensitivity of the electrometer. The slopes of the curves only are of significance.

(2) *The determination of the photoelectric work function from the characteristic long wave-length limit.* In this work the method employed in determining the long wave-length limit was that used by DuBridge[1] and Cardwell[2] in which filters were used to cut out certain portions of the spectrum of the irradiating light. The filters consisted of organic solutions prepared according to the specifications given by Dahm,[5] and of certain glass screens obtained from Corning Glass Company. Immediately after a filter was used its transmission was photographed with a quartz prism spectograph. The long wave-length limit of the specimen taken after the baking but before heating the specimen itself was found to lie between 2536 A.U. and 2652 A.U. Observations upon the wave-length limit were not made in the earlier stages of the out-gassing due to the fact that the characteristics of the specimen would undergo a change in the time required for a set of observations. After the specimen had reached a stable condition, frequent determinations

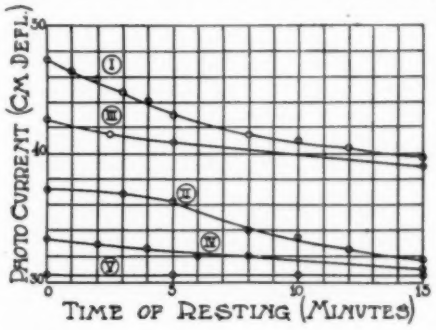

Fig. 3. Decrease of photoelectric sensitivity with time.
Curve I, taken after 4 hours total heating;
Curve II, taken after 40 hours total heating;
Curve III, taken after 112 hours total heating;
Curve IV, taken after 184 hours total heating;
Curve V, taken after 300 hours total heating.

of the long wave-length limit were made. The long wave-length limit of thoroughly out-gassed molybdenum was found to lie between 3650 A.U. and 4047 A.U. Upon interposing a screen which transmitted the 3650 line of mercury strongly, a small but decided photoeffect was always observed. When a screen was used that transmitted the 3650 line very weakly leaving the lines above 3650 with approximately the full intensity, the effect was very small, so small that it was at times doubtful whether an effect was present. When a screen was used that cut out the 3650 line completely no effect was observed. It is probable then that the 3650 line is the last active line in the mercury spectrum and it is undoubtedly a very close approximation to the long wave-length limit of "gas-free" molybdenum. It is at any rate certain that the next mercury line that could be isolated with the screens used, 4047, is not active. The work function corresponding to a wave-length limit of 3650 A.U. is 3.38 volts while a wave-length limit of

[5] Dahm, Jour. Opt. Soc. **15**, 266 (1927).

4047 A.U. yields a value for the work function of 3.05 volts. The average value of the photoelectric work function so determined may therefore be given as $3.22 \pm .16$ volts. These results were repeated daily for more than a week with no conflicting results. Independent observations were made by two observers.

(3) *The determination of the thermionic work function from the slope of the logarithmic graph of Richardson's equation.* In a few cases other observers have compared the value of the photoelectric work function with the value of the thermionic work function obtained from the same specimen. DuBridge[6] has compared the photoelectric and thermionic work functions of platinum and finds them to agree within the limits of experimental error. Warner[7] reports a close agreement between the two work functions of tungsten. In the case of molybdenum, thermionic currents between the temperatures of 1300°K and 1600°K were measured with a Leeds and Northrup galvanometer having a sensitivity of 2.2×10^{-10} amperes per millimeter at a scale distance of approximately two meters. Figure 4 is a logarithmic graph of Richardson's equation from data taken after the specimen had been heated a total of 330 hours. The slope of this curve yields a value for the constant b in Richardson's equation of 39,600. The corresponding value of the thermionic work function is 3.48 volts. The maximum error introduced into the result due to inaccuracy of temperature determination was estimated at 2 percent. The value of the thermionic work function determined from these experiments may then be given as $3.48 \times .07$ volts. The photoelectric and thermionic work functions of molybdenum are thus found to agree within 0.26 volts which is within the limits of error of this experiment, inasmuch as the apparatus was not expressly designed for thermionic measurements.

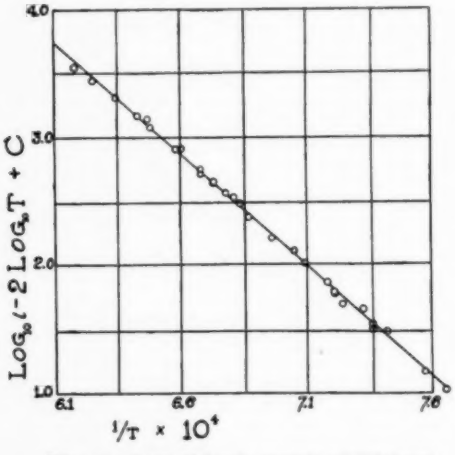

Fig. 4. Logarithmic graph of Richardson's equation from data taken after specimen had been heated 330 hours.

(4) *The variation of the photoelectric sensitivity with temperature.* Very few experimenters have investigated a temperature variation of the photoelectric effect over a wide range of temperature. DuBridge[1] reports for platinum an increase in the photocurrent with temperature up to 1100°C. Cardwell[2] finds that iron shows a decrease up to the temperature at which the iron undergoes a change in crystal structure and then begins to increase. The present work with molybdenum indicates a steady decrease in photocurrent with temperature which amounts to approximately 30 percent in going from room temperature to 1000°C. Figure 5 is a curve in which the

[6] DuBridge, Phys. Rev. **31,** 236 (1928).
[7] Warner, Proc. Nat. Acad. Sci. **13,** 56 (1927).

total photocurrent is plotted as a function of the heating current. The circles with dots in the centers indicate observations taken with increasing temperature and the circles with crosses in the centers represent points taken with decreasing temperature. The temperatures in this interval were below the range of the optical pyrometer. It was not possible to take observations of the photocurrent at temperatures above 1000°C owing to the fact that the enormous thermionic currents completely masked the photoeffect. No

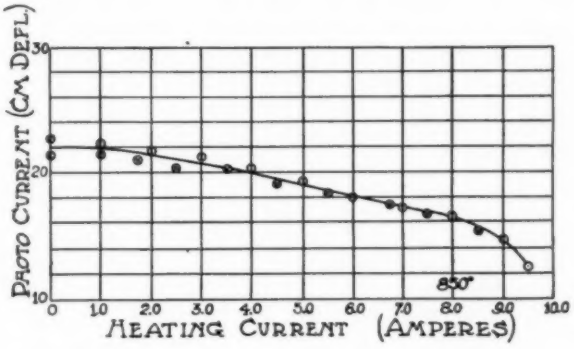

Fig. 5. Total photo-current as a function of heating current.

evidence was obtained in these experiments to determine whether or not the variation in photoelectric sensitivity with temperature is actually due to a change in the work function. The thermionic work function, which is an average value between 1300°K and 1600°K, was higher than the value obtained from the wave-length limit at room temperature. All that can be inferred from these data is that the temperature variation is in the proper sense to be caused by such a change in the work function.

Summary

Specimens of molybdenum subjected to long periods of heat treatment in a high vacuum showed an increase in photoelectric sensitivity as the heat treatment progressed, accompanied by a shift in the long wave-length limit from approximately 2600 A.U. to approximately 3800 A.U. The value of the photoelectric work function was found to be $3.22 \pm .16$ volts. The value of the thermionic work function between the temperatures of 1300°K and 1600°K was found to be $3.48 \pm .07$ volts. The photoelectric sensitivity of molybdenum showed a decrease with rise in temperature in the range from 0°C to 1000°C.

In conclusion the author desires to express his sincere appreciation to Professor C. E. Mendenhall under whose direction the work was done, to Professor R. C. Williamson and Professor H. B. Wahlin for many helpful suggestions, and to Mr. Howard E. Nelsen for his valuable assistance in the final part of the work.

University of Wisconsin,
Madison, Wisconsin,
March 11, 1929.

THE RECTIFICATION OF RADIO SIGNALS BY A THERMIONIC TUBE CONTAINING ALKALI METAL VAPOR

By K. H. Kingdon and E. E. Charlton

Abstract

The cathode of a thermionic triode tube is surrounded by a region of minimum potential caused by electron space-charge. If the cathode is of thoriated tungsten, and the tube contains caesium vapor, a few positive ions are formed by ionization of caesium atoms striking the hot cathode. Some of these ions accumulate around the potential minimum, raise the potential at that point, and allow a larger electron current to flow to the anode. The ions have a natural frequency of oscillation about the potential minimum, which is usually several hundred kilocycles. If an alternating voltage is applied to the tube, of a frequency agreeing with this natural frequency, the ions are set in oscillation about the potential minimum. This oscillation of the ions makes the potential minimum more negative, and decreases the anode current. In addition the amplitude of oscillation may build up by a resonance effect to such a large value that the ions are able to discharge to one of the neighboring conductors, leading to a still greater decrease in anode current. This kind of rectification is much greater for small alternating voltages than that resulting from curvature of the triode characteristics.

I. Introduction

SOME years ago one of the writers (E.E.C.) while studying triode thermionic tubes containing caesium vapor, found that under certain conditions these tubes were very sensitive radio detectors.[1] Subsequent experiments have shown that detector action (rectification) by these tubes is due mainly to causes entirely different from those which determine rectification in the ordinary high vacuum triode (curvature of characteristics). In the alkali metal tubes the rectification is caused by the action of the signal on the motion of positive ions formed by ionization of alkali metal atoms coming in contact with the hot filament.[2] These ions change space-charge conditions in the tube, and so change the electron current to the anode. In this article we shall give an account of some fundamental experiments with these tubes, and of the theory to which they lead, leaving to another article a more detailed account of practical alkali metal detector tubes and their characteristics in radio circuits.[3]

[1] The UX 200 A radiotron is a detector of this kind. See also Brown and Knipp Proc. I. R. E. **10**, 451 (1922) and **15**, 49 (1927); Donle, Proc. I. R. E. **11**, 97 (1923) and **12**, 159 (1924).

[2] Langmuir and Kingdon, Phys. Rev. **21**, 380 (1923); Proc. Roy. Soc. **107**, 61 (1925).

[3] Charlton and Hitchcock, to be submitted to Proc. I. R. E. Most of the ideas which we describe in the present article have been under discussion in our laboratory for some time, and all those who have worked with these tubes have made some contribution to them. In this article we try to reduce these ideas to precise form. We therefore wish to express our indebtedness to Messrs. A. L. Samuel, L. P. Smith, and W. J. Hitchcock for their contributions. We are also particularly grateful to Mr. H. M. Mott-Smith, Jr. for his suggestions in connection with the frequency characteristic of these tubes, and the experiments on this point.

II. Experimental Tubes

Most of the experiments to be described here were made with two tubes, *A* and *B*. Both tubes had V-shaped filaments of thoriated tungsten wire 0.00406 cm diameter and about 5 cm total length. The apex of the V was steadied by a flexible wire hook. The thoriated filaments were usually in a well-activated condition. The grids were of the conventional oval wire-wound type, and were surrounded by the usual oval anode. Both tubes had an amplification constant of about 25. In tube *B* portions of grid and anode at one corner were cut away and mounted on separate leads, as shown in Fig. 1. This construction made it possible to study separately phenomena at one end of the filament, usually the negative end. Unless otherwise stated the tube was connected so as to use the whole filament. The tubes were well exhausted, but contained a small amount of metallic caesium, giving a vapor pressure[2] of 1.8×10^{-3} barye when the bulb was at 25°C. This pressure is so low that ordinary ionization by collision phenomena play no appreciable part in the operation of the tube.

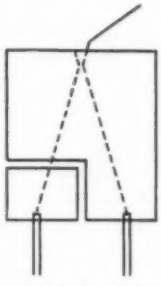

Fig. 1. Construction of grid and anode.

III. Static Rectification Characteristics

The tube was placed in a constant temperature bath, and filament temperature, and grid and anode voltages (E_g, E_p) fixed at the desired values. The multi-range ammeter in the anode circuit had a compensating battery and high resistance connected across it, so that most of the anode current (i_p) could be balanced out, and the residual read on one of the low-current ranges of the ammeter. An alternating current signal of any desired frequency and voltage was then applied between filament and grid, and the resulting change Δi_p in i_p noted. Thus Δi_p is the change in i_p due to an unmodulated signal, and may be said to measure the "static rectification" of the tube.

The a.c. signal was taken from one of two small oscillators, so as to cover the frequency range desired. The coil of a wave-meter was placed near the coil of the oscillator chosen, and a "pick-up coil" was placed on the opposite side of the wave-meter coil. The wave-meter thus served both to measure the frequency and as a filter to free the wave of harmonics. The leads from the pick-up coil went to a variable mutual inductance, the secondary of which was connected from filament to grid of the tube. A thermocouple connected across the secondary served to measure the signal voltage. This voltage was not appreciably affected by the grid current, even when the latter was large.

Fig. 2 shows Δi_p as a function of E_g for tube *B* (whole filament) at filament voltages of 3.1 and 5.0. E_g was measured from the negative end of the filament. The other conditions were—bulb temperature 30°C, $E_p=22.5$, signal voltage 0.050 RMS, signal frequency 600 kilocycles. The filament temperature was about 1700°K at $E_f=3.1$, and 1940°K at $E_f=5.0$. Both curves start at the left with small positive values of Δi_p. This is the same

phenomenon as rectification by curvature of anode characteristic in an ordinary high vacuum triode. Throughout the rest of the curves the values of Δi_p are negative and usually much greater. This is the type of rectification

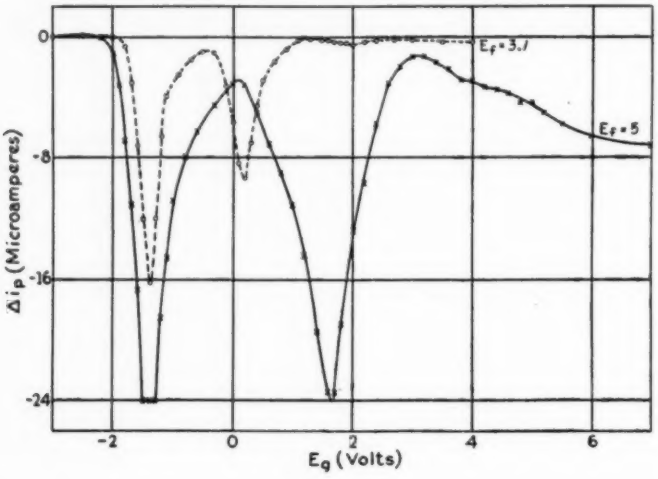

Fig. 2. Δi_p as a function of E_g for tube B at filament voltages of 3.1 and 5.0.

with which we are particularly concerned. Both curves show two main negative peaks, separated by a voltage difference slightly greater than $E_f/2$. For the $E_f = 5$ curve the rectification is large even at large positive values

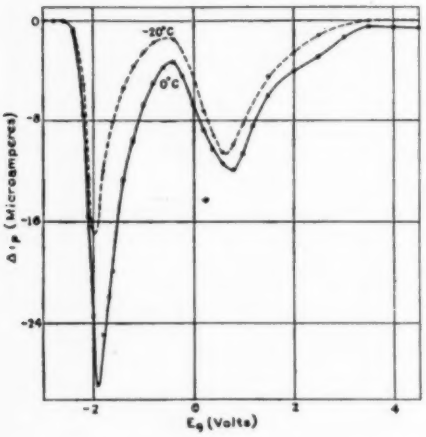

Fig. 3. Δi_p as a function of E_g for tube B at bulb temperatures of 0°C and −20°C.

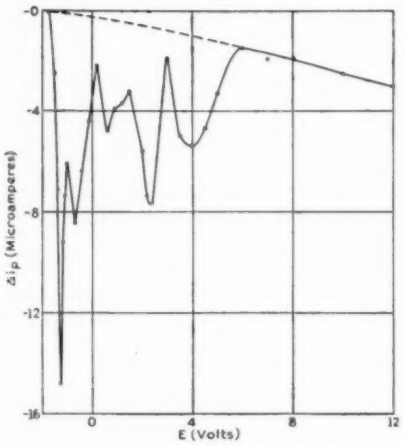

Fig. 4. Δi_p as a function of E, the common potential of grid and anode of tube B.

of E_g. For the $E_f = 3.1$ curve at high E_g the sum of anode and grid currents approaches the saturation emission from the filament, and Δi_p becomes small.

Fig. 3 shows Δi_p as a function of E_g for tube B at bulb temperatures of 0°C and −20°C. The other conditions were $E_p=45$, $E_f=5$, signal voltage 0.044, frequency 1050 kilocycles. The state of activation of the thoriated surface of the filament was different from that in Fig. 2. The rectification at −20°C is less than at 0°C and the effect gradually disappears as the vapor pressure of the caesium is reduced to zero.

For the experiment illustrated in Fig. 4 the grids and anodes of tube B were connected together and put at the common potential E. Fig. 4 shows Δi as a function of E. As before, E was measured from the negative end of the filament. The other conditions were—bulb temperature 29°C, $E_f=5$, signal voltage 0.044, frequency 1050 kilocycles. At the left the curve shows large negative peaks, somewhat more jagged than those found when the tube was used as a triode. There is a steady rise in the region of positive E, as in the right-hand part of the $E_f=5$ curve of Fig. 2. Note that in Fig. 4 the right-hand part may reasonably be extrapolated to the left by the dotted line, suggesting that the whole Δi curve is the sum of two different effects, one of which predominates at low values of E, and the other at high. This will be shown to be the case (see below, section 8).

IV. Evidence for Localization of Sensitivity in Limited Region of Filament

The peaks in the left-hand portions of the curves of Figs. 2 and 4 are very striking, and they indicate the presence of effects which vary rapidly with E_g. The signal voltages applied between grid and filament are small, and it is to be expected that they will produce the greatest effect on the motion of electrons or ions between filament and grid when the steady electric field in this region is smallest. In Fig. 2 the tube constants and contact potentials are such that when E_g is about −2, the combined fields of grid and anode are just able to produce a field at the negative end of the filament which accelerates electrons away from the filament, or more correctly, from the potential minimum (due to electron space charge) which surrounds the filament. As E_g is made more positive, this region of zero or small field moves along the cathode towards the positive end. Note that in the $E_f=3.1$ curve of Fig. 2 the peaks extend over a range of 3 volts from $E_g=-2$ to +1, and that in the $E_f=5$ curve they extend over a range of 5 volts from $E_g=-2$ to +3. That is, the "peak" phenomenon extends over a range of E_g wherein the combined values of grid and anode voltages are such as to produce a very small or zero field at some point on the filament. For larger positive fields the phenomenon changes over to the "steady rise" shown at the right. In Fig. 4 the "peak region" extends over a range of E slightly greater than E_f.

This discussion would lead us to expect that if we consider only the current coming from a limited region of the filament, then the contribution from this region to the total rectification will be greatest when the electric field in this region is small. This conclusion is supported by an experiment

made with tube B. The polarity of the filament was such that the small anode (Fig. 1) covered the negative end of the filament. The two sections of the grid were connected together, and the signal applied as before. The anode circuit was arranged so that either the resulting change Δi_p in the total anode current, or the change $\Delta i_p'$ in the current to the small anode only, could be measured. Fig. 5 shows Δi_p and $\Delta i_p'$ as functions of E_g for filament voltages 3.67 and 5.0. The other conditions were: bulb temperature 25°C, $E_p = 45$, signal voltage 0.044, frequency 1050 kilocycles. In the $E_f = 3.67$ curve we note that the left hand negative peak in Δi_p is matched by the negative peak in $\Delta i_p'$ showing that at $E_g = -2$ the greater part of the

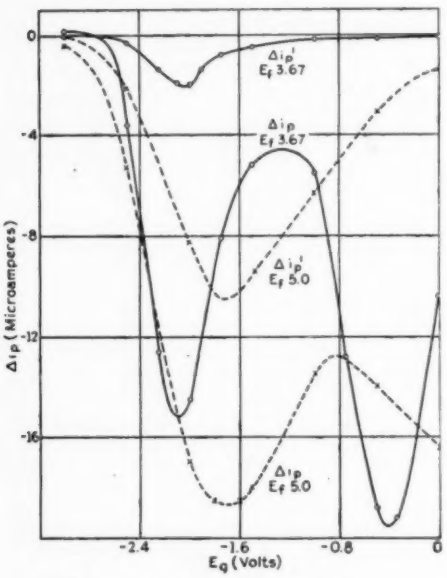

Fig. 5. Δi_p and $\Delta i_p'$ as functions of E_g for filament voltages 3.67 and 5.0.

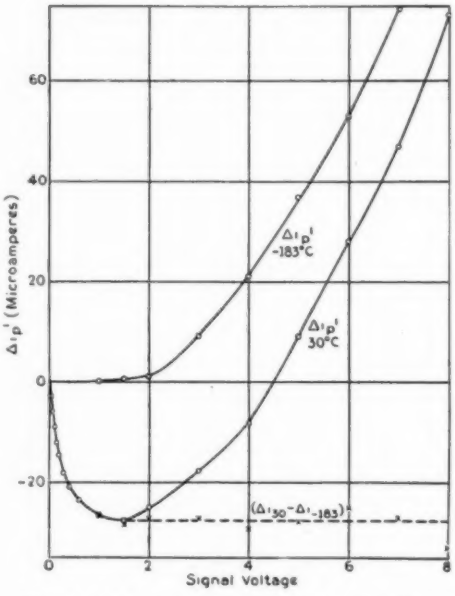

Fig. 6. $\Delta i_p'$ as a function of signal voltage for temperatures of 30°C and −183°C. The difference between the two curves (dotted curve) is a measure of the caesium type rectification.

rectification is taking place near the negative end of the filament. On the other hand there is no trace of a peak in $\Delta i_p'$ corresponding to the peak in Δi_p at $E_g = -0.4$, thus showing conclusively that this peak is due to rectification at a portion of the filament entirely outside the small anode. A similar behavior is evident in the $E_f = 5$ curves.

We are thus led to the idea that in the peak region the rectification is due to a phenomenon taking place chiefly over a limited region of the filament where the field acting on ions or electrons is small. The reason for the rectification being greater at some parts of the filament than at others, thus giving rise to the peaks, is best deferred until later (section IX).

V. Variation of Static Rectification with Signal Voltage

We have seen in the preceding sections that a small radio frequency signal applied between grid and filament causes a decrease in i_p. If however the signal voltage is made much larger (several volts) it produces an increase in i_p. This increase is due to ordinary rectification by curvature of the anode characteristic, which at these large signal voltages over-balances the other type of rectification which we have been discussing. The two types of rectification may be separated in the following way. The experiment to be described was done with the current to the small anode only of tube *B*. The conditions of the experiment where $E_f=5$, $E_p=45$, signal frequency 600 kilocycles. In Fig. 6 the curve marked $\Delta i_p'(30°)$ shows $\Delta i_p'$ as a function of signal voltage, with the bulb at 30°C. The tube was then put in liquid air and a second curve taken $\Delta i_p'(-183°)$. The first curve includes both the caesium type rectification, and the anode characteristic curvature rectification; the second, only the latter. The difference between the two curves is therefore a measure of the caesium type rectifi-

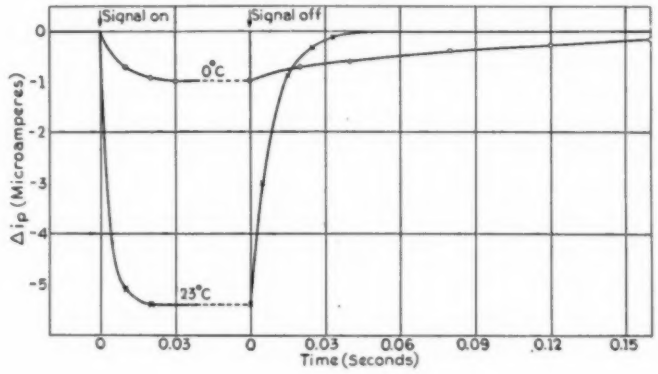

Fig. 7. Time lag effects.

cation, and is shown by the dotted curve. This dotted curve reaches a constant value at a signal voltage of about 1.5, and remains at that value for stronger signals.

This saturation behavior suggests that the caesium ions, whose motion is affected by the signal in such a way as to produce rectification, may all be removed from the vicinity of the cathode by a moderately strong signal, so that stronger signals can produce no greater effect.

VI. Time-lag Effects

Tube *A* was placed in a bath at 23°C, with $E_p=22.5$, $E_g=-1.65$, $I_f=0.194$ amp. (filament temperature about 1700°K). An Einthoven galvanometer was connected in the anode circuit, with a compensating battery and high resistance connected across it, so that only a small residual fraction of the anode current flowed through the galvanometer fiber. An alternating voltage (0.053 volt, 1050 kilocycles) was applied between grid and filament

at the time marked "signal on" Fig. 7, and removed at the time marked "signal off." The curve marked 23°C is a plot of the photographic record obtained in this way. The tube was then placed in ice and water, E_g changed to -1.8, and the record marked 0°C in Fig. 7 taken in a similar way. Both records show that when the signal was applied i_p fell rapidly to a minimum value, and when the signal was removed recovered at a rate which depended markedly on the bulb temperature. Fig. 8 shows semi-logarithmic plots of the rate of recovery of the anode current. Time is measured from the instant of removing the signal, and the ordinates measure the amount by which i_p lies below its final value. If Δi_{p0} is the maximum change in i_p, then both recovery curves are of the form

$$\Delta i_p = \Delta i_{p0} e^{-t/\tau}.$$

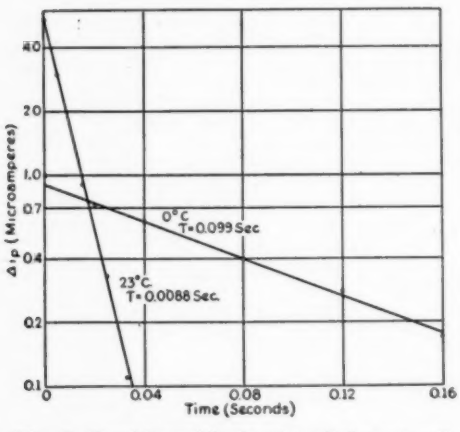

Fig. 8. Semi-logarithmic plot of the rate of recovery of the anode current.

The time constants τ are 0.0088 and 0.099 sec. at 23° and 0°C respectively. The pressures of caesium vapor at these temperatures are respectively 14.7×10^{-4} and 1.12×10^{-4} barye, so that the time constants are approximately proportional to the pressures. (There is some error in τ for the 23° curve, resulting from sluggishness of the Einthoven).

Similar time-lag records were taken for tube B, with the bulb at 0°C, and other conditions varied. Fig. 9 shows two records illustrating the effect

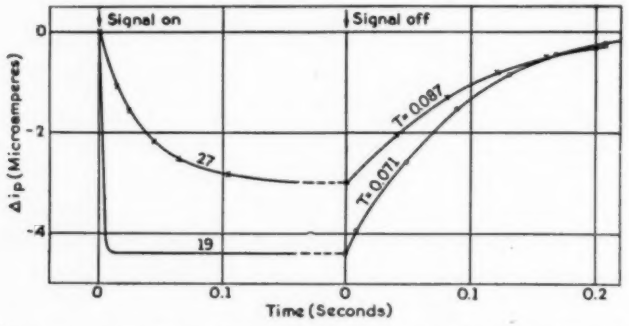

Fig. 9. Two records, tube B, illustrating the effect of strong and weak signals.

of strong and weak signals. For record 19 the conditions were $E_f=3.1$ (1700°K), $E_p=22.5$, $E_g=-1.7$, signal voltage 0.050, frequency 600 kilocycles. The current fell to its minimum value in about 0.01 sec. after applying the signal. The recovery was slow, with a time constant 0.071 sec. For record 27 the conditions were $E_f=3.1$, $E_p=22.5$, $E_g=-1.6$, signal

voltage 0.004, frequency 600 kilocycles. With such a weak signal a time of about 0.15 sec. was required for the current to fall to its minimum value after applying the signal. The rate of recovery was not very different from that of record 19, τ being 0.087 sec.

The decrease in i_p when the signal was applied was due, according to the theory mentioned in section I, to the removal of caesium ions from the region around the filament, with a consequent enhancement of electron space charge limitation of current. The initial parts of the records of Fig. 9 are in agreement with this idea, for it is to be expected that a weak signal (curve 27) would take much longer to sweep away the ions than would a strong signal (curve 19).

The recovery time lags observed at 0°C indicate that a time of several tenths of a second is required for the ion concentration around the filament to build up to its original value. This time is enormous compared with the time required for an ion to move from filament to grid (of the order one microsecond). The positive ion supply around the filament is renewed by ionization of caesium atoms at the surface of the hot filament, and the ion current from the filament depends on the amount of caesium adsorbed on its surface. When the caesium ion concentration around the filament is depleted by the signal, the amount of caesium adsorbed on the filament is also decreased. Hence, when the signal is removed the amount of caesium adsorbed on the filament must first be built up to normal value before the ion concentration around the filament can return to normal. That is, the recovery time lag measures the time required for a certain small fraction of the filament surface to become coated with adsorbed caesium. The initial loss time lags measure the time required for this adsorbed caesium to be removed from the filament (as ions) by the signal.

Some support is given this view by the fact that when the filament temperature is higher the time lags are smaller, although the actual values of Δi_p are larger. One would expect the amount of caesium adsorbed on the filament to be less at higher filament temperatures. The conditions for record 9 (Table I) were $E_f=5$ (1940°K), $E_p=22.5$, $E_g=-1.6$, signal voltage 0.010, frequency 600 kilocycles. The fall in i_p was complete in about 0.015 sec., and the time constant of the recovery was about 0.028 sec. The recovery time constant is thus about one third of that obtained in record 27, when the filament was at 1700°K.

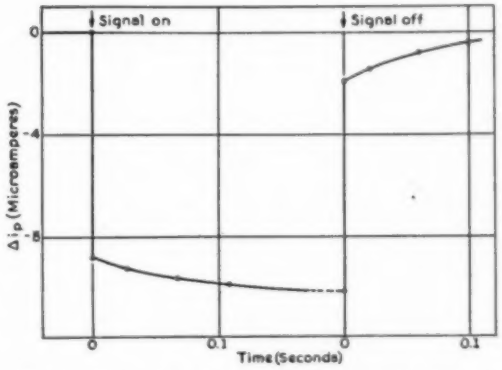

Fig. 10. Time lags (tube *B*) when steady change of potential was applied between grid and filament.

Fig. 10 (record 22) shows the time lags observed when a steady change of potential was applied between grid and filament of tube *B*. The con-

ditions were $E_f = 3.1$, $E_p = 22.5$, $E_g = -1.7$, signal voltage -0.05, bulb temperature 0°C. When the change in voltage was applied to the grid there was first an extremely rapid decrease in i_p (corresponding to the ordinary mutual conductance change in a high-vacuum tube), followed by a slow decrease taking about 0.15 sec. to reach completion. This slow decrease represents the removal of caesium ions from a portion of the filament which became positive to the grid when E_g was changed. When the grid voltage was restored to its original value, there was first a rapid change in i_p, followed by a slow change as the caesium ion concentration was gradually built up to its normal value. The recovery time constant was 0.068 sec.

A summary of some of the time-lag records is given in Table I.

TABLE I. *Time lags.*

Tube	Record	Bulb °C	E_f	E_p	E_g	Signal *Volts*	Signal k.c.	τ sec.
A	—	23	3	2.25	−1.65	0.053	1050	0.0088
	—	0	3	22.5	−1.8	0.053	1050	0.099
B	8	0	5	−1	−1	0.012	600	≪.01
	9	0	5	22.5	−1.6	0.010	600	0.028
	19	0	3.1	22.5	−1.7	0.050	600	0.071
	20	0	3.1	22.5	−0.15	0.050	600	0.083
	22	0	3.1	22.5	−1.7	−0.050	0	0.068
	24	0	3.1	6	6	0.150	600	≪.01
	25	0	3.1	−0.9	−0.9	0.020	600	0.128
	27	0	3.1	22.5	−1.6	0.004	600	0.087
	29	0	3.1	22.5	−1.6	0.004	250	0.097
	30	0	3.1	22.5	−1.6	0.050	100	0.099

Note that in record 24, where both grid and anode were strongly positive to the most positive part of the filament, there is no appreciable recovery time lag. This must mean that in this type of rectification (the steady-rise part of curves like Fig. 4, but at $E_f = 3.1$ instead of $E_f = 5$) there is no drainage of caesium ions from the region around the filament. This is to be expected, since the ions could hardly move, under the influence of a small a.c. voltage, to an electrode which was at least 3 volts positive to their point of origin. The rectification in this case must arise from a redistribution of the ions in the space between filament and grid, under the influence of the signal. (See section VIII).

VII. Static Rectification at Various Frequencies

The experiments to be described were made with tube *B*. The values of E_p, E_g and signal voltage were held constant, and the signal frequency was varied from 15 to 1700 kilocycles, Δi_p being noted at each frequency.

Fig. 11 shows two frequency characteristics for which the conditions were $E_p = 22.5$, $E_g = -1.6$, signal voltage 0.050, bulb temperature 31°C. For the upper curve the filament temperature was 1700°K, and for the lower 1940°K. The values of Δi_p are largest for frequencies of 250 and 350 kilocycles respectively.

Figure 12 shows frequency characteristics for changes in the current to the small anode only of tube *B*. The conditions were $E_p = 45$, signal voltage 0.050, bulb temperature 30°C, filament temperature 1940°K, and various values of E_g ranging from -2.7 to -1.7 as marked on the curves. Note that the maximum of rectification moves from 300 to 900 kilocycles as the grid voltage goes from -2.7 to -1.7.

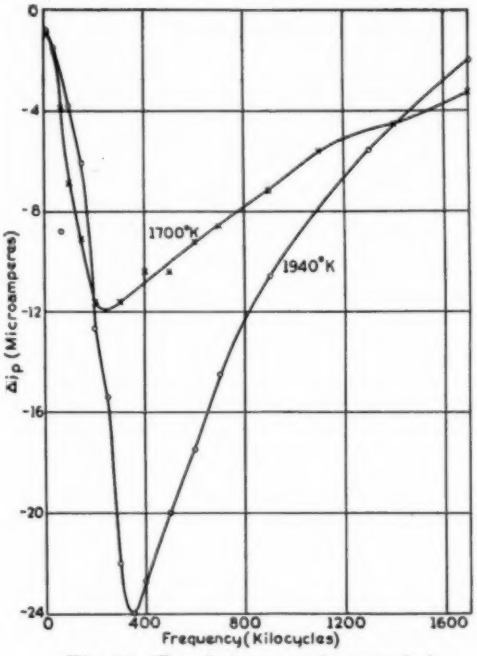

Fig. 11. Two frequency characteristics for tube *B*.

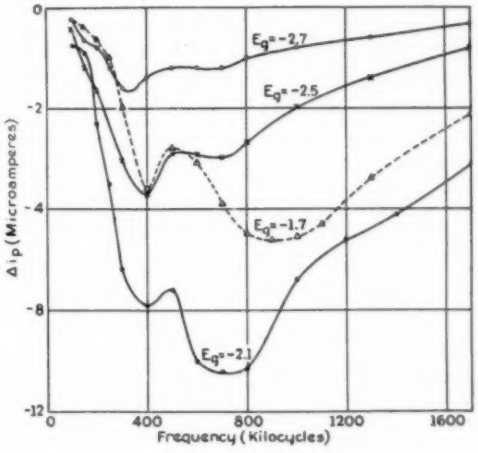

Fig. 12. Frequency characteristics for changes in current to small anode only of tube *B*.

Fig. 13 shows a frequency characteristic for tube *B* (whole filament) when grid and anode were both positive to the most positive part of the filament. The conditions were $E_p = 10$, (both measured from the negative end of the filament as usual), filament temperature 1940°K ($E_f = 5$) bulb temperature 29.5°C, signal voltage 0.044. The rectification is largest at 670 kilocycles.

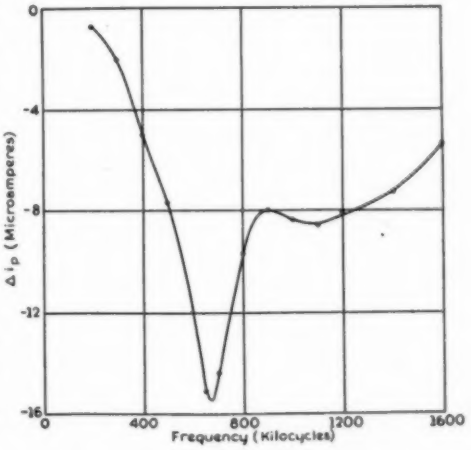

Fig. 13. Frequency characteristic for tube *B* when grid and anode were both positive to most positive part of filament.

The shape of these frequency characteristics suggests that some resonance phenomenon is involved in the mechanism of rectification. It seems

likely that the maximum rectification is obtained when the period of the applied signal agrees with the natural period of oscillation of the positive ions about the potential minimum surrounding the cathode. We shall defer further discussion of this to the next section.

VIII. Theory of the Rectification Effects

We shall make first some calculations of the potential distribution and space-charge density in the region near the cathode. We shall have to make these calculations for the case of parallel plane electrodes, instead of for a wire between two planes, which is the actual geometry of the tubes. However, the calculations will have qualitative, and some quantitative, interest. The necessary equations, with reference to earlier work, have been given by Langmuir[4] in a convenient form for calculation.

The distance from filament to grid in tubes A and B was about 0.1 cm. For calculation involving the field near the cathode we may replace the triode by a diode having an (effective) anode at the position of the triode grid. Accordingly we shall make our calculations for two parallel plates of thoriated tungsten each of area 1 sq. cm and 0.1 cm apart. The cathode is at zero potential, and at a temperature (T) either 1700°K or 1940°K. As we are interested in cases where the potential difference between cathode and (effective) anode is small, we shall suppose the anode potential (V_2) to be +0.5 volt. We need the following data

$T=1700$	$T=1940$
$i_0=0.224$ amps.	$i_0=2.79$
$V_2=0.1464(\eta_2-\eta_1)$	$V_2=0.1671(\eta_2-\eta_1)$
$\xi_2=\xi_1+348.5(i)^{1/2}$	$\xi_2=\xi_1+314(i)^{1/2}$

where i_0 is the saturation emission, i is the actual current, and η and ξ are the voltage and space parameters defined in Langmuir's paper. By assuming values of i and finding the corresponding values of V_2, we find by interpolation that when $V_2=0.5$ the values of i, V_m (voltage at the potential minimum) and x_m (distance of potential minimum from cathode in cm) are as given in Table II.

Table II.

T	i (amp)	i/i_0	V_2	V_m	x_m
1700°K	9.56×10^{-4}	0.00427	0.5	−0.790	0.0219
1940	15.3	0.000549	0.5	−1.259	0.0207

Using these values for i/i_0 we may then calculate the potential V_x at any distance x from the cathode. The result of this calculation is shown in the curves of Fig. 14.

We see from these curves that an electron leaving the surface of the cathode is in a retarding field, and only those electrons will escape to the anode whose initial thermal velocities perpendicular to the cathode are

[4] Langmuir, Phys. Rev. **21**, 419 (1923).

greater than $(2eV_m/m)^{1/2}$. On the other hand, a positive ion, formed by surface ionization at the cathode will be attracted towards the potential minimum. If the initial velocity of the ion is less than that corresponding to 0.5 volt it will be unable to reach the anode, and will oscillate out through the potential minimum and back to the cathode. Then it may be reemitted as a positive ion. If the ion loses energy by collision with gas molecules (caesium vapor plus residual gas) it will not return to the cathode, but will execute oscillations of diminishing amplitude about the potential minimum. In this connection it may be noted that the addition of an inert gas at low pressure increases the rectification considerably, presumably because the

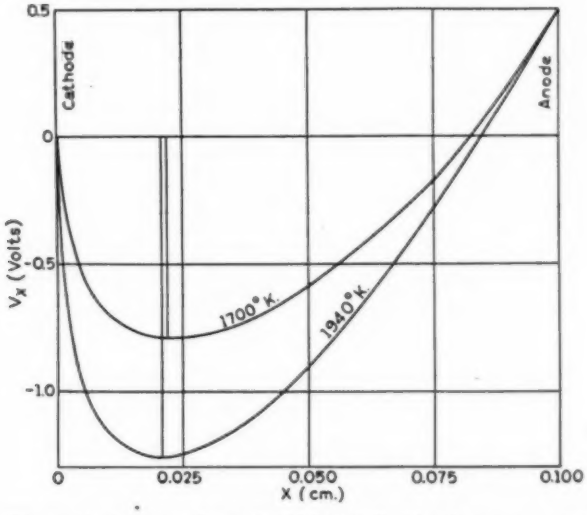

Fig. 14. Theoretical curves for potential distribution between parallel planes of thoriated tungsten.

increased number of collisions leads to the accumulation of more caesium ions at the potential minimum. Now if an a.c. signal is applied between cathode and anode whose period agrees with the period of the ions in this potential "trough," the ions will build up large oscillation amplitudes by a resonance effect, and may finally be able to flow to the cold anode, where they acquire electrons and escape as neutral atoms.

To estimate the natural period of the ions about the potential trough, we try to fit parabolas $x^2=aV$, where a is a constant, to the potential distribution curves on each side of the potential minimum. Then by adding together the half-periods for the two parabolas we obtain the total period. If the potential follows the law $V=x^2/a$ we have that the force on an ion is

$$-edV/dx=-2ex/a=Md^2x/dt^2$$

whence the period τ is

$$\tau=2\pi(Ma/2e)^{1/2}.$$

Taking the mass of the caesium ion (M) to be 2.21×10^{-22} gm, we have

$$\tau=5.23\times10^{-5}(a)^{1/2}$$

where $a=x_m/(V_m)^{1/2}$, x_m and V_m being expressed in cm and volts respectively.

In this way we find the natural periods at 1700°K and 1940°K to be 2.43×10^{-6} and 1.96×10^{-6} sec. respectively. The corresponding frequencies are 411 and 510 kilocycles respectively. These agree as to order of magnitude, and relative value, with the frequencies for maximum rectification in Fig. 11 (250 and 350 kilocycles).

Thus it appears that if the (effective) anode voltage is near that of the cathode, this resonance oscillation phenomenon explains how ions are drained away from the potential minimum region, thus increasing the electron space charge there, making V_m slightly more negative, and reducing the flow of electrons to the anode. On the other hand, when the anode is highly positive to the cathode (as in the right hand part of Figs. 2 and 4, and in record 24, Table I) this explanation cannot be valid.

We have suggested above that if the ions lose energy by collision with neutral atoms, their amplitude of oscillation will decrease, and they will accumulate around the position of the potential minimum at x_m. If we have a fixed total number of ions between cathode and anode, it may be that these will be most effective in raising the potential at x_m (and thus allowing a larger electron current to flow) when they are clustered together at x_m. When the signal is applied the ions will be set in motion and will, on this view, be less effective in raising the potential at x_m, so that the electron current to the anode will decrease. When the signal is removed the ions, as they lose energy by collision with neutral atoms, will again accumulate at x_m and the anode current will rise. There has been no drainage of ions to an electrode in this process, so that time lags of the kind discussed in section VI will be absent. This agrees with record 24 in Table I, where the recovery time lag was too short to be measured.

That the ions are most effective in raising the potential at x_m when they are grouped at x_m, may be shown by a simple argument suggested to the writers by Dr. L. Tonks. In Fig. 15 the two points A and B are held at the same potential. If we place a positive charge ρ at C, the potential will rise linearly along AD and fall linearly along DB, the slopes of these lines being fixed by ρ. If instead of concentrating ρ at C we distribute it between A and B, the potential distribution will follow some curve such as $AD'B$. Since the total ρ is the same as before, it follows from Gauss' theorem that AD and DB will be the tangents to the curve $AD'B$ at A and B. Hence D' must lie below D. This shows then that the ions will be most effective in raising the potential at x_m when they are grouped together at x_m.

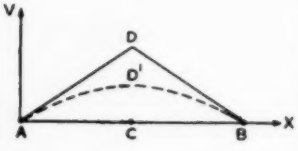

Fig. 15.

In the discussion in this section it has been assumed that the electron density between the electrodes is so small that an ion may travel back

and forth across the potential minimum many times before being neutralized by an electron. We shall therefore make a calculation of space-charge density to see if this is actually the case. We follow a method used by Dr. Langmuir in unpublished work, and start from Eq. (11) of reference 4.

$$\xi = \int_0^\eta [\epsilon^\eta - 1 \pm \epsilon^\eta P(\eta^{1/2}) \mp 2(\eta/\pi)^{1/2}]^{-1/2} d\eta \tag{1}$$

where $\eta = e(V - V_m)/kT$ and $\xi \propto (x - x_m)$. P denotes the Gauss probability function, and $\epsilon = 2.718 \ldots$. The upper signs are for $x < x_m$ and the lower for $x > x_m$ (Fig. 14). When $x > x_m$ we find from Eq. (1)

$$(d\eta/d\xi)^2 = \epsilon^\eta \operatorname{erf} \eta^{1/2} - 1 + 2(\eta/\pi)^{1/2} \tag{2}$$

$$d^2\eta/d\xi^2 = \tfrac{1}{2}\epsilon^\eta \operatorname{erf} \eta^{1/2} \tag{3}$$

where $\operatorname{erf} \eta^{1/2} = 1 - P(\eta^{1/2})$.
and when $x < x_m$

$$(d\eta/d\xi)^2 = 2\epsilon^\eta - 1 - \epsilon^\eta \operatorname{erf} \eta^{1/2} - 2(\eta/\pi)^{1/2} \tag{4}$$

$$d^2\eta/d\xi^2 = \epsilon^\eta(1 - \tfrac{1}{2} \operatorname{erf} \eta^{1/2}) \tag{5}$$

If ρ_m is the charge density at x_m we find from Poisson's equation and Eqs. (3), (5).

$$\rho = \rho_m \epsilon^\eta \operatorname{erf} \eta^{1/2} \text{ for } x > x_m \tag{6}$$

$$\rho = 2\rho_m \epsilon^\eta (1 - \tfrac{1}{2} \operatorname{erf} \eta^{1/2}) \text{ for } x < x_m \tag{7}$$

Now the density ρ_1 at the cathode surface is connected with the temperature and the saturation emission i_0 by the relation

$$\rho_1 = i_0(2\pi m/kT)^{1/2} = 6.43 \times 10^{-6} i_0/T^{1/2} \tag{8}$$

when i_0 is measured in amperes.
Hence from Eq. (7) knowing i_0 and ρ_1 we can find ρ_m. For the case of the thoriated tungsten plates, cathode at 1700°K, we have $i_0 = 0.224$ amp, whence by Eq. (8), $\rho_1 = 2.2 \times 10^{11}$ electrons/cm^3. We found previously (Table II) $V_m = -0.790$, whence η_1, the value of η at the cathode is found to be 5.4. From Eq. (7) we find $\rho_m = 4.7 \times 10^8$ electron /cm^3.

From the equations above we can find the electric field at any point between the electrodes. Thus for $x > x_m$

$$(dV/dx)^2 = -8\pi\rho_m(kT/e)(\epsilon^\eta \operatorname{erf} \eta^{1/2} - 1 + 2(\eta/\pi)^{1/2} \tag{9}$$

and for $x < x_m$

$$(dV/dx)^2 = -8\pi\rho_m(kT/e)(2\epsilon^\eta - 1 - \epsilon^\eta \operatorname{erf} \eta^{1/2} - 2(\eta/\pi)^{1/2} \tag{10}$$

Now dV/dx is zero at x_m, so that from Gauss' theorem and the values of dV/dx at anode and cathode, we may find from Eq. (9) and Eq. (10) the total charge between x_m and the anode, and between the cathode and x_m.

Adding the results we find for the total charge between the plates (1 sq. cm in area) in the case we are considering

$$N_e = 1.75 \times 10^8 \text{ electrons.}$$

Since the plates are 0.1 cm apart, this corresponds to an average electron density $n_e = 1.75 \times 10^9$ per cm^3.

We wish to calculate the average time which will elapse before an ion immersed in an electron atmosphere of this density will recombine with an electron. There appears at present to be no accurate method[5] for making this calculation, but we can estimate a lower limit for the life of an ion by calculating the rate at which electrons come close enough to the ion to have their paths deflected through $\pi/2$. It seems reasonable that a much closer encounter would be required for capture. We use Maxwell's formula as quoted by Richardson or Jeans.[6] For Coulomb's law of force this formula reduces to

$$\sin\theta = 1/(1+\alpha^2)^{1/2}$$

where θ is half the angle through which the path of an electron is turned,

$$\alpha = -bmv^2/e^2 \quad ,$$

and b is the perpendicular from the ion to the path of the electron when at a great distance from the ion. m, v, and e are the mass, initial velocity and charge of the electron. When $\theta = \pi/4$, $\alpha = 1$. For an electron having the average Maxwellian velocity for 1700°K, $mv^2/e^2 = 3.08 \times 10^6 \text{cm}^{-1}$, so that $b = 3.25 \times 10^{-7}$cm. The total number of electrons per second whose paths are deflected through $\pi/2$ or more will be given by the number of electrons flowing per second through the surface of a sphere of radius b. This number is

$$4\pi b^2 n_e (kT/2\pi m)^{1/2} = 14500.$$

Hence our minimum estimate of the life of an ion is 10^{-4} sec. Since the time required for an ion to cross between the electrodes is about 10^{-6} sec, it follows that the ion may oscillate back and forth many times without recombination. This is the condition we have postulated in the theory.

The probability of such a long life for a positive ion raises a question as to whether the time-lag effects of section VI might not be due to an accumulation of caesium ions around the potential minimum region, rather than to an accumulation of caesium on the filament. Quantitative deductions from the theory of the parallel plane case make this seem improbable. We have found the number of electrons between the plates to be 1.75×10^8 in the case considered above. The presence of caesium vapor does not change the anode

[5] Oppenheimer's formulae for hydrogen recombination (Phys. Rev. 31, 349 (1928)) cannot be applied directly to the case in point.

[6] Richardson: Electron Theory of Matter (1914) p. 417 Jeans: Dynamical Theory of Gases (1916) p. 231.

current a great deal, so that the number of caesium ions between the electrodes must be less than 10^8;—if it were greater, there would be complete neutralization of electron space charge, and large currents would flow. We now wish to calculate the time required to supply 10^8 ions to the space between the electrodes, by ionization at the surface of the cathode. From unpublished data it appears that 0.02 of the caesium atoms striking a fully thoriated tungsten surface at 1700°K leave it as ions. With the bulb at 0°C ($p=1.12\times10^{-4}$ barye) the number of atoms striking a sq. cm surface per sec is 1.55×10^{13}. Hence the number of ions emitted per sec. is $3.1\times10.^{11}$ This would supply the quota of 10^8 for the space between the electrodes in 3×10^{-4} sec, so that no time lags of tenths of a second should be found. It thus seems likely that accumulations of caesium on the filament (section VI) is the correct explanation of the time lags. The time lags observed at 0°C correspond roughly to the time required for enough caesium atoms to strike the filament to cover 1/1000 of its surface.

IX. The Flow of Ions Along the Potential Minimum

In the preceding sections we have confined the discussion to the flow of ions perpendicular to the filament surface. Since there is a drop of potential along the filament, there will be a flow of ions parallel to the filament. It is necessary to take this into account in order to understand the tube characteristics fully.

The potential at a point just outside the filament surface in one of our tubes is indicated semi-quantitatively by the full line in Fig. 16 for $E_f=3.1$. Starting at the cold negative terminal where the filament is coated with caesium, as we go to the right the potential first falls as the caesium layer is driven off the hot filament. This drop is about -1.3 volts, the contact potential difference[7] between an adsorbed caesium layer and thoriated tungsten. The potential then rises as we move to the right, the rise being caused by the voltage drop in the filament. At the center the filament is cooled by the anchor wire (Fig. 1) caesium deposits on it, and causes a little hump in the potential. The potential curve proceeds in a similar way up to the positive terminal.

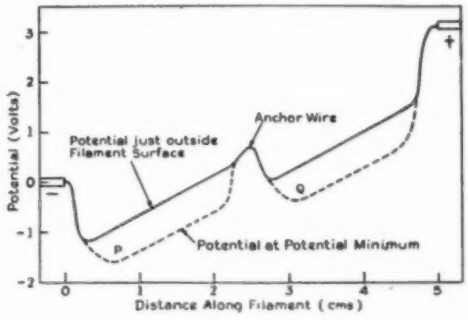

Fig. 16. Distribution of potential along filament.

At the ends and center of the filament, where there is very little electron emission, the filament surface itself will be the "potential minimum." In the regions where there is large electron emission the potential of the "po-

[7] See an article on contact potential measurements by Langmuir and Kingdon to be submitted to the Physical Review.

tential minimum" may be lower than that just outside the filament surface by an amount of the order of 1 volt (Table II). The course of the potential minimum is indicated by the dotted curve in Fig. 16.

Ions will therefore flow along the potential minimum trough from the more positive parts of the filament towards P and Q. There seems little doubt (section 8) that the life of the ions is great enough for this flow to increase appreciably the concentration of ions at P and Q. This accounts for the two peaks usually observed in the static rectification curves (Fig. 2). Contamination of parts of the filament surface or incomplete formation of the thoriated surface might produce several regions like P and Q, leading to several peaks, as in Fig. 4. In this connection it may be noted that the characteristics of Fig. 2 were taken some days after Fig. 4, and that the filament had been given a severe thermal treatment between.

X. Comparison of Static Rectification with the Rectification of Modulated Radio Frequency Signals

The static rectification curves of section III represent the response of the tube to radio frequency signals of zero frequency of modulation. The occurrence of the time lags described in section VI indicates that if a modulated signal is used the ion concentration around the cathode will not have time to return to its normal maximum value in the interval between the peaks of

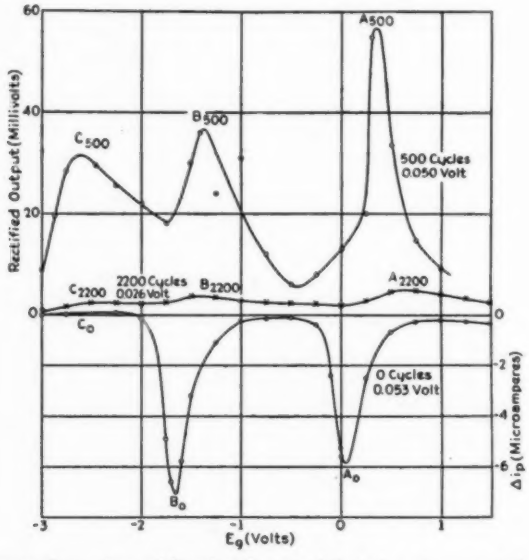

Fig. 17. Comparison of rectification for modulated and unmodulated signals.

the modulating wave. The rectified currents will therefore be smaller than those observed in the static rectification tests, and will decrease as the frequency of modulation is increased.

The first point may be illustrated by an experiment made with tube A. The conditions were $E_f = 3.3$ (1700°K), $E_p = 22.5$, bulb at room temperature,

signal frequency 1000 kilocycles. In the first test the signal was modulated at 500 cycles, signal voltage 0.050, and the 500 cycle voltage generated across a 50,000 ohm output impedance in the anode circuit was measured. This voltage in RMS millivolts for various settings of E_g is indicated in the curve of Fig. 17 marked 500 cycles. The tube was then placed in another test set and a similar run made, this time using 2200 cycle modulation, 0.026 volts signal, and a 690,000 ohm output impedance. The curve obtained is that marked 2200 cycles in Fig. 17. We are indebted to Messrs. Darlington and Hitchcock for these measurements. Finally, a static rectification curve was taken using a signal voltage 0.053. The values of Δi_p are plotted in Fig. 17, using the ordinate scale on the right (microamperes.)

The two negative maxima A_0, B_0 and the positive maximum C_0 of the static rectification curve, are reproduced at approximately the same grid voltages in the curves for modulated signals. It is interesting to note that although C_0 is insignificant compared with A_0 and B_0, yet C_{500} and C_{2200} are about as large as their companion maxima. This is because the C maxima represent rectification by curvature of the anode characteristic, and involve no appreciable time lag (electron flow only) whereas the A and B maxima involve relatively large time lags (section VI). At the normal filament temperature, 1940°K, A_{500} and B_{500} would be much greater than C_{500}.

It is instructive to compare the maximum changes in anode current for the B_0 and B_{2200} maxima. The double amplitude of the current through the output impedance at the B_{2200} maximum, when the RMS voltage across it was 4×10^{-3} must have been 1.64×10^{-8} amp. The internal resistance of the tube anode circuit at $E_p=22.5$, $E_g=-1.4$ was 91,000 ohms, so that if this had been the only resistance in the circuit (as in the static rectification test) the maximum change in anode current would have been

$$1.64\times10^{-8}\ \frac{690000+91000}{91000}=1.4\times10^{-7}\ \text{amp.}$$

The B_0 maximum was 7μa for a 0.053 volt signal, or since a nearly linear law is followed at very low voltages (Fig. 6), the maximum would have been about 3.4μa for 0.026 volt. This current change is 24 times as great as that at the B_{2200} maximum, the difference being due to a time lag of the order of that given in the 23°C curve of Fig. 8.

The variation of rectified output with modulation frequency is illustrated by Fig. 18, compiled from a report by Mr. Oakley. This was taken with another tube. The filament temperature was 1940°K. The signal voltage was 0.1, carrier frequency 1000 kilocycles, modulated at various frequencies from 20 to 10,000 cycles. The modulation frequency is plotted as abscissas, while the ordinates measure volts generated across a 100,000 ohm resistance in the anode circuit. Curves are shown for the bulb at 40°C and at 0°C. The variation in output with frequency is quite pronounced, and is caused by the time lag effects discussed in section VI.

Thus there are two frequency effects,–(1) a high-frequency effect due to the natural period of oscillation of the caesium ions about the potential minimum, and (2) a low-frequency effect due to the time taken for the concentration of caesium ions around the filament to be built up to normal value when the signal is removed (or falls to a minimum in modulation).

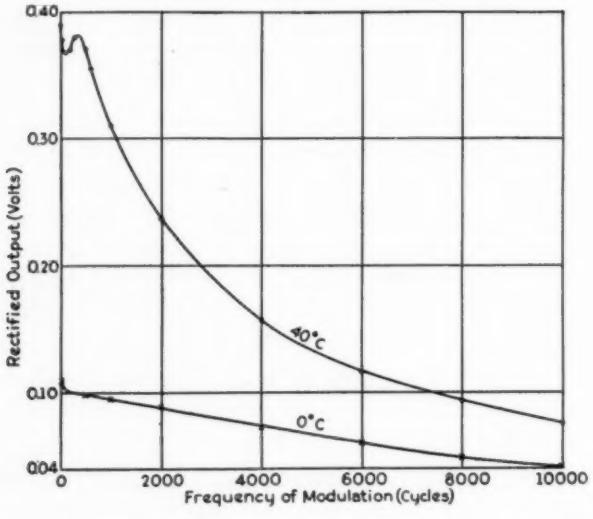

Fig. 18. Variation of rectified output with modulation frequency.

XI. Static Rectification at Low Frequencies

We saw in Fig. 10 that a d.c. change in grid voltage produces both an "instantaneous" and a slow change in anode current, the latter being due to a change in the density of caesium ions around the filament. Since this density changes as we move along the filament, we have corresponding changes in the mutual conductance curve. This is illustrated by Fig. 19 (Tube A). The ordinates measure the change in i_p when the grid was made 0.05 volt more negative; the abscissas are E_g. The negative peak at -1.8 volts is due to the caesium ion effect mentioned above, and corresponds roughly in position to the B_0 peak of Fig. 17.

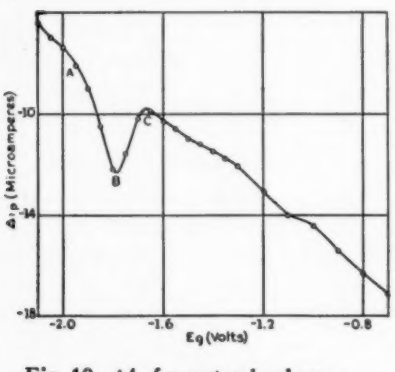

Fig. 19. $\Delta 4_p$ for a steady change in grid potential.

Proceeding now to low frequency alternating voltages applied between grid and filament, it is obvious from section VII that at frequencies below a few thousand cycles the natural period of the positive ions can play little part in the rectification. At very low frequencies the concentration of caesium ions around the cathode

can keep pace very nearly with the fluctuations in signal voltage, so that rectification due to the drainage away of these ions is small. Fig. 20 shows some static rectification curves at various frequencies taken by Mr. A. L. Samuel, using another tube. The 60 cycle curve has a marked positive peak at $E_g = -2.6$. This is "rectification by curvature," and corresponds to a region of the $i_p E_g$ characteristic where the curvature has been enhanced by the effect shown in the AB portion of Fig. 19. At higher frequencies this peak becomes much smaller, since the ion concentrations depart more and more from the steady value. Following the positive peak on the 60 cycle curve is a small negative peak. This corresponds to the region BC of Fig. 19, where the curvature of the $i_p E_g$ characteristic is small, and the "ion drainage" rectification is able to overbalance the "curvature" rectification. At more positive E_g the rectification is small, and of uncertain sign, as might be expected from the conflict between the two types of rectification, each of them giving only small effects. The curve for a 970 kilocycle signal is included in Fig. 20. Here the ion drainage rectification far outbalances the curvature type except at very negative E_g.

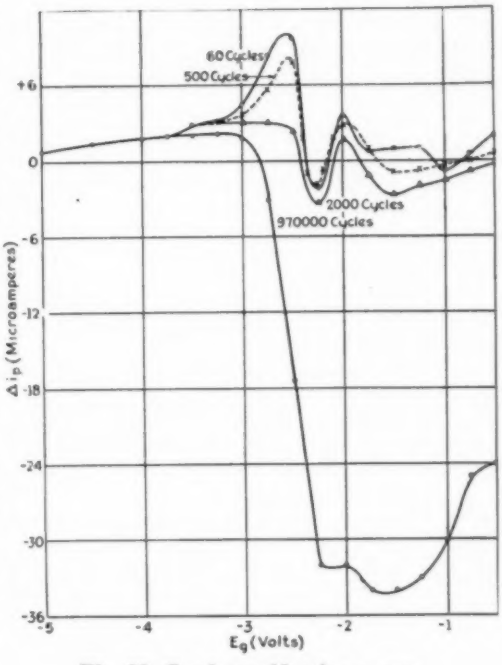

Fig. 20. Static rectification curves.

XII. Effect of State of Activation of Thoriated Cathode

The static rectification of tube A was measured when the thoriated cathode was activated to different degrees. The curves are shown in Fig. 21, the emissions being marked on them. The other conditions were $E_f = 3.25$ (1700°K), $E_p = 22.5$, signal voltage 0.053, frequency 1050 kilocycles, bulb at room temperature.

XIII. Comparison of Rectification with and without Grid Leak

The ordinary high vacuum tube is about 4 or 5 times as sensitive a detector when used with grid leak and condenser as when used without. This is not true of the alkali vapor tubes, the sensitivity being about equal in the two cases. The grid leak serves to keep the grid current small, and hence in the alkali vapor tubes fixes the point of operation at about the B maximum in Fig. 17. Since the use of a grid leak does not increase the rectification, the

change in grid current when a signal is applied must be relatively much smaller than the change in anode current. This may be accounted for as follows. The grid current is small, so the potential of the grid must be about the same as that (V_m) of the potential minimum region at the negative end of the filament. When the signal is applied and caesium ions drained off,

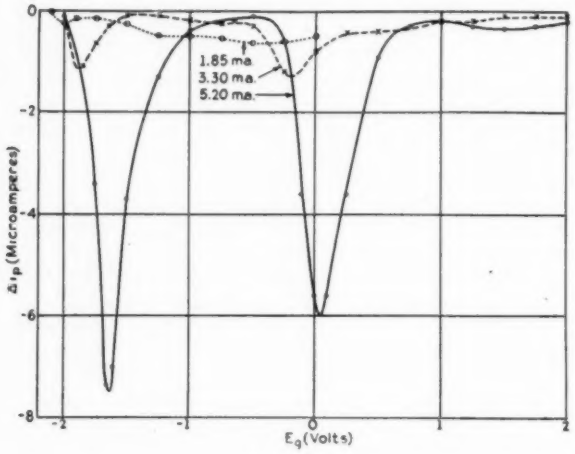

Fig. 21. Static rectification curves for tube *A* with thorium cathode activated to different degrees.

V_m becomes more negative. This reduces the total number of electrons escaping through the potential minimum, but at the same time will increase the fraction of the escaping electrons which goes to the grid since the grid is now on the average appreciably more positive to V_m. This action reduces fluctuations in the grid current, and thus reduces grid leak rectification.

RESEARCH LABORATORY,
GENERAL ELECTRIC COMPANY,
SCHENECTADY, N. Y.
February 18, 1929.

PATHS OF CHARGED PARTICLES IN ELECTRIC AND MAGNETIC FIELDS

By W. Bartky and A. J. Dempster

Abstract

A combination of electric and magnetic fields is described which is suitable for positive-ray analysis experiments, or precise determinations of the ratio of charge to mass. The orbits of charged particles in the radial electric field and transverse magnetic field of the system are computed, and it is shown that a beam of rays of various velocities diverging from a point are brought to a focus provided the variations are not too large. Formulas are given for computing the errors introduced by variations in direction and velocity.

IN DETERMINATIONS of the specific charge of the electron and in methods of positive-ray analysis, the question of bringing a divergent beam of charged particles to a focus is of fundamental importance. Semicircular paths in a constant magnetic field have been used in many experiments.[1] A related problem is the focusing of a beam of charged particles after it has suffered deflections, so that a range of velocities are brought to

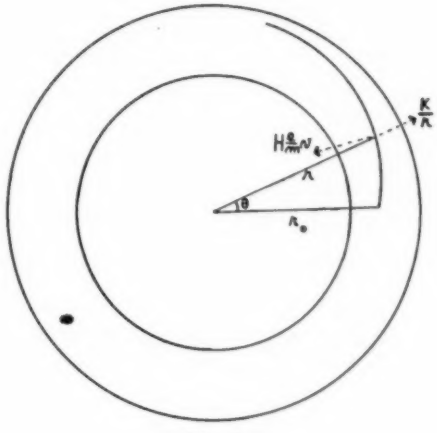

Fig. 1.

the same point. This type of focusing has been developed by Aston in his mass spectrograph.[2] In a previous paper[3] it was suggested by one of the authors that this velocity-focusing might be combined with direction-focusing to obtain greater sharpness than could be obtained by either alone. In this paper one combination of electric and magnetic fields is discussed which seems specially suitable for experimental use.

[1] J. Classen, Phys. Zeits. **9**, 762 (1908); H. Busch, Phys. Zeits. **23**, 438 (1922).
[2] F. W. Aston, Phil. Mag. **38**, 709 (1919).
[3] A. J. Dempster, Phys. Rev. **20**, 638 (1922).

Suppose the charged particles to move in a cylindrical condenser, shown in section in Fig. 1. If a magnetic field H is established perpendicular to the plane of the paper a particle describes an orbit under the influence of a radial acceleration, K/r due to the electric field, and of an acceleration due to the magnetic field which acts at right angles to its direction of motion at any point, and is given by $H(e/m)(ds/dt)$. Let us suppose the electric force to be directed outwards and the magnetic force inwards; the equations of motion, in polar coordinates, are then:

$$\left.\begin{aligned} \frac{d^2r}{dt^2}-r\left(\frac{d\theta}{dt}\right)^2 &= \frac{K}{r}-H\frac{e}{m}\frac{ds}{dt}\left(r\frac{d\theta}{ds}\right)=\frac{K}{r}-\lambda\frac{rd\theta}{dt} \\ \frac{1}{r}\frac{d}{dt}\left(r^2\frac{d\theta}{dt}\right) &= H\frac{e}{m}\frac{ds}{dt}\cdot\frac{dr}{ds}=\lambda\frac{dr}{dt} \end{aligned}\right\} \tag{1}$$

where $\lambda=He/m$. From the second equation

$$\frac{d}{dt}\left(r^2\frac{d\theta}{dt}\right)=\frac{\lambda}{2}\frac{dr^2}{dt}, \tag{2}$$

so that $d\theta/dt=\lambda/2+A/r^2$ where $A=r_0^2(\theta_0'-\lambda/2)$
Substituting for $d\theta/dt$ in (1) we obtain

$$\frac{d^2r}{dt^2}=\frac{A^2}{r^3}+\frac{K}{r}-\frac{\lambda^2r}{4}. \tag{3}$$

We are interested only in orbits which are nearly circular, since only these may be described in the condenser considered.

For the circular orbit $r=\rho$, the magnetic force is always directed along the radius vector, and from (3) $\lambda^2/4-K/\rho^2=A^2/\rho^4$
Substituting $r=\rho+x$ in (3), we obtain

$$d^2x/dt^2=-x(\lambda^2-2K/\rho^2) \tag{4}$$

If the magnetic and electric fields and initial angular velocity θ_0' are adjusted so that $A=0$ or $\lambda^2=4K/\rho^2$, then (4) reduces to

$$\frac{d^2x}{dt^2}=-\frac{\lambda^2}{2}x \tag{5}$$

and $d\theta/dt=\lambda/2$. The solution of (5) is $x=P\sin\lambda t/2^{1/2}$, showing that a divergent bundle of rays is reunited after a time $t_0=2^{1/2}\pi/\lambda$ when the angle described is $\pi/2^{1/2}$, that is 127° 17′.

If we substitute $r=\rho$ in the first equation of (1) and consider ρ as a function of $d\theta/dt$ we find that ρ passes through a minimum for $d\theta/dt=\lambda/2$, so that for the adjustment of the electric and magnetic fields which makes $A=0$ that is $\lambda^2=4K/\rho^2$, we have particles with slightly different velocities describing approximately the same circular orbit.

To find the sharpness of the focus, it is necessary to compute the orbits described by particles with different directions and velocities to a further approximation.

Since

$$\frac{d^2r}{dt^2}=\frac{d}{d\theta}\left[\frac{dr}{d\theta}\cdot\frac{d\theta}{dt}\right]\frac{d\theta}{dt}=\frac{d^2r}{d\theta^2}\left(\frac{d\theta}{dt}\right)^2+\left(\frac{dr}{d\theta}\right)\cdot\frac{d}{d\theta}\left(\frac{d\theta}{dt}\right)\cdot\frac{d\theta}{dt}$$
$$=\left(\frac{\lambda}{2}+\frac{A}{r^2}\right)^2\frac{d^2r}{d\theta^2}-\frac{2A}{r^3}\left(\frac{\lambda}{2}+\frac{A}{r^2}\right)\left(\frac{dr}{d\theta}\right)^2$$

it follows from (3) that

$$\frac{d^2r}{d\theta^2}-\frac{2A}{r^3}\left(\frac{\lambda}{2}+\frac{A}{r^2}\right)^{-1}\left(\frac{dr}{d\theta}\right)^2=\left(\frac{A^2}{r^3}+\frac{K}{r}-\frac{\lambda^2 r}{4}\right)\left(\frac{\lambda}{2}+\frac{A}{r^2}\right)^{-2} \tag{6}$$

This equation may be solved for the special case in which A is small and the orbits are nearly circular by putting

$$A=\mu a \qquad \text{and} \qquad r=\rho(1+\mu z) \tag{7}$$

where μ is a parameter, and where ρ satisfies

$$\frac{K}{\rho}-\frac{\lambda^2}{4}\rho=0\,; \qquad \rho^2=\frac{4K}{\lambda^2}\cdot$$

For on substituting (7) into (6) and neglecting powers of μ greater than the second we find the following equation for z,

$$\frac{d^2z}{d\theta^2}=\left[\frac{\mu a^2}{\rho}-\frac{K}{\rho^2}(2z-\mu z^2)\right]\left[\frac{\lambda}{2}+\frac{\mu a}{\rho^2}\right]^{-2}=-2z+\mu z^2+8\epsilon\mu z+4\epsilon^2\mu \tag{8}$$

when $\epsilon=a/\lambda\rho^2$. Assume the solution of (8) to be of the form

$$z=z^{(0)}+\mu z^{(1)}$$

then

$$\begin{aligned} d^2z^{(0)}/d\theta^2&=-2z^{(0)}\\ d^2z^{(1)}/d\theta^2&=-2z^{(1)}+z^{(0)^2}+8\epsilon z^{(0)}+4\epsilon^2. \end{aligned} \tag{9}$$

With the initial conditions

$$z\Big|_{\theta=0}=c_0 \qquad \frac{dz}{d\theta}\Big|_{\theta=0}=c_1$$

the solution of the first equation is

$$z^{(0)}=c_0\cos 2^{1/2}\theta+(c_1/2^{1/2})\sin 2^{1/2}\theta.$$

Substituting this in the second equation of (9) we obtain

$$\frac{d^2z^{(1)}}{d\theta^2}=-2z^{(1)}+\left(\frac{c_0^2}{2}+\frac{c^2}{4}+4\epsilon^2\right)+\left(\frac{c_0^2}{2}-\frac{c_1^2}{4}\right)\cos 2^{3/2}\theta+\frac{c_0c_1}{2^{1/2}}\sin 2^{3/2}\theta$$
$$+8\epsilon\left(c_0\cos 2^{1/2}\theta+\frac{c_1}{2^{1/2}}\sin 2^{1/2}\theta\right)$$

The solution of the last equation subject to the conditions

$$z^{(1)}\Big|_{\theta=0}=0 \qquad \frac{dz^{(1)}}{d\theta}\Big|_{\theta=0}=0 \text{ is;}$$

$$z^{(1)}=\left(\frac{c_0^2}{4}+\frac{c_1^2}{8}+2\epsilon^2\right)-\frac{1}{12}\left(c_0^2-\frac{c_1^2}{2}\right)\cos 2^{3/2}\theta-\frac{c_0c_1}{6\cdot 2^{1/2}}\sin 2^{3/2}\theta$$
$$+\frac{4\epsilon\theta}{2^{1/2}}\left(c_0\sin 2^{1/2}\theta-\frac{c_1}{2^{1/2}}\cos 2^{1/2}\theta\right)-\left(\frac{c_0^2}{6}+\frac{c_1^2}{6}+2\epsilon^2\right)\cos 2^{1/2}\theta$$
$$+\frac{1}{2^{1/2}}\left(\frac{c_0c_1}{3}+\frac{4\epsilon c_1}{2^{1/2}}\right)\sin 2^{1/2}\theta.$$

For $\theta=\pi/2^{1/2}$, $z^{(0)}$ and $z^{(1)}$ reduce to

$$z^{(0)}=-c_0, \quad z^{(1)}=\frac{c_0^2}{3}+\frac{c_1^2}{3}+4\epsilon^2+2^{1/2}\pi\epsilon c_1.$$

For $A=0$ we have by (2) that the angular velocity is $\lambda/2$. Let the initial angular velocity θ_0' for $A=\mu a$ be $(\lambda/2)(1+\delta)$. Then as a first approximation from (2) $\mu a=\rho^2\lambda\delta/2$. Suppose the parameter $\mu=1$ then the initial conditions for $\theta=0$ become

$$r_0=\rho(1+c_0), \quad dr/d\theta=\rho c_1, \quad \theta_0'=\lambda(1+\delta)/2$$

Since $\epsilon=a/\lambda\rho^2=\delta/2$, the value of r at $\theta=\pi/2^{1/2}$ is;

$$r=\rho\left(1-c_0+\frac{c_0^2}{3}+\frac{c_1^2}{3}+\delta^2+\frac{\pi}{2^{1/2}}c_1\delta\right) \tag{10}$$

If the extreme variation in velocity is 3 percent and if the angular aperture of the beam is 1 in 25 ($c_1=0.02$), the value of r is $\rho(1-c_0)$ with an error of less than 1 in 1000. With the old simple magnetic focusing, the values of r for the different velocities would have varied fifteen times as much.

Equation (10) shows that in general there are two values of the velocity for which r is equal to r_0. These may be made to coincide by altering c_0, that is by altering the electric or magnetic field, since $c_0=(r_0/\rho)-1=(r_0\lambda/2k^{1/2})-1$. If c_1 is sufficiently small, this occurs for $c_0=0$ or $He/m=\lambda=2k^{1/2}/r_0$ thus giving e/m in terms of the electric and magnetic fields and the radius of curvature.

RYERSON PHYSICAL LABORATORY,
UNIVERSITY OF CHICAGO,
March, 1929.

ON TIME-LAGS IN FLUORESCENCE AND IN THE KERR AND FARADAY EFFECTS

By E. Gaviola

Abstract

A critical study of the experimental literature is made in regard to the existence of time-lags or "dark-times" in fluorescence and it is found that not a single experiment shows the existence of such things. Moreover experiments seem to show that in all the cases when the emitting state is the state reached directly as a result of the excitation process, the emission begins immediately upon excitation and decreases exponentially. Experiments interpreted as showing the existence of time-lags in the Kerr and Faraday effects are also considered and it is found that they do not prove the reality of such time-lags. An analysis is made of the way in which the "optical shutter" of Beams' works, with the result that it is found to behave quite differently from what it was supposed to do. Wave trains of light that were supposed to be cut off by it in parts of 3 cm length are certainly not reduced to less than 300 cm, or 100 times more than assumed.

Introduction

IT IS common to find in the literature references to time-lags or "dark-times" in fluorescence and the names of R. W. Wood, Gottling, Vavilov and Lewshin, Hoxton and Beams, W. Wien, and others are mentioned as having proved experimentally the existence of such "dark-times" between the moment of excitation and the beginning of emission for different fluorescent substances. The assumption made in most of the cases is that if one illuminates a fluorescing substance for a very short time, the substance will remain dark for a certain finite time after excitation, "bursting then into luminosity," luminosity which will decrease exponentially; and this assumption is supposed to be supported by many experimental results. The purpose of the present paper is to examine the experimental material in connection with time-lags in fluorescence and to see how far the mentioned assumption is justified. The investigation indicates there is not a single experiment which has shown the existence of "dark-times" in fluorescence, when the state reached due to the excitation is the state directly responsible for the emission of the light observed. Even when this last condition is not fulfilled, the emission always begins at the moment of excitation.

The Origin of the Idea of Time-Lags

In the classical theory there is no possibility of time-lags in fluorescence: If a classical oscillator is excited at a given moment, it will begin to emit radiation (if capable of doing so) at the very time of excitation and the intensity of the radiation will decrease exponentially with time, because of the damping of the oscillator.

The Bohr atom, with its stationary states in which the electrons could remain for some time without radiating, gave rise to the possibility of con-

ceiving the existence of "dark-times." In fact, the statement that the excited stationary states had a measurable mean life was often misinterpreted in the sense that *most* atoms, if not all, would remain in the excited state during the said mean life and then fall to the normal level emitting radiation. Curiously enough, this misinterpretation seemed to be supported by the extinction-curves of canal-beams as obtained by W. Wien and especially by an experiment of R. W. Wood.

The Extinction-curves of Canal-beams

As is well known, W. Wien[1] has repeatedly measured the intensity of light emitted by a canal-beam when it enters a vacuum as a function of the distance from the canal, or, what amounts to the same, as a function of the time after traversing the canal. The extinction-curves that he found originally were not exponential in the neighborhood of the canal: the intensity seemed to increase at first up to a certain maximum and then to decrease exponentially. This unexpected result gave rise to interesting theories of Mie[2] and Stark,[3] which with some assumptions about the emission-process of light, explained the increase found beyond the canal. This increase has later been shown to be due wholly to defective experimental conditions and a recent investigation[4] made in W. Wien's laboratory, in which the experimental difficulties were eliminated, has shown that the extinction-curve of canal-beams in vacuum is an exponentially falling line from the very beginning and that there is no increase in intensity after passing the canal. This result makes it unnecessary to consider the theories of Mie and of Stark.

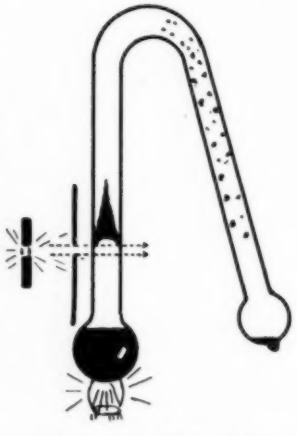

Fig. 1. Wood's experimental arrangement for showing "dark time" in mercury fluorescence.

The Experiment of R. W. Wood

R. W. Wood[5] performed in 1921 a very interesting experiment, which was generally accepted as a proof of the existence of "dark-times" at least in some special cases. His experimental arrangement is reproduced here in Fig. 1. An inverted quartz U-tube contains liquid mercury in one side, which is heated by a bunsen burner. Mercury evaporates in this side, rises with considerable velocity (about 10 m per sec.) and condenses on the walls of the other side of the U-tube. A narrow region of the rising vapor is illuminated by an aluminum spark as shown in the figure. It is known that mercury vapor at sufficient density illuminated by an aluminum spark emits

[1] Wien und Harms, Handbuch d. Experimentalphysik **14**, 706.
[2] G. Mie, Ann. d. Physik **66**, 237 (1921).
[3] J. Stark, Ann. d. Physik **49**, 731 (1916).
[4] J. Port, Ann. d. Physik **87**, 581 (1928).
[5] R. W. Wood, Proc. Roy. Soc. **A99**, 362 (1921).

a blue-green fluorescence which can be easily seen with the naked eye. Now, Wood found that this green fluorescence was carried away from the illuminated zone by the rising vapor and that the maximum of it occurred a few millimeters above the primary light-cone. The green fluorescence appeared in the form of a flame, as indicated in Fig. 1. Let us consider now what one should expect in a case like this: It is known that mercury vapor has an absorption-band at about 1850A, which is certainly due to molecular mercury, and that light of the spark absorbed in this region is responsible for the emission of the green fluorescence. The absorption of the 1850A quant will bring the molecule to an excited state which will correspond to the level 2^1P_1 of the atom. On the other hand, it is known that the green fluorescence is emitted by molecules in an excited state corresponding to one of the 2^3P levels, probably 2^3P_1 of the atom. Before the green band can be emitted a process must occur which brings the excited molecule from the state corresponding to the 2^1P_1 level to the state corresponding to the 2^3P_1 level. This process may be a radiation jump, it may also be the result of collisions of the second kind. Fig. 2 illustrates the case. The levels indicated are not to be understood as levels of the atom, but as corresponding levels of the molecule where they are certainly multiple because of oscillation and rotation. The case we are considering is similar to a well-known one in radioactivity: If we start with a substance A which after a mean life τ_1 gives birth to a second substance B, which on its side decomposes after a mean life τ_2 emitting a certain radiation, and if we have at the beginning the substance A alone and observe the growing in the amount of B as a function of the time by measuring its radiation, we will find that B starts growing at the moment zero, reaches a maximum at a time

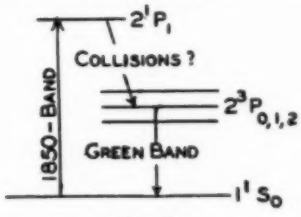

Fig. 2.

$$t_m = [\tau_1\tau_2/(\tau_1-\tau_2)]\cdot ln\tau_1/\tau_2 \qquad (1)$$

and decreases again more or less exponentially. The amount of B is given by the formula

$$N_B = N_A^0(e^{-t/\tau_1}-e^{-t/\tau_2})[\tau_2/(\tau_1-\tau_2)]. \qquad (2)$$

These formulas are to be found in any treatise on radioactivity and are illustrated in Fig. 3.

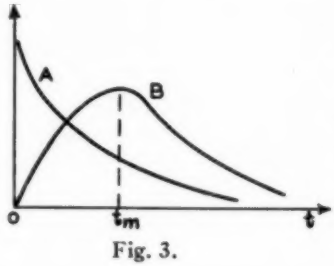

Fig. 3.

We should expect then the green band in the case of Wood to behave like the substance B in the radioactive case: The green fluorescence should start at the moment of excitation, it should grow to a maximum at a time given by formula (1) if τ_1 and τ_2 mean now the mean life-times of the levels of 2^1P_1 and 2^3P_1 of the molecule respectively,* and should decrease afterwards more or less exponentially. Now in the flame drawn in Fig. 1, its lower limit is

* One of these two levels of the molecule, or both, seem to be metastable.

sharply separated from the illuminated region, but it is not so in the photographs reproduced in Prof. Wood's paper (see Figs. 4 and 5, Plate 5, reference 5), we can see there that the green flame really starts in the illuminated region and that its intensity distribution along the axis of the tube can be well accounted for by formula (2). Figs. 6 and 7 in Wood's paper, which have often been believed to be photographs, are in reality drawings made after subjective observation and the absolutely dark spaces between excitation and maximum of emission indicated in the drawings are certainly optical illusions due to the effect of contrast.

The delay in the appearance of the green fluorescence in the case of Wood is due then to the fact that the state which emits it is not the level reached as a result of the excitation, and the slow increase of the intensity at first indicates the growing number of molecules in the said state. The results of Wood can be readily interpreted without assuming the existence of any "dark-times" or time-lags in fluorescence.

The Experiment of Gottling

Using the arrangement of Abraham and Lemoine for the measurement of short times of fluorescence, as suggested by Wood, Gottling[6] attempted to determine the extinction-times of the fluorescence of rhodamine and barium-platino-cyanide. He obtained some values which he interpreted as time-lags in the fluorescence of the substances. Now, with the arrangement used by Gottling the only thing that can be measured is the displacement in time of the center of gravity, so to say, of the emission in regard to the absorption, but nothing can be said about the form of the emission-curve. The values obtained by Gottling could as well be interpreted as mean extinction-times of exponentially falling emission-curves. But these values were falsified by the fact that Gottling did not take into consideration the color-dispersion of the Kerr effect, and when he tried to measure time-lags he was really determining the different values of the Kerr effect for the blue light of the spark, the red light of rhodamine, and the green one of barium-platino-cyanide.[7]

The Experiments of Beams, Brown, Hoxton, Rhodes, Allison, Lawrence and Locher

We shall consider now a group of thirteen publications by the authors mentioned above, in which they claim to have found and measured "dark-times" and time-lags for the appearance of the lines in the spark, for fluorescence, and for the Kerr and Faraday effects in different liquids. These publications can be divided into three groups according to the experimental devices used in determining the time-lags. To the first group belong the ones

[6] S. I. Vavilov and W. L. Lewschin, Zeits. f. Physik **35,** 920 (1926).

[6] Gottling, Phys. Rev. **22,** 566 (1923).

[7] Compare E. Gaviola. Ann. d. Physik **81,** 681 (1926); Zeits. f. Physik **42,** 853, 862 (1927).

in which a single Kerr cell is used, placed between crossed nicol-prisms, which, charged by a transformer to high voltage, discharges through a spark gap; to the second one belong the experiments made with the "optical shutter" of Beams; and to the third one the determination of lags in the Faraday effect.

First Group.—The apparatus used is a modification of the one of Abraham and Lemoine[8] and is shown schematically by Fig. 4. The Kerr condenser, K, placed between crossed nicols N_1 and N_2 is charged to a certain potential by a transformer or by an electrostatic machine, and discharges through the spark gap S. The light of the spark is observed directly or after reflection in mirrors through the shutter N_1KN_2. Instead of the eye a spectrograph can be placed behind N_2. The lines of the spark will be seen or not, depending on the length of the light-path before they cross the shutter and on the capacity and self-induction of the circuit. It was found[9] that the different lines emitted by the spark appear in a certain succession, the air-lines first, the spark-lines later, and the arc-lines last. It was also found that there was a difference in the time of appearance of different spark-lines and of different arc-lines among themselves. The times measured ranged from 0.2 to 15×10^{-8} sec. Now, these results can be readily interpreted without assuming the existence of any time-lags in fluorescence. That the air-lines appear first is obviously due to the fact that the spark-discharge must begin by ionizing and exciting the air between the electrodes, after which metal from the electrodes will evaporate as a result of local heating and it will be ionized and excited by collisions. Since the spark-lines of the metal appear sooner than the arc-lines, it seems that at first most metal atoms are ionized and that it takes some time before they recombine and have a chance of emitting arc-lines. The fact that different spark-lines and arc-lines do not appear simultaneously among themselves can be easily understood by applying the same considerations that were used for explaining the experiment of Wood. An explanation in detail of the sequence of appearance of the lines can not yet be attempted because the quantitative measurements are not reliable. They are mostly calculated upon the assumptions that the Kerr condenser discharges suddenly (instantaneously) a certain time after the beginning of the spark, which is given by the length of wire between spark and condenser divided by the velocity of light; that a capacity-induction circuit does not oscillate even if there is no appreciable resistance in it, and that a Leyden jar connected in parallel with the spark-gap does not modify the time at which the condenser discharges. These three assumptions

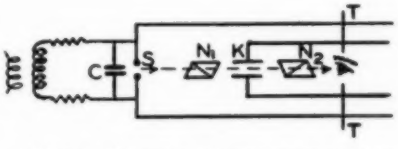

Fig. 4. Diagram of apparatus used to measure "dark time" and "time-lags."

[8] Abraham and Lemoine, C. R. **129,** 206 (1899).

[9] F. L. Brown and J. W. Beams, J. O. S. A. **11,** 11, (1925); J. W. Beams, Phys. Rev. **27,** 805 (1926), **28,** 475 (1926); J. W. Beams and P. N. Rhodes, ibid. **28,** 1147 (1926); G. L. Locher, J. O. S. A. **17,** 91 (1928).

are obviously incorrect and falsify the measurements. Furthermore, there is not sufficient consideration paid to the very large color dispersion of the Kerr effect. The fact that Beams finds that different terms of the same multiplet appear at different times may be due in part to this and in part to the method of measurement which was by changing the light-path, or the wire-length, until a line appeared or disappeared, the time of which will depend (since the Kerr condenser discharges in reality rather slowly) on the sensitivity of the eye or plate and on the intensity of the particular line. Moreover Locher found recently that multiplet-lines appear together.

Another experiment made with the same arrangement of Fig. 4 in a slightly modified form was performed by Hoxton and Beams[10] in order to measure the extinction-time of the fluorescence of solutions of fluorescein. They found a time $(3.2\pm0.3)\ 10^{-8}$ sec. for an aqueous solution and interpreted it as the "time elapsing between the beginning of incidence and the beginning of fluorescence emission." The considerations applied to the experiment of Gottling have here full validity and need not be repeated. This measurement is also not free from the objections outlined above. Furthermore, the extinction-time of fluorescein in water has been determined by Gaviola who found $(4.5\pm0.5)\ 10^{-9}$ sec. for it, a value confirmed by a quite independent calculation of Perrin[11] who found 4 to 6×10^{-9} sec. The value measured by Hoxton and Beams is then about six times too large and indicates by no means the existence of a time-lag in fluorescence.

Second group: The optical shutter of Beams.—We shall consider here a group of experiments made with the so-called "optical shutter" of Beams. The shutter was originally defined as "a method of obtaining light-flashes of uniform intensity and short duration" and it was assumed to "open abruptly, remain open any desired time from 10^{-9} to 10^{-7} seconds and then close abruptly."[12]

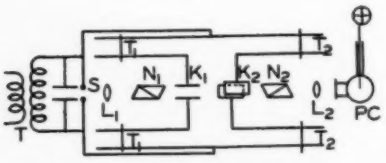

Fig. 5. The optical shutter of Beams.

Fig. 5 shows the experimental arrangement used. Two identical Kerr cells, K_1 and K_2 are placed, one inclined 90° to the other, between crossed nicols N_1 and N_2. Light of the spark S, or of a steady light-source placed instead of it, will not pass the optical system $N_1K_1K_2N_2$ as long as the electrical fields in K_1 and K_2 are equal, owing to the fact that the difference of phase produced by K_1 on the light will be compensated by K_2. If the fields in K_1 and K_2 are different, light will pass the system and fall for instance upon the photocell PC. The shutter was originally supposed to work in the following way: The transformer T will charge the two cells K_1 and K_2 to equal potentials until the spark S strikes, before which moment no light will pass the shutter, since the two cells will compensate; at a time $t_1=l_1/c$ (where l_1 is the total length of wire from the

[10] L. G. Hoxton and J. W. Beams, Phys. Rev. **27**, 245 (1926).
[11] F. Perrin, C. R. **182**, 219 (1926).
[12] J. W. Beams, J. O. S. A. **13**, 597 (1926).

spark S to the cell K_1 and c the velocity of light) after the spark strikes the condenser K_1 will discharge abruptly; at a time $t_2=l_2/c$, where l_2 is the length of wire to the second cell, K_2 will discharge abruptly. If $l_1=l_2$, the two cells will discharge at the same time and no light will pass the shutter, but if l_2 is for instance longer than l_1, the second cell will discharge (abruptly) a certain time $\Delta t=t_2-t_1$ later than the first. During this time Δt the electric field will be present only in cell K_2 and light incident upon the system will be able to pass through it. This time Δt, during which the shutter is open, is then $\Delta t=(l_2-l_1)/c$ and can be varied at will by changing the positions of the trolleys T_1 and T_2.

As we see, the assumptions made in the above reasoning of Beams were: First, "that the fall of potential travels along the lead wires at about the velocity of light"; second, that a change Δl in the length of the wire will change the time at which the condenser discharges "abruptly" by $\Delta t=\Delta l/c$, and third that a spark circuit with capacity and self-induction will not oscillate even if there is not sufficient resistance in it to damp out the oscillation.

That these assumptions were incorrect has been recognized by Beams and Lawrence themselves who in a recent publication[13] make an approximate calculation of the way in which the shutter works under the assumption that the discharge of the Kerr cells occurs aperidocially with a time constant α ($1/\alpha$ is the time in which the field decreases to $1/e$). The same calculation in a more exact form has been repeated by v. Hámos,[14] who assumes also aperiodic discharge. Both authors come to the conclusion that the shutter neither opens nor closes abruptly and that the time during which it remains open does not depend in first approximation on the position of the trolleys. Only the total light intensity allowed to pass through depends on it. The curves published by v. Hámos in Fig. 3 of his paper show that the duration of the opening of the shutter is of the magnitude of $1/\alpha$ if we define arbitrarily this duration as the time between the beginning of the opening and the instant at which the light let through decreases to $1/e$ of its maximum value. Now Beams and Lawrence show that their previous results can be accounted for by assuming $1/\alpha=10^{-8}$ sec. in spite of which they state later (p. 177) that "the shortest flashes produced were more probably of the order of magnitude of 10^{-9} sec." The value of α found by Beams and Lawrence applied to the curves of v. Hámos would indicate a value ten times larger.

Beams and Lawrence and v. Hámos find also that the apparent time-lags of the Kerr effect measured before[15] were all probably due to the differences in the dielectric constants of the substances which produced differences in the capacities of the cells and with them also in the duration of their discharges.

[13] J. W. Beams and E. O. Lawrence, Jour. Franklin Inst. **206**, 169 (1928).

[14] L. v. Hámos, Zeits. f. Physik **52**, 549 (1928).

[15] J. W. Beams and F. Allison, Phil. Mag. **3**, 1199 (1927); J. W. Beams and E. O. Lawrence, Proc. Nat. Acad. Sci., **13**, 505 (1927).

Now the calculations mentioned above are based on the assumption of an aperiodic discharge of the Kerr cells. This assumption requires the existence of suitable resistances in the circuits, resistances which, according to the statements of Beams and Lawrence were not present (pp. 166 and 177). Moreover they point out that "the discharge, instead of falling off exponentially, ... was less rapid initially and more rapid in its later stage." All of this makes certain that the discharge in the shutter was actually a periodic oscillation with a certain damping coefficient. Furthermore, Locher detected actual oscillations in his circuit with a wave meter, but he disregarded them because their period seemed to him too long to affect the working of the apparatus. The period was on the contrary of the order of magnitude that one may expect for the oscillatoric discharge of the Kerr cell. It is necessary, therefore, to analyze how the shutter works in the case of a periodic damped oscillation under the conditions that actually existed in the original experiments.

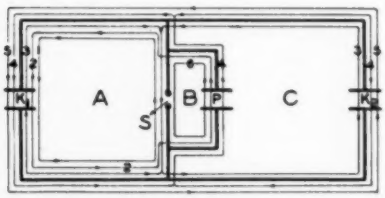

Fig. 6. Diagram of electrical circuit in the optical shutter of Beams.

Figure 6 shows a diagram of the electrical circuit. K_1 and K_2 are the Kerr condensers, S the spark-gap, and P the Leyden jar connected parallel to it. As we see, we have three circuits A, B, and C, coupled together and they will be capable of oscillating in many different ways. The thin lines drawn in Fig. 6 indicate the possible oscillation affecting directly the Kerr condenser K_1. As is well known, in a spark-discharge circuit every possible oscillation does actually take place with its own amplitude and frequency, which can be calculated knowing the capacities, inductances, and resistances of the circuit. Since the ohmic resistances of the circuit were probably low, all the indicated oscillations were certainly periodic with a certain damping coefficient. Let us consider some of the oscillations: Oscillation 1 is the discharge of the Kerr condenser K_1 through the spark S; oscillation 2 is the discharge of the same through the large capacity P; oscillation 6 is the discharge of the Leyden jar P through the spark S, which will probably be of large amplitude and induce a forced oscillation of the same frequency upon the circuit A, and so on. The discharge of the Kerr condenser K_1 will then be determined by the superposition of six periodic damped oscillations, each of them with its own frequency and amplitude. Not knowing the inductances and resistances of the circuit (they have not been published), we can not calculate the amplitude of each of the oscillations and so we can not know which of them will be strongest and which can be neglected, but we can try to eliminate some of them by general considerations. Oscillation 5 will be surely weak, 6 will be strong as said before and have a long period, but we may arbitrarily assume that the induced forced oscillation upon K_1 be of small amplitude and thus eliminate these two. But oscillations 1, 2, 3, and 4 will probably be of comparable amplitude, and none of them should be neglected. Of these four 1 has the shortest period and is the only

one that has been considered by the authors working with the shutter. The fact that Locher found that a change in the inductance connecting the jar P with the spark S increased the values he was measuring up to five times, indicates that the main oscillation in his case was 2, or 4, or 6, all of which have a longer period than 1. But let us assume the most favorable case for the quick closing of the shutter, let us assume that only oscillation 1 affected the Kerr cell K_1 and let us make a similar assumption for the Kerr cell K_2. The period of oscillation 1 can not be exactly calculated because the inductance of the circuit has not been published but one can estimate, according to the dimensions of the apparatus, that the inductance, L, was of the order of 10 microhenries. The capacity of the condenser K_1 was of about 5 cm and the capacity of the wires of about 20 cm so that the period will be approximately $T=2\pi(LC)^{1/2}=10^{-7}$ sec. Let us consider now how the cells will discharge: If we limit ourselves to the consideration of the first quarter period of the oscillation, that is, to the first breakdown of the field in K_1 we can assume that the electric field E_1 in the cell will diminish following a sine curve

$$E_1=E_1^0 \sin\left[(2\pi t/T)+\pi/2\right] \tag{3}$$

Now, the amount of light passing the shutter at a given moment will be

$$J=A \sin^2 \alpha/2 \tag{4}$$

if α is the resultant phase-difference produced by both Kerr cells (see Fig. 6), which is given by

$$\alpha=2p(E_2^2-E_1^2) \tag{5}$$

where p is a constant and E_2 the field in the cell K_2, therefore

$$J=A \sin^2\left[p(E_2^2-E_1^2)\right]. \tag{6}$$

In Fig. 7 curve 1 represents E_1^2 as a function of the time and it gives the decrease of the square of the field in the cell K_1. If the trolleys T_1 and T_2 (Fig. 6) are placed symmetrically the cell K_2 will discharge also following curve 1 and the difference of phase α will be constantly equal to 0 and so will the light-intensity J. If we displace now the trolley T_2 a certain amount, say 83 cm, the cell K_2 will *begin* to discharge $83/c$ sec. later than K_1, that is, the phase of the discharge in K_2 will have a delay of $83/c$ sec. At the same time the self-induction of the circuit of K_2 will increase and with it the period of the discharge, but since a small change in the position of the trolley will produce a still smaller change in the self-induction and since the period changes only with the square root of the self-induction, a small change in the position of the trolley will in first approximation not modify the period of the discharge. The square of the field in K_2 will be given then by curve 3 (Fig. 7), which is the same curve 1 displaced 83 cm to the right. The curve "diff.(3–1)" of Fig. 8 gives the difference $E_2^2-E_1^2$ as a function of the time in a five-times larger scale, difference to which α is proportional

[formula (5)]. The curve "$J(3-1)$" indicates the light-intensity which will pass the shutter according to formula (6). We see that light will pass practically during the whole time that the condensers take to discharge. Let us consider now what happens if we reduce the difference in the positions of the trolleys to 25 cm: Curve 2 will represent now E_2^2, curve "diff.(2–1)" the difference $E_2^2-E_1^2$ and curve "$J(2-1)$" the light-intensity which will pass the shutter. As we see the total intensity allowed through has diminished but not the time during which the shutter remains open. The bringing of 2 still nearer to 1 will flatten down curve J. All this means is that the displacement of the trolleys will in first approximation not change the time during which the shutter remains open but only the total light-intensity

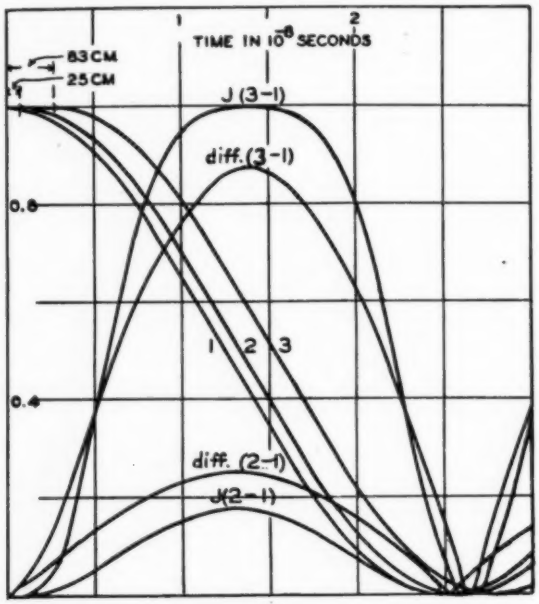

Fig. 7.

allowed through, and that in no case will the shutter remain open for less than about 10^{-8} sec.

The optical shutter behaves then in quite a different way from what it was originally supposed to do and since the fundamental assumptions upon which all measurements made with it are based are incorrect, every result obtained with it has to be considered as doubtful. So, for instance, in a paper "On the nature of light"[16] it is claimed that trains of light-waves have been cut in pieces of 3 cm of length, while we have seen that the shutter can by no means reduce the length of a wave-train to less than 300 cm, or one hundred times more than what the authors claim.

In a recent paper on "The element of time in the photoelectric effect,"[17] assumptions are made which can not be regarded as free from the con-

[16] E. O. Lawrence and J. W. Beams, Proc. Nat. Acad. Sci. **13**, 207 (1927).
[17] E. O. Lawrence and J. W. Beams, Phys. Rev. **32**, 478 (1928).

siderations outlined above in connection with the optical shutter. None of the experiments of this group proves then the existence of any time-lags.

Third group. Using an arrangement similar to the optical shutter, in which the two Kerr cells are substituted by Faraday cells, Beams and Allison find time-lags for the Faraday effect in various liquids. In a first publication[18] values for the time-lags are found which are reproduced in the second column of Table I.

TABLE I

Substance	Time-lag in seconds according to Beams and Allison	Allison
CCl_4	$(1.1\pm0.3)10^{-9}$	$(3.3\pm0.2)10^{-9}$
Benzene	$(1.9\pm0.3)10^{-9}$	$(3.5\pm0.2)10^{-9}$
Xylene	$(2.1\pm0.3)10^{-9}$	$(4.4\pm0.2)10^{-9}$
Chloroform	$(2.4\pm0.3)10^{-9}$	$(4.6\pm0.2)10^{-9}$
Toluene	$(2.5\pm0.3)10^{-9}$	$(2.7\pm0.2)10^{-9}$
Bromoform	$(4.1\pm0.3)10^{-9}$	$(6.6\pm0.2)10^{-9}$

In a second publication by one of the same authors[19] which appeared a few months later, the lags reproduced in the third column are found for the same substances under the same conditions. As we see the differences between both measurements are about ten times larger than the limits of error indicated and are of the order of magnitude of the quantities measured themselves. Since no explanation is offered for the divergence, these results can not be considered as proving the existance of time-lags in the Faraday effect.

SUMMARY

(*a*) The idea of the existence of time-lags in fluorescence was probably conceived because of a misunderstanding of the concept introduced by Bohr, that excited atoms can live for finite time without radiating.

(*b*) The extinction-curve of the light emitted by canal-beams has now been established by J. Port to be an exponentially falling curve from the very beginning.

(*c*) The experiment of Wood with streaming mercury vapor, which was accepted as a proof of the existence of "dark-times," is explained as due to the fact that the light observed is emitted by a state which is not directly reached as a result of the excitation. It is shown that there is no real "dark-time" even in this case.

(*d*) The time-lags measured by Gottling were in reality mainly due to the color dispersion of the Kerr effect.

(*e*) The successive appearance of different lines in the spark can be readily understood without the assumption of time-lags. A detailed explanation could be attempted if the quantitative material were more reliable.

[18] J. W. Beams and F. Allison, Phys. Rev. **29**, 161 (1927).

[19] F. Allison, Phys. Rev. **30**, 66 (1927).

(*f*) The time-lags measured by Hoxton and Beams for the fluorescence of liquid solutions were probably due to color dispersion of the Kerr effect, as in the case of Gottling, and to an inaccurate method of measuring and calculating.

(*g*) The optical shutter of Beams which was supposed to "open abruptly, remain open any desired time from 10^{-9} to 10^{-7} seconds and then close abruptly" is analyzed and found to open and close during a time of the order of 10^{-8} sec. and to remain open for at least 10^{-8} sec. in the best case. The time during which it remains open does not depend in first approximation on the position of the "trolley" as was assumed.

(*h*) The former result indicates that in the experiment of Lawrence and Beams where it was claimed that light wave-trains were cut in pieces of 3 cm length by the optical shutter the wave-trains were really not shortened to less than 300 cm in the best case.

(*i*) The time-lags found for the Kerr effect in liquids with high dielectric constants were probably due to the fact that increase in dielectric constant means increase in the capacity of the Kerr condenser and with it of the time that it takes to discharge.

(*j*) The time-lags measured by Beams and Allison for the Faraday effect can not be considered as proving the existence of the said lags.

DEPARTMENT OF TERRESTRIAL MAGNETISM,
CARNEGIE INSTITUTION OF WASHINGTON,
January 8, 1929.

DEPENDENCE OF ULTRA-VIOLET REFLECTION OF SILVER ON PLASTIC DEFORMATION

By Henry Margenau

Abstract

The change in electrical conductivity of metals with mechanical strain suggests the possibility of a dependence of optical reflecting power on plastic deformation. To study this matter, and to obtain additional evidence with regard to the nature of cold working, the behavior of the minimum of reflecting power of silver in the near ultra-violet (at 3160A according to Hagen and Rubens) was examined for silver surfaces of varying degrees of strain, produced by vigorous and moderate polishing, etching, and electroplating. Reflection curves were obtained by measuring directly, by means of two quartz photoelectric cells, incident and reflected intensities. It is shown that the minimum is very low and lies at 3160A, in accordance with Hagen's and Rubens' measurements, only for highly polished plates. For unstrained surfaces it is shifted to lower wave-lengths by about 20A and the reflecting power rises appreciably. The results presented in the paper, as well as other allied phenomena, are accounted for by assuming a change in the number of free electrons and a consequent change in the index of refraction of the metal.

Introduction

THE effects of cold working upon metals are usually explained by assuming two distinct types of changes in the arrangement of the crystal lattice: translational slipping of portions of the crystal along important crystallographic planes and the process commonly known as twinning. Although metallurgists have been fairly successful in assigning the observed features of plastically deformed metals to these two causes, there has recently been an accumulation of evidence pointing to their inadequacy for an exhaustive explanation of electrical properties of cold worked metals. Geiss and van Liempt[1] present a summary of observations which cannot be accounted for by reference to changes in the geometrical configuration of the crystal. The authors are led to suggest a deformation of electronic orbits accompanying the rearrangement of atoms. However, they advance this hypothesis on purely speculative grounds.

The original object of the experiment described in this paper was to decide, by studying with some precision those properties of plastically deformed metals which do not depend on atomic arrangement, whether or not such assumptions are necessary. The reflecting power R of Ag in the ultra-violet was selected for the following reasons: *a.*—If the fundamental assumptions of Drude's theory are correct, R is determined in the ultra-violet region by electrons only, free or bound. (The reasoning in this paper will be consistently classical, since the quantum theory is not readily applicable to the phenomena of reflection and dispersion.) The residual ray frequencies

[1] W. Geiss and J. A. M. van Liempt, Zeits. f. Metallk. 18, 216–218 (1926).

for silver as computed roughly from Madelung's theory lie at about 75μ, while the electronic resonance frequencies fall in the near ultra-violet. *b.*—Ag has a sharp minimum of reflection at 3160A, which, it was hoped, would be particularly sensitive to changes. *c.*—Ag is capable of sustaining high degrees of plastic deformation, which can be easily produced. Polishing is known to cause very severe surface strains. *d.*—A silver surface is not likely to undergo rapid chemical changes; disturbing effects resulting from impurities are less likely to arise than with other metals. *e.*— Optical constants of silver are accurately known; they have always been obtained for highly polished surfaces.

Experimental Method

To carry out the investigation it was necessary to use a method not dependent on specular reflection; furthermore it had to permit a comparison of reflecting powers of specularly and diffusely reflecting specimens. Photographic methods were not employed (except as a check) because of the uncertainty that attends densitometer readings taken on plates which are given very unequal times of exposure. Hence it seemed preferable to make direct photometric measurements. Figure 1 illustrates the experimental arrangement.

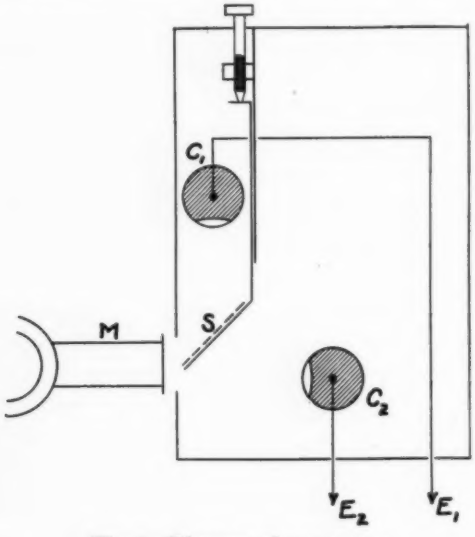

Fig. 1. Diagram of apparatus.

The light source used (not shown in the figure) was a mercury quartz lamp. An iron arc, preferable because of its greater abundance of lines, was not sufficiently steady in its performance to give good results. It will be noticed that the precision of the results is unaffected by intensity variations, but depends essentially on the constancy of the position of the light source. The mercury arc was found to emit a moderately strong continuous spectrum if it was operated with high current densities. This latter condition was suitable for taking readings. After passing through a Gaertner monochromator the light was admitted to a tin box containing the silver plate and the measuring devices. The dispersion of the optical system was such that a spectral line in the region under investigation had a width of about 12A as measured on the drum of the monochromator.

The interior of the box and all parts exposed to the light were coated with lamp black. A silver plate *S* rested on an inclined holder, which could be made to move vertically by means of a spring and a screw extending through

the top of the box. By turning the screw the relative amounts of light falling on S and passing below the holder were adjusted. C_1 and C_2 are photo-electric cells measuring reflected and directly transmitted light respectively. They are made completely of quartz, Pyrex cells with quartz windows having proved unsatisfactory. It was attempted for some time to construct two photo-cells (potassium cells) with similar characteristics for the complete region of measurements, but without success. There was a change in the ratio of the sensitivities of the two cells in different portions of the spectrum. This variation had to be determined by calibrations. The cells used in the experiment were carefully tested and shown to have a linear intensity-current relation for intensities of the order of magnitude here used. Readings were taken both with white light and various definite ultra-violet wave-lengths selected at random. Each cell was connected with a separate electrometer kept in a different compartment of the same case. Deflections could be observed on the same scale through a longitudinal slit in the wall of the box. Measurements were made by the rate method. The electrometers could be used at very low sensitivities (400 mm per volt) during the greater part of the experiment, the photo-currents being of the order of 10^{-13} amperes.

At the beginning of a series of observations the top screw was adjusted until a suitable ratio of deflection rates was obtained. This adjustment was maintained until all readings on a single plate were taken. The apparatus was repeatedly calibrated, usually after three sets of readings had been made on different specimens which were to be compared. This was done by inserting in place of S a totally reflecting quartz prism, designed to deviate the incident beam upward through an angle of 90°. The absorption of the quartz was assumed to be non-selective over the range of measurements.

The preparation of the silver surfaces needs a few words of comment. Two different conditions of plastic deformation were imposed by moderate and vigorous polishing. Moderate polish was produced by rubbing the specimen on emery and fine sand paper, while high polish was the result of grinding and subsequent careful buffing. The former surface was fairly regularly reflecting, but showed a multitude of minute scratches, while the latter appeared highly specular and exhibited no irregularities visible to the naked eye. "Unstrained" surfaces were prepared by slow etching in dilute nitric acid. They showed a distinctly crystalline structure of fine grain. The "electrolytic" plate carried a deposit produced with current densities of 1.5 milliamperes per cm^2 in a bath of $KAg(CN)_2$. All plates were of dimensions $2\times4\times0.1$ cm. To avoid the formation of disturbing impurities on the plates or at least to insure the existence of similar surface films the specimens were washed in alcohol and rinsed in distilled water after their preparation. It was found, however, that great precautions of this character were unnecessary to obtain reproducible results in the spectral region of primary interest.

Experimental Results

The range of investigation extended from 2500A to 3500A. Only the significant portion of the curves, that covering the minimum, is reproduced.

Readings about and below $\lambda = 2500$A were found to be irregular and incapable of reproduction within the limit of experimental error. The cause of such variations appears to be the disturbing action of occluded impurities which overshadow the spectral peculiarities of the silver surface. For accurate determinations in this region it will be necessary to place the plates in a vacuum.

The values of R plotted against λ represent in all cases reflecting powers at an angle of incidence of 45°, not at normal incidence. For comparison, R has been assumed arbitrarily to be 1 for some wave-length in the visible portion of the spectrum, and all other points have been adjusted accordingly. This procedure, which was applied equally to all curves compared on a single

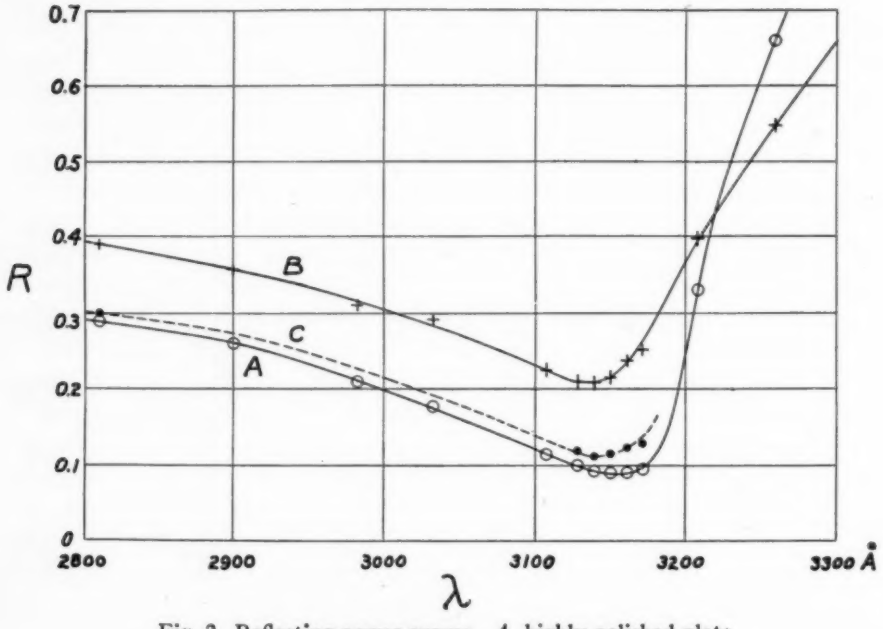

Fig. 2. Reflecting power curves. *A*, highly polished plate. *B*, etched plate. *C*, highly polished plate after heating.

diagram, may possibly introduce an unavoidable constant error throughout. However, it can not vitiate the conclusions of the paper.

Curve *A* in Figure 2 refers to the reflecting power of a highly polished plate. For this curve, particular care has been taken in determining R for visible light ($\lambda = 5400$A was the wave-length for which these three curves were normalized), so that the actual height of the ordinates at the minimum should be correct and in agreement with results obtained by absolute methods of measurement. Computing the minimum ordinate on the basis of Minor's data[2] the value 0.0883 is found[3] while the experimental height is 0.088. An accurate location of the minimum on the wave-length scale afforded some

[2] R. S. Minor, Ann. d. Physik **10**, 617 (1903).
[3] Cf. table on p. 11.

difficulties. Calibration curves without the silver plates could not be taken with a precision equal to that of the actual measurements, the electrometer deflection being more rapid. (Reducing the intensity of the light source introduced erratic readings as it entailed a shift of the center of illumination and a consequent change in the relative amounts of transmitted and reflected light.) The error due to the uncertainty in the calibration affects only the absolute position of the minima, not their distance apart. For curve *A* the minimum lies at 3157A, and the range of uncertainty is estimated to be about ±5A. Curve *B* represents the reflecting power of an etched surface. There is a slight irregularity to the right of the minimum which occurs on almost all curves taken for etched samples. Though this feature can not be said definitely to be real, it is probable that there is a fine structure.

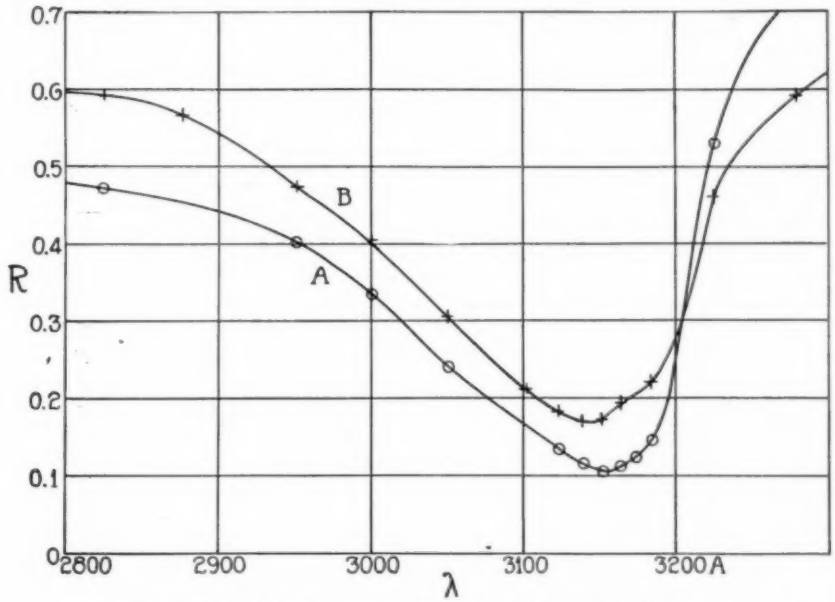

Fig. 3. Reflecting power curves. *A*, highly polished plate. *B*, moderately polished plate.

Curve *C* illustrates the behavior of a silver plate which was first highly polished and subsequently heated for a few minutes above the annealing temperature. It shows that the changes which are due to polishing are partly reversible if the metal is allowed to free itself from strain.

In Figure 3 the optical behavior of a moderately polished surface *B* is compared with that of a highly polished one *A*, while in Figure 4 *B* is an electrolytic plate and *A* a highly polished one.

The experimental method here outlined, if applied carelessly, is susceptible to errors for several reasons. First, proper account has to be taken of the variations in the spectral sensitivities of the two photo-cells. They necessitate frequent calibrations such as were referred to previously. Another very annoying source of error is the lack of parallelism of the two monochro-

mator slits. If a spectral line, the inclination of which is determined by the position of the collimator slit, makes a small angle with the second slit, the various portions of this slit will be illuminated successively as the line passes across it, and the constant ratio of the amounts of reflected and transmitted light as fixed by the position of the top screw will be disturbed. It is therefore necessary to make an extremely fine adjustment of the monochromator. Small residual disturbances of this character which could not be eliminated were rendered ineffective by calibrating the arrangement exactly for the wave-lengths at which measurements of R were made. For the diffusely reflecting surfaces selective action of photo-cell C_1 was to be expected on account of partial polarization of the reflected light. This matter was investigated by introducing a ground quartz plate in place of S and taking read-

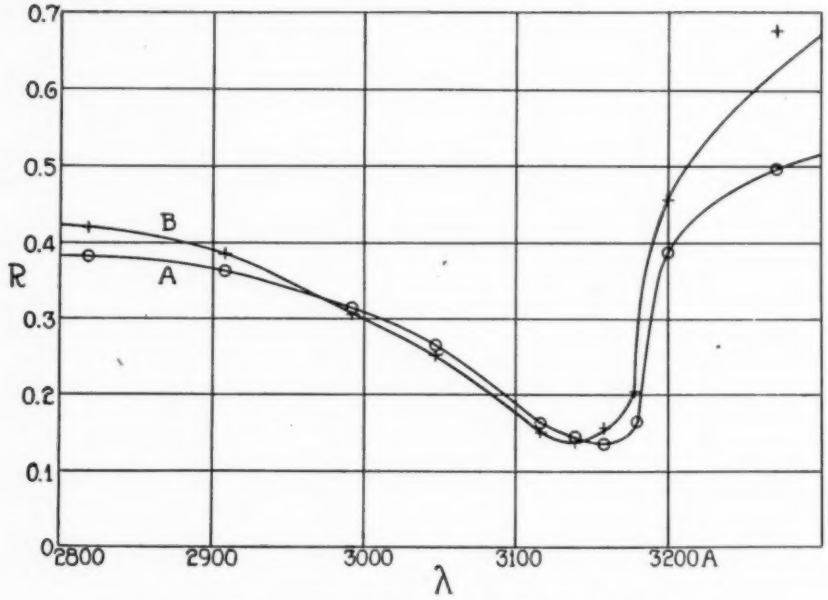

Fig. 4. Reflecting power curves. A, highly polished plate. B, electrolytic plate.

ings. Thus it was found that the sensitivity of C_1 did not increase markedly up to about 3500A, where a change, attributed to selective photoelectric emission, became noticeable. Potassium is well known to behave in this way, its maximum selective effect occurring at 4350A.

The experimental results, as apparent from the curves, can be summarized as follows: Cold working displaces the minimum of reflecting power of silver to longer wave-lengths by about 20A (in the extreme case of Fig. 2) and causes it to be more pronounced. High polish, regarded as an extreme form of plastic deformation, reduces the ordinate at the minimum by about one half.

It may be objected that the results here stated are not consequences of cold working, but arise from the difference in smoothness of the surfaces.

There is indeed an effect of this character, and its magnitude requires investigation. If the wave-length of light becomes smaller than the size of pits in the surface, it may, under suitable conditions, undergo several reflections. Its intensity will thereby be reduced. Hence an uneven surface should show diminished reflection for small wave-lengths. At the minimum the opposite is observed. Another influence will result from the difference in inclination of the small reflecting portions of a rough surface. Consider a rough surface as being made up of small facets of equal area, whose normals have a certain angular distribution about the normal of the "plane" surface. The latter was inclined, in this experiment, at an angle of 45° to the incident parallel light. Let $p(\theta)$ be a distribution function measuring the proportional number of facets the normal of which is inclined at θ to the parallel incident light, such that $\int_{-45°}^{135°} p(\theta)d\theta = 1$. For any angle of incidence θ the reflecting power of a metal surface is given by

$$R(\theta)=\frac{1}{2}\left\{\frac{n^2(1+k^2)-2n\cos\theta+\cos^2\theta}{n^2(1+k^2)+2n\cos\theta+\cos^2\theta}+\frac{n^2(1+k^2)\cos^2\theta-2n\cos\theta+1}{n^2(1+k^2)\cos^2\theta+2n\cos\theta+1}\right\} \tag{1}$$

Here n = index of refraction; nk = index of absorption. Neglecting a constant multiplier, which in the experiment is disposed of by the indicated process of adjusting the values of R, the reflecting power of a diffusely reflecting surface at a general angle of incidence 45° becomes

$$R=\int_{45°-\delta}^{45°+\delta} p(\theta)R(\theta)d\theta \tag{2}$$

where δ is one quarter of the angle subtended by the diameter of the transparent area of C_1 at S. This integral, evaluated for all wave-lengths, gives the values of R over the spectral range. They will not, in general, agree with those obtained from (1). (2) was evaluated for $\lambda = 3130$A, $\lambda = 3150$A. $\lambda = 5400$A, using Minor's[2] data for n and nk. The difference between (1) and (2) will evidently be greatest for the case $p(\theta) = 0$ if $\theta < (45° - \delta)$ and $\theta > (45° + \delta)$; $p(\theta) = \text{const.}$ if $(45° - \delta) \leq \theta \leq (45° + \delta)$, the constant being chosen in accordance with $\int p(\theta)d\theta = 1$. This amounts to assuming all facet orientations as equally probable, while actually there will be a preponderance of facets having their normals nearly coincident with the general normal of the surface. For this extreme case

$$R=\overline{R(\theta)} \tag{3}$$

where the average is taken between $(45° - \delta)$ and $(45° + \delta)$. Taking $\delta = 5°$, the following figures are obtained:

	$R(\theta)$ (Specular reflection)	R(diffuse reflection)
5400A	0.938	0.939
3150A	0.073	0.073
3130A	0.083	0.084

It is apparent that the experimental results are not due to surface roughness.

After the displacement of the minimum had been measured in this manner the reflection spectrum from silver plates illuminated by a carbon arc was photographed, first by means of a small grating, then, to get greater dispersive power, with a prism spectrograph. The first photographs showed a definite indication of the shift, while the latter (dispersion about 15A/mm) permit a comparison as to its order of magnitude, which checks well with conclusions from the curves. Densitometer readings were not made.

Hagen and Rubens[4] found that the reflecting power of Ag depends to some extent on the age of the surface. R at the minimum is greater for "old" silver than for a freshly polished surface. In the present work this was also found to be the case. R at the minimum rose through a succession of intermediate values by an amount of 37 percent after 15 days, the plate being kept near the radiator of the research room (temperature about 85°F). Another plate polished in the same manner at the same time was placed in a glass tube, which was evacuated and deposited at the same place. Its minimum reflecting power showed no change on examination after 15 days. Moreover, a highly polished plate exposed to evaporating SC_2 acquired an increase in R of 12 percent within one hour. Hence this effect is attributed to the formation of impurities, probably sulfide, on the reflecting surface. Any foreign substance could reasonably be assumed to obliterate the spectral peculiarities of metallic silver in the region of the minimum. Accompanying changes in R in the farther ultra-violet were measured, but appear erratic. The position of the minimum is not noticeably altered by ageing of this type.

Discussion of Results

A change in R can be accounted for by a variation of two parameters: n and k. The trend of both is sketched in Fig. 5, which is taken from Minor's[2] paper. The rapid downward slope of n is characteristic of a narrow transmission band. It is difficult to produce agreement with the experimental findings by assuming changes in k. A simple shift of the k-minimum to the left will not displace the minimum of R. At any rate such procedure would seem very arbitrary. The curve shows, on the other hand, that the minimum of k lies at 3140A, not at 3160A, where that for R is found. It is the rapid slope of n which causes the latter to appear 20A beyond the former. Tilting the straight line portion of the curve about a fixed point for which n is about 1.1 so that $dn/d\lambda$, whose value for the polished surface is -0.006/A, becomes -0.0032/A, moves the minimum of R to 3140A. This reduction in the rate of variation of n with λ is chosen, *a*) on account of its simplicity, all other possible methods of accounting for the displacement being more complicated, *b*) because of its influence on other properties. It is well known that, on the basis of the classical dispersion theory, $dn/d\lambda$ depensd in a definite manner upon the number of bound electrons vibrating with a resonance frequency which lies on the short wave-length side of the trans-

[4] R. Hagen and H. Rubens, Ann. d. Physik 8, 1–21 (1902).

mission band. If this number decreases the slope of n at the point in question becomes less steep.[5] We shall assume, therefore, that for an unstrained surface the number of electrons vibrating with a certain ultra-violet frequency is smaller than that for a polished one. Therefore, relieving the surface from

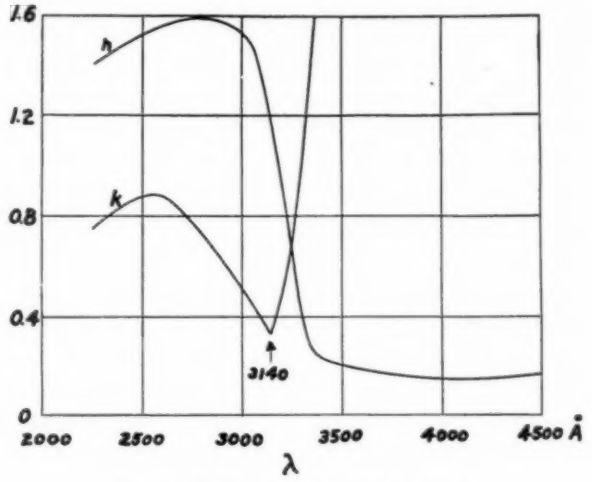

Fig. 5. Variations of n and k with λ.

strain affects the values of k for two reasons. (1) The maximum of k will be reduced in proportion to the decrease in the number of bound electrons of the resonance frequency, which follows directly from

$$n^2k = A \sum_i \frac{n_i \omega l_i}{(k_i^2 - \omega^2) + 4\omega^2 l_i^2},$$

where A is a constant, n_i the number of resonating electrons of frequency k_i, and l_i a damping factor. The effect of neighboring frequencies is here neglected. The effect upon the minimum of k can not be calculated since it depends essentially on other resonance frequencies, but if conditions in the latter frequencies remain fixed it is probably small. (2) The electrons which, in the undeformed state, are no longer constrained to vibrate with a definite frequency must be supposed to be free. Their presence adds to k the amount $C/2\omega n^2$, C being the conductivity due to these electrons. If the curves in Fig. 5 are redrawn in qualitative agreement with these considerations, the values for R obtained from them are in accord with experimental observation. The hypothesis here outlined also agrees with the reduction of electrical conductivity which occurs with plastic deformation.

M. de Sélincourt[6] has shown that heating a silver surface causes the minimum of R to be displaced to longer wave-lengths. His explanation seems unsatisfactory to the writer, since it is out of harmony with accepted theories

[5] Numerical calculations can easily be made; but they have little meaning since the value of the resonance frequency is not known. See note added in correction of proof.

[6] M. de Sélincourt, Proc. Roy. Soc. A107, 247–254 (1925).

of metallic reflection (the effect of bound electrons is neglected, the occurrence of the minimum being attributed to lack of resonance of free electrons) and it shows no connection with the decrease in electrical conductivity. The assumptions made in the present paper account well for the changes found by M. de Sélincourt, if heating, as well as cold working, is supposed to reduce the number of free electrons, i.e. bind some electrons into vibrational frequencies. Cooling would then shift the minimum to shorter wave-lengths and raise it, which is actually shown in his curves, while heating would displace it still further to greater wave-lengths. ($dn/d\lambda = -0.012/\text{A}$ causes it to appear at 3180A.) The shallowness of the minimum at 150° does not follow from a change in the slope of the n-curve; it would call for a more radical modification which would result, for instance, if other resonance frequencies were affected.

It is interesting to apply the hypothesis, here found valid to explain the effects of plastic deformation on the reflecting power of silver, to other known influences of cold working on optical properties. Lord Rayleigh[7] and Lummer and Sorge[8] have shown that polishing changes the sign of Δ, the phase-difference between the components of the reflected amplitude vibrating in and perpendicular to, the plane of incidence. The latter authors have also discussed the incompetence of Drude's theory of surface layers for explaining this effect. They used a glass prism with $n = 1.5196$ for $\lambda = 5460\text{A}$. It would follow from our assumption that polishing increases the number of electrons vibrating with a resonance frequency in the ultra-violet. The consequent effect on n in the visible region of the spectrum is an increase as is apparent from the dispersion curve for glass. Denoting the new index of refraction by n', we have $n' > n$. Passing from the polished surface into the prism we should encounter surface layers whose indices of refraction vary from a maximum value n_m to n. But according to Drude's theory,

$$\tan \Delta = \frac{4\pi}{\lambda} \frac{n^2}{1-n^2} \frac{\sin \alpha \tan \alpha}{\tan^2 \alpha - n^2} \int_0^d \frac{(n'^2-1)(n'^2-n^2)}{n'^2} dl,$$

where α = the angle of incidence. (See Fig. 11 on page 339 of Lummer and Sorge's paper.) l is the distance of an infinitesimal surface layer with index of refraction n' from the regular prism surface. The change in sign of Δ can only be caused by a change in the sign of the integral, which is negative as long as $n' < n$. Drude assumed the surface layers to be occluded air, hence there should be no change in sign. Strain will produce a surface film of glass with $n' > n$, which renders it possible for the preponderance of surface layers dl to have an index of refraction greater than n, and for the integral to change sign.

In concluding the writer wishes to express his gratitude for the encouragement he received from the members of the department throughout

[7] Lord Rayleigh, Phil. Mag. **16**, 444–449 (1908).

[8] O. Lummer and K. Sorge, Ann. d. Physik **31**, 325–342 (1910).

his work, particularly to Professor McKeehan, who suggested the problem, and under whose sympathetic guidance it was a pleasure to carry on the investigation.

SLOANE PHYSICS LABORATORY,
YALE UNIVERSITY,
March 11, 1929.

Note added in proof:—More detailed calculations have been carried out on the basis of the following assumptions:

1. The frequencies corresponding to the two persistent spectral lines $\lambda_2 = 2413$A (spark) and $\lambda_1 = 3280$A may be considered as principally responsible for the value of the index of refraction at the minimum. λ_1 involves the neutral state of the atom.

2. Cold working changes only the number of electrons per atom (n_1) vibrating with frequencies corresponding to λ_1.

For Δn_1, the change in n_1 due to plastic deformation, one easily derives

$$\Delta n_1 = -\Delta\left(n\frac{dn}{d\lambda}\right)(\lambda_1^2-\lambda^2)^2/A\lambda\lambda_1^4, \quad \text{where } A = \frac{Ne^2}{4\pi^2c^2m}.$$

We find for n_1 the value 0.023, indicating that only about 2 percent of the silver atoms are in their neutral state; and for Δn_1 due to plastic deformation, by inserting the experimental value for $\Delta(ndn/d\lambda)$ at the minimum,

$$\Delta n_1 = -0.008,$$

which is equivalent to a reduction of the number of neutral atoms by about one-third. This would call for a change in electrical conductivity of about 0.8 percent.

COMETS AND TERRESTRIAL MAGNETIC STORMS

By H. B. Maris and E. O. Hulburt

Abstract

A recent theory of the authors attributed terrestrial magnetic storms and auroral displays to the effect of unusual flares of ultra-violet light from the sun falling upon the terrestrial atmosphere. Such flares would be expected to cause changes in comets, and therefore comet changes should be closely connected with magnetic storms. This connection is supported by the evidence brought out in the present paper in a discussion of the behavior of 31 comets scattered through the years 1848 to 1927. A general statistical result was that in the month preceding each comet's activity there occurred on the average 6, 4, 2.9 and 1.5 times as many magnetic storms of strength 4, 3, 2 and 1, respectively, as there should have occurred according to chance. Outstanding comet changes, 28 in number, were observed on the average 5 days after strong magnetic storms. The positions of the comet, sun and earth at the epochs of the comet changes indicated that the solar flare was in a wide angle, contrary to the narrow beam hypothesis of Maunder.

1. *INTRODUCTION.* It is known that strong auroral displays are accompanied by terrestrial magnetic storms,[1] and it is an accepted belief, based on a long accumulation of evidence, that these phenomena are caused by unusual bursts of radiation of some sort from disturbed areas of the sun. The assumption that the solar disturbance is a flare of ultra-violet light has been shown in a recent paper[2] to explain in detail the prominent features of the aurora and of the complicated magnetic effects observed during a magnetic storm. In a simple case the flash was assumed to blaze out at full intensity for some minutes or hours and then to die away in a few hours or days; it might of course flare out again irregularly or intermittently. The flash was such as would come from a spot 1/10,000 part of the solar disk in area and at a temperature of 30,000°K, the temperature of the normal surface being 6,000°K. Assuming black-body conditions the hot spot would increase the solar energy in the visible spectrum by about 1 percent and in the extreme ultra-violet spectrum below 1000 angstrom units by a factor of 10^4 or more; it was realized that the black-body calculations could be little more than illustrative approximations, for the radiations from the flare would probably be in the nature of bright line and continuous spectrum emissions. The unusual ultra-violet energy of the flash, upon being absorbed in the high atmosphere of the earth, caused an unusual ionization and excitation of the atmospheric gases and these effects in turn gave rise to the auroral display and the magnetic disturbance. The solar flashes might be expected to cause activities in comets. Very extraordinary and apparently lawless changes in comets have often been observed and it was of interest to see whether the comet changes were connected with terrestrial magnetic

[1] Røstad, Geofysiske Publ. Oslo 5, 1 (1928), and references *infra*.

[2] Maris and Hulburt, Phys. Rev. 33, 412 (1929).

storms. It is the purpose of this paper to offer evidence in support of this connection based on the data of 31 comets.

Unquestionably the main ideas of the present paper have been foreshadowed by others, who have remarked on the similarity in the appearance of the flickering luminosity occasionally seen in comet's tails and the terrestrial auroral displays. Barnard,[3] in discussing the nature of the influences which may retard, accelerate and disrupt a comet's tail, suggested that these "may come from energies originating in disturbances on the sun—perhaps of a similar nature to those that cause magnetic disturbances and auroral effects on the earth." In the present instance we give point and development to Barnard's idea. One may go farther and suggest that certain planetary phenomena such as the appearance of Jupiter, of Venus, of Saturn's rings of the zodical light, etc., may be related to unusual solar activity. Köhl[4] has remarked that the luminosity which has been observed on the unilluminated part of Venus may occur at the same time as terrestrial auroras. During sunspot maximum when the solar radiation is most intense Köhl[4] thought that the northern cloud belts of Jupiter were relatively weak and Antoniadi[5] that the polar caps of Mars melted most rapidly.

2. *Brief theory of comet behavior, quiet sun.* Before taking up the effects produced in a comet by the solar disturbance we must first give a brief description of the action of the light of the quiet sun upon an ideally simple comet. We may imagine the comet to have travelled for a number of years in extra-planetary space. The mass of the comet may be 10^{-15} to 10^{-6} of the mass of the earth, its temperature is fairly low, below 10°K; the comet is perhaps nonluminous. Comets may collect matter from space, by sweeping through dust or gaseous clouds or the ions of space,[6] but we will neglect such possibilities as these The comet will be more or less sperical in shape and its material may be in lumps or may be gaseous if the temperature is so low that the thermal velocities of the atoms and molecules are below the velocities of escape from the gravitational attraction. Upon coming near the sun the comet is warmed by the solar radiation and some of its material becomes gaseous. The comet expands and gives out light, either scattered sunlight or absorbed sunlight which it has transformed into its own characteristic emissions. In this stage it is a round hazy object with no tail; it is seen mainly by the luminous coma, the nucleus being hardly noticeable. The gaseous particles of the coma being warm and therefore no longer held by gravitation, escape and are pushed out into a tail by the pressure of the sunlight. Since the thermal velocities are low, of the order of meters per second, as compared with the velocities caused by light pressure the tail may be narrow and may stretch out from the comet with little lateral spreading. Other effects, however, may result from the sunlight energy absorbed in the comet. In particular short wave-length ultra-violet light causes ioni-

[3] Barnard, Astrophys. J. **29**, 70 (1909) and Lick Observatory Pub. **11**, (1913).
[4] Köhl, Astr. Nach. **201**, 403 (1915).
[5] Antoniadi, Monthly Notices, Roy. Ast. Soc. **76**, 413 (1915–16).
[6] Eddington, "The Internal Constitution of the Stars," p. 373 (1926).

zation and excitation of the molecules and atoms of the cometary gases. Upon collision with the excited particles or with ions undergoing recombination some of the atoms (or molecules) may receive high velocities of 10 or even 100 km sec,$^{-1}$ which are much greater than the temperature velocities. (See reference 2 for a more complete discussion of collisions with excited atoms). A tail of a comet which contains an appreciable number of such fast moving particles will spread out as it recedes from the nucleus, and it is well known that the observed spreading of many comet's tails indicates the presence of particles moving with velocities too fast to be explained by temperature or light pressure effects.[7]

3. *Active sun.* Turning now to the case of the active sun, a comet under the influence of the ultra-violet flare would be expected to undergo changes similar to those just described for the quiet sun but in modified or accentuated form. The strong ultra-violet energy will cause the comet to increase in brightness, this increases its chance of discovery. Of the 31 comets discussed in the following pages, 12 were discovered a few days after strong magnetic storms under circumstances which indicated that the storm had caused an unusual brightening of the comet; for example, Holmes' comet 1892 III (see section 21) was discovered five months after it had begun to move away from the earth. Sixteen of the comets appeared during intervals of solar quiescence, and were discovered roughly when they should have been according to their brilliancy, accessibility, etc. It is difficult to say whether the discovery of the remaining 3 comets was attendent upon magnetic storms or not. The effect of the ultra-violet light flare is to increase greatly the solar radiation pressure on the cometary gases and if the flare lasts long enough may be sufficient to sweep away the coma and the tail leaving only the nucleus glowing as a star. The unusual amount of energy absorbed in the nucleus, probably in the form of heat, chemical effects, ionization and excited atoms and molecules, may cause an explosion. The nucleus may shoot out a new tail in a random direction, the tail may be of a variety of forms, narrow, fan-like, etc.; the nucleus may break into pieces. As the result of a mild solar flash one might expect the nucleus to give off an envelope of luminous gas, or several outward spreading envelopes if there were several successive flashes. Changes of these types are often seen in active comets.

4. *Observational data.* In order to bring out the connection between the changes in the comets and the terrestrial magnetic storms 31 comets were selected pretty much at random through the years 1848 to 1926, some were of historical interest, some were active, others were inactive, etc. In general we have given attention mainly to prominent changes such as unusual brightening, loss of tail, breaking up of nucleus, etc., and have left out of mention less striking variations, such as changes in spectra, etc. The data of the comets have been gathered for the most part from standard text books of astronomy, Chamber's "The Story of the Comets" (1909), the Monthly Notices of the Royal Astronomical Society, the Astrophysical Journal, and

[7] Russell, Dugan and Stewart, "Astronomy" 1, 441 (1926).

references therein. The orbits of the 31 comets were plotted, four of which are given in Figs. 1 to 4. The circle in each figure is the orbit of the earth. The comet's orbit must be rotated, about the dotted line in the figure as axis, through the angle i in such a direction as to tilt up from the page the portion of the orbit on the same side of the dotted line as i.

The data of the magnetic storms have been taken from Maunder's lists in the Monthly Notices of the Royal Astronomical Society, from the Journal of Atmospheric Electricity and Terrestrial Magnetism, the "Charactère Magnétique" and the records of the United States Coast and Geodetic Survey. In the descriptions of the comets given in paragraphs 5 to 35 the intensities of the magnetic storms are given by numbers in parenthesis, thus (1), (2), (3) and (4) mean a disturbance of moderate, strong, very strong and very, very strong intensity, respectively. In the lists of storms for the years after 1881, Maunder (Roy. Ast. Soc., Monthly Notices, *65*, 2(1904-5)) changed the system of assigning intensities; before 1882 no (4) storms appeared in his records, these being included in the category (3); after 1881 (4) storms were listed. Many storms were of several days duration with varying intensities on different days, but to avoid unnecessary complication we have given in most cases only the data of the beginning of the storm; in a few instances, however, the duration of the storm is indicated. In addition we shall be interested in the a and b angles. The a angle is the angle subtended at the sun on a particular date by the earth and the comet. The b angle is the angle subtended at the sun by the earth and the projection of the comet in the plane of the ecliptic, the sign of b being positive if the angle measured from the earth to the comet is in the direction of the sun's rotation. In illustration, June 4 to 6 (2), $35°a$, $-20°b$, means that on June 4 there began a magnetic storm of intensity (2) which lasted 3 days and that the a and b angles were 35° and $-20°$, respectively.

5. *Encke's comet 1848 II*, discovered August 27, 1848, early in November developed a spreading tail pointed at the sun; a tail pointed in the direction of the sun is an unusual feature. At this period the magnetic storms were July 11 (2), September 8 (1), October 18 (3), 23 (2), 25 (1), 27 (2), 29 (2), 30 (1), November 17 (3), 18 (2), 21 (2), $30°a$, 26 (1), December 17 (2). The month from October 18 to November 18 was the most active magnetic month in a period of four years. The abnormal tail is regarded as arising somehow from the unusual solar activity.

6. *Comet 1851 IV*, discovered October 22, visible 4 weeks,had a bristly tail pointing towards the sun. Storms September 3 (2), 4 (2), 6 (2), 7 (3), 27 (1), 29 (3), October 1 (2), 2 (3), 28 (2), $10°a$, November 11 (1), December 6 (3), the most active period since 1848. Another case of an abnormal tail and exceptional solar activity.

7. *Donati's comet 1858 VI*, discovered June 2 , visible 25 weeks. A very large comet which exhibited no very great changes. The nucleus at first was very bright; on September 20 two envelopes were visible, on September 30, one had gone. Seven successive envelopes rose up and disappeared the last one on October 20. Storms May 7 (1), June 22 (2), 23 (2), 24 (1), July 5

(1), August 25 (1), September 20 (1), 21 (1), 22 (1), October 17 (1), 27 (2). About all that can be said is that the comet was mildly active at a time when the sun was mildly active, with no clear connection between events on the comet and individual storms.

8. *Comet 1860 III*, discovered June 19, 1860, visible 8 weeks, exhibited complex changes in its tail. The period was one of great magnetic activity, the storms being, June 10 (1), 29 (2), 30 (2). July 1 (2), 4 (2), 5 (1), 11 (2), 19 (1), 20°*a* to 80°*a*, August 6 (2), 7 (2), 8 (2), 9 (2), 10 (3), 11 (2), 12 (3), 16 (1).

9. *Great comet 1861 II*, discovered May 13, visible 52 weeks, showed no prominent changes, although some envelopes appeared. Storms April 15 (1), August 18 (1), 19 (1), October 10 (2), 24 (1), November 7 (1), December 19 (2), a relatively quiet period. The comet passed perihelion on June 1, and in October was probably so far away that the October 10 storm had no effect upon it.

10. *Comet 1862 III*, discovered July 15, visible 13 weeks, exhibited an active tail all through August. The storms were, April 2 (1), 10 (1), July 5 (3), 7 (2), 120°*a*, 90°*b*, 23 (1), August 3 (2), 4 (3), 5 (2), September 24 (2). The discovery on July 15 may have resulted from an unusual brightening of tne comet caused by the strong solar disturbance of July 5 and 7; the comet activity in August coincides with the magnetic activity at that time.

11. *Winnecke's Comet 1871 V* was a faint nebulous object nearly round, when discovered on September 19, visible 11 weeks. Storm August 6 (2), 21 (1), 24 (3), September 7 (1), October 14 (1), November 2 (3), 9 (2), 10 (3), 19 (1), 10°*a*,–10°*b*, and no more storms this year. By the beginning of November the comet had acquired a remarkable fan-like form. A bright nucleus developed between November 5 and 8, which may be attributed to the solar activity in November; one has to go back six years to find equal solar activity.

12. *Tempel's comet 1873 II* was discovered July 3 after its perihelion passage on June 25; visible 15 weeks, a quiet comet. Storms May 15 (1), 23 (1), June 1 (1), 20 (1), 26 (2), 70°*a*, 60°*b*, 29 (1), July 9 (1), 12 (1), 16 (1), August 5 (1), September 20 (1), and no more storms this year. The discovery may have resulted from the disturbance of June 26. The subsequent normal behavior of the comet was in keeping with the small solar activity at the time.

13. *Coggia's comet 1874 III*, discovered April 17, visible 26 weeks, exhibited complex changes in the head beginning about June 22. Further changes took place during July, envelopes appeared, the nucleus varied in shape and brightness, two jets of light were seen, etc. Storms February 4 (3), 5 (1), March 7 (2), April 1 (2), 2 (2), 7 (2), 70°*a*,–70°*b*, 13 (1), 28 (1), May 26 (1), June 3 (1), September 29 (1), October 3 (3), 4 (2), 5 (1), 16 (1), and no more storms this year. The discovery followed 8 days after the strong April disturbances. June and July being a period of relative solar quiescence one must perhaps look to some other cause than unusual solar activity to

account for the changes in the head of the comet which occurred at this period.

14. *Comet 1877 II*, discovered April 5, visible 14 weeks, developed in June a tail pointing at the sun. Storms January 6 (1), May 2 (1), 11 (1), 28 (2), 120°*a*,–100°*b*, October 11 (1), and no more storms this year. The abnormal tail may have been due to the May solar activity.

15. *Swift's comet 1881 II*, discovered May 30, visible 2 weeks, had the longest tail on record. There were no changes observed in the comet and there were no storms at all from April 21 to September 11.

16. *Great Comet 1882 III*, discovered September 3, visible 39 weeks, was one of the largest comets known. Its orbit is given in Fig. 1. The comet was intact when it passed out of view behind the sun in the middle of September. When it emerged into view again on October 9 the nucleus was shattered into a number of bright pieces. The disruption of the nucleus became more apparent during the following weeks. Storms August 4 (2), September 12 (2), October 2 (4), 5 (2), November 11 (3), 16 (1), 17 (4), 21 (3), 25 (2), December 20 (2); a very active period. The storm of November 17 was the

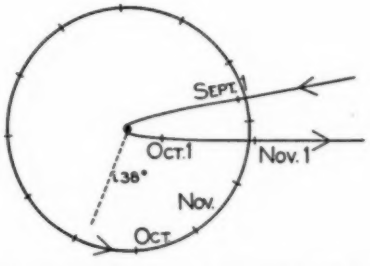

Fig. 1. Orbit of Great Comet 1882 III.

greatest ever recorded. We may suppose that during its close circuit around the sun the comet encountered the tremendous solar disturbance and was torn to pieces. The comet was a "sun grazer," it went very near to the sun, and it may be that the tidal action of solar gravitation was an important factor in causing the disruption. It is an unusual coincidence that the greatest comet on record should have met disaster at the hands of the greatest solar outburst on record. It seems hardly conceivable that the comet itself could have created the solar disturbance, for calculation showed that the tidal effect on the sun of the heaviest of comets assumed to approach within 1,000 km of the solar surface was vanishingly small.

17. *Pons-Brooks' comet 1884 I*, discovered September 2, visible 39 weeks, was an active comet, its changes being described as "rapid and lawless." About September 22 it increased very much in brilliancy; in February 1885 its head was nebulous and changed about March 2 to show a bright star-like nucleus. Storms 1883, August 18 (1), September 16 (3), 18 (2), 80°*a*, October 5 (3), 16 (2), 19 (1), November 1 (2), 19 (1), 22 (2), 1884, February 23 (2), 29 (3), 50°*a* March 28 (1). The brightening followed closely after the

strong September storms, and the change to the stellar nucleus after the strong February storms.

18. *Sawerthal's comet 1888 I*, discovered February 2, visible 24 weeks, exhibited a triple tail on March 27; it had only a single long tail on April 11 and experienced a sudden outburst of brilliancy on May 20. Storms January 13 (3), 23 (2), 60°*a*, 50°*b*, March 15 to 17 (1), April 11 (2), May 7 (1), 20 (2), 140°*a*, 130°*b*, June 3 (1), August 3 (1). The discovery followed 12 days aft the strong January storms and the triple tail was seen about 12 days afterthe long March storm. The remaining two comet events fell on the dates of strong solar activity.

19. *Brook's comet 1889 V*, discovered July 6, visible 19 weeks, changed little until August 1 when it threw off 4 fragments; after 3 weeks one fragment expanded and disappeared. There were no storms in April, May and June, on July 17 a (2) storm, 15°*a*, 15*b*, and August 13 (1), September 8 (1), 22 (1), October 5 (1), 18 (1), 20 (1). The disintegration of the comet was seen 14 days after the only large storm in the period.

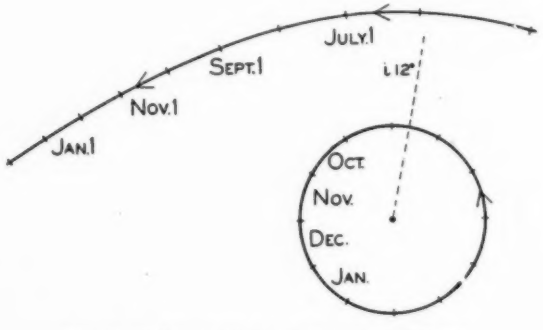

Fig. 2. Orbit of Holmes' Comet 1892 III.

20. *Swift's comet 1892 I*, discovered March 6, visible 32 weeks, brightened greatly after March 7. In the early part of April a new tail appeared, making 3 tails in all; the tails experienced a number of changes from April 5 to 10. On May 7, the nucleus divided and on May 15 material left the nucleus. Storms January 4 (3), February 13 (4), 15 (1), 20 (1), 27 (2), 29 (3), March 6 (3), 30°*a*, 30°*b*, 11 (4), 24 (1), April 25 (3), May 1 (3), 90°*a*, 90°*b*, 16 (1), 18 (4), 19 (1), June 2 (3), 27 (3). The discovery of March 6 and the brightening of March 7 followed 3 days after a group of strong storms. The April changes in the tails find no direct counterpart in the storms. The disintegration of the nucleus followed 4 days after very intense storms. The comet was far away at the time of the intense June storms.

21. *Holmes' comet 1892 III*, visible 12 weeks, was discovered November 6, five months after perihelion passage, June 13. In Fig. 2 are given the orbits of the comet and the earth. In November the comet was round and nebulous with no nucleus; on December 6 it changed to the elongated comet form, still with no nucleus. It then grew so faint and transparent that on January 4

it could hardly be seen. On account of bad weather Barnard[8] was unable to observe the comet from January 4 to January 16. When seen again on January 16 the comet had contracted in size and had a bright stellar nucleus. The comet then gradually expanded in diameter and faded out.

Storms 1892, May 1 (3), 16 (1), 18 (4), 19 (1), June 2 (3), 27 (3), July 12 (3), 16 (4), August 3 (1), 4 (1), 12 (4), September 5 (1), October 17 (2), November 4 (2), 20°*a*, 20°*b*, December 4 (2), 5 (1), 1893, January 5 (1), 21 (1), February 4 (2), March 14 (1). The discovery of the comet on November 6, undoubtedly due to an unusual brightening, followed 2 days after the (2) storm of November 4. We must suppose that the strong solar flares which caused storms from May to October did not strike the comet. The change in the comet on December 6 followed immediately after the solar activity of December 4 and 5. The brightening of the comet seen on January 16 may have been due to the January 5 flare which, to be sure, was not strong enough at the earth to cause more than a (1) storm, but which may have fallen upon the comet with greater intensity. At this time *a* was about 40°.

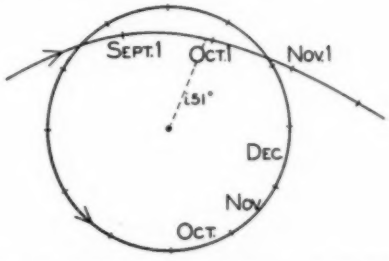

Fig. 3. Orbit of Brooks' Comet 1893 IV.

22. *Brooks' comet 1893 IV*, discovered October 17, visible 7 weeks, exhibited extraordinary changes in its tail. Barnard's series of pictures[3] of this comet are very beautiful and his discussion of the activity very illuminating.[3] The orbits of the earth and of the comet are given in Fig. 3. On October 17, 18, 19 and 20 the comet was normal with a fair sized tail. On October 21 "The tail was shattered. It was bent, distorted and deflected, while the larger part of it was broken up into knots and masses of nebulosity, the whole appearance giving the idea of a torch flickering and streaming irregularly in the wind.—If the comet's tail, in its flight through space, had suddenly encountered a resisting medium which had passed through the tail near the middle, we should have precisely the appearance presented by the comet.—What makes this explanation all the more probable is that the disturbance was produced from the side of the tail that was advancing through space."[9] During the latter part of October the tail of the comet became normal again and then on November 2 was observed to have experienced a violent change.[10] The tail was thrown forward (in the direction of its

[8] Barnard, Astrophys. J. **3**, 41 (1896).
[9] Barnard, Popular Astronomy **1**, 416 (1893).
[10] Barnard, Lick Observatory Pub. **11**, p. 32, plates 110 and 114 (1913).

motion) from its normal position; the end of the tail had a sharp bend. On November 3 the tail had partially returned to its normal form. Barnard gives no photographs of the comet on November 4 and 5. His photograph of the comet on November 6 shows the outer end of the tail to be broken and irregular. He says (Reference 10, plate 112), "Another disturbance seems to have occurred at this time, or shortly before. The entire tail does not seem to have been affected, or perhaps the disturbance itself had ended and the straight part of the tail had been newly formed in the mean time."

Storms 1893, April 26 (2), June 9 (1), 18 (2), July 15 (3), 21 (1), August 6 (2), 18 (2), September 8 (1), 26 (1), 29 (2), 160°*a*, 150°*b*, November 1 (3), 3 (1), December 5 (1) 1894, January 3 (3). The violent changes in the comet on October 21 need no further explanation here. Fortunately there is nothing in the magnetic storm list to indicate a solar outburst toward the comet around October 21. The conclusion seems clear that the comet change in this case was not due to the solar influence, and that Barnard's resisting medium theory of this change remains complete and compelling.

In the violent disturbance of November 2 the forward motion of the tail with the bend at the end was exactly the type of change which the unusual light pressure from a solar flare would be expected to produce. This change was clearly due to the intense solar activity of November 1. The changes in the tail observed on November 6 followed closely after the storm of November 3. It is interesting to quote again from Barnard. In the Astrophysical Journal, **24,** 258 (1906), he wrote, "Indeed, the more I see of comet photographs and of the changes they show in a comet's tail, the more I am convinced that the phenomena of the tail of Brooks' comet were unique, and that they were due to a disturbing influence foreign to the comet and the sun." We would only suggest that this remark apply to the change of October 21 and not to the other changes.

23. *Gale's comet 1894 II*, discovered April 1, visible 7 weeks, was not very active but was observed about May 1, to have developed a number of long slender tails. Storms March 21 (1), 30 (3), 20°*a*,–10°*b*, April 17 (3), 30°*a*, 10°*b*, June 9 (2). The discovery followed 2 days and the tail activity 13 days after intense solar disturbances.

24. *Swift's comet 1899 I*, discovered March 3, visible 21 weeks, experienced no important changes in March and April. After passing through perihelion on April 12 rather close to the sun it was found to have brightened considerably. On May 7 the nucleus was observed to be double; the tail exhibited twisting and other small variations. Material near the extremity of the tail was formed of matter which had left the nucleus on May 15. Storms 1899, January 28 (1), February 11 (3), 23 (1), March 21 (2), 23 (1), April 18 (1), May 1 (1), 3 (1), 15 (1), 20°*a*, 10°*b*, June 28 (2); a fairly active period. There seemed to be no strong storms with which to associate the splitting of the nucleus, although one can not be sure what solar influence may have been active on the comet during its close approach to the sun. The general tail activity in May and the departure of matter from the nucleus

on May 15 fall in with the moderate storms of May 1 and 3 and of May 15, respectively.

25. *Brooks-Borelly comet 1900 II*, discovered July 23, visible 10 weeks, experienced no unusual changes; minor variations occurred in the structure of the tail. There were no magnetic storms at all in the last half of 1900.

26. *Great comet 1901 I*, discovered April 12, visible 5 weeks, was seen on May 6 to have a long tail and two short ones at 20° to 40° from the main tail. The only storms in 1901 were March 13 (2), May 10 (2), September 10 (1). The comet peculiarity is not directly attributable to the known solar activity. The comet came in fairly well over and fairly close to the south pole of the sun and may have experienced some solar activity which did not reach the earth.

27. *Brooks' comet 1902 I*, discovered April 14, visible 6 weeks, had no nucleus and exhibited no changes. The only storms in 1902 were January 15 (1), April 10 (2), 160°*a*, 160°*b*, August 21 (2). The discovery followed 4 days after the strong April disturbance, and the lack of comet activity thereafter was in keeping with the lack of solar activity.

28. *Borelly's comet 1903 IV*, discovered June 11, visible 19 weeks, exhibited a tail of complex structure which underwent various minor changes from June 22 to August 18. About July 24 a portion of the tail was rejected, as if the tail-forming emission from the nucleus had suddenly shifted slightly to one side. Storms April 5 (1), June 29 (1), 90°*a*, August 21 (1), September 19 (1), October 12 (2). The comet variations find no direct counterpart in the solar activity. In August, however, the comet was well over the north pole of the sun and may have received some solar influence not felt by the earth. Barnard[11] has suggested that the agitation of July 24 might have been caused by a meteor plunging into the nucleus.

29. *Kopff's comet 1905 IV*, was discovered with the telescope on March 3, 1906, 15°*a*, 15°*b*. On looking back it was found on the photographic plates of January 10, 1904, 35°*a*–35°*b*, and January 14, 1905, 5°*a*,–5°*b*. On these three dates the distance of the comet from the earth was about 3, 6 and 3 astronomical units, respectively. Storms 1903, December 13 (3), 30 (1), 1904, January 28 (1), April 1 (1), April 17 (1), June 15 (2), July 6 (1), August 3 (1), September 24 (1), October 21 (2), 1905, January 5 (2), February 3 (3). The discovery on January 10, 1904, may possibly have been due to a brightening of the comet caused by the solar activity of December 13; the connection, however, is uncertain. The discoveries of January 14 and March 3, followed 12 and 7 days, respectively, after strong solar outbursts.

30. *Morehouse's comet 1908 III*, discovered September 1, visible 26 weeks, experienced three very striking and pronounced outbursts[12] which began on, or a short time before, the dates September 29, October 14 and November 14. The orbits of the comet and the earth are given in Fig. 4. Storms August 11 (1), 21 (1), September 5 (1), 11 (4), 29 (4), 50°*a*, 0°*b*,

[11] Barnard, Astrophys. J. **18**, 210 (1903).

[12] Barnard, Astrophys. J. **28**, 292 and 384 (1908); **29**, 65 (1909).

October 12 (2), 60°a,–20°b, November 8 (2), December 4 (4), 140°a,–130°b. The three violent changes in the comet occurred 0, 2 and 6 days after intense solar disturbances. Apparently the solar flare of September 11 did not touch the comet. It is scarcely necessary to emphasize the agreement between the magnetic storms and the comet activity in this case. The facts of this comet alone would perhaps be sufficient to justify the present theory.

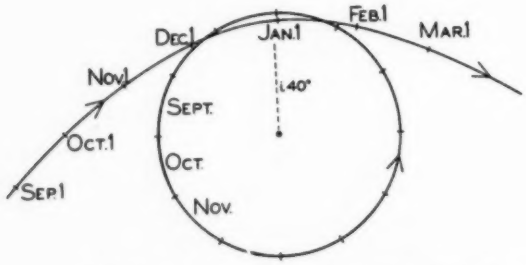

Fig. 4. Orbit of Morehouse's Comet 1908 III.

31. *Halley's comet 1910 II*, visible August 1909 to July 1911, was a disappointment to us. There were a number of strong solar outbursts well spaced, and the comet underwent many small variations and some fairly pronounced ones. There seemed, however, to be no clear connection between the solar and comet activities. We must leave it to the astronomer to overhaul the vast literature bearing on this comet's latest apparition.

32. *Brooks' comet 1911 V*, discovered February 27, visible about 30 weeks, increased in brightness about the middle of October and developed

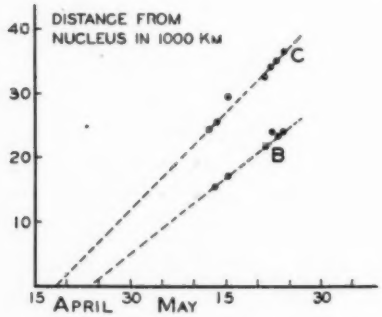

Fig. 5. Movement of fragments *B* and *C* of Mellish's Comet 1915 II.

a wealth of structure in the tail at this time. Storms May 14 (1), October 10 (3), 80°a, 80°b, December 11 (1). The activity of the comet followed shortly after the October 10 disturbance.

33. *Mellish's comet 1915 II*, discovered February 10, visible some 70 weeks, exhibited many changes in form and structure, none of which were of outstanding violence. There were many storms during this period, some fairly intense. In general the active periods of the comet fell in with the more intense storms. The splitting of the nucleus, observed in May, offered

data for the following calculation. Storms April 1 (1), 7 (1), 15 (2), 70°*a*, 20°*b*, 25(1), 30 (1), May 14 (1), 19 (1), 26 (1), 30 (1). Two fragments *C* and *B*, *C* brighter and farther from the nucleus than *B*, were found to be moving away from the nucleus with velocities which were approximately constant. The distances of the fragments from the nucleus were measured[13] from May 12 to May 24. The values are plotted in Fig. 5 as ordinates against the times as abscissas. The points where the lines of the figure intersect the time axis give the dates on which the fragments actually left the nucleus. The dates are April 18 and 24 for *C* and *B*, respectively, which are fairly close to the strong storm of April 15.

34. *Taylor's comet 1916 I*, discovered November 24, visible 26 weeks, was observed on February 9, 1917, to have a double nucleus. Storms 1916 September 29 (2), October 5 (2), 19 (2), November 2 (2), 11 (2), 25 (2), 20°*a*, 20°*b*, December 11 (1), 14 (1), 26 (1), 1917 January 4 (1), 7 (1), 9(1), 21 (1), 30°*a*, February 6 (1), 14 (1). The discovery occurred during a period of intense solar activity. It is not certain whether the moderate activity of January and February had anything to do with the breaking up of the nucleus.

35. *Skjellerup's comet 1927 k*, discovered December 2, was a brilliant comet visible in the day. On December 20 it was observed to have a tail towards the sun. Storms November 17 (1), December 5 (1), 13 (1), 14 (1), 15 (1), 16 (1), 17 (1), 18 (1), 30°*a*, 5°*b*. The abnormal tail occurred after solar activity which, although of moderate intensity, continued for an unusual length of time.

36. *Some statistics*. A general correlation of magnetic and comet activity may be made as follows: The total numbers of magnetic storms of intensities 1, 2, 3 and 4 were 952, 439, 135 and 24, respectively, for the 78 years from 1848 to 1926. Of the 31 comets considered here all but three were more or less active. The 30 day periods preceding the activities of each comet were added together and gave a total of 3 years for the 28 active comets. In this three years there were 55, 49, 20 and 6 magnetic storms of intensities 1, 2, 3 and 4, respectively; whereas according to chance there should have been 3/78 of 952, 439, 135 and 24, or 37, 17, 5 and 1, respectively. In other words, during the active periods of the comets, totalling 3 years out of 78, there occurred 1.5, 2.9, 4 and 6 times as many storms of intensities 1, 2, 3 and 4, respectively, as there would have occurred if the periods had been selected at random among the 78 years. This result and the facts brought out in the detailed discussion of the 31 comets are regarded as substantiating the hypothesis that an unusual change in a comet was caused in a majority of cases by an unusual flare or emission from the sun, the same emission, if it strikes the earth, giving rise to a magnetic storm and possibly an auroral display.

37. *Characteristics of the solar flare*. One would naturally suppose the solar outburst to be a flare of wide angle, or of an angle which may be wide, narrow, irregular, etc., but Maunder,[14] in order to explain the tendency for

[13] Helwan Observatory Bull. **1**, 145 (1911–1922).

[14] Maunder, Monthly Notices, Roy. Ast. Soc. **65**, 19 (1904); **76**, 68 (1915); Astrophys. J. **21**, 101 (1905).

the recurrence of magnetic storms approximately with the period of a solar rotation, made the hypothesis that the emission was in a narrow beam. The facts of the comets however, support the wide flare idea. To show this we turn to the 28 comet events of sections 5 to 35, such as brightening, change in tail, etc., which were associated with terrestrial magnetic storms. The data of these events are plotted as dots in Fig. 6; the abscissas are the b angles (defined in section 4) and the ordinates are the number of days between the terrestrial magnetic storm and the observation of the comet event. Taking the direction of rotation of the sun on its axis to be positive, negative and positive b angles mean that the comet was behind and ahead of the earth, respectively. Positive and negative values of the days mean that the comet event occurred after and before the storm, respectively.

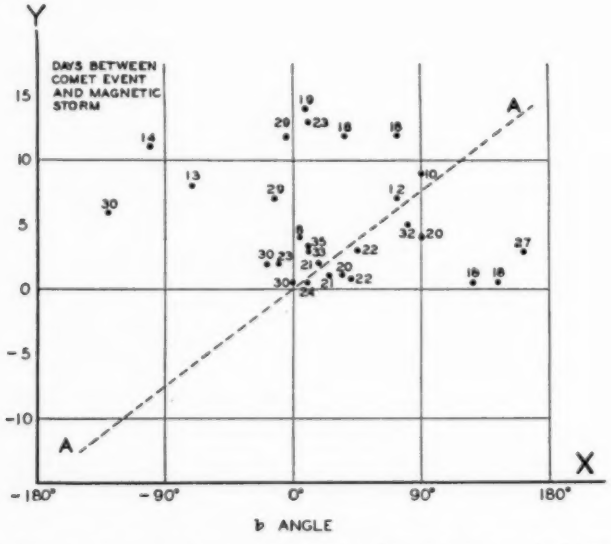

Fig. 6. Data of 28 comet events. Abscissas, the b angles; ordinates, the time interval in days from the magnetic storm to the comet event.

The number along side of each dot of Fig. 6 is the number of the paragraph in which the data of the comet event are given. If the solar flare is in a wide angle, the time interval between the date of the storm and the comet event should be independent of the relative positions of the comet and the earth, and the dots of Fig. 6 should fall on a straight line parallel to the X axis. It is seen that they do this very roughly. The grouping of the dots into the region of small values of the b angles is to be expected on the wide flare theory, for the probability that a flare strike a comet and the comet be observed falls off with increasing b angle. Accurately, for the discussion of the grouping one should use a plot similar to Fig. 6, but with the a angles instead of the b angles as abscissas; such a plot, however, does not differ materially from Fig. 6. The fact that there are more points with positive than with negative b angles is in keeping with the facts that the comet

velocities were greater than the velocity of the earth, that there were about twice as many direct moving comets as retrograde, and that the comets usually experienced their events after getting near to the sun.

If the solar emission is in a narrow beam which rotates with the sun as in Maunder's theory[14] the chance that the same beam strike both the comet and the earth would be expected to be low, for many comets were not in the plane of the ecliptic. Therefore a direct association of comet events with magnetic storms, as has been brought out here, is incompatible with the narrow beam hypothesis. If, however, for the sake of argument we imagine the beam to be a thin sheet, as would be formed by two planes through meridians of longitude at an angle of, say 4° with each other, then the time between the occurrence of the terrestrial storm and the comet event will be proportional to the b angle. The dots of Fig. 6 should in this case fall along a line parallel to the line AA, which passes through the points (0°, 0 days) and (180°, 14 days), taking the solar rotation period to be 28 days. The dots clearly do not do this. It is concluded that the evidence offered by the comet data is in favor of the wide angle flare hypothesis and against the narrow beam hypothesis. This conclusion leaves the recurrence tendency of magnetic storms without an explanation. To account for the recurrence tendency one might suggest that the flare bursts out approximately with the solar rotation period. Such a geyser action might possibly be due to tides on the sun caused by the planets, although calculation using standard formulas neglecting resonance indicates that such tides are very small, less than 1 cm, or to pulsations of some sort arising from deep seated actions in the sun.

Earlier theories of the aurora[15] have been based on the hypothesis that the emission from the solar outburst which caused the aurora was corpuscular, as ions, electrons, neutral particles, etc. It was suggested[16] that the corpuscular emission required a day and a half or more to travel from the sun to the earth, a distance of 1 astronomcial unit. The recent theory[2] regarded the emission to be ultra-violet light; the behavior of wireless waves[17] during a magnetic storm was found to support the ultra-violet light hypothesis. One might expect to obtain evidence about the nature of the solar emission from the time interval between the magnetic storm and the comet event. The evidence from the comet data of this paper is, however, mainly noncommital. The average ordinate of the points of Fig. 6 is 5 days, which means that the comet event followed the magnetic storm by 5 days on the average. This delay is not regarded as indicating that 5 days were required for the solar emission to travel to the comet, but rather as representing approximately the average time required for the comet to change sufficiently to be perceptible to an observer on the earth.

[15] Gehrke, Handbuch d. Phys. Optik **11**, 178 (1927).

[16] See references given by Greaves and Newton, Monthly, Notices, Roy. Ast. Soc. **89**, 84 (1928).

[17] Maris and Hulburt, Proc. Inst. Rad. Eng., **17**, 494 (1929).

[18] Hazard, Records of the Magnetic Observatory, Cheltenham, Maryland, U. S. A., (1911).

Light travels 1 astronomical unit in 8 minutes. The ultra-violet light theory of magnetic storms indicated that the storm commences immediately possibly within seconds or minutes, after the light falls upon the terrestrial atmosphere. The change in the comet caused by the light might or might not occur immediately, and might or might not be immediately perceptible to a terrestrial observer. To get accurately the time interval between the beginning of the storm and the observed change in the comet, the comet and the earth should be at distances from the sun as widely different as possible, the commencement of the magnetic storm should be sharp and definite, and the change in the comet should be pronounced and well observed. These requirements are not satisfactorily fulfilled in any of the cases which we have examined. Perhaps the best case was that of the change in Morehouse's comet (section 30) on September 29, 1908. On this date the comet was about 1.7 and 0.9 astronomcial units from the sun and the earth respectively. Barnard's pictures[12] of September 21 to 26 showed that the comet was fairly inactive. On account of bad weather he obtained no pictures on September 27 and 28. His photograph on September 29 at 10 hr. 45 min., P. M., Central Standard time (U.S.A.) taken with an exposure of 2 hr. 30 min. "shows a disturbed condition of the comet which possibly was the forerunner of the great change that followed in the next two days." The magnetograph record[18] showed a slight disturbance beginning on September 28 at about 8 hr. 40 min., Greenwich Mean Civil Time, which died out pretty well after a few hours, and an intense disturbance beginning sharply on September 29 at 1 hr. 30 min., G. M. C. T. Taking this latter storm to be the one which influenced the comet, we see that the comet change had already set in 27 hours after the beginning of the storm. Since the September 29 photograph was obtained with an exposure of 2.5 hours, the change in the comet was slow and probably had begun many hours before, and therefore the time interval was probably much less than 27 hours. This result is regarded as being more in keeping with the 13 min. (1.6 astronomical units) required by light than with the longer time required by material corpuscles. Possibly astonomers may be able to come upon better data for the calculation.

In conclusion it is a pleasure to express our thanks to Dr. E. B. Frost of the Yerkes Observatory for sending us a very fine series of reprints of publications of Professor Barnard.

NAVAL RESEARCH LABORATORY,
WASHINGTON, D. C.
February 6, 1929.

SOUND RADIATION FROM A SYSTEM OF VIBRATING CIRCULAR DIAPHRAGMS

By Irving Wolff and Louis Malter

Abstract

From the expression for the velocity potential due to a point source radiating into a semi-infinite medium Lord Rayleigh has determined the sound radiation from a vibrating circular diaphragm in an infinite wall. With the same method, the radiation due to any shaped diaphragm or combinations of diaphragms can be determined. Curves are given for circular diaphragms which show the distribution of pressure over the surface bounding the semi-infinite medium. These curves enable the determination of the radiation from any combination of vibrating circular diaphragms placed in the surface. Calculations have been carried out for a number of special cases. At low frequencies the diaphragms react upon each other to increase the efficiency of radiation. This effect vanishes at high frequencies. The mutual aid of the diaphragms decreases very rapidly as the distance between the diaphragms is decreased. In certain cases the combination may result in decreased efficiency over particular frequency ranges. These results are all explainable on the basis of phase differences between motion of a diaphragm and the pressure over the surface of another diaphragm due to the motion of the first.

THE sound energy radiated by a vibrating diaphragm can be determined if its velocity of motion and the pressure over its surface are known. The pressure on the surface depends on the shape of the space into which the sound is radiated and the pressure caused by other vibrating diaphragms or sound sources in the neighborhood of the first one. In considering the radiation from a number of diaphragms placed near each other, the effect of each diaphragm on the others must therefore be taken into account in getting the radiation from the combination.

In this study we shall consider in particular the sound radiation from a number of vibrating circular diaphragms moving in phase and set in an infinite plane wall.

General Theory

The pressure due to a very small source vibrating with S. H. M. and radiating into a semi-infinite medium (a medium bounded by an infinite plane surface in which the source is set) is given by

$$P=\frac{i\rho\omega V_0 e^{i\omega t}e^{-i\omega r/c}}{2\pi r}dS$$

where $\omega=2\pi f$; ρ = density of medium; $V_0e^{i\omega t}$ = velocity of source; dS = area of source; r = distance from source; c = velocity of sound in medium; λ = wave-length of emitted radiation.

The pressure at any point due to a plane surface moving with the velocity $V_0e^{i\omega t}$ is therefore given by:

$$P=\frac{i\rho\omega V_0 e^{i\omega t}}{2\pi}\int\int \frac{e^{-i\omega r/c}}{r}dS$$

where the integral is taken over the vibrating surface.

The pressure at any point on an infinite plane surface moving with velocity $V_0e^{i\omega t}$ is $\rho CV_0e^{i\omega t}$ and could be obtained by carrying out the integration indicated in Eq. (2) between the limits for $r=0$ and $r=\infty$ and for angles from 0 to 2π. The pressure $\rho CV_0e^{i\omega t}$ may be thought of as a pressure which is contributed by all points on the vibrating surface and which aids the radiation from any particular section of the surface by making it move into a more resistant medium. It will be noted that the pressure on the infinite surface is independent of the frequency showing that the radiation from the infinite surface moving with the same velocity at all frequencies is independent of the frequency. In making radiation calculations it is found very convenient to compare the pressure in phase with the velocity at any point on a vibrating surface with the pressure on an infinite surface moving with the same velocity. We shall call the ratio of the pressure to the pressure due to an infinite surface the acoustic-aid coefficient of a vibrating surface at a point. Expressed this way from Eq. (2) the acoustic-aid coefficient at any point due to a vibrating surface is

$$\frac{i\omega}{2\pi c}\int\int \frac{e^{-i\omega r/c}}{r}dS$$

the integral being taken over the surface.

For an infinite surface this coefficient is of course unity. The average radiation per unit area from any surface compared to the radiation per unit area from an infinite surface moving with the same velocity can be obtained by averaging the aid-coefficient over the surface. This will be called the radiation coefficient of the surface. For an infinite surface the coefficient is unity.

Radiation from a Single Diaphragm

The expression for the radiation from a single vibrating circular diaphragm set in an infinite wall has been obtained by Lord Rayleigh. The radiation coefficient is

$$\left[1-\frac{J_1(4\pi R/\lambda)}{2\pi R/\lambda}\right]$$

and shown in Fig. 1.

It will be noted that at low values of R/λ the coefficient is proportional to the square of R/λ. For large values of R/λ the coefficient oscillates about unity with decreasing amplitude. This is what might be expected since for these values the finite diaphragm approaches the case of an infinite diaphragm.

Radiation from a Combination of Diaphragms

In order to determine the radiation from any surface with other vibrating surfaces in the neighborhood, it is only necessary to know the radiation coef-

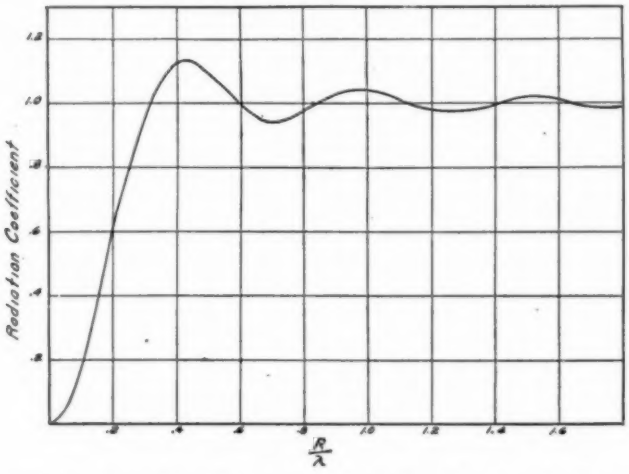

Fig. 1. Acoustic radiation coefficient of a vibrating circular diaphragm. (Set in an infinite wall).

ficient, of the surface in question and the average aid-coefficient over the surface contributed by the other vibrating surfaces. The curve given in Fig. 1 in combination with the set of curves in Fig. 2 permits this calculation

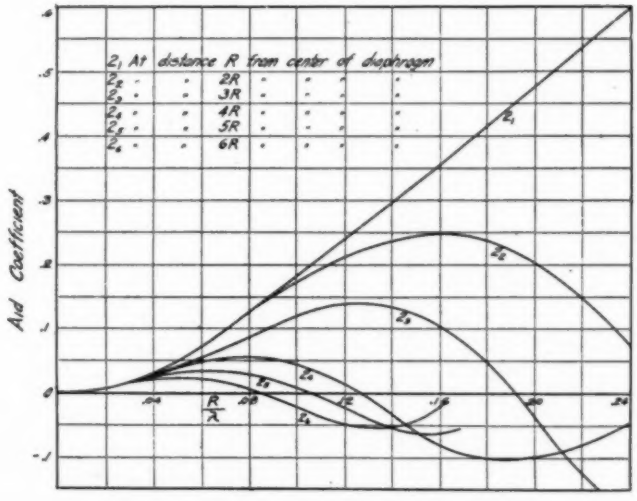

Fig. 2. Acoustic aid coefficient of a vibrating circular diaphragm. (Set in an infinite wall).

to be easily made for any combination of vibrating circular diaphragms moving in phase and set in a large wall.

The curves in Fig. 2 show the aid coefficients at a number of points at specified distances from the center of a circular diaphragm. In order to make the calculations general the curves are plotted for a series of distances expressed in terms of R, the radius of the disk, and R/λ. The integration was carried out by the method of quadrature.

Examination of this set of curves shows that the aid extends equally to comparatively large distances for small values of R/λ. As R/λ increases the aid for the larger distances becomes comparatively less than for the smaller distances, eventually even decreasing and becoming negative. The negative value means that the point is far enough away so that the aid-pressure has a component in opposite phase to the motion at the point (which motion is assumed to be in phase with the diaphragm which is contributing the aid).

Application to Problems

The problem before us is to determine the increase of efficiency of a single diaphragm due to the action of other diaphragms upon it. In order to show the manner in which the curves can be used in a simple case it will be assumed that the diaphragms are alike and that each is being fed with the same amount of energy.

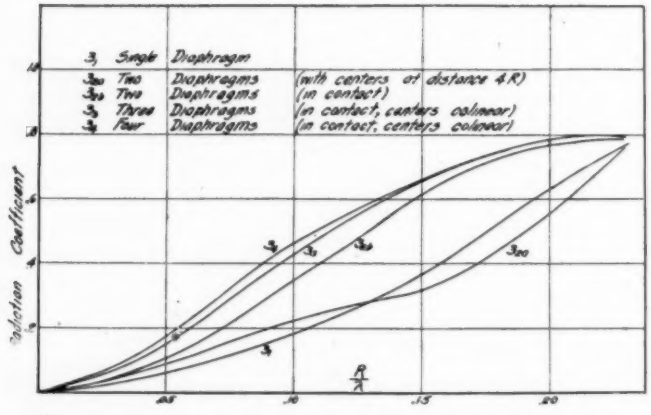

Fig. 3. Acoustic radiation coefficient of circular diaphragm combinations. (Set in an infinite wall).

In order to make the example concrete we shall first take the case in which two diaphragms are set in an infinite wall with their centers 4 R apart. Fig. 1. gives the radiation coefficient of a single diaphragm. At a frequency such that $R/\lambda = 0.05$ the radiation coefficient of a single diaphragm turns out to be 0.05. Since the two diaphragms have their centers 4 R apart, the one diaphragm extends from a distance of 3 R to 5 R from the center of the other diaphragm. A sufficient approximation is obtained by taking the aid-coefficients at $3R$, $4R$, $5R$ and averaging them. On curves Z_3, Z_4 and Z_5 we find respectively for the aid coefficients at $R/\lambda = 0.05$, 0.043, 0.035, and 0.028 averaging 0.035. At this value of R/λ the radiation coefficient of the

diaphragm is therefore increased from 0.05 to 0.085 by the presence of the other at a distance $4R$ from it.

By repeating this process for a series of values of R/λ a curve determining the radiation coefficient of the diaphragm in the presence of the other is determined. If more than two diaphragms had been present it would have been necessary to add the aid-coefficients due to each one of them in the same manner, the final aid being the sum of the aids due to all the diaphragms.

In a combination in which the radiation coefficients for the individual members do not turn out to be the same (such as three diaphragms in line) the radiation coefficient of the combination is expressed as the average of the separate radiation coefficients.

Fig. 3 shows the radiation coefficients of a number of diaphragm combinations. In order to show the effect a little more clearly the ratio of these coefficients to the coefficient of a single diaphragm is shown in Fig. 4.

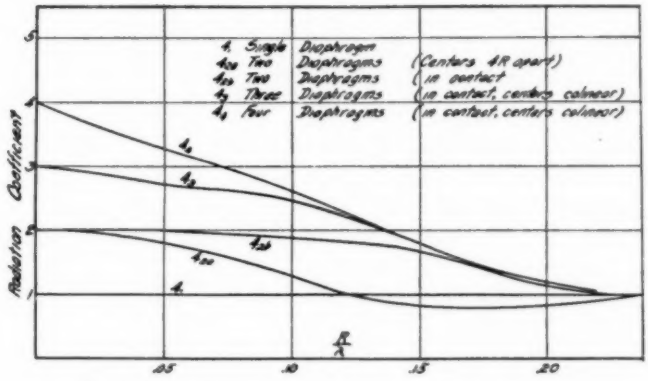

Fig. 4. Relative radiation from circular diaphragm combination. (Set in an infinite wall).

An examination of these curves leads to some interesting conclusions. At very low values of R/λ increasing the number of diaphragms increases the radiation coefficient in almost the same ratio. At somewhat higher values of R/λ the increase is rapid for the first diaphragms added but does not change very much as the number of diaphragms is further increased. At still higher values of R/λ the extra diaphragms have no effect upon the radiation coefficient. The diaphragms help each other most when very close to each other. The extension to diaphragms of different sizes or moving with different velocities and not in phase follows without much difficulty and will not be elaborated upon here.

RADIO CORPORATION OF AMERICA,
NEW YORK CITY,
January 15, 1929.

BOOK REVIEWS

Strukturbestimmung mit Röntgeninterferenzen. H. OTT. **Gitter-Theorie der festen Körper.** K. F. HERZFELD. Bd. VII. 2 Teil. Wien-Harms Handbuch der Experimentalphysik. xii+433 pp. 196 figs. Akademische Verlagsges. m.b.H., Leipzig, 1928. Price, unbd. RM. 37, bd. RM. 39.

The monograph by Ott (322 pp., 187 figs.) deals with the physical part of structure analysis by x-ray methods for which the mathematical basis was laid by Niggli in the preceding section of this volume. There are some differences in the symbols used, the notation of Ott being the more cumbersome. There are now so many German treatises on this subject that comparisons become interesting. The present example excels in two particulars: in the treatment of the intensity factors, and in the number of experimental hints for the conduct of the various types of analysis. This is the only place known to the reviewer where the "kinematic" and "dynamic" theories of crystal diffraction are clearly contrasted, and where the useful operation of rolling a thin paper tube in which to pack a powder is carefully described. The systematic way in which the several possible experimental methods are reviewed is especially to be commended. The treatment of interference from liquids and other more or less amorphous materials is, although brief, refreshingly better than the usual vague generalities. A few errata deserve correction: p. 35, 3rd line from bottom 1-cos χ should be 2(1-cos χ); p. 50, eq. 40a $(1+\cos^2\theta)$ should be $(1+\cos^2 2\theta)$; p. 117 ($h=4n$, *bzw.* $4n\pm1$) should be ($\Sigma h=$etc.); p. 121, Tabelle 7 last entry $1, 32\cdot10^{-6}\pm0, 4$ should be $13, 2\cdot10^{-6}\pm0.4$; p. 225, Tabelle 14 entry for $\Sigma h^2=38$ should include $235(z=24)$, entry for $\Sigma h^2=46$ has two redundant values of z; p. 307 near middle θ should be $90°-\theta$; p. 310 §4, l. 8 "erste" should be "siebente."

The monograph by Herzfeld (98 pp., 9 figs.) is a review, as far as possible from a single view-point, of the diverse and practically independent studies which have been made in this debatable ground. The subject has suffered thus far from the circumstances that few students having enough chemical and crystallographical foundation to build upon have had enough mathematics to build with. The work under discussion here reflects this unsatisfactory state of affairs. After a good start at the general lattice theory in the static case, followed by a well-reasoned treatment of oscillations—both "optical" and "acoustical"—and of the complications necessary to explain temperature effects, the text disintegrates into a series of paragraphs recording the successes and failures of special assumptions in particular cases. The author has been well-advised to take a non-partisan stand in reporting these skirmishes, and is modest enough to admit (p. 418) that a gratifying agreement between calculations and observations by Herzfeld and Wolf may be accidental. The reviewer is sorry to note that the lattice-theory of ferromagnetic crystals, developed in a considerable series of papers, principally from Scotland and Japan, has been omitted *in toto*. Except for this the bibliography appears to be reasonably complete. There are a few misprints of no great importance and some terms that have been invented without much regard for standard usage, e.g. "kubisch zentrischer Diagonalgitter."

Paper and printing are good, as is usual in books from this press. The binding could not be duplicated in this country for twice what is charged.

L. W. MCKEEHAN

PROCEEDINGS

OF THE

AMERICAN PHYSICAL SOCIETY

MINUTES OF THE WASHINGTON MEETING, APRIL 18–20, 1929

The 157th regular meeting of the American Physical Society was held in Washington, D. C., on Thursday, Friday and Saturday, April 18–20, 1929. The Thursday and Friday sessions were held at the Bureau of Standards in the East Building and the Industrial Building. The Saturday sessions were held at the National Academy of Sciences. The presiding officers were Professor H. G. Gale, President of the Society, and Dr. W. F. G. Swann, Vice-President of the Society. Friday morning was devoted to a Symposium on Dielectrics. The papers for the Symposium were invited and the titles appear with the following abstracts, numbers 47 to 54, inclusive.

On Friday evening there was a dinner for the members of the Society and their friends at the Cosmos Club. President Gale presided and the speakers were the guests of honor, Professors F. Hund, W. Heisenberg, L. S. Ornstein and A. Sommerfeld. Music was furnished by Professor Sommerfeld, Professor Heisenberg and Dr. Swann.

At the regular meeting of the Council held on Friday, April 19, 1929, one was elected to fellowship, two were transferred from membership to fellowship and twenty-eight were elected to membership. *Elected to Fellowship:* Addams S. McAllister. *Transferred from Membership to Fellowship:* Carleton C. Murdock and J. R. Oppenheimer. *Elected to Membership:* Walter E. Albertson, Thomas Alty, Arthur H. Barnes, Ralph W. Barnes, Julius V. C. Bucher, J. D. Cockcroft, Mabelle C. Dame, N. A. de Bruyne, J. B. Derieux, A. A. Dixon, J. B. Edwards, Lawrence Y. Faust, F. E. Fowle, Bernhard Frey, Robert C. Garth, Samuel D. Gehman, Walter A. Greig, Harvey Hall, Albert G. Ingalls, Montgomery H. Johnson, Jr., Ben Kievit, Jr., Gerald Kruger, S. E. Rodgers, Albert E. Shaw, A. Melvin Skellett, Szczepan E. Szczeniowski, J. Chester Swanson, Morgan Williams.

The regular program of the American Physical Society consisted of 135 papers, numbers 6, 10, 17, 18, 33, 38, 39, 40, 44, 45, 46, 68, 85, 89, 90, 98, 99, 105, 107, 108, 112, 114, 117, 126, 129, 130, 131, 132 133 and 135 being read by title. The abstracts of the papers are given in the following pages. An **Author Index** will be found at the end.

W. L. SEVERINGHAUS, *Secretary*

ABSTRACTS

1. Electron scattering in hydrogen. G. P. HARNWELL, *Princeton University.*—With an apparatus which has been previously described (Phys. Rev. **31**, 634 (1928)) an analysis has been made of the scattering of electrons in hydrogen. The electrons used had energies of from

40 to 200 equivalent volts. The angular distribution of the scattered electrons varied but little throughout this range. The only tendency noticeable was that the curves in which the number of elastically scattered electrons was plotted against the scattering angle dropped more sharply for the electrons with higher velocities. An attempt has been made to compare the observed distribution curves with those which would be expected on the assumption of different laws of force for the scattering centers. The results show that the scattering is very much greater than can be accounted for by an inverse square law or a law based on either Hartree's or Thomas' atomic field theories. No direct wave-mechanical calculations have been made for the scattering of electrons by molecular hydrogen, but the calculations have been carried through in detail for the scattering by atomic hydrogen. These calculations are the only ones which approach the experimental results in order of magnitude. The experimental points obtained in molecular hydrogen lie quite well on the calculated curve for atomic hydrogen.

2. On the theory of electron scattering in gases. ALLAN C. G. MITCHELL, *Bartol Research Foundation of the Franklin Institute.*—The scattering of electrons in gases is here treated by the Born wave-mechanical method, using however for the potential energy of the electron in the field of the atom, an energy calculated on the basis of the Fermi statistical theory of atomic fields the first approximation wave equation, in spherical coordinates r, θ, ϕ, is

$$\nabla^2\psi_1+k^2\psi_1=k^2(V/E)\psi_0; \qquad k=8\pi^2mE/h^2$$

where $\psi_0=e^{ikz}$ and $x=r\cos\theta$, the equation for the oncoming electron wave, and ψ_1 is the wave function for the scattered wave. From the statistical potential theory we take $V(r)=-(Ze^2/r)\Phi(r/\mu)$. The solution of the wave equation is

$$\psi_1=\frac{k}{2E}\,\frac{Ze^2}{\sin(\Theta/2)}\,\frac{e^{ikr}}{v}\int_0^\infty \Phi\left(\frac{\rho}{\mu}\right)\sin\left(2k\rho\,\sin\frac{\Theta}{2}\right)d\rho.$$

The ratio of the number of particles scattered through an angle Θ to the number falling on the atom is

$$P=\left|\frac{\psi_1}{\psi_0}\right|^2=\left[\frac{k}{2E}\,\frac{Ze^2}{r}\right]\frac{1}{\sin^2(\Theta/2)}\left[\int_0^\infty \Phi\left(\frac{\rho}{\mu}\right)\sin\left(2k\rho\,\sin\frac{\Theta}{2}\right)d\rho\right]^2.$$

For $\Theta=0$ the number, of particles scattered is finite. The number of particles scattered is a maximum for $\Theta=0$ and a minimum for $\Theta=\pi$. The results are in qualitative agreement with a modification of Born's method proposed by Sommerfeld and with experiment.

3. A new method of recording electrons. PERCY H. CARR, *Cornell University.* (*Introduced by F. K. Richtmyer.*)—When electrons even at relatively low velocities impinge upon the surface of some metals, the properties of the metal surface are changed so that some vapors react toward the bombarded portion in a different manner than toward the unbombarded portion. Use is made of this fact to record the electron "lines" in a magnetic spectrograph. For instance, a gold plate after exposure in the spectrograph is held over hot mercury. Generally, the mercury vapor amalgamates the gold more readily on the unbombarded portions, and the exposed "lines" appear dark against a gray background. Metal plates when "developed" in the proper vapor are the equal of photographic plates for this purpose when the speed of the electrons is about 30 equivalent volts. For slower speeds the metals are much superior, and definite traces have been recorded below 15 volts. The metals used are gold, silver, copper, and zinc.

4. The diffraction of electrons by a copper crystal. H. E. FARNSWORTH, *Brown University.*—A sharply defined beam of electrons is directed normally against the {100} face of a copper crystal. The apparatus is so arranged that the total secondary electron current may be measured under the same conditions as the angular distribution, for bombarding potentials as low as 1 volt. Electron beams are found to issue from the crystal in the low voltage region at the bombarding potentials for which maxima occur in the total secondary electron curve. Electron beams which are the x-ray analogues, and which require a refractive index greater than unity, have been found in the region below 150 volts. In addition, other sets of beams are found

which may be accounted for by assuming a wave-length for the electron which is one-half that given by the formula $\lambda = h/mv$. These beams also require a refractive index greater than unity. The sets of low voltage beams, with one exception, are of this latter type. This exceptional set, which occurs at about 3 volts, is not accurately reproducible.

5. The absorption coefficient of slow electrons in alkali vapors. ROBERT B. BRODE, *University of California.*—The absorption coefficient (α) or the reciprocal of the mean free path of electrons has been measured in the vapors of Na, K, Rb, and Cs. The apparatus used was a modified form of the type originally described by Ramsauer. The velocity of the electrons was varied between 0.5 volts and 400 volts. The shapes of the absorption curves for the 4 vapors were nearly the same except in magnitude. From 400 volts down to about 4 volts the curves were approximately hyperbolic, fitting the equation $\alpha = K/(\text{volts})^{1/2}$ where K has the values 1350, 1850, 2060, 2600 for Na, K, Rb and Cs respectively. α is expressed in cm^2/cm^3 for a pressure of 1 mm of Hg at 0°C. Below 4 volts the curves rise to maximums between 2 and 3 volts and then decrease to minimums at less than a volt. A further increase is then observed for lower velocities although the measurements are there not in close agreement. The size of the atoms as compared with the electron probability distribution is in good agreement. Except for the maximums at low velocities the shape of the curves is in agreement with the shape predicted by the wave mechanics for hydrogen atoms.

6. Refocussing of electron paths in a radial electrostatic field. A. L. HUGHES, V. ROJANSKY, AND J. H. MCMILLEN, *Washington University, St. Louis.*—If a beam of electrons of identical velocities enters a uniform magnetic field through a narrow slit in a partition bounding the field, the electrons describe circular paths. It is well known that if the entering electrons make but small angles with the normal to the partition a refocussing of the paths occurs after the path of the normally entering electrons has turned through 180°. The behaviour of electron paths in an inverse first power, radial, electrostatic field has been investigated, and it has been found that refocussing should occur when the path of the normally entering electrons has been turned through 127° 17′. This position should play the same part for the electrostatic case as does the 180° position for the magnetic case. The departure from perfect refocussing, and the resolution between different velocities, should be of the same respective orders as the corresponding quantities in the magnetic case. An apparatus was constructed to test the theory. The radial field was produced by a difference of potential between two pieces of metal machined to co-axial cylindrical surfaces. Satisfactory refocussing of electron paths entering the field at $\pm 5°$ with the direction of perpendicular entrance was found.

7. Wave-length measurements of γ rays from radium and its products. LUVILLE T. STEADMAN, *Yale University.*—These measurements as reported in the Physical Review **33**, 120 (1929) have been continued with greater accuracy. Also, counting has been done with the crystal turned through an angle of 10°, thereby causing the diffracted rays of all wave-lengths to be changed in direction so that they cannot enter the chamber, but all other conditions remain the same. This method gives the background of the spectrum directly and from it a simple means of obtaining the relative intensities of the lines. Counts taken when the chamber slits are at a position which gives a line but taken now with the crystal turned, counts obtained both for the crystal set and when turned with the slits not on the line but nearby where a continuous spectrum would show up, are all of the same value which points to the absence of a continuous spectrum of γ rays. The twelve lines of shortest wave-length measured are as follows in X.U.: 8.72, 7.45, 6.78, 5.55, 4.97, 4.12, 3.38, 2.86, 2.38, 1.59, 0.95, 0.42. A diamond crystal will be used to check these short wave-lengths.

8. Basis for computing the age of a mineral. ALOIS F. KOVARIK, *Yale University.*—Calculation of the age of a mineral is based on the analysis data giving the uranium, thorium and lead contents and the atomic weight of the lead. Presence of common lead, various disintegration constants and atomic weights, and no alteration of contents except by radioactive changes are assumed. Formulae for the age and for the amount of common lead are deduced. Also, a formula giving the amount of common lead in a mineral to a fair degree of approximation is

developed in terms of the same data which when applied as a correction to the lead found by analysis makes it possible to obtain the amount and the atomic weight of the lead formed by the radioactive disintegration, thus enabling the use of the formulae ordinarily used when the presence of common lead is ignored as is the usual but erroneous practice.

9. An apparatus for the determination of ionic mobilities. OSWALD BLACKWOOD, *University of Pittsburgh.*—A device for determining ionic mobilities has been made which is analogous to Fizeau's apparatus for determing the velocity of light. An electrometer plate and two pairs of grids are mounted at distances 5.6 cm, 5.4 cm, and 3.5 cm above a 20 cm brass disk. Ions produced by a polonium plaque near the disk tend to be driven upward by electric fields in the lower and upper compartments. Opposing fields in each of the grid pairs prevent the passage of ions except for brief intervals, periodically, when two commutators simultaneously reverse the fields. Passage of a thin sheet of ions through both grid pairs will occur when the period of the commutator equals the time for the ions to pass from the lower to the upper grid. From this period, the voltage between the grid pairs, and their distance of separation, the mobility of the ions may be computed. Using this arrangement, the time required for the elimination of fifty percent of the initial, positive, monomolecular (?), ions in undried air has been found to be 0.011 seconds, which is in accordance with Erikson's value. This method is superior to the "blast" method in that turbulence is eliminated and that the purity of the gases may be controlled by enclosure of the apparatus.

10. Factors affecting the nature of the ions in the air. HENRY A. ERIKSON, *University of Minnesota.*—It has been previously found that the rate of transition of the initial positive ion in air depends upon how the air used has been treated. In this paper results are given showing that in the case of air dried by passing through drying agents like P_2O_5 and $CaCl_2$ the transition is very rapid, but that when the air is dried by passing through coils immersed in liquid air the initial positive ion transforms very slowly. It is also shown that products due to the ionizing process cause a rapid transition of the initial ion.

11. Motion of positive ions in a plasma. L. TONKS AND I. LANGMUIR, *General Electric Co.*—Heretofore it has been assumed that positive ions in a plasma have a "temperature" approximating one-half the electron temperature to account for the positive ion currents which flow to electrodes and the walls. This assumption causes theoretical difficulties which are overcome by supposing that each new positive ion has the small temperature of a gas atom and accelerates only under the influence of fields arising from the tendency of the high temperature electrons to flow away. Thus a collector does not measure a positive ion current which exists independently of its presence but rather causes fields which impel positive ions toward it. The calculated potential distribution across the positive column of an arc checks the observed quantitatively, and other experimental results can be explained. The theory gives a new relation $a\lambda = s_0(2kT_e/m_p)^{1/2}$, a = discharge tube radius, λ = ions per electron per second, s_0 = known constant. This equation, an ion current equation, an ion generation equation, an electron mobility equation, and the energy balance equation are available now and are sufficient to fix λ, T_e, ion current density, ionization intensity, and longitudinal field in terms of arc current.

12. The influence of shape on the efficiency and stability of permanent magnets. D. P. RANDALL, *Syracuse University.*—The magnetic energy delivered to an air gap by a given weight of steel depends on the following factors: inherent magnetomotive force of the steel, degree of stabilization required, leakage and fringing flux between the limbs and pole pieces of the magnet. Each of these factors is greatly modified by the shape and proportions of the magnet and its pole pieces. A method is developed for correlating these various factors with the magnetic characteristics of the steel: residual induction, coercive force or potency, and incremental permeability. Curves are given showing efficiencies attainable with various gap energy densities and degrees of stabilization. Efficiency is defined as the ratio of magnetic energy in the air gap to maximum magnetic energy inherent in the steel; degree of stabilization, as the ratio of the maximum stray field not permanently affecting the magnetization to the field intensity

maintained in the air gap. Comparison is made on this basis between tungsten, chromium, and some of the high coercive cobalt steels. Advantages of cast magnets in relation to stability are also considered. As applied to a meter magnet of tungsten steel, charts are given showing proper proportions for maximum efficiency over a considerable range of gap lengths and degrees of stabilization. By application of the principle of similitude these charts may be made to give specific dimensions for a magnet of any desired size.

13. Determination of the average size of the discontinuities in magnetization. RICHARD M. BOZORTH, *Bell Telephone Laboratories.*—The theory of the determination is analogous to that of the small shot effect. Instead of determing ne, the charge that moves as a unit in a conductor, nm_a is determined, where m_a is the change in magnetic moment corresponding to the reversal of one atom and n is the number of atoms which act together to produce one of the impulses of the Barkhausen effect. Since the moment corresponding to one atom reversal is known, the mean value of n can be determined from the equation which is derived for a cylindrical sample of magnetic material: $\overline{i^2} = A\bar{n}m_a(dB/dt)/\mu_r$, where $\overline{i^2}$ is the mean square current measured, A is a known constant depending on the amplifier and other apparatus, dB/dt is the mean time rate of change of induction, and μ_r is the reversible permeability. The fundamental relation used in deriving this formula is that deduced by T. C. Fry in his theory of the small shot effect [Jour. Frank. Inst. **199**, 203–20 (1925)]. The value of $\bar{n}$ (about 10^{18}) is found to be greatest near the steepest part of the hysteresis loop and to diminish rapidly as the end of the loop is approached.

14. Magnetic properties of iron crystals. DONALD FOSTER, *Bell Telephone Laboratories.*—Large crystals were grown by annealing hard drawn wires of electrolytic iron in vacuum. The method of growing differs from the well-known means developed by Edwards and Pfeil in several essential respects. The crystals are 0.1 cm in diameter and from a few millimeters to 15 cm in length. Measurements by an x-ray rotation method show that the wire axis always lies at a considerable angle to the nearest (111) direction, but is otherwise unrestricted. The magnetic data were obtained by means of a new method whereby the demagnetizing field is experimentally determined for each crystal. The hysteresis loop is characterized by extremely steep sides with sharp corners and high remanence. The coercive force for $H_{max} = 30$ gauss is 0.4 gauss and in respect to the effect of orientation there is qualitative agreement with earlier work. Contrary to reports by previous investigators we find no "breaks" at the knee of the magnetization curve. The initial permeability is about 175. The maximum permeability occurs at a field intensity of about 0.8 gauss. The effect of tension is being investigated.

15. A theory of light. GLEN H. DRAPER, *U. S. Naval Observatory, Washington, D. C.*—Accepting the law of cause and effect as an absolute law and accepting the mathematics perdicated on this law, the theory propounds: (a) That space is a three-dimensional void, except as occupied by matter and light. (b) That the nature of matter is determined by its normal light content or the normal energy relations existing between electrons and their nuclei. (c) That the velocity of light through any substance tends toward a constant velocity by a measurable value. (d) That the velocity of light indicates the center of force, as gravitation indicates the center of mass. The theory may be applied to the Michelson-Morley experiment and offers an explanation of why Dr. Roy Kennedy obtained a zero result from his recent experiments, while Dr. Dayton C. Miller obtained a small positive result.

16. The electronic theory of light and other forms of electromagnetism. HERBERT J. BRENNEN, *Department of Chemistry, Northwestern University.*—My hypothesis, (Journal of the Franklin Institute, **202**, 828–831 (1926)) that light is corpuscular and that the corpuscles are electrons, is further developed on the basis of Newtonian dynamics. It is found that (1) the electric charge e of a moving electron is given by: $e = e_0(1-\beta^2)^{1/2}$ where e_0 is the electric charge in E. S. U. of a stationary electron, whence follows (2) the Lorentz-Einstein formula and (3) Sommerfeld's Theory of the fine spectral structure. From (1) when $\beta = 1$, we have: (4) the electric charge of an electron moving with the speed of light is zero and hence will not be deflected by an electric or a magnetic field. It is further shown that (5) the velocity of light is given by: $c = e_0/(Kmr)^{1/2}$ where m and r are the mass and radius of the electron and K is the

specific inductive capacity of the medium. Since K is known by experiment to be proportional to the square of the refractive index of the medium, we have (6) the velocity of light is inversely proportional to the refractive index of the medium. For a vacuum, $K=1$, and hence (7) the number of natural constants is reduced by one.

17. Group velocity. D. G. BOURGIN, *University of Illinois.*—In the Phys. Rev. **33,** 239 (1929) Tonks suggests the interesting empirical theorem; $\mu E = vE_i$ where μ and v are the group and phase velocities and E and E_i are the total and doubled reactive energies/unit length respectively. The conditions for the validity of this and similar theorems have been developed. In particular, it turns out that the theorem does not hold in general if the characteristic linear differential equation involves higher space derivatives than the second—the physical interpretation is immediate.

18. The optical constants of solid mercury. ROLLIN SMITH BALDWIN, *Yale University.*—The optical method and apparatus used was essentially the same as that of O'Brien (Phys. Rev. **27,** 93 (1926)). A vacuum of the order of 10^{-5}mm of Hg and suitably placed liquid air traps reduced any error due to adsorbed gases or vapors condensing on the free surface of the Hg below an amount detectable by the method of measurement. Distillation of the Hg both in vacuo and a continuous current of air (2–3 cm press.) was found necessary to obtain Hg of the required degree of purity. The values for the absorption coefficient showed no appreciable change, but the values of the index of refraction for the solid state were greater by approximately 10 percent or more than those of the liquid state for the wave-lengths of light used (λ5790–69, λ5460, λ4358). Although this is contrary to results of Haak and Sissingh (Proc. Royal Acad. Amsterdam **21,** 691 (1919)), it is believed that the change is due to a change in the optical constants with the change of state of the Hg itself, and not to spurious effects.

19. On the continuous spectrum of mercury. LIEUT. W. N. THORNTON AND W. H. CREW, *Postgraduate School, U. S. Naval Academy.*—The continuous spectrum of mercury has been photographed with a small quartz spectrograph and evidence supports the view that it is due to the recombination of electrons with molecules, or, what amounts to the same thing, with atoms held in molecular bond. The source of radiation was a mercury arc [J.O.S.A. **17,** 261 (1928)] operating at atmospheric pressure and at about 500°C. A low current, low voltage, high frequency, condensed discharge in the vapor between two liquid mercury surfaces gave a spectrum consisting of two very strong bands (maximum intensities at about λ4500 and λ3300) and four extremely weak lines: (λ5461; λ4358; λ4047; λ2536).

20. The refractive index of sodium vapor. S. A. KORFF, *Princeton University.*—Continuing the study of the refractive index of sodium vapor in relation to the widths of the D lines in absorption, (Phys. Rev. **32,** 584 (1929)) more accurate values are obtained. Plates showing the fringes formed by the rapidly varying refractive index were obtained, and measured on a microscope, showing classically predicted values to hold to better than 1 percent an increase in accuracy over the previously reported value (8 percent). The plates were also examined on a densitometer.

21. Energy distribution in the solar ultra-violet spectrum. BRIAN O'BRIEN, *Buffalo Tuberculosis Association, Perrysburg, N. Y.*—Energy distribution in the solar spectrum was measured by a method previously described (Phys. Rev. **33,** 640 (1929)) from Dec. 24 to Mar. 21 from λ3300A to λ3007A on Dec. 24, and to λ2939A on Mar. 21 at a station 42° 27′ N. lat. and 1480 ft. elevation. Where necessary scattered light of longer wave-length was eliminated by preliminary dispersion with a 30° quartz prism. Atmospheric transmission was measured to λ2953A on several days near the equinox of uniform sky conditions as determined by a recording radiometer. A curve of atmospheric opacities reduced to zenith sun lies parallel to but slightly below that of Fabry & Buisson (Astrophys. J. **54,** (1921)). Error of a single log intensity determination is less than 0.05 and systematic errors are an order of magnitude less than this as has already been shown. Error in λ is less than 1A. Intensities were reduced to absolute units by a calibrated thermopile and silver film on quartz filter.

22. The attenuation of ultra-violet light by the lower atmosphere. L. H. DAWSON, L. P. GRANATH AND E. O. HULBURT, *Naval Research Laboratory.*—Measurements were made with a quartz mercury lamp, a quartz spectrograph and a recording densitometer of the attenuation of ultra-violet light from 3000A to 2050A by the atmosphere at sea level. For wave-lengths longer than 3000A no absorption could be observed at distances up to 400 meters; for wave-lengths below 2800A there was pronounced absorption above that attributable to molecular scattering. The absorption was the same day and night, was unaffected by changes in the humidity, but increased with haze. The thicknesses of clear air necessary to reduce the light to 10^{-2} were about 22, 5, 0.57 and 0.20 km for 2800, 2500, 2200 and 2050A, respectively. The absorption in the lower atmosphere around 2800 to 2900A was not sufficient to account for the sharp cessation of the solar spectrum in this region. This result is in keeping with the fact that the ultra-violet limit of the solar spectrum is due to ozone in the high atmosphere. The absorption in the lower atmosphere at 2200 to 2050A, a spectrum region where ozone is relatively transparent, is great enough to prevent sunlight of these wave-lengths from penetrating to sea level.

23. The absorption of light by fog. L. P. GRANATH AND E. O. HULBURT, *Naval Research Laboratory, Washington, D. C.*—Measurements between two stations 0.4 km apart with a thermocouple and galvanometer and with spectrograms, properly calibrated, of the absorption of light by fog for wave-lengths from 0.4 to 3μ showed that the absorption increased slightly with decrease in wave-length, but hardly enough to indicate that red light is appreciably better than blue light for the purpose of penetrating fog. For a fairly dense fog, such that in daylight dark colored objects at about 0.6 km could barely be seen, the distances necessary to reduce the light to 10^{-2} of its original value were about 710, 843, 910, 970, 980 and 980 meters for wave-lengths 0.4, 0.5, 0.6, 1.0, 2.0 and 3.0μ, respectively.

24. Absorption of ultra-violet light by oxygen, water vapor and quartz. L. P. GRANATH, *Naval Research Laboratory.*—Quantitative measurements were made of the absorption of light by oxygen, water vapor and crystalline quartz in the spectral region 1900 to 2100A, by means of a quartz spectrograph and a recording densitometer. Defining the absorption coefficient α by $I = I_0 10^{-\alpha d}$ where d is the distance in cm, values of α were obtained for oxygen at atmospheric pressure in tubes up to 5 meters in length which showed the peaks of absorption due to the Schumann-Runge band system below 1970A. From 2000 to 2100A the absorption appeared continuous with no marked peaks, α being 0.00025, 0.00032, and 0.00050 cm^{-1} at 2100, 2050 and 2000A, respectively. The values of α for saturated water vapor at 25°C were 0.0005, 0.0013 and 0.003 cm^{-1} for wave-lengths 2050, 1950 and 1900A. For a specimen of crystalline quartz 2.5 cm thick α was found to be 0.086, 0.11, 0.13 and 0.17 cm^{-1} for wave-lengths 2040, 2000, 1940, and 1870A.

25. The development of "thermodynamic symbolism"—second paper. JOHN Q. STEWART, *Princeton University.*—At the February meeting the proposition was advanced that the formulae and concepts of thermodynamics, when interpreted symbolically, form a structure of mathematical relations which is applicable for the coordination (and discovery) of principles in each of numerous special fields in physics. The present paper treats in this manner a problem in mechanics and electrostatics—that of particles acting on one another with forces which vary as some function of the distances. To such a system energy can be communicated in two ways. When a given particle is moved under the influence of an arbitrary force, work is supplied. On the other hand energy must be supplied when the mass present in any volume-element in the field of potential is varied. Such increments of energy may be taken as the analogue of heat in thermodynamics. Potential is the analogue here of temperature. Accordingly the discussion of the mechanical problem proceeds along thermodynamical lines.

26. Classification of physical laws: periodicity of physical concepts. VICTOR COFMAN, *E. I. du Pont de Nemours and Co.*—A tabular arrangement of the *extensive* factors: mass (M) volume (V), entrophy (S), time (t), and their corresponding *intensive* factors: molar free energy (dE/dM), pressure (dE/dV), temperature (dE/dS) and power (dE/dt), gives a set of 28 laws.

Some of these are well-known laws; other have not been clearly stated as such. They can all be deduced from an extension of a well-known thermodynamic equation, namely $(FdM-PdV)+(TdS-Xdt)=0$. The symmetry of this equation suggests that entropy extends in time, just as mass extends in space. This is a fruitful concept because entropy can be taken as a measure for change or happening, and time becomes a thermodynamic variable. Planck's constant h, as shown by J. Q. Stewart also, is the entropy analogue in the radiation system; a quantum wave has constant value at different *places* for the same reason that a gram weight has the same mass at different *times*. Laws of electronic or gravitational systems can also be tabulated, by the substitution of suitable variables: i.e., gravitational force, or e.m.f., in place of gas pressure, (velocity)^2 instead of temperature, etc. Equations like

$$dP/dp=v/V; \qquad dP/(pdh)=-g/(RT);$$
$$E=E_0+RT/(nF)\ \ln\ c;$$
$$-P_0=(RT/V)\ \ln\ p+\text{const};\ \Gamma=-(cd\sigma)/(RTdc)$$

should be identical in form.

27. The curvature radius of space-time derived from 24 Cepheid variables and 35 O-stars. LUDWIK SILBERSTEIN, *Research Laboratory, Eastman Kodak Co.*—The combination of the expressions for the spectroscopic radial velocity and the transversal velocity (proper motion) of a star in isotropic (deSitterian) space-time gives for the curvature radius R the statistical formula

$$R^2/c^2=\left[(\overline{r_1^2v_{r2}^2/v_1^2})-(\overline{r_2^2v_{r2}^2/v_2^2})\right]/(\overline{v_1^2}-\overline{v_2^2})$$

where r is the distance, v the resultant, v_r the radial velocity of a star belonging to one of two groups of stars, marked by the suffixes 1 and 2, and the bars indicate averages taken over each of these groups. This formula applied to two groups of Cepheid variables, each consisting of 12 objects, gives $R=3.01\times10^{11}$ astron. units, and applied to thirty-five 0-stars, split into groups of 17 and 18, yields $R=3.25\times10^{11}$ astron. units. Since scarcely more that two figures are dependable, these two estimates of the world radius are to all purposes identical. Both are about 20 times smaller than that derived (1924) from 18 globular clusters and the Magellanic clouds. But there are weighty reasons for relying more upon this new value. This is most impressively corroborated by the results just obtained (April 7) from 246 stars from Young and Harper's list, viz. 3.39×10^{11}.

28. A new electromagnetic effect and its application to a theory of the permanent magnetic field of the sun and earth. ROSS GUNN, *Naval Research Laboratory.*—A study of the motions of ions as they spiral about an impressed magnetic field shows that a two-fold effect is produced (1) a diamagnetic effect, dependent on the field strength (2) a systematic ion drift, dependent on the gradient of the field. The ion drift is considered and expressions obtained for the current density. Under the conditions of radial symmetry and a closed circuit a current flows, in such a direction as to reduce the inhomogeneity of the impressed field and *increase* the total flux enclosed by the current circuit. This increase in flux suggests that the phenomenon is regenerative. Application to the sun shows that westward currents flow in the solar atmosphere accounting for the observed magnetic moment. Diamagnetic data indicate, however, that the observed vaule is 1/230 of the actual value. The seat of the largest currents appears to be in regions of short free paths well within the sun. Similar arguments apply to the earth and the correct magnetic moments are found in each case if the mean gradient is taken equal to that observed at the surface and if the mean free paths of the ion approach 10^{-6} cm. On the present view the magnetic field arises from the thermal energy of the sun and earth and has no direct connection with its rotation.

29. Resonance in circuits with parallel resistances. ALLEN ASTIN, *National Research Fellow, Johns Hopkins University.*—Jezewski (Zeits. f. Physik, **48**, 123 (1928)) and Doborzynski (Zeits. f. Hochfrequenz., **31**, 15 (1928)) have shown theoretically that in a resonance circuit of inductance, capacity and parallel non-inductive resistance the value of the capacity for maximum p.d. across it is independent of the value of the parallel resistance. The author (Disserta-

tion, New York, 1928) has shown that the same condition holds when a non-conducting condenser is placed in series with the shunted condenser. This type of resonance may be detected with either a vacuum tube voltmeter or a thermocouple connected as the parallel resistance. By using the former method of detection the relation is verified at a frequency of 2×10^6 with resistances as low as 100 ohms (d.c. value) for the first circuit and down to 30 ohms for the series circuit. The resistances used for the test are capillaries filled with carbon particles. In comparing the two circuits it is shown for small values of the parallel resistance (less than 1000 ohms) the voltages across the shunted condenser at resonance are much greater in the series circuit than in the simple one. The circuits are considered because of their value in measuring the dielectric constants of conducting liquids.

30. Rectification by oscillation of positive ions about the potential minimum of a thermionic triode. K. H. KINGDON, *General Electric Co.*—Positive ions are trapped in the potential minimum surrounding the cathode and have a natural frequency of oscillation about it. An alternating voltage of the same frequency (10^5 to 10^6 cycles) applied between grid and cathode sets the ions in motion, and leads to a decrease in the electron current to the anode. This rectification effect has been reported previously [Science, **68**, 599 (1928)] for caesium ions generated at the cathode. It has now been studied for ions of other gases made by electron collision between grid and anode. By using a low voltage caesiated filament as cathode, separate rectification peaks may be obtained for the ions of each of the argon and neon isotopes. Helium shows two peaks whose separation is that of ions having masses 4 and 5. It is uncertain whether the 5 peak can be attributed to He H (Aston). Oxide coated equipotential cathodes apparently usually do not have sufficiently uniform surfaces to separate the isotopic peaks. Detection in the old argon filled detector tubes is due to this ionic rectification.

31. Forced electric oscillations in three circuits with electromagnetic coupling. W. J. SETTE AND R. E. MARTIN, *Lehigh University*.—Three circuits containing inductance, capacitance, and resistance, each of the circuits being coupled by a mutual inductance to the others, were considered. From the differential equations showing the potential drops in the networks with a sinusoidal electromotive force in the circuit designated 1, the values of the currents flowing in the circuits were obtained. The expressions for the current amplitudes in the networks 2 and 3, I_2 and I_3, are symmetrical, but the expression for I_1 is different. The resonance relations were calculated. To check the theory apparatus in accord with the hypotheses was set up. Taking each current as a function of the reactance in its own network the curve I_k against X_k exhibits the ordinary resonance peak and zero asymptote. Considering I_2 with X_3 variable, it has a maximum, minimum, and a horizontal asymptote not zero. Supposing I_1 a function of X_3 there are again a maximum, a minimum, and a determined asymptote. The experimental curves agree with those indicated by the theory. Some equations have been checked to within a few percent though accurate check is difficult.

32. Some characteristics of electric sparks excited by an ignition coil. R. A. WOLFE AND O. S. DUFFENDACK, *University of Michigan* AND D. W. RANDOLPH, *The A C Spark Plug Co.*—Investigations have been made with a high vacuum cathode-ray oscillograph on various characteristics of an electric spark excited by an ignition coil. The peak voltage depends on the material of the electrodes and is less for materials of low work of extraction of electrons. Th. peak voltage of a spark gap has been correlated with the thermionic emission of the electrodese The voltage across the gap rises from zero to its maximum in from one to two microseconds, the time being affected to some extent by the capacitance of the circuit. The spark current has small superposed oscillations at its beginning. Increasing the capacitance in parallel with the gap increases the duration of the superposed oscillations, increases the maximum value of the current, and also increases the time required for the current to reach its maximum. Added capacitance completely changes the amount of energy dissipated in the several phases of the spark. The maximum power of a spark with a capacitance of $750\mu\mu f$ in parallel with the gap has been observed to reach 66 kilowatts.

33. Resistance of air condensers. R. R. RAMSEY AND B. D. MORRIS, *Indiana University.*—The method of measurement is the differential thermometer method as used by Ramsey (Phys. Rev., **27**, 815 (1926)) except that iron-advance thermocouples were used to determine thermal equilibrium. Measurements were made at wave-lengths of 125 to 410 meters with capacities varying from 0.00001 to 0.00054μf. The resistances obtained ranged from 0.076 to 11 ohms. When these results are reduced to "standard conditions" by the empirical formula, $(R_s = R(300/\lambda)(C/.001)^{3/2})$ the value of R_s ranged from 0.0078 to 0.0132 ohms. The values obtained by applying the formula to Ramsey's data are practically the same as the above. Applying the formula to Dye's (Proc. Phys. Soc. Lon., **40**, 285 (1928)) data, which were obtained by a substitution method, R_s ranged from 0.0021 to 0.006 ohms. Dye's measurements were made at 200 to 15000 meters. Applying the formula to measurements made by the resistance variation method higher results are obtained. The measurements by Weyl and Harris (Proc. Inst. Rad. Eng., **13**, 109 (1925)) made at wave-lengths 96 to 260 meters with resistances from 0.71 to 18.5 ohms give values of R_s ranging from 0.41 to 1.33 ohms. Callis' (Phil. Mag., **1**, 428 (1926)) data give a mean value of 0.98 ohms for R_s. Brown, Wiebusch and Colby's (Phys. Rev., **29**, 887 (1927)) data give values for R_s ranging from 0.26 to 0.56 ohms.

34. Properties of Rochelle salt as a dielectric with Braun tube oscillograms. C. B. SAWYER AND C. H. TOWER. *The Brush Laboratories Co., Cleveland, O.*—Both saturation and hysteresis appear in Braun tube oscillograms made at various temperatures with a condenser whose dielectric consists of Rochelle salt slabs cut perpendicular to the a-axis. Some polarization effects are observable. Curves are also given, showing the variation in mechanical and electrical saturation with temperature. These correspond in only a general way to the piezoelectric constant's variation with temperature. Certain marked peculiarities are noted in the resulting mechanical deformation when Rochelle salt is excited with alternating potentials. Clear Rochelle salt half-crystals have been produced up to forty-five centimeters in length.

35. Mechanism of dielectric breakdown in thin layers. F. E. NULL AND J. B. EDWARDS, *Georgia School of Technology.*—Whitehead has shown that it is practically impossible to remove the last traces of moisture from paper insulation. To determine whether moisture was responsible for pyroelectric breakdown in impregnated papers on d.c. potential, we made a study of the electrical characteristics of 0.0005 inch, unimpregnated, linen condenser paper for different moisture contents. We were able to separate the effects of hot spots and ionization by collision, upon the breakdown potential, by the variation with the number of layers tested, of the current-voltage characteristics, the conduction current, and the breakdown potential. For atmospheric pressure and a relative humidity of 22.5 percent breakdown was due to hot spots, the breakdown potential per layer being approximately constant from 1 to 16 layers, thus indicating lateral, thermal conduction from the hot filaments. Breaks in the characteristics present strong evidence of some ionic discharge wich does not affect the breakdown potential. Tests for paper dried in vacuum are complete; others for paper dried by heat and vacuum, and impregnated with dry air under pressure are in progress.

36. Dielectric polarization potential and the law of superposition for hard rubber. H. H. RACE AND J. R. CAMPBELL, JR., *Cornell University.*—If a constant potential E_1 is applied to an imperfect dielectric like hard rubber, there is evidence that an electric potential E_p is built up in the dielectric. If, after a long time charge at E_1, the applied potential is suddenly reduced to a lower value E_2, current will flow in a negative direction if E_p is greater than E_2. Therefore a sample of hard rubber was subjected to several exactly similar conditions of charge at $E_1 = 750$ volts ($G = 884$ v/cm), but different conditions of discharge in that E_2 was varied from 703 to 748.5 volts. The results indicate that for hard rubber the polarization potential built up during a long time charge is approximately equal and opposite to the charging potential. Under the assumption that Curie's law of superposition held true for the existing conditions, the curve of current against time, was predicted from data obtained for the same test piece over two years ago. (Fig. 8, "Electric Conduction in Hard Rubber, Pyrex, Fused and Crystalline Quartz," by Hubert H. Race, A.I.E.E., Quarterly Trans. **47**, 4 (1928)). The time when this current changed

direction (measured from the instant the lower voltage was applied) was also predicted. The close correspondence between the predicted and actual curves bore out the truth of the law of superposition for the gradients used.

37. On the red shift of spectral lines through interstellar space. F. ZWICKY, *California Institute of Technology.*—Distant objects in the skies show an average receding velocity which is approximately proportional to the distance. Assuming that a light quantum $h\nu$ has a gravitational mass $h\nu/c^2$, an exchange of momentum and energy might be expected between the quantum and the masses around its path (essentially the masses in a 90° cone behind the quantum, because of the finite velocity of the gravitational waves). This gravitational analogy to the Compton effect would lead to a red shift roughly given by $\Delta\nu/\nu=\alpha f\rho l^2/c^2$, where f is the gravitational constant. The density ρ of matter in space is taken to be uniform. l is the distance travelled by the quantum, c the velocity of light and α a constant of the order one. For very great distances l^2 has to be replaced by ll_1, where l_1 is a constant. For the clusters outside of the galactic system ($l\sim15000$ parsecs, $\rho\sim10^{-29}$ to 10^{-24} gr/cm^3) we should expect $1.5\times\alpha\times10^{-8}>\Delta\nu/\nu>1.5\times\alpha\times10^{-7}$, whereas the observed values given in the following paper are about 3×10^{-4}. The above formulae will be changed (*a*) if the density ρ is not uniform, (*b*) if there are systematic motions of matter in space which might cause violet shifts also, (*c*) by the irregular motions of matter in space.

38. On the radial velocities of globular clusters. P. TEN BRUGGENCATE, *p. t. Mt. Wilson Observatory.* (*Introduced by F. Zwicky.*)—Radial velocities of spirals, corrected for solar motion, show a linear correlation with distances. Zwicky's explanantion (the foregoing note) predicts a similar correlation for globular clusters, since the larger densities inside the galactic system compensate the smaller distances. Preliminary examination of the data for clusters indicated a correlation between velocities and galactic latitude, the red shift increasing with decreasing latitude. Since the star counts of Seares offer a means of estimating densities between us and the clusters, correlations were sought between velocities and total numbers of stars inside cones, whose axes were lines joining the sun and the clusters. No correlations were found for cones whose solid angles are 1° and 30°, but for a solid angle of 60°, a definite linear correlation appeared, giving a red shift of 100 ± 60 km/sec ($\Delta\nu/\nu\approx3\times10^{-4}$) for 15000 parsecs and a density of matter of about 10^{-23} gr/cm^3. The large solid angle of the cones makes an explanation based on the ordinary Compton effect improbable; the correlation between star numbers inside such cones and velocities rules out a deSitter effect. Thus the results, obtained from globular clusters, suggest the real existence of the new effect proposed by Zwicky.

39. On the spherically symmetrical statical field in Einstein's unified theory of electricity and gravitation. NORBERT WIENER AND M. S. VALLARTA, *Massachusetts Institute of Technology.*—In Einstein's new unified theory of electricity and gravitation (Berliner Sitzungsber. 1928, p. 217 and p. 224; 1929, Feb. 1) the electromagnetic and the gravitational fields are described in terms of an antisymmetrical tensor ${}^a h_\lambda$ which associates with each point of a continuum X_4 a quadruple of axes and consequently determines a parallelism of directions valid for the whole of space. In this paper the components ${}^a h_\lambda$ are determined under the same assumptions made in the previous (1916) Einstein theory to obtain Schwarzschild's solution. It is shown that an electromagnetic field is incompatible in the new Einstein theory with the assumptions of static spherical symmetry and of symmetry of past and future. Further, with the same assumptions, it follows from the new Einstein field equations that the gravitational field also vanishes. Since all experimental confirmations of general relativity are essentially tests of the Schwarzschild solution, the new Einstein theory lacks at present all experimental confirmation.

40. Note on the statistical interpretation of Maxwell's equations. M. S. VALLARTA, *Massachusetts Institute of Technology.*—Following a method given by Dirac it is shown that the energy density and the Poynting vector of Maxwell's theory, respectively, can be interpreted as the probability that n photons be wholly within a given region at a given time, and the probability that n photons cross a given boundary in a given direction. Further, the change in

probability of n photons being within a given closed region is equal to the probability of their having crossed the boundary of that region. These considerations lead to a discussion of the relations between Maxwell's equations and Dirac's equations of the spinning electron (Proc. Roy. Soc. **117**, 610 (1928)).

41. Indetermination principles. ARTHUR E. RUARK, *Mellon Institute, Gulf Oil Companies and University of Pittsburgh.*—The writer has shown (Proc. Nat. Acad. **14**, 322) that in experiments on a single electron we encounter limits to the accuracy with which its position can be measured. It will be shown that this circumstance is connected with Heisenberg's indetermination principle. It is a consequence of Heisenberg's principle, together with the fact that there is an upper limit to the uncertainty of a measured velocity, since a particle cannot move with velocity greater than that of light. Conversely, the existence of a limit of accuracy in length measurements, together with the upper limit for velocity, enables us to prove a theorem which resembles and is related to Heisenberg's indetermination principle. We do not encounter a limit to the accuracy of length measurements when Newtonian dynamics is used, which shows clearly that the existence of this limit is connected with the validity of relativistic mechanics.

42. Interpretation of deviations from Ohm's law on Fermi statistics. HENRY MARGENAU, *Yale University.*—K. T. Compton (Proc. Nat. Ac. Sci., 12, 1926) has shown that the classical free electron theory, applied to Bridgman's observations on deviations from Ohm's law, leads to a value of the mean free path $l=3.13\times10^{-6}$cm. Compton's method has been used, with certain modifications required by the new statistics, to recalculate l assuming a Fermi distribution of electrons. The only points of departure from his procedure lie in the circumvention of the use of Langevin's formula for mobilities—Sommerfeld's expression for conductivity being employed instead—and the substitution of different relations between arithmetic mean speed and root mean square speed. The resultant formula for l becomes

$$l=[(kT)/(Ee)][(22.5m/M)(\sigma_0-\sigma)/\sigma_0)]^{1/2}$$

it differs from Compton's formula only by a numerical constant slightly greater than one. The value of l if computed on the basis of Compton's figures (taken from Bridgman's work) is 3.29×10^{-6} cm. Calculated from the classical conductivity formula, with the number of free electrons equal to that of atoms, (assuming $T=500°$K, corresponding to Compton's figures) it would be 3.6×10^{-7} cm. Sommerfeld's theory, on the other hand, (gives $l=3.1\times10^{-6}$ cm). It is seen that the mean free path here computed agrees better with Sommerfeld's value. The evidence from Bridgman's work appears to favor distinctly the Pauli-Sommerfeld point of view.

43. Solution of problems in quantum mechanics by operator analysis. R. B. LINDSAY AND R. J. SEEGER, *Yale University.*—The operator method of Hilbert, Neumann and Nordheim (Math. Ann. **98**, 1 (1928)) is based upon a set of physical axioms interpreting quantum laws statistically. With the introduction of Dirac's function $\delta(x-y)$ and the fundamental operators $p\equiv\epsilon\partial/\partial x$, $q\equiv x\cdot$, satisfying $pq-qp=\epsilon I$ (where $\epsilon=h/2\pi i$ and I is the unit operator), they derive the equations

$$(1)\qquad (F-y)\phi(x,y)=0 \qquad \text{and} \qquad (2)\quad \left(G+\epsilon\frac{\partial}{\partial y}\right)\phi(x,y)=0,$$

where F and G are any two canonically conjugate hermitian operator functions of p and q and x and y any two dynamical quantities. If $F\equiv H$, the Hamiltonian, $y\equiv W$, the energy, and x is the position coordinate, (1) becomes the usual Schrödinger equation, where $\phi_n\bar{\phi}_n dx$ measures the probability that for $W=W_n$, the coordinate lies between x and $x+dx$. The present paper investigates the special cases: (I) free particle, $H=p^2/2m$ and G found to be $-m/2(qp^{-1}+p^{-1}q)$; (II) uniform field, $H=p^2/2m+kq$, $G=p/k$; (III) harmonic oscillator, $H=p^2/2m+k^2q^2$, $G=(i/4)\{\log[(p/(2m)^{1/2}+ikq)2^{-1/2}]-\log[(p/(2m)^{1/2}-ikq)2^{-1/2}]\}$. A partial differential equation method for finding G is introduced, and the problem of uniqueness and the introduction of transcendental functions are discussed. The associated equation (2) is not unique, and more general equations are constructed whose properties are investigated. In (I) (2) determines the dependence of ϕ on W; in (II), (2) appears to add nothing new. The normalized solutions for ϕ are obtained.

44. On the principle of microscopic reversibility. G. E. UHLENBECK AND H. C. WOLFE, *University of Michigan.*—It is shown that for collisions in which energy, momentum, and number of particles are conserved—e.g. elastic collisions between particles with spherical symmetry, scattering of light quanta by electrons, the probability coefficients for direct, inverse, and reverse collisions are equal. Following Pauli (Zeits. f. Physik **18,** (1923)) the particles are represented by their "four-vectors" of energy and momentum. A collision means a rotation of the two vectors about their resultant. The fundamental geometric constants of the collision are obtained as functions of the energies and momenta. These functions are invariant to Lorentz transformations and are also invariant if we make the substitutions which correspond to the inverse and reverse collisions. Hence, all functions of the collision variables (energies and momenta, before and after collision), which are invariant to Lorentz transformations, are invariant to the inverse and reverse substitutions. From invariance to Lorentz transformations of the six dimensional phase volume (where the space range is a volume element moving with the particle), there follows the Liouville theorem of the conservation of extension in phase in a collision. Using, in addition, the invariance to Lorentz transformations of the number of collisions of a specified type in a specified time, the equality of the probability coefficients for the direct, inverse, and reverse collisions is proved.

45. Some critical points in a study of recent quantum theories. R. J. SEEGER, *Yale University.*—A critical survey is made of several recent quantum theories: matrix; q-number; operator of Born and Wiener; operator of Hilbert, Neumann, and Nordheim. A presentation is given in the symbolical manner of Dirac upon a new algebraical postulate for non-permutable variables q, p. Suppose $u(q)$ and $v(p)$ or $u(q^m p^m)$ and $v(q^n p^n)$ are homogeneous. Let $uv^2u = vu^2v$. Hence, it can be shown that $uv - vu$ is equivalent to a parameter. Identify one such parameter with the symbolical idemfactor. From this, old formulae are extended in meaning and in use. Several new ones are developed for convenience. The inverse of a polynomial is proved to be a non-permutable binomial expansion. Throughout, equivalence and identity are kept distinct. The symbols are interpreted as matrices, and then as operators. The Hermitian conditions of both suffice to prove canonical conjugates unique. Differences arise in the kinds of functions allowable and in the use of the inverse function. Schrödinger's equation and the diagonal matrix H are found to be different possible interpretations of an equation mathematically incidental to the problem of finding canonical conjugates. The matrix $q \equiv \left| q(nm) e^{2\pi i \nu(nm) t} \right|$ is extended to allow $q(nm)$ dependent on t. The damped linear oscillator is then solved by the matrix theory, as well as by the methods of Schrödinger and of Born and Wiener. The matrix theory is applied to the physical pendulum with an approximate solution.

46. Saturation of electric and magnetic polarization of gases on the basis of quantum mechanics. K. F. NIESSEN, *International Education Board Fellow, University of Wisconsin. (Introduced by J. H. Van Vleck.)*—Van Vleck's previous calculations are extended to include higher powers of the field F. The electric polarization is calculated (1) to all powers of F for rigid molecules, (2) to terms in F and F^3 for deformable ones. In (1) we obtain the ordinary Langevin formula, if the rotational frequencies are small compared to kT/h. In (2) only the chief terms agree with Debye's classical formula. Analogous calculations for the magnetic case yield the following results

$$(3a) B(l, \beta, H, T) + B(s, 2\beta, H, T), \qquad (3b) B(j, g\beta, H, T),$$

$$(4a) L(\sigma_l, \beta, H, T) + B(s, 2\beta, H, T), \qquad (4b) L(\sigma_l + 2\sigma_s, \beta, H, T)$$

where $L(l, \beta, H, T)$ is the result of putting $\mu = l\beta$ in the Langevin function and $B(l, \beta, H, T)$ is the same for Brillouin's function. Cases 3 and 4 apply to atoms and diatomic molecules respectively, and a and b to narrow and wide multiplets respectively. Here s, j, l, g have their usual spectroscopic meaning, β is the Bohr magneton and σ_l, σ_s are the components of l and s along the molecular axis. The relation $B(l, \beta, H, T) = L(l + \frac{1}{2}, \beta, H, T) - L(\frac{1}{2}, \beta, H, T)$ brings B in accordance with Nernst's theorem. The influence of the electric (magnetic) polarization by magnetic (electric) field is calculated for rigid molecules and is a small second order effect.

47. "Dielectrics and insulation" (10 minutes) by J. B. WHITEHEAD, *Chairman of the Committee on Insulation of the National Research Council and Dean of Engineering, Johns Hopkins University.*—Present knowledge and theory as to the fundamental properties of dielectric materials, as revealed in the literature of physics, is not sufficient to explain the behavior of dielectrics as employed in the insulation of electric circuits. This discrepancy has been the chief concern of the Committee on Electrical Insulation, of the Division of Engineering and Industrial Research of the National Research Council. A brief description will be given of those properties of electrical insulation which seem to limit its performance and life, and of the gap which exists between knowledge of these properties and the products of fundamental physical research and of classical theory. The picture presented emphasizes the importance of a closer knowledge of dielectric absorption and other anomalous properties of dielectrics.

48. "On the mechanical and electrical strength of dielectric crystals" (30 minutes) by F. ZWICKY, *California Institute of Technology.*

49. "Electrical convection phenomena in oil" (10 minutes) by LEWI TONKS, *Research Laboratory, General Electric Company.*

50. "The effect of temperature, pressure and frequency on the electrical properties of rubber" (10 minutes) by H. L. CURTIS, A. T. MAC PHERSON AND A. H. SCOTT, *Bureau of Standards.*—The dielectric constant, power factor, and resistivity of rubber are dependent on the percentage of sulphur with which it is vulcanized, on the temperature and pressure, and, for the first two properties, on the frequency at which the measurements are made. At normal temperatures, pressures, and frequencies, the curve showing the relation between dielectric constant, or power factor, and the percent of sulphur has a maximum in the neighborhood of 12 percent sulphur and a minimum near 19 percent. For 60 cycles both the maximum and minimum occur at higher percents of sulphur than for 1000 cycles or for 3000 cycles. At lower temperatures the maxima and minima are shifted in the direction of lower percentages of sulphur and become less pronounced until at $-76°C$ they entirely disappear. Increasing the pressure in the range from 1 to 700 atmospheres has the same effect as slightly reducing the temperature. This behavior of rubber can probably be interpreted from a consideration of the electric moments of molecules or molecular groups, and their rotational mobility. Electric moment is a function of chemical composition; rotational mobility is conditioned by temperature and pressure.

51. "Influence of surfaces and space charges on the apparent conductivity of dielectrics" (30 minutes) by KARL F. HERZFELD, *Johns Hopkins University.*

52. "Electron bombardment of hydrocarbons" (10 minutes) by V. KARAPETOFF, H. A. TREBLER AND E. G. LINDER, *Cornell University.*—As a part of a study of the mechanism of the deterioration of dielectrics in underground cables, hydro-carbon vapors have been subjected to electron bombardment and the resulting chemical changes observed. The bombardment results in the condensation and polymerization of the hydrocarbons, and in the evolution of gases, chiefly hydrogen. An attempt has been made to find the relationship between the amount of gas evolved and the molecular structure of the hydrocarbons.

53. "Electrical insulation from the engineering viewpoint" (30 minutes) by G. M. J. MACKAY, *Research Laboratory, General Electric Company.*

54. "The dependence of dielectric polarization upon molecular condition" (10 minutes) by C. P. SMYTH, *Princeton University.*—The equation of Debye for the variation of dielectric polarization with temperature, which has been found accurate for gases, gives misleading results when applied to pure dipole liquids because of the mutual action of the dipoles. When the dipoles are sufficiently separated from one another by the molecules of a non-polar solvent, the equation is found to apply satisfactorily and the value obtained for the electric moment is the same as in the gas. When the distance of separation of the dipoles decreases with increasing concentration, the polarization commonly decreases, but, in the case of strongly associated liquids like the alcohols, may increase. Because of the conflicting effects of thermal agitation and

intermolecular attraction, solutions may be obtained in which the polarization is almost independent of temperature. Many liquids show an increase in polarization with temperature instead of the decrease required by the Debye equation, and acetic acid and some of the octyl alcohols even show an increase in dielectric constant with rising temperature. The polarizations and dielectric constants of the isomers of octyl alcohol, the molecules of which presumably differ little in electric moment, differ greatly because of the different molecular force fields resulting from the different locations of the doublet in the molecule.

55. Location of the electromotive force in a photovoltaic cell. W. NORWOOD LOWRY, *Cornell University.*—A method was used patterned after that of Murdock (Nat. Acad. Sci. 12, 1926). In a Pt-Rhodamine B-Pt cell, curves plotted with e.m.f. and position of electrode in respect to the window, showed no sudden break in the slope of the curve when passing from a dark to an illuminated region, as had been previously observed in the case of current measurements. In another investigation it was found that the voltage sensitivity of the above type of cell increased with the concentration of the electrolyte. A voltage amplifier system was developed utilizing a 4-element vacuum tube, with which a sensitivity greater than 5,000 mm. per volt was obtained, with a current drain of an order of magnitude comparable to that of an electrometer, and with a period shorter than the latter. Some of the data were taken with this device, and the rest of the measurements were made with a Compton type electrometer.

56. Departure from Einstein's photoelectric equation with certain alkali metal films. W. B. NOTTINGHAM, *Bartol Research Foundation.*—Photoelectric current measurements with light near the long wave-length limits for sodium and potassium films on platinum gave 3.0×10^{-14} amp. at 8200A and 1.3×10^{-13} amp. at 9400A respectively. Light from the anode of a 15 amp. carbon arc was used. The long wave-length limit is probably greater than 8400A for sodium and 9600A for potassium. Miss J. Butterworth (Phil. Mag. **6**, 1 (1928)) reports 9700A for potassium from measurements of the "complete" photoelectric effect. Departures from Einstein's photoelectric equation have been found for both metals near their long wave-length limits with very thin films. The cell potential for zero current plotted versus the quantum energy for the different wave-lengths, expressed in their voltage equivalent, showed that the equation $Ve=\alpha h(\nu-\nu_\alpha)$ held with $\alpha=1$ for wave-lengths shorter than 5200A; $\alpha=2$ between 5200A and 5400A; $\alpha=3$ between 5400A and 6200A; and $\alpha>3$ for wave-lengths greater than 6200A. The range over which α has a constant value depends on the film thickness. When the film has the thickness which makes the photoelectric response and the long wave-length limit the maximum, α is unity over almost the entire range of wave-lengths.

57. Use of dielectrics to sensitize alkali metal photoelectric cells to red and infra-red light. A. R. OLPIN, *Bell Telephone Laboratories, Inc.*—A technique is described for greatly enhancing the photoelectric response of sodium and potassium surfaces in vacuum by the introduction of very small amounts of such dielectrics as sulphur vapor, water vapor, benzene, and organic dyes. Cells thus produced are far more sensitive to light of color temperature 2848°K than the best vacuum cells heretofore studied; the increase being due mainly to a striking red sensitivity, especially in the case of the sodium cells. Spectral distribution curves show the presence of new maxima, lying between λ5000 and λ5500A for sodium and between λ6000 and λ6500A for potassium, the former being much more pronounced. In each case λ_0 = approximately 1μ. The frequency difference between the regular and new maxima for each surface corresponds to a wave-length of about 1μ. This is the wave-length region at which the dielectrics used exhibit strong absorption bands. A theory is proposed which suggests a modulation of the exciting light at the cathode surface, the incident frequency combining with the characteristic vibration frequency of the dielectric. Extension of the theory to explain similar phenomena in the sensitization of photographic plates and in the field of fluorescence is suggested.

58. The preparation of photoelectric cells with thin films of lithium as the photoactive material. HERBERT E. IVES, *Bell Telephone Laboratories, Inc.*—Lithium is a difficult material to handle in a vacuum tube for the following reasons: (1) the shell of oxide which forms on a slug cut in air is too stiff for molten lithium, which is very light, to break through; (2) the

oxide distills at a lower temperature than the pure metal; (3) lithium rapidly attacks glass and platinum. It has been found possible to prepare thin films of lithium by the following process: A thin walled steel tube is driven through a slug of lithium so that on withdrawal of the tube a cylindrical rod of lithium is obtained which is protected from the air except on its two ends. A heavy steel rod is then inserted in the steel tube, above the lithium, and this, when the whole system is heated in vacuo by a high frequency field, forces the lithium out in a globule from which a thin film may then be distilled on to a plate of tungsten. This film at one stage in its formation is sensitive to red light as far out as λ6708.

59. On the emission of positive ions from hot tungsten. LLOYD P. SMITH, *Cornell University, Ithaca, N. Y.*—A decay in the positive ion emission over a long period of time has been noted at temperatures above 2600°K which were not previously found for a temperature of 2500° following a flash treatment. For a given temperature the ion current seems to approach a steady value. When the temperature is increased there is a decay from the new value down to a steady value which is higher than the previous steady value. Before the ion current is allowed to decay appreciably the heat of evaporation of the ions, determined by plotting the data according to the Langmuir evaporation equation for tungsten, may be as high as 8.3 volts. After heat treatment and partial decay of the ion current, it gradually decreases to 6.5 volts. After this value has been reached there is no further change regardless of further decay or heat treatment. Theoretical considerations have thus far failed to establish the nature of the ions but experiments are now under way to determine the ratio of their charge to mass.

60. Thermionic emission as a function of the amount of adsorbed material. J. A. BECKER, *Bell Telephone Laboratories, Inc.*—It is commonly assumed that the logarithm of i, the thermionic current from a cm² of tungsten at a fixed temperature, increases linearly with θ, the fraction of the surface covered with an electropositive element. Experiments with barium-on-tungsten show, however, that this assumption is untenable and that for $0 < \theta < 0.85$

$$\log i/i_0 = 1.1(\log i_1/i_0)(1-\epsilon^{-2.0\theta}) \qquad (1)$$

Subscripts indicate values of θ. θ is determined from the deposition time and is unity at the optimum activity. Log i increases principally because the work function ϕ decreases. Probably $\Delta\phi$ is caused by the existence of adsorbed Ba^+ ions. If N_p = number of ions/cm² and l = diameter of Ba^+,

$$\Delta\phi = -300 \cdot 4\pi N_p 4.77 \times 10^{-10} l \text{ volts} \qquad (2)$$

From Richardson's equation and (1) and (2) we conclude: for small θ, about 1 in 5 Ba particles are adsorbed as ions, the remainder being adsorbed as atoms; as θ increases the ratio of ions to atoms decreases; the tendency to form adsorbed ions is approximately proportional to the amount by which ϕ exceeds the resonance potential of Ba; when $\theta = 1$, about 1 in 10 adsorbed particles are ions.

61. Thermionic and photoelectric emission from caesium at low temperatures. L. R. KOLLER, *General Electric Co.*—Cathodes consisting of very thin films of caesium on caesium oxide on silver have been found to give high values of thermionic emission at very low temperatures. Measurements of emission have been made at different temperatures and the emission was found to follow the equation $I = AT^2 e^{-b/T}$ over a range of from 373 to 443°K. Above this temperature the cathode surface deteriorates. The constants determined from a plot of this equation were $A = 9.8 \times 10^{-2}$; $b = 8{,}700$. The cathodes used had an area of 10 cm² and were formed directly on the bulb wall so that it was possible to heat them by immersing them in a temperature bath. This large surface makes it possible to measure thermionic emission at temperatures below 473°K. These cathodes are also highly photo-sensitive, giving about 5 microamperes per lumen of incident light from a tungsten filament at 2465°K. The photoelectric current was measured over the same range of temperature as the thermionic current. Under these conditions it was possible to measure at the same time photoelectric and thermionic currents of the same magnitude. The photo-current was found to show a slight positive temperature coefficient.

62. Thermionic emission from tungsten and the Schottky equation. H. L. VAN VELZER AND W. R. HAM, *Pennsylvania State College.*—Values of the thermionic currents from tungsten filaments show that the Schottky relation

$$\log i = \log i_0 + e^{3/2}(dV/dx)^{1/2}/(kT)$$

can be verified with sufficient accuracy to furnish a satisfactory method of determining the electronic charge, e. The behavior of the current from small wires during the process of "clean up" is similar to that found by Millikan and others and there is a temporary clean up by intense electrical fields above that that may be obtained by ordinary methods. Using extended high voltage clean up, Shottky's equation appears valid for tungsten up to 10^8 volts/cm. No upper limit is indicated.

63. Schottky effect and contact potentials of thoriated tungsten filaments. N. B. REYNOLDS, *Princeton University.*—Becker and Mueller's experiments on the lack of saturation of thermionic currents from thoriated filaments have been repeated under a variety of conditions. The point of departure of the curves from the theoretical Schottky line seems independent of the amount of thorium present on the surface, and to depend only on the field. At gradients of 10000 volts/cm and higher, Schottky's equation applies accurately. Subjecting the filament to positive ion bombardment with ions of above 500 volts velocity causes a subsequent greater deviation from this line, making it difficult to attain saturation with gradients of 30000 volts/cm. The emission at high fields may be actually increased by this process, suggesting a possible roughening of the surface. The variation in contact potential of a thoriated filament with θ, the fraction of the surface covered with thorium, has been investigated by a method of retarding fields. There is a positive temperature coefficient, and taking this into account, the change in contact potential with θ agrees quantitatively with the resultant change in b_0 of the thermionic emission equation. The emitted electrons are found to have a Maxwell's velocity distribution, except near the zero of potential, which is now being investigated.

64. The use of the Schottky relation in the determination of the thermionic work function of tungsten. W. R. HAM, *Pennsylvania State College.*—Thermionic emission data for tungsten suggest a method, independent of T, of measuring and examining ϕ, the work function, as follows. The thermionic equation assumed is $i_0 = A\,\epsilon^{-(\phi_0/kT)}$. Substituting in Schottky's equation $i = i_0 \epsilon^{e^{3/2}(dV/dx)^{1/2}/kT}$ we have $i = A\,\epsilon^{\phi_0/kT + e^{3/2}(dV/dx)^{1/2}/kT}$ and taking logarithms

$$\log i = \log A - [\phi e + e^{3/2}(dV/dx)^{1/2}]/kT.$$

If data of $\log i$ and $(dV/dx)^{1/2}$ are plotted for a particular T

$$\log A - \phi e/kT = I \qquad \text{(the intercept)} \qquad (1)$$

$$e^{3/2}/kT = S \qquad \text{(the slope)} \qquad (2)$$

or

$$\log A = I + \phi S/e^{1/2}.$$

And for a family of such curves taken at different temperatures and ϕ considered constant

$$\phi = e^{1/2}(-\delta I/\delta S)$$

Hence, if plotting I against S for such data, we obtain a straight line we may conclude that ϕ is constant for the thermionic equation with which we started; i.e., the T^2 equation. If, on the other hand, a linear relation is not found, we can determine by the deviation from a straight line just how ϕ varies with temperature and hence experimentally arrive at the correct form of thermionic equation for ϕ constant. An advantage of this method is that precise measurements of temperature are not necessary and the values of dV/dx, the potential gradient, need be only relatively accurate.

65. Molecular rays of hydrogen chloride in an electric field. M. J. COPLEY AND W. H. RODEBUSH, *University of Illinois.*—In this work a beam of hydrogen chloride molecules of initial temperature −80°C is passed through the inhomogeneous electrostatic field between a wire and a cylinder which are at a difference of potential of about 10,000 volts. The beam

is 0.04 mm in width and the value of $\partial E/\partial r$ is 10^8 volts/cm^2. The field is produced by a transformer and condenser with a kenetron. The hydrogen chloride molecules are condensed on a liquid air-cooled target upon which a layer of ammonia has first been condensed and an image of ammonium chloride is formed which is easily seen, although difficult to photograph. Preliminary results indicate that a large fraction of the molecules are deflected in the field since the central portion of the image is almost obliterated but it has not yet been possible to obtain a clear image of the deflected beam.

66. Effect of crossed electric and magnetic fields on the helium spectrum. J. S. FOSTER, *McGill University.* (*Assisted by National Research Council of Canada.*)—New lines appear in the helium spectrum when the source is subjected to crossed electric and magnetic fields. Some of these are found near the diffuse series lines (λλ4472, 4388, 4026) with nearly twice the separations observed for the fundamental combination lines in the Stark-effect.

67. Zeeman effect in MgH. F. H. CRAWFORD AND G. M. ALMY, *Harvard University.*—The MgH band at λ5211 ($^2P \rightarrow {}^2S$) consists of three branches of narrow doublets. In a magnetic field the behavior of each branch is qualitatively the same. For high j it is about as follows: At 8300 gauss the doublets are unsymmetrically widened to around 5/4 of their no-field separation and fairly sharp, with a faint continuous band between. As the field is increased, this faint band increases in intensity, its width remaining slightly less than the no-field separation. The outside components move out and become fainter. Their separation at 16000 gauss is about twice that of no-field, at 28400 about three times (observed only in P branch). For lower j (4 1/2 to 9 1/2) the above behavior is modified. At 8300 gauss each member of the doublet is diffusely broadened to approximately $2\Delta\nu_n$ the intensity distributions being complementary. Thus the low frequency member is most intense in the center, while the high frequency one appears as a doublet. As the field is increased, a single pattern is obtained for the doublet, most intense at the edges, of width somewhat less than the no-field separation. For lowest j (1/2 to 3 1/2) the patterns of the observable lines are resolved, increasing in width and complexity with the field.

68. Interaction of the Stark effect and electronic spin in alkalis. V. ROJANSKY, *Washington University.*—As pointed out to the writer by Professor J. H. Van Vleck, the matrix approximation formulas for the energy levels of a non-degenerate system, when applied to the evaluation of the Stark levels of non-hydrogenic atoms in a weak electric field, cannot be expected to give accurate results throughout the range of the (weak) field. In fact, in the case of alkalis, after the original Hamiltonian H_0+H_1 is transformed by the proper first order canonical transformation, terms of the type $(n, l, j; n, l, j \pm 1)$ appear in the new (second order) Hamiltonian. The frequencies associated with these terms are relatively very small, and thus the system should be treated by methods appropriate to degenerate systems, especially when the Stark separation (which is a second order effect in non-hydrogenic atoms) is comparable to that of the fine structure. Physically, in fields which produce such separations the multiplet structure should be distorted, and intensity redistributed. For small fields the effect should be negligible. The corrected expressions for the energy levels and the transformation functions necessary for the calculation of relative intensities were thus found. Comparison with experiment has not yet been carried out.

69. Relative intensities of Stark components in helium. G. O. LANGSTROTH (*Canadian National Research Bursary*), *McGill University.* (*Introduced by J. S. Foster.*)—Quantitative measurements of the relative intensities of individual Stark components in two typical helium line groups (λλ4388, 4026) have been made. The agreement with the theory based on quantum mechanics is somewhat better that that noted by Dewey, (Phys. Rev. **30**, 770 (1927)), there being no really serious departure from the predicted values. The method of measurement employed is a variation of Koch's procedure and depends on the use of a neutral wedge for the production of the intensity marks. A useful feature in this research is the development of a Lo Surdo tube in which the electric field is uniform through an appreciable portion of the Crookes' dark space. This permits the Moll photometer to operate at its maximum efficiency.

70. Extreme ultra-violet spectra of Ne and A excited by electrodeless ring discharge. K. T. COMPTON, J. C. BOYCE AND J. L. NICKERSON, *Princeton University.*—High frequency currents from an oscillator giving between 0.25 and 3.5 K. W. traversed ten turns of wire surrounding a discharge tube located at the slit of the vacuum spectrograph. Whereas spectra excited by controlled electron impacts show only arc and first spark lines, the electrodeless ring discharge brings out higher stages of excitation. Some differentiation between these is possible, since increased gas pressure and decreased energy input relatively intensify lower stages of ionization, and vice versa. Gas is driven in large quantities into the glass of the discharge tube, whence it gradually comes out again to contaminate later spectra unless special precautions are taken. We find for Ne III, ionization potential 63.2 volts or 511,700ν, and higher limits at 545,350 and 566,517 approximately. Metastable singlet states are at about 22,300 and 52,250 above the low triplet state. Two triplet series of three members each and one singlet series of two are found, as well as the low quintet state, and the low states associated with the higher limits. All predicted a–b lines are found. Similar though less complete analysis of A III gives its ionization limit as 329,476. a–b lines of Ne IV and A IV are strong, but those of Ne V and A V are, if present, too weak for identification.

71. Low voltage electron impacts in hydrogen. F. G. SLACK, *Vanderbilt University.*—Observations were made on the effect of electron impacts with hydrogen in a three electrode tube with unipotential, oxide coated, hot filament. The gas was streamed through the tube at pressures from 0.05 to 0.50 mm of Hg. Curves showing the variation of current from filament to grid-plate with varying accelerating potentials agree in general with those reported by Duffendack (Phys. Rev., **20,** (1922)), Olmstead (Phys. Rev., **20,** (1922)), and by Richardson and Tanaka (Proc. Roy. Soc., **106A,** (1924)). The breaks below 10.2 volts in the curves of Richardson and Tanaka, attributed by them to the presence of Hg vapor, are entirely missing thus confirming their suspicions. Spectroscopic observations were made in the field free region between the grid and plate. Photographs show no Balmer lines but some of the secondary spectrum at 13 volts in pure hydrogen. No means other than the electron impacts were used to increase or produce radiation.

72. Simultaneous ionization and excitation by positive ions and excited atoms. O. S. DUFFENDACK AND H. L. SMITH, *University of Michigan.*—An extension of an investigation of the simultaneous ionization and excitation of diatomic gases admixed with a rare gas (Phys. Rev. **29,** 914 (1927)) reveals that both ions and excited atoms are effective. By adding hydrogen to He-CO and Ne-CO mixtures a comparison of the effectiveness of the two types of impacts in producing certain excited states of CO^+ could be made. Hydrogen has a marked quenching action on the production of the A′ state of CO^+, the initial level on the comet tail bands, particularly when excited Ne atoms were used for its excitation. This action is probably due to the nearness of the values of the ionizing potential of H_2 and the minimum radiating potential of Ne.

73. The excitation of N lines by controlled electron impact. LOUIS A. TURNER AND E. W. SAMSON, *Princeton University.*—The $3s^4P - 3p^4P$ lines of N at 8200A are produced by bombardment of N_2 at a pressure of 0.05 mm with electrons having 22.3 volts or more of energy. The behavior of the intensity of the lines with changes of exciting current and pressure indicates that they result from a primary process of dissociation of N_2 into a neutral atom and an excited atom, as suggested by Herzberg. Since the excited atom has 11.8 volts of energy an upper limit of 10.5 volts for the heat of dissociation of N_2 is obtained in agreement with the conclusion of Mulliken and Birge that its value is considerably less than 11.4 volts. The correction to the applied voltage was obtained by determining the ionizing potential of Hg vapor present, using the Hertz-Kingdon method. The value of 22.3 volts may be several tenths of a volt too high because of the difficulty of determining the exact voltage for disappearance of the lines and a slight uncertainty concerning the correction to the voltage to be deduced from the measurements of the ionizing potential of Hg.

74. The mean life for the spark spectrum of mercury. L. R. MAXWELL, *National Research Fellow. The Bartol Research Foundation.*—By using the method for determining the life of excited states recently described by the writer (Phys. Rev. **32,** 721 (1928)), the following results have been obtained for several lines of the mercury spark spectrum;

Wave-length (A)	Type of Spectrum	Mean Life (sec.)
3090 (E_2)	Hg III	6×10^{-7}
3312 (E_2)	Hg III	4×10^{-7}
3114 (E_3)	Hg IV	9×10^{-7}
2572 (E_3)	Hg IV	8×10^{-7}

These results indicate that the life of the excited states for the triply charged ion is slightly greater than for the doubly charged. The mean life for the lines of Hg II have not been measured but are estimated to be of the order of 10^{-8} seconds. From current-light intensity measurements it is found that at a single electron collision the atom is multiply ionized and excited. This experimental result substantiates the assumptions made in calculating the mean lives given in the above table.

75. Decay of the spectrum of the afterglow of nitrogen mixed with argon. A. G. WORTHING AND H. E. WAY, *University of Pittsburgh.* The afterglow chamber consisted of a glass bulb with tungsten terminals and was filled with a mixture of the order of 99 percent A and 1 percent N at a pressure of about 2 cm of Hg. Periodic discharges, followed in succession by exposures to different parts on a photographic plate in a spectrograph, yielded three spectrograms of the afterglow in succeeding stages. Using notation of the I. C. Tables, the early stage showed a maximum in the orange sequence for the 8→4 vibrational transition and in the red sequence for the 8→5 and the 4→1 transitions. The third stage showed maxima for 11→7, 9→5, and 9→6 transitions, and a tendency to a maximum at 11→8. The second stage showed an intermediate shift. At the same time decay tended to strengthen the orange sequence relative to the red sequence. With time the afterglow spectrum seemed to approach that in pure nitrogen. Metastable argon atoms interspersed with the neutral nitrogen molecules transferring energy by collisions of the second type to neutral nitrogen molecules and exciting them to B_3 and B_4 stages seems a possible explanation. It is necessary to suppose that this process decays faster than does the normal pure nitrogen afterglow.

76. Spectra in condensed discharges. J. W. BEAMS, *University of Virginia.*—Light emitted by an electric spark occurring between metallic electrodes in air together with that emerging from condensed discharges at low pressures has been studied by means of a mirror rotating 1600 revolutions per second. The rotation of the mirror was obtained by the method of Henriot and Hunguenard (Jour. d. Phys et Ra. **8,** 443 (1927)) as modified by Lawrence, Beams and Garman (Phys. Rev. **31,** 1112 (1928)). Photographs of single discharges were obtained, one millimeter on the plate corresponding to 5×10^{-8} sec. The velocities of propagation of the luminosity of various metallic vapors in the spark previously studied by Schuster and Hemsalech and others (Baly Spectroscopy, Longmans, 1912) have been measured. The time of appearance of the spectrum lines was found to be in accord with the values obtained by the Kerr cell method (Phys. Rev. **28,** 475 (1926)). The air lines appeared first followed by the spark lines and later the arc lines of the metal. The air lines die out first followed by the spark and finally the arc lines of the metallic vapor. The photographs indicate that the spark at first appears as a narrow thread then, during its initial stage, expands radially.

77. The photo-ionization of the vapors of caesium, rubidium and potassium. ERNEST O. LAWRENCE AND N. E. EDLEFSON, *University of California.*—A modification of the space charge method of Foote and Mohler has been devised which compensates out the effects of temperature changes, thereby allowing full use of the great inherent sensitivity of the space charge method. A water-cooled hydrogen discharge tube carrying 5 amperes at 3000 volts served as a source of continuous ultra-violet light of great intensity. The ionization efficiency of the light in caesium and rubidium falls off continuously from their respective series limits to shorter

wave-lengths. Potassium shows a striking dissimilarity in qualitative confirmation of the previous observations of Williamson (Proceedings of the National Academy, **14,** 793 1928)) and Lawrence (Philosophical Magazine, **1,** 345 (1925)). The probability of ionization in potassium vapor is a maximum at the series limit and falls off rapidly to 2710A where the ionization increases to a second maximum at 2340A where it again rapidly decreases. The ionization efficiency at 2340A is about three times its value at the series limit. The separation of these two maxima is equivalent to 0.96 volt. Spectroscopic data give 0.8 to 1.0 volt for the heat of dissociation of K_2, indicating dissociation plus ionization as the origin of the second maximum.

78. Photo-ionization of alkali vapors. F. L. MOHLER AND C. BOECKNER, *Bureau of Standards.*—Relative measurements of photo-ionization of caesium, rubidium and potassium as a function of the wave-length have been made by the space charge method as well as absolute determinations by a direct method for the first two elements. The sensitivity drops rapidly from the limit to about a tenth of the maximum value at 600A beyond the limit in both caesium and rubidium. Ion current measurements give the atomic absorption coefficients at the limits as 2.3 and 1.1×10^{-19}, respectively. The sensitivity of potassium is low at the limit and increases rapidly from 2600A to 2200A in agreement with published results. Absorption measurements in caesium vapor at low pressure, as well as computations using the principle of detailed balance and the intensity of the recombination spectrum, give values agreeing in magnitude with the photo-ionization value of atomic absorption at 3184A.

79. Determination of the orientation of single crystal specimens of metals of the hexagonal system. THOMAS A. WILSON, *General Electric Co., Department of Chemistry, Union College.*—The x-ray method previously described (Bulletin of the Physical Society Vol. **4,** No. 1) for cubic metal single crystals has been extended to crystals of the hexagonal system. The equations for the interperpendicular angles have been derived. The necessity of using symmetrical photographs has been eliminated, so that one Laue photograph alone is needed to fix the orientation. The method has been applied to zinc crystals grown according to the method of Mathewson and Phillips (Am. Inst. Min. Met. Eng. Preprint 1623-E Feb. 1927). A twin has been shown present in a poorly formed crystal.

80. Experimental evidence for the filling of electron levels from the relative intensity of x-ray lines. SAMUEL K. ALLISON, *University of California.*—According to the accepted theory of the periodic system, electrons first enter the 5_3 orbits at 57 La; only one electron remaining in these orbits until 72 Hf from whence the orbits fill up to 10 electrons at 78 Pt or 79 Au. The $L\beta_3$ line is double, representing the transitions 5_{22}, $5_{23} \rightarrow 2_{22}$. In a previous paper (Phys. Rev. **32,** 1 (1928)) the author found that this line was about 32 times more intense (relative to lines involving more deeply buried orbits) in the uranium than in the tungsten L series. This paper reports intensity measurements involving this line in 76 Os, 77 Ir, 78 Pt, 79 Au, 81 Tl, 82 Pb, 83 Bi. The experiments were carried out at a voltage about 2.66 times the average of the critical excitation voltages for the L series in each case. A curve showing the ratio of the intensities $L\beta_3/L\beta_1$ as a function of the atomic number rises rapidly with increasing atomic number and takes a sharp upward jump between 78 Pt and 79 Au. This indicates that the first element in which 10 electrons occupy the 5_3 orbits in an approximately undisturbed condition in the solid state is 79 Au. The curve is similar to one obtained in the region about 46 Pd for the lines $L\beta_2$ and $L\gamma_1$ by Jönsson (Zeits. f. Physik **41,** 221 (1927)).

81. Diffraction of x-rays in liquids: isomers of n-octyl alcohol. G. W. STEWART, *University of Iowa.*—Through the kindness of Professor E. Emmet Reid of Johns Hopkins University, the following carefully prepared isomers of n-octyl alcohol were tested: four octanols and sixteen heptanols. The conclusions are: (1) That the polar group OH produces a molecular chain doubling only when it is attached to the carbon at the end or next to the end of the chain. (2) That the molecular space arrangement or cybotactic condition in the isomers is usually sufficiently marked to give two sets of intersecting planes containing diffracting centers. (3) That the arrangement of molecules in a second set of planes is most conspicuous when the OH is attached at the center of the molecule. (4) That the CH_3 in a branch causes an increase in the

diameter of the chain of 0.25A and 0.50A, apparently depending upon the distance from the OH group. (5) That the chain remains a fairly rigid one, in contrast to the chain in the case of paraffins. The results as stated assume the validity of Bragg's Law and the correctness of the view of the author as to the cybotactic condition.

82. Wave-length measurements of L lines (Zn to Ca). CARL E. HOWE, *University of Chicago.*—Using the first inside order from a plane grating, (600 lines to the millimeter) L lines of Zn, Cu, Ni, Co, Fe, Mn, V and Ca have been measured. The wave-lengths extend from Zn $L\alpha_1$ (12.2A) to Ca L_1 (39.7A). With few exceptions, for the elements from Zn to Mn inclusive, four lines ($L\alpha_1$, $L\beta_1$, $L\eta$, L_l) have been measured. The $L\alpha_1$ line of V (origin $M_{32}\rightarrow L_{22}$) appears to be present thus indicating at least one electron in the M_{32} level of V. Measurements of the lines of Cr, V and Ti now in progress will probably give definite information on this point. Neither the $L\alpha_1$ nor the $L\beta_1$ line of Ca was observed as is to be expected. Separation of the lines was attained by adjusting the grating so that the angle between the inside order and the plane of the grating is small. Under this condition the angular dispersion is given by $\Delta\alpha=\Delta\lambda/(D\beta)$ where D is the grating space and β the small angle between the plane of the grating and the first inside order. All measurements are absolute.

83. On the determination of the wave-length of x-ray satellites. F. K. RICHTMYER, *Cornell University.*—A densitometer record of an x-ray (diagram) line and its satellites shows the latter as a complex structure on the side of the former. Only if one knows the exact shape of the densitometer record through the diagram line alone (i.e., without satellites) can one, by substraction, determine the satellite structure, and thus the wave-lengths of the satelline components. For this purpose, advantage may be taken of the fact that the excitation potential of the satellites is some 25 percent higher than that of the parent line. If a spectrum plate of the parent line be obtained at, say, 20 percent above its excitation voltage, the satellites are either absent or relatively very weak. By comparing the densitometer record of such a plate with one obtained at higher voltages, a less ambiguous record of the satellite structure is obtainable

84. Absolute wave-length of the $K\alpha$ and $K\beta$ lines of Cu. J. A. BEARDEN, *University of Chicago.*—Using plane optical gratings ruled with 50 and 600 lines per mm, spectra of the K series of Cu have been obtained. The $K\alpha$ lines were not resolved but the mean wave-length was found to be $K\alpha=1.5439\pm0.0002$. This is about 0.36 percent higher than previously reported measurements by this method and also 0.36 percent higher than given by crystal measurements. The $K\beta=1.3940\pm0.0002$, which is about 0.34 percent higher than the crystal measurements give. The $\pm$ values given are the probable errors obtained in taking the average of 10 plates. All of these plates were taken under different conditions and many of the plates had 8 measurable orders. The angles were measured by using two plates, one 8 cm from the grating and the other 205 cm from the grating. The plates were parallel to within 5 sec. of arc and the distance between them was measured to one part in 50000. The gratings were centered over the axis of rotation of the spectrometer by the use of an interferometer. The interferometer was also used to make sure that the grating did not move during an exposure. The measurements of the distance between the plates and the separation of the lines on the plates have been carefully checked by independent observers in order to find if there was a consistent error which was being overlooked. These results give a value of the electronic charge $e=4.824\times10^{-10}$ and Avogadro's number $N=5.999\times10^{23}$.

85. Temperature and the Compton effect. G. E. M. JAUNCEY AND H. BAUER, *Washington University, St. Louis.*—The intensity of x-rays reflected from a crystal decreases with temperature. According to Debye (Ann. d Physik **43**, 49) this decrease in intensity should be accompanied by an increase in the intensity of the rays diffusely scattered by a crystal, but Jauncey (Phys. Rev. **20,** 405 and 421) has shown that this increase is either zero or very small. The effect of temperature on the ratio of modified to unmodified scattered x-rays has therefore been examined. Using DeFoe's method (Phys. Rev. **27,** 675) an aluminum absorbing sheet was transferred from the primary beam to the scattered beam and the ratio of the two ionization cur-

rents found at room temperature and also when the scattering substance was heated to 565°C. Wave-lengths ranging from 0.35A to 0.62A were scattered by carbon at angles of 60°, 75° and 90° and no definite effect of temperature was observed. In five cases the ratio was slightly less and in four cases slightly greater at the higher temperature. In each case the difference between the cold and hot ratios was not greater than the probable error of each ratio. Similar results were obtained for scattering from aluminum and copper.

86. Fine structure in the Compton effect. BERGEN DAVIS AND HARRIS PURKS, *Columbia University.*—A continuation of two crystal analysis of fine structure of scattered radiation: A special x-ray tube was constructed with small piece of graphite near the target spot. Mean angle of scattering was $\theta = 155°$. The displaced radiation had fine structure as follows going toward long wave-lengths: A relatively strong line 0.0421A from Mo $K\alpha_1$ position, and then three weaker lines at 0.0012A, 0.002A and 0.0109A from this strong line. These agree with the fine structure previously found in the undisplaced scattered radiation. (Davis and Mitchell, Phys. Rev. **32,** 331 (1928)). The two pictures are alike but the displaced one is shifted 0.0421A from the undisplaced. The displacement is less than is to be expected from $d\lambda = 0.0243\,(1-\cos\theta)$. Our results give $d\lambda = 0.022\,(1-\cos\theta)$. This is about 9 percent smaller than required by theory. Our errors cannot be as great as this. Beryllium, investigated at $\theta = 163°$, gives a strong main line at $0.0446\text{A} = 0.0228\,(1-\cos\theta)$ from $K\alpha_1$ position and a line at 0.0051A from this main line. This agrees with the Be K energy level. A weak line 0.00087A toward short wave-length from main line. The last two were also observed in undisplaced radiation by Mitchell and described at the December meeting of this society.

87. On the polarization of x-radiation from mercury vapor. WILLIAM DUANE, *Harvard University.*—Experiments have been described on the x-radiation coming from the impacts of homogeneous electron rays against mercury vapor atoms. This paper deals with experiments on the polarization of this x-radiation. The x-ray tube employed was substantially the same as that previously described, except that the mercury vapor from the electric furnace passed down into a tube cooled with liquid air. The polarization was tested by means of the secondary radiation scattered from a block of carbon struck by the primary radiation. The secondary radiation was detected and its intensity measured in different directions by means of a point counter, similar to that which I described in the Comptes Rendus for July 18, 1910. (Since that date, these point counters have been greatly improved by Geiger and others.) Experiments on the radiation coming from the mercury vapor at right angles to the stream of electrons showed that this radiation was largely, but not completely, polarized. The secondary radiation coming from the block of carbon in a direction parallel to the stream of electrons was about 0.37 as intense as that coming from the block of carbon at right angles to the stream.

88. Reflection of electrons and its application to the design of molybdenum target water cooled Coolidge tubes. H. R. KIEHL, W. R. HAM, M. W. WHITE AND W. P. DAVEY, *Pennsylvania State College.*—Calorimetric measurements previously made on molybdenum target Coolidge tubes indicated that approximately twelve percent of the energy input to the tube was reflected to the walls at 14 kv and 3.00 ma. Later experiments on similar tubes showed an electron current along the walls to the anode during this reflection, which was probably due to the increased conductivity of the glass during electron bombardment. Failure of the tube due to cracked glass was attributed to local heating. Occasionally minute portions of the walls even become melted. The tube was accordingly redesigned by one of us in order to reduce the reflection to the walls by decreasing the cathode-anode distance to 0.3 centimeter. Using the new design, calorimetric measurements showed a reflection of roughly 1/3 that of the old type tubes. The average life of 26 old type tubes was 538.5 hours. On the same group of apparatus, one new type tube has already been run 5340 hours, one 3607 hrs. and one 1830 hours at 20–25 ma, 30 kv, and one tube 556 hours at 40–45 ma, 30 kv. All of these tubes are still in successful operation. These results clearly show the dependence of the length of life of such tubes upon the electron reflection to the walls.

89. Separation and relative intensity of the diagram-components of the $L\beta_2$ line by means of the double x-ray spectrometer. SAMUEL K. ALLISON, *University of California.*—According to the energy level diagram applicable to atoms which have lost one electron from an inner level the $L\beta_2$ line should be double, since it consists of electron transitions from the levels N_{IV}, $N_V \rightarrow L_{III}$. Crofutt (Phys. Rev. **24,** 9 (1924)) claims to have measured the weaker component of β_2 in tungsten (74) calling it β_{1b}. The present paper describes the results of investigation of the line $L\beta_2$ in 77 Ir, 81 Tl, and 92 U. In 77 Ir the line $L\beta_2$ has such a great intrinsic breadth that $L\beta_{1b}$ cannot be separated from it although the dispersion and resolving power of the instrument are ample. In 81 Tl a better but not complete resolution is obtained, due to the fact that in this case $L\beta_2$ is considerably narrower. In 92 U a practically complete resolution is obtained with the crystals both in the first order since here the lines are intrinsically narrower still. The average of two results for uranium gives $\Delta\lambda = 1.85$ X.U. or $\Delta\lambda/\lambda = 0.24$ percent. Calculation from the combination principle using M-series wave-lengths by Lindberg (Zeits. f. Physik **50,** 82 (1928)) gives $\Delta\lambda = 1.93$ X.U. The ratio of the intensity of β_2 to β_{1b} should be 9 to 1 by the Burger-Dorgelo rules; the average of 1 value for 81 Tl and two for 92 U gives 9 to 0.9 which is within the experimental error.

90. The band spectrum of silver chloride. BROOKS A. BRICE, *New York University.*—A system of bands in the ultra-violet due to AgCl has been obtained with a special discharge tube by viewing the region immediately above a trough-shaped Pt electrode covered with the fused salt. Excitation is by means of an induction coil or a transformer. Hydrogen is present at 1 to 2 mm pressure. Lines of H and Cl and Ag also occur. The bands are not obtained when AgBr or Cu_2Cl_2 are used on the electrode, or when bare Pt electrodes are used. The bands are shaded to the red, and extend from λ3140 to λ3226. Three sequences are observed, the bands of each sequence being closely grouped. The intensity distribution indicates a small change in the moment of inertia in the emission. The heads of the bands are given by

$$\nu = 31570 + n'(275.6 - 6.25n') - n''(344.7 - 1.86n'')$$

No evidence of electronic multiplicity is found. Four bands due to the fainter isotopic system $AgCl^{37}$ are observed. The theoretical isotopic displacements for the (0,1), (1,2) (2,3) (3,4) bands are 7.1, 8.5, 10.1, 11.9 cm^{-1} respectively. The measured values are 7, 9, 11, 10 cm^{-1}.

91. Fine structure of the beryllium fluoride bands. F. A. JENKINS, *New York University.*—The ultra-violet band spectrum of BeF, first observed by Datta, has been photographed with sufficient resolving power to permit the quantum analysis of the rotational structure. Each band has six branches, designated (in the order of decreasing frequency) R_2, R_1, Q_2, Q_1, P_2, P_1. Heads are formed by R_2, R_1, and Q_1. The combination relations between the R and Q branches have been found for the (0,0) and (1,0) bands, as well as the relations $R - Q \cong Q - P$ in the (0,0) band. These show a double initial set of terms, and a single final set. Hence the bands are probably $^2P \rightarrow {}^2S$, similar to those of the homologous molecules BO and CN. The system-origin is at $\nu = 33{,}186.0$, and for the ^2P state $\Delta\nu = 19.6$, approximately. Preliminary values of the band constants are, $B' = 1.405 - 0.018\ n'$, $B'' = 1.474 - 0.015\ n''$. The internuclear distance in the ^2S normal state is therefore 1.365×10^{-8}cm. The relatively small value of $\Delta\nu/B$ in the upper state gives a large rotational distortion, the doublet separation contracting rapidly and approaching a nearly constant value of 2.0 cm^{-1} above j_k = about 30. The doublet separations are accurately the same for $R(j_k - 1)$, $Q(j_k)$, and $P(j_k + 1)$.

92. A new band system probably due to singly ionized HCl. BROOKS A. BRICE AND F. A. JENKINS, *New York University.*—When a transformer discharge occurs in a continuous flow of HCl at a pressure of about 1 mm, a bright green glow is observed in the region close to the electrodes. Lines of H, and spark lines of Cl and Pt are obtained from this glow. A system of bands is obtained extending from λ2830 to λ3966. Their coarse structure shows them to be due to a hydride. The experimental evidence shows Cl to be the other element of the emitter. The same bands appear in a discharge in hydrogen with Pt electrodes covered with AgCl or Cu_2Cl_2, but not with AgBr, and not with bare Pt electrodes or bare Ag electrodes. Exact meas-

urements of the heads are difficult because the origin is apparently very near the head, and the structure is coarse. On account of an unusual intensity distribution, it has not yet been possible to assign true vibrational quantum numbers. The bands form a doublet system with $\Delta\nu = 663$ cm^{-1}. The heads are given by

$$\nu = \begin{cases} 28446 \\ 27783 \end{cases} + 1561p - 36.3p^2 - 2569n$$

the observed values of (p, n) being $(-1,0)$, $(0,0)$, $(1,0)$, $(2,0)$, $(3,0)$, $(4,0)$, $(5,0)$, $(0,1)$, $(3,1)$. Preliminary examination of the structure indicates that of a $^2S \rightarrow {}^2P$ system, which is to be expected for HCl^+ on theoretical grounds.

93. Vibrational levels and potential energies of diatomic molecules. PHILIP M. MORSE, *Princeton University.*—An exact solution is obtained for the Schroedinger equation representing the motions of the nuclei in a diatomic molecule, when the potential energy function is assumed to be of a form similar to those calculated by Heitler and London and others. The allowed vibrational energy levels are found to be given by the formula

$$E(n) = E_e + h\omega_0(n+\tfrac{1}{2}) - h\omega_0 x(n+\tfrac{1}{2})^2$$

which is known to express the experimental values quite accurately in most cases. An empirical law is found relating the normal molecular separation r_0 and the classical vibration frequency ω_0, which is that $r_0^3\omega_0 = K$ to within a probable error of 4 percent for 21 cases. Constant K has the same value for all diatomic molecules and for all electronic levels. By means of this law, and by means of the solution above, a quite accurate representation of the potential energy function can be obtained for any electronic level where ω_0 and $\omega_0 x$ are known experimentally.

94. The explanation of a critical potential of oxygen ($O_2 \rightarrow O^+ + O$) and the intensities of the ultra-violet O_2^+-bands. E. C. G. STUECKELBERG, *Princeton University.*—Observations by Hogness and Lunn, Smyth and Stueckelberg give evidence that O^+ is formed from the neutral molecule by a single electronic impact of energy between 20 and 21.6 volts. Potential energy curves of several states of O_2 and O_2^+ were plotted by a method given by Philip M. Morse in the previous paper. The values of r_0 for the states of O_2^+ (not known experimentally) were calculated from the law $r_0^3\omega_0 = 3000$A cm^{-1}, mentioned in the previous paper. The most probable transition from the normal state of the neutral molecule to the initial state of the ultra-violet O_2^+-bands goes to a part of the curve of this state, where the vibrational energy is equal to the energy of dissociation. This explains the above experiments. The intensities of the ultra-violet O_2^+-bands were calculated by the method of Condon from the obtained energy curves. The good agreement with the observations by Johnson provides an additional check for the above assumptions and the law for r_0.

95. New terms of the oxygen arc spectrum. RUDOLF FRERICHS (*Fellow of The International Education Board*), *University of Michigan. (Introduced by R. A. Sawyer.)*—The oxygen arc spectrum consists of three systens, *A*, *B*, *C*, which are built up respectively from the three low terms, ^4S, ^2D, ^2P of the configuration $2s^2$, $2p^3$ of the oxygen ion. The system *A* was analyzed by Runge and Paschen and completed by Hopfield's discovery of the lowest ^2P term. It consists of triplets and quintets. Terms of the two other systems have not been found previously, although they are of especial interest since the green auroral line has been explained as forbidden transition between the lowest terms ^1S and ^1D of the systems *C* and *B* respectively. With the use of an intense source and a 6.5 meter concave grating the structure of some of the unclassified oxygen groups has been determined and some new groups have been discovered. A low term of the *B* system is a ^3D term (8702, 8690, 8682) which combines with the *P* term (21206) of system A. A combination of the ^3D term with the lowest ^3P term of system *A* is the diffuse triplet λλ988–990 given by Hopfield. The ^3D term also combines with negative terms of the *B* system, two of which give the two triplets given by Runge and Paschen at λλ6260 and 5410. A strong incompletely resolved group of fine lines at λ8230 gives an additional negative ^3D term. The investigation is being continued.

96. Some multiplets in the spectrum of doubly ionized copper, Cu III. R. C. GIBBS AND ALICE M. VIEWEG, *Cornell University.*—The lowest terms in the spectrum of doubly ionized copper arise from the electron configuration $3d^9$, and successively higher terms from the configurations $3d^84s$, and $3d^84p$. Aided by analogy with the arc spectrum of cobalt, Co I, and the first spark spectrum of nickel, Ni II, some of the quartets and doublets, as well as intercombinations, arising from the transition $3d^84p$ to $3d^84s$, have been identified in copper. Several lines arising from the transition $3d^84p$ into the lowest configuration, $3d^9(^2D_{2\frac{1}{2}})$, have also been classified in the region of 800A. The authors expect to extend this analysis into the spectrum of Zn IV, and possibly Ga V.

97. The infra-red arc spectra of carbon and nitrogen. S. B. INGRAM, *National Research Fellow, University of Michigan.*—The spectrum of a carbon arc in air at sufficiently high current densities brings out strongly the arc spectra of carbon, nitrogen and oxygen. Using as a light source such an arc run at 125 amperes the wave-lengths and approximate intensities of about one hundred and twenty lines between 9000A and 20000A have been measured. The apparatus consisted of an infra-red spectrometer with a plane grating, a linear vacuum thermopile, and a Moll thermo-relay to amplify the galvanometer current. The wave-lengths appear to be accurate to about 2A and in the second order lines as close as 6A have been resolved. About ninety of the observed lines have been classified as combinations between terms in C I and N I. A number of new terms have been fixed in both of these spectra and many of the terms provisionally identified by Fowler and Selwyn in C I and Compton and Boyce in N I have been definitely confirmed. The relative values of these terms which previously depended on extreme ultra-violet measurements have been revised to conform to the more accurate infra-red data.

98. The infra-red absorption spectrum of chlorophyll and xanthophyll. R. STAIR AND W. W. COBLENTZ, *Bureau of Standards.*—Through the generosity of Dr. F. M. Schertz who isolated the material, we have been able to study the infra-red absorption bands in leaf pigments (chlorophyll, xanthophyll, carotin) using a mirror spectrometer and rock-salt prism. The xanthophyll was dissolved in carbon disulphide, and also examined in a thin film melted on a plate of rock-salt. Absorption bands were located at 1.3, 3.05, 3.45, 4.3, 6.0, 6.9, 7.3, 8.05, 8.45, 8.80, 9.05, 9.60, 9.75, 9.9, 10.4, 10.9, 11.3, 11.6, 11.9, 12.1, 12.5, 12.9, 13.2, 13.4, 13.8, 14.2 μ. The chlorophyll films were formed by evaporation from an alcoholic solution, on plates of fluorite and rock-salt. Absorption bands were located at 1.3, 3.05, 3.5, 3.8, 4.7, 6.0, 6.2, 6.5, 6.9, 7.3, 7.8, 8.2, 8.6, 9.1, 9.6, 10.1, 10.4, 10.8, 11.1, 11.9, 12.6, 12.9, 13.4, 13.7 μ. The chemical constitution of xanthophyll is unknown. Hence the band at 3μ is of interest since it is found in compounds containing OH and NH-groups. The bands are 3.4, 6.9, and 7.3μ are found in compounds containing CH_2 and CH_3-groups. None of these numerous absorption bands are so deep as found in molecules having a simpler chemical structure.

99. The infra-red absorption spectrum of carbon tetrachloride as related to the Raman spectrum of scattered radiation. W. W. COBLENTZ AND R. STAIR, *Bureau of Standards.*—Langer (Nature, March 9, 1929) has shown that it is not the frequency of a certain infra-red absorption band, but the difference between the frequencies of pairs of infra-red absorption bands, that corresponds to the Raman shift between the modified lines and the exciting line. In carbon tetrachloride the absorption band at 12 to 14μ (obtained with a rock-salt prism) is very complex and further measurements with a larger dispersion are contemplated. In the rest of the spectrum the agreement between the latest observed and Langer's calculated values are in good agreement, as follows: Calc., 13.14, 12.69; 10.24, 9.97; 9.30, 9.07; 8.20, 8.02; 6.57, 6.46μ. Obsd., 13.10, 12.67; 10.22, 9.95; 9.32, 9.08; 8.20, 8.02; 6.57, 6.45μ. Between the wave-lengths 6 and 12μ there are no conspicuous absorption bands other than the pairs just noted, and there is no doubt that the calculated values refer to these bands. Other absorption bands occur at 14 to 15μ.

100. The near infra-red absorption bands of organic compounds. E. K. PLYLER, *University of North Carolina.*—An experimental study has been made of the infra-red absorption

bands of some organic compounds of the methyl, ethyl, propyl and butyl groups. In the region from 1μ to 7μ there were similarities in the bands of all the different compounds. These observed bands were identified with combinations and overtones of four assumed fundamental frequencies at about 3.4μ, 6.8μ, 10μ and 15μ. These fundamental bands are probably produced by the vibrations of the C-H linkage. In some compounds such as the alcohols additional bands appeared which were attributed to other groups of atoms in the molecule. A study of the experimental work of Barnes, Ellis, and Sappenfield support the classification of the bands given in the present work.

101. A transmission-reflection grating for the infra-red. A. H. PFUND, *Johns Hopkins University.*—This type of grating consists of a large number of equidistant and parallel metallic ribbons, separated by air spaces and mounted so that the flat sides of the ribbons stand perpendicular to the "plane of the grating." By allowing radiations to fall on the grating with its lines vertical under an angle of incidence such that incident radiation is just refused direct transmission, a "blaze" of light is reflected from the ribbon surfaces. This blaze, which is similar to that obtained from echelette gratings, has a very large fraction of the incident radiations concentrated in superposed orders. Applications to infra-red investigations are discussed.

102. Series relationships in Be I. R. F. PATON AND R. E. NUSBAUM, *University of Illinois.*—Recent work on the spectrum of beryllium with a high vacuum tungsten furnace, together with data obtained by Sanders and Albers in the vacuum spark, has led to the discovery of the sharp and diffuse series of singlets for this element. These results, and those on the triplet series of Be I, indicate that the combination line $2^1S_0 - 2^1P_1$ should occur at about 4550 ± 5A. A strong line at 4554 ± 1A was observed in the furnace spectrograms but could not be assigned to beryllium finally, as a strong line of barium has this wave-length and other barium lines showed faintly. With greater resolution and a low pressure arc as a source the beryllium line has been resolved from the barium line and its wave-length (4553.07A) determined. This establishes a relationship between the singlet and triplet series of Be I and makes possible a more exact determination of the term values for this atom.

103. The equilibrium between surface and volume concentrations of dissolved substances. J. M. EGLIN, *Bell Telephone Laboratories, Inc.*—The composition of the surface of a solution is not the same as that of the solution as a whole. There is an equilibrium between the solute in the bulk of the solution and that adsorbed on the surface. This equilibrium is similar to the one between a vapor and the mass of that vapor adsorbed on the surface of a solid. An equation has been developed to fit the vapor-solid case from a study of the evaporation of thin films of barium on tungsten, and also from theoretical considerations. Applying this equation to the surface-volume equilibrium of a solute in a liquid, and more particularly to the surface tension changes resulting therefrom, a relation giving the surface tension as a function of the volume concentration of solute has been found. This relation is $\theta_i = |\Delta\sigma| \epsilon^{-a-b(\Delta\sigma)}$ where $\Delta\sigma$ is the change in surface tension from that of the pure solvent, θ_i is the volume concentration of solute, and ϵ, a, and b are constants. This result is found to fit observed data as well as the best empirical equation so far developed; viz. that of v. Szyszkowski.

104. Anode spots and their relation to the absorption and emission of gases by the electrodes of a Geissler discharge. C. H. THOMAS AND O. S. DUFFENDACK, *University of Michigan.*—In a Geissler discharge containing H_2, N_2, or CO_2 at pressures of 0.5 to 12 mm and electrode separations of 5 to 30 cm, the anode glow breaks up into a number of bright hemispherical spots, more or less symmetrically arranged, when the polarity of a direct current discharge is reversed. Mackay found under different conditions a similar effect in helium (Phys. Rev. **15**, 309, 1920). One necessary condition for the formation of spots is that the anode evolve gas under electron bombardment. This assumption is proved correct by the absence of spots on a thoroughly degassed anode and by the formation of spots in oxygen on an anode previously saturated with CO. As many as 75 spots arranged in 5 concentric rings have been observed on an anode 34 mm in diameter. Conditions governing the number, size, and duration of the

spots have been determined. The formation of anode spots has been used to prove that the cathode and anode absorb and emit gas, respectively, at rates which are functions of the current density, gas pressure, kind of gas and electrode temperature. Spots form on anodes of all the metals tried; iron, nickel, copper, brass and aluminum. The phenomena indicate that the gas penetrates the metal to a considerable depth.

105. The gas content of sputtered films. L. R. INGERSOLL, *University of Wisconsin.*—Using a special deposition tube, which allows the cathode to be withdrawn without altering vacuum conditions, films of nickel have been sputtered in residual atmospheres of argon and helium and their gas content investigated. This is large, although, in general less than one molecule per metal atom. Upon heating, the gas is emitted copiously at 300–400°C—just the (baking) temperature range for which, as previously shown (Phys. Rev. **26,** 86 (1925); **32,** 649 (1928)), such films become magnetic and also become much better conducting. It seems probable that this gas content is primarily responsible for the abnormal magnetic and other properties of such sputtered films. These films also possess to a remarkable extent the ability to absorb or "clean up" hydrogen when a certain critical temperature is exceeded. This temperature depends on the previous heat treatment given the film and may be as low as 100°C. The amount of hydrogen absorbed is many times that required for a monomolecular layer and the process is probably one of solution. Preliminary experiments indicate no effect of this hydrogen on the crystal lattice.

106. Thermal conductivity of Pyrex glass as a function of temperature. HERMAN E. SEEMANN, *Cornell University.*—Preliminary measurements of the thermal conductivity of Pyrex glass indicate that this property increases linearly with the temperature, within experimental error, from 0.0025 cal./cm deg. sec. at 0°C to about 0.0046 cal./cm deg. sec. at 600°C. The specimen was in the form of a hollow cylinder, closed at one end with a hemispherical cap. Energy to maintain a steady temperature gradient was supplied by means of an electrically heated filament mounted axially inside the specimen. Thermal contact with the specimen was made with molten metal baths inside and outside. Temperatures were measured with thermocouples. Details of the method have been published in connection with similar work on clear fused quartz (Phys. Rev. **31,** 119, (1928)). A radiation correction for the measurements on Pyrex glass is being considered.

107. The Pierce acoustic interferometer as an instrument for the determination of velocity and absorption. W. H. PIELEMEIER, *Pennsylvania State College.*—Sputtered quartz crystals of known natural frequency were used as sources in a Pierce acoustic interferometer. The reaction of the returning waves on the crystal driver is a periodic function of the mirror displacement, causing a cycle of change in galvanometer deflection each half wave-length. Curves show that multiple reflections take place at the mirror and at the crystal where the pressure antinodes in the gas cause deflection maxima. Indications that wave velocity depends on intensity are 1st, asymmetry of the deflection peaks; 2nd, *increasing* asymmetry with increasing mirror displacement; 3rd, non-uniform peak spacing; 4th, abrupt changes in logarithmic decrement of peak height. Air and CO_2 were tested at frequencies from $3(10)^5$ to $12(10)^5$ c.p.s. The average peak spacing indicates a slightly higher velocity than for audible sound. Absorption measurements indicate that air and CO_2 become more absorbent with rising frequency, CO_2 being nearly opaque at $12(10)^5$ c.p.s. The observed absorption by air at this frequency agrees well with Lebedew's theory and with a torsion vane determination which was used as a check. At the lower frequencies the determinations are not so reliable because the absorption is rather small.

108. Application of microphotometers for the analysis of photographic sound records. J. TYKOCINSKI-TYKOCINER, *University of Illinois.*—Variable density sound records may be used in connection with many acoustic problems. In 1923 (Transactions of the Society of Motion Picture Engineers, **17,** p. 112) the author suggested the use of microphotometers for analysis of photographic sound records. Thanks to the cooperation of O. S. Duffendack, University of Michigan, and H. Siedentopf, University of Goettingen, the author has obtained microphotometric reproductions of his early sound records made in 1922 by modulating the

light of a mercury arc discharge. Records taken on negative and positive cinema films and representing sounds of a violin, man's voice, woman's voice and also variations of an alternating current 830 cycles were thus investigated by the Moll thermoelectric microphotometer and also by a modified Koch-Kruss photoelectric microphotometer. Both instruments gave satisfactory results showing the quality and intensity of the recorded sounds. Imperfections of the records can be traced by this method to their origin. Poor modulation of the light source and faults due to the graininess of the film or to photographic processes can be detected by comparing microphotometric curves with those obtained with a sonometer or phonodeik actuated directly by the sound. Variable density records produced by an alternating current and analyzed by a microphotometer, show this method to be equivalent to an oscillograph for higher frequencies.

109. Some experiments on rubber at various temperatures. PAUL C. MITCHELL AND W. W. STIFLER, *Amherst College.*—Several cylindrical specimens of rubber were subjected to torsion and stretching when at room temperature, when immersed in ice-water, and when frozen in liquid air. The changes in length between room and liquid air temperatures were also observed As would be expected, the numerical values vary with the composition of the specimen Typical results for one sample at liquid air temperature are:—Young's modulus $=1.5\times10^{10}$ dynes/cm^2; rigidity modulus $=1.8\times10^{10}$ dynes/cm^2; mean coefficient of expansion between 22°C and -188°C $=1.65\times10^{-4}$.

110. Solution of elastic vibration problems with solid damping. A. L. KIMBALL, *General Electric Co.*—It has been previously demonstrated, experimentally, for various types of solids of different physical properties, that the internal friction, active in damping out vibrations of these solids is independent of frequency of vibration, and depends only upon amplitude. (Phys. Rev. **30,** 948, (1927)). The dissipation per unit volume per cycle is expressed by the formula $\Delta W_1=\xi\sigma_m^2$ where σ_m is the maximum stress amplitude of the vibration cycle, and ξ a friction constant. Approximately sinusoidal elastic vibrations (free or forced) with this "solid damping" can be analyzed mathematically for any case susceptible of analysis on the basis of ideal viscous friction. This is accomplished by assuming that the actual hysteresis loops of internal friction, of lenticular form, are replaced by elliptical loops of exactly the same area. On this assumption a vibration with solid friction can be exactly represented by a differential equation involving viscous friction terms derived from the law $\eta d\epsilon/dt$ where $\eta=$ frictional force per unit area per unit velocity of strain. The coefficient η must be looked upon as a parameter and is evaluated on the basis of the law $\Delta W_1=\xi\sigma_m^2$ previously given. For simple vibrating systems η is found equal to $(\xi E^2)/(\pi\omega)$, where E is Young's modulus and ω is the angular frequency of the applied stimulus.

111. Quantitative measurements of wind tunnel turbulence. H. L. DRYDEN AND A. M KUETHE, *Bureau of Standards.*—Apparatus has been developed for quantitative measurements of the mean amplitude of the fluctuations of air speed about a mean value in turbulent air flow. The basic element is a fine wire (0.017 mm in diameter) electrically heated, the temperature and resistance of which vary as the air speed varies. A special compensating circuit is used to compensate for distortion introduced by the lag of the hot wire. The compensation is effective for frequencies up to 100 cycles per second. With this apparatus it has been found that the turbulence is different in different parts of the same wind tunnel. Furthermore the wind force on certain types of bodies is found to vary and to correlate with the amount of turbulence. It therefore appears possible to adopt a suggestion of Prandtl to use the force on a sphere as a measure of turbulence and to make the measurement a quantitative one as soon as the variation of the force on the sphere with the turbulence has been determined. A full account of this work will appear in the Technical Reports of the National Advisory Committee for Aeronautics.

112. The velocity of sound in Rochelle salt crystals. ELIAS KLEIN, *Naval Research Laboratory.*—Numerous crystal slabs, their widths lying in the *bc* plane and their lengths carefully oriented with respect to the crystallographic axes, were allowed to excite oscillations in an

electrical circuit the frequency of which was determined entirely by the dimensions of the crystal. The velocity was calculated from the length of the crystal and the frequency of the circuit as obtained from a heterodyne frequency meter. Over 200 plates of various sizes cut at 45° with the b and c axes yielded an average of 4.15×10^5 cm/sec. The velocity in plates whose lengths are parallel to the c axis is not greatly different from that in plates parallel to the b axis. For long thin crystals they are approximately 5×10^5 cm/sec. This investigation is one of a series which was initiated to determine certain physical properties of piezo-active Rochelle salt *dynamically* as compared with its *static* characteristics which Valasek and others have found to pass through marked changes at 23°C. The present experiment shows no abrupt changes at this critical temperature and indicates that the velocity of sound in crystal plates is independent of temperature between 15° and 28°C

113. The extension, period, and modulus of rigidity of a spring wound in the form of a truncated cone. GYFFORD D. COLLINS AND OLIN B. ADER, *Duke University.*—On the assumption that the whole of the extension of a spring was due to torsion, the effect of shear being negligible (being about 0.2 percent in the spring used in this experiment), O. B. Ader has derived an expression for the extension of a truncated conical spring in the following form:

$$z=2MgN(R+r)(R^2+Rr+r^2)/3nr_1^4$$

in which z is the extension produced by an axial load Mg, N is the total number of coils in the spring, R and r the radii of the two end coils, n the rigidity modulus, and r_1 the radius of the wire of which the spring is made. The period of the spring is given by $T=2\pi[(1+xm/M)(z/g)]^{1/2}$ in which x is the fraction of the mass of the spring accelerated, m the mass of the spring, and z the extension produced by the load M. The fraction x varies from 1/7 in a conical spring (r equal to 0) to 1/3 in the helical spring (r equal to R).

The rigidity modulus may be calculated from

$$n=8\pi^2MN\left(1+x\frac{m}{M}\right)(R+r)(R^2+Rr+r^2)/3r_1^4T^2$$

where the symbols have the same meaning as above. All these expressions have been checked experimentally with good agreement. Further, the period is noticeably different when the spring is inverted, due to the difference in the fraction of mass accelerated, since all the other factors are constant. In the spring used the fraction was 0.2034 when the small end was up, and 0.5075 when inverted, the mass of the spring was 67.091 gm, and the load varied from 50 to 450 gm.

114. Raman effect for HCl liquid. E. O. SALANT, *National Research Fellow*, AND A. SANDOW, *New York University.*—Pure HCl liquid, at −100°C, shows the Raman effect when illuminated with a mercury arc. The modified scattering indicates an absorption band at 3.6μ for HCl liquid.

115. Note on the Raman effect in gases. E. C. KEMBLE AND E. L. HILL, *National Research Fellow, Harvard University.*—Recent experiments of Wood on the Raman effect in HCl gas show that the spectrum correlated with the 3.4μ vibration-rotation band is a sharp line at the position corresponding to the missing line of the band. He also finds some six lines, of whose genuineness he is uncertain, close to the exciting wave-length, but which he correlates with alternate lines of the pure rotation absorption spectrum. A theoretical consideration of the dispersion formula using matrix elements appropriate to a diatomic molecule in a Σ state shows that the Raman spectrum for a vibration-rotation band should consist of a Q branch, appearing as a single line at the position of the "missing line," together with "double R"-form and "double P"-form branches corresponding to $\Delta j=\pm2$. No true R and P branches exist. The apparent absence of the transitions $\Delta j=\pm2$ in the Raman vibration-rotation spectrum is presumably due to weak intensity. The pure rotation Raman spectrum should consist of a double-R branch in conformity with the observations. Detailed intensity calculations are in progress.

116. The Raman effect in gases and liquids. R. W. Wood, *Johns Hopkins University.*—(I) Lines of modified wave-length have been obtained in the radiations scattered by HCl, NH_3 and other gases at atmospheric pressure with exposures of only five hours. A "light-furnace" of improved type was employed in conjunction with an F·2 spectrograph. HCl gave the "missing line" corresponding to vibration without change of rotation, unaccompanied by the vibration-rotation lines shown in absorption. There was, in addition a group of lines very near the exciting line which can apparently be identified with the alternate lines of the pure rotation band found by Czerny in the region between 40μ and 100μ. NH_3 also gave a single line identified with the absorption band at 6.5μ, other strong absorption bands not being represented.

(II) Improved technique in the excitation of the Raman effect shown by liquids—Monochromatic excitation by a helium lamp and a method of identifying the infra-red absorption bands without wave-length measurements.

117. Singlet spectrum of Ge III. R. J. Lang, *University of Alberta.*—The author's previous analysis of the triplet spectrum of Ge III has been extended to include the following combinations for singlet terms: 4^1S-4^1P, 4^1P-4^1D, 4^1D-4^1F and the intercombinations $4^1S-4^3P_1$, 4^3D-4^1F, 4^3P-4^1D, 4^1D-4^3F, 4^1P-4^3D. Assuming a term value $F=63000$ the ionization potential is 32.6 volts. Some of the terms from the $(4p4d)$ configuration have also been found.

118. The theory of incoherent scattering. R. M. Langer, *National Research Fellow, Bureau of Standards.*—In a note to Nature (March 9, 1929) it was indicated that the wave mechanics as treated by Dirac seems to be capable of explaining the observations in scattering experiments. Since the note was sent in, others (Czerny in Naturwissenschaften, and Rasetti, Ellis, and Wood in Nature) have reported experiments which give difficulty on the commonly accepted point of view. These experiments confirm the suggestion in the note cited. For example, CO being diatomic has only one series of vibration states and therefore as Rasetti found, gives frequency shifts in scattered light which also occur in the infra-red. On the other hand, CO_2 has several series and therefore combination frequencies appear in scattering as noticed by Rasetti. The line observed by Wood at the frequency of the Q branch in HCl is of course to be expected since it does not correspond to a zero rotation change as it would in the infra-red. The absence of the P and R branches would be harder to account for especially as the diffuse shifted lines in CCl_4 at 761 and 788 cm^{-1} seem to be P and R bands. The evidence for this is that if we use the 27 cm^{-1} difference between them to calculate the moment of inertia we find $J=6.35\times10^{-39}$. This corresponds to a molecular radius $r=2.1\times10^{-8}$ cm which is very plausible since $CHCl_3$, which is similar but larger, has $r=2.4\times10^{-8}$.

119. The first spark spectrum of gallium. R. A. Sawyer, *University of Michigan,* and R. J. Lang, *University of Alberta.*—The gallium spectrum has been excited in a hollow cathode discharge in helium and photographed both with the vacuum spectograph and in the quartz and visible regions. Many new lines have been measured in the gallium spark spectrum. The chief triplet series have been established permitting the computation of term values. Several of the prominent singlet lines have also been identified.

120. The first spectrum of krypton. William F. Meggers, T. L. de Bruin and C. J. Humphrey, *Bureau of Standards.*—A new list of estimated intensities and measured wave-lengths has been obtained for more than 200 lines (3302.54 to 9751.77A) characterizing the first spectrum of krypton photographed with concave grating and with quartz spectrographs. Analysis of these new data has resulted in the identification of the main spectral terms analogous to those of the similarly constructed neon and argon spectra. Practically all of the Kr I lines have been classified in series of various types. From the series limits and combinations absolute term values are derived and the ionization potential of 13.940 volts is deduced for Kr. The general features of the Kr I spectrum closely resemble those of the preceding rare gases, Ne I and A I, and are found to be in excellent accord with the theoretical expectations. This analysis shows that the krypton line (5649.56A) which has been proposed as a primary standard of wave-length has relatively low intensity and involves a metastable level. These objections do

not apply to the stronger line 5870.92A, but none of the lines can be recommended as primary standards until they have been reexamined for hyperfine structure.

121. The vector coupling in the nickel-, palladium-, and platinum-like spectra. JULIAN E. MACK, *National Research Fellow, Princeton University.*—The spectra of the platinum-like isoelectronic sequence offer evidence of an extreme departure from the normal "Russell-Saunders" type as might be expected from the position of platinum in the periodic table. Comparison of relative energies and g-values shows almost a complete transition from normal or LS coupling to jj coupling, with increasing nuclear charge and increasing atomic number, in the d^9s and d^9p configurations of the nickel-, palladium-, and platinum-like spectra. New assignments are given in Pt I and new levels in Tl IV, and Pb V. The problem of assigning conventional names (values of L and S, total orbital and spin angular momenta) to energy levels showing other than LS coupling, is closely related to the problem of coordinating levels with respect to series limits. For these problems to have any meaning, it is necessary to consider quantum numbers and atomic numbers as continuous variables.

122. Spectral terms of platinum and classification. PAUL J. OVREBO, *West Virginia University.*—Forty-nine new terms have been found for platinum. Of these seventeen are low, twelve intermediate and nineteen upper levels. Combination of these and previously known levels give 250 lines of which 150 are newly described lines. This leaves about 95 lines to be classified, excepting the lines of very low intensity. A number of combinations have been found between low and high levels. The term 29,600.8 combines with high, intermediate and low terms; 31,900.5 combines with low as well as other intermediate terms, while 44,760.9 acts as both intermediate and high levels. A number of the new levels have been classified by means of combinations. A. C. Hausmann's classification of the old low levels from the Zeeman effect has been used as a basis for these predictions of classification. In this work the tables of platinum wave-lengths of W. F. Meggers and Kayser have been assumed to be accurate to 0.05A.

123. Spectral relations between certain iso-electronic systems and sequences in the "iron group." H. E. WHITE, *Cornell University.*—Recent identifications in the spectra of V II, III, IV, V, Cr III, IV, V, Mn IV, V, Fe V are sufficient to bring out a number of interesting relations between the various electron configurations and the corresponding energy levels in these elements. The combination of ordinary energy level diagrams, for each of the elements in a sequence of iso-electronic systems, with a Moseley diagram brings out several new regularities among the iron group of elements. Such diagrams drawn for each of the four sequences of iso-electronic systems (1) K I, Ca II, Sc III, Ti IV, V V; (2) Ca I, Sc II, Ti III, V IV, Cr V; (3) Sc I, Ti II, V III, Cr IV, Mn V; (4) Ti I, V II, Cr III, Mn IV, Fe V appear to be almost identical. The combination of the ordinary energy level diagrams of neutral vanadium V I, with singly ionized vanadium V II, doubly ionized vanadium V III, triply ionized vanadium V IV, and quadruply ionized vanadium V V, with a Moseley diagram brings out a new relation between the spectra of one element in its successive stages of ionization. The above mentioned diagrams are obtained by plotting downward the square root of the term values (values computed from the series limits as zero) against atomic number.

124. Atomic levels and wave-lengths in the spectrum of the vacuum iron arc. KEIVIN BURNS AND FRANCIS M. WALTERS, JR., *Carnegie Institute of Technology.*—In the interval 2800A to 8800A some 600 lines in the spectrum of the vacuum iron arc have been compared directly with neon standards by simultaneous exposure. The atomic levels, including a large number hitherto unpublished, have been derived from these wave-lengths, and by means of these levels 1200 lines have been computed between 2100A and 9000A. Several hundred lines have been classified for the first time. The new classifications rest partly on the new levels, and partly on published levels whose combinations have been observed in the ultra-violet. The region of spectrum containing numerous precise standards has been extended from 3370A to 2100A. The intensities of the classified lines have been plotted according to the level values for both iron and titanium, and these intensity diagrams have proven to be very useful in assigning the types to newly found levels.

125. New terms in he spectrum of Al I. R. F. PATON AND W. D. LANSING, *University of Illinois.*—The spectrum of Al was investigated in the tungsten vacuum furnace described by Paton and Rassweiler (Phys. Rev. **33,** 16 (1929)). The lines of the sharp and diffuse series were obtained in absorption and emission, confirming previous work. In addition the two well-known lines 3057.15 and 3050.07 appeared in emission at the same temperature as the first lines of the diffuse series, and with comparable intensity. These lines, along with a weaker one at 3060.20 measured in the vacuum spark are assigned to the transition $3^2P-3p'\ ^2D$, where the $3p'\ ^2D$ term arises from the configuration $3s3p^2$. A pair observed by Sawyer and Paschen at 1910.91 and 1906.57 are assigned to the transition $3^2p-3p'\ ^2S$. The term values are $3p'\ ^2D_3 = 15468$, $3p'\ ^2D_2 = 15504$, $3p'\ ^2S_1 = -4166$. All these term values are based on the $^1S_0$ state of the Al II core. These identifications are confirmed by the irregular doublet law and the Moseley law.

126. A theory of the magnetic field associated with sun-spots. ROSS GUNN, *Naval Research Laboratory.*—Theory of sun-spot magnetic fields based on the ion drift produced by ions spiralling around a nonhomogeneous magnetic field. The Hale-Bjerknes theory is retained almost completely. It is shown that the small initial symmetrical magnetic field produces currents in such a direction that regeneration is possible and that the currents flowing in the steady state are ample to account for the observed fields. The computed fields are found to be proportional to the square root of a logarithmic function of the radius of the sun-spot and the depth of the conducting layer.

127. Quantum mechanics of chemical reactions. R. M. LANGER, *National Research Fellow, Bureau of Standards.*—An important class of chemical reactions can be treated as a simple quantum mechanical problem in which a system changes from one configuration to another. Reaction, i.e., configuration change, takes place only when the two configurations have states of equal energy. Since in general the states of equal energy will be higher vibration states, only molecules having more energy than the average will react. This explains the success of the "Activation hypothesis." However, the old form of this hypothesis is incorrect in several respects. For example, molecules may have energy in excess of the measured activation energy and still be incapable of reaction because the final configuration has no state of the same energy. Metathetical reactions, decompositions, including radioactive decompositions, and other classes may be treated in this manner. Most interesting is the possibility that sometimes the function of a catalyst is to change the energy levels so that there is an equality where there was none before.

128. The Clausius' equation of state. HERBERT J. BRENNEN, *Department of Chemistry, Northwestern University.*—I have recently pointed out [Proc. Nat. Acad. Sci. **15,** 11–18 (1929)] that equations of state must contain, in general, (at least) three volume parameters and hence, van der Waals' equation, which contains only two such parameters, a and b, must, in general, be mathematically absurd. Therefore Clausius' equation, which has long been condemned as having one too many such parameters becomes no more logical than that of van der Waals. It is shown that the values of the "reduced" parameters can be very easily calculated from the observed critical ratio, RT_c/P_cV_c; if this ratio is 8/3, the value of the third reduced parameter is zero and hence the equation becomes that of van der Waals; if the critical ratio is 3.75, the mean of a large number of substances, the value of the reduced volume of the molecules is 1/16, whereas the experimental value is approximately 1/4; if the critical ratio is above 4.0, we obtain the absurd result that the volume of the molecules is negative. Hence Clausius' equation must be rejected.

129. Ionization of caesium vapor by line absorption. F. L. MOHLER AND C. BOECKNER, *Bureau of Standards.*—Further experiments on the effect discovered by Mohler, Foote and Chenault (Phys. Rev. **27,** 37 (1926)) have been undertaken. Ionization by light on the red side of the limit is produced largely, if not entirely, by absorption by the principal series lines beyond the third line. Measurements of the line effect relative to the photo-ionization produced by light on the violet side of the limit show no measurable change of the effect with temperature

between 150°C and 230°C at constant pressure. A comparatively small change with vapor pressure can probably be explained by absorption in the layer of vapor outside of the ionization chamber. Residual gas in the tube reduces the effect. Measurements of the reduction of the photo-ionization by a separate absorption cell containing caesium are being made. A column of vapor 30 cm long at a pressure of 0.015 mm reduced the effect at 3600 to ten percent, while on the violet side of the limit the change is unmeasurable (less than one percent).

130. Incoherent scattering in Rochelle salt. R. M. LANGER, *National Research Fellow, Bureau of Standards,* AND ELIAS KLEIN, *Naval Research Laboratory.*—The spectrum scattered by crystalline Rochelle salt differs in character from that of calcite and quartz; the latter substances show sharp as well as hazy lines while the modified lines observed in Rochelle salt are all very diffuse. Furthermore, there are two broad continuous bands, which conicide with those obtained with pure water and water solutions. These bands are undoubtedly due to water of crystallization and correspond with two which are found in infra-red absorption (Coblentz). However, the scattered lines do not correspond with the infra-red absorption maxima observed by Coblentz nor with the reflection maxima noted by Pfund. But the combinations among these seem to account for most of the numerous (about ten) frequency shifts which is in accord with the theory (Nature, Mar. 9, 1929) of the effect. The shifts range from about 500 to 3000 wave-numbers. Measurable plates were obtained by an exposure of one half hour.

131. Lattice energetics of plastic flow in metals. R. H. CANFIELD, *Naval Research Laboratory, "Bellevue," Anacostia, D. C.*—Previous work of the author having supplied data on the width of the negative part of the energy diagram for metals, ("Lattice energetics of thermal vibrations in metals," December meeting) an attempt has been made to obtain a formula for the stress at which plastic flow commences in a metal crystal or polycrystalline aggregate. The assumption made is that the elastic energy in the grain is made available to augment the work of the external force in overcoming the resistance to sliding in a single plane. The formula involves the geometry of the lattice and the plane and direction of slip, and is in good agreement with experiment for polycrystalline Armco iron.

132. The formation of spiral nebulae. H. B. MARIS, *Naval Research Laboratory, Washington, D. C.*—It is shown that a star cluster 1.3×10^{22} cm in diameter, as our galaxy, moving through intergalactic space filled with gas of density 10^{-26} grams cm^{-3} will sweep up this gas and leave a cone of low density in its wake. Due to the gravitational attraction of the surrounding gas the cone expands, the outward velocity of its wall being 2 km sec^{-1} after 10^8 years and 650 km sec^{-1} after 10^9 years. At this time the diameter of the cone is 10^{24} cm, which is about the average distance between the spiral nebulae, and it is assumed that the expanding walls are broken up by other galaxies, etc. The condensations of galactic size and mass thus formed contract under gravitation with little increase in temperature for, say, 10^8 years. With increasing density diffusion becomes important and the temperature of the entire mass rises rapidly until radiation pressure stops the gravitational fall and gives the component parts of the total mass outward velocities of hundreds of km sec^{-1}, such as are observed in the spiral arms of the expanding nebulae. Temperatures of 10^{10} degrees would be reached even at the surface and conditions suitable for the emission of penetrating radiation would prevail.

133. The distribution of electrons between the plate and grid of a three electrode tube as determined by positive caesium ions. J. M. HYATT, *Union College, Schenectady, N. Y.*—It is impossible to determine the exact distribution of primary electrons to the grid and plate of a tube on account of secondary electron emission. It can be shown that the paths of positive ions are the same as those of electrons at the same potentials. Hence, if the distribution of positive ions is determined, taking into account the emission of secondary electrons, the electron distribution becomes known. The source of the positive ions was a tungsten filament in the bulb of a radiotron UX201A containing caesium vapor. The emission and plate currents were observed at given negative grid potentials as the plate potential was varied from +45 to −600 volts. The part of the observed plate current due to secondary electrons from the grid and plate was calculated and the true positive ion current determined. The fraction of

the positive ions caught by the plate increased to 0.86 for a plate potential to grid potential ratio (E_p/E_g) of 0.70 and remained constant for higher ratios of $E/_pE_g$. The ratio of the open to the closed areas of the grid was found to be 0.87. This indicates that the electron distribution may be calculated from the dimensions of the grid in this general type of tube.

134. An extension of the spark spectrum of copper. GERALD KRUGER, *Cornell University*, (*Introduced by R. C. Gibbs*).—It has been shown that the ground term of copper II is a ^1S which arises from $3d^{10}$ electrons. The next higher terms are $3d^94s\ ^1D^3D$ and still higher are found the terms $3d^94p\ ^3(PD^1F)\ ^1(PD^1F)$. One term of the $^1S_0$ series, two terms of the $^1D^3D$ series, and one term of the $^3(PD^1F)\ ^1(PD^1F)$ series have been found. It was the object of the present work to extend the $^1D^3D$ series so that an accurate calculation of the limit would be possible. A Schueler lamp of the hollow cathode type was used as a light source. The spectrum was photographed by using a vacuum spectrograph which was so designed that the region (0–2600A) could be photographed on one plate. A grating (15000 line per inch) giving a dispersion of 11.12A per mm was used. Two higher members of the $^1D^3D$ series have been found and the limit of the series calculated on this basis. These calculations show that the $^1S_0$ lies 163738 cm^{-1} below the $^2D_3$ level of Cu III from which the ionization potential was calculated to be 20.2 volts. This places the first members of the $^3D_{123}$ series at 141813 cm^{-1}, 140894 cm^{-1}, and 139743 cm^{-1} respectively. In addition, several lines in the region 90000 cm^{-1} and 110000 cm^{-1} have been found, which have the $^3D^1D$ separation, but they have not been completely classified.

135. The fine structure and satellites of the *K*-alpha lines of the light elements. C. B. BAZZONI, L. Y. FAUST AND B. B. WEATHERBY, *University of Pennsylavnia*.—The x-ray spectra of certain light elements have been measured including boron, oxygen and carbon both free and in various compounds. A grating on glass 1179 lines per mm furnished by Professor R. W. Wood was employed in a special vacuum spectrograph. The lines were analyzed with a densitometer involving a Moll vacuum thermocouple. The lines are complex the width of boron $K\alpha$ being about three Angstroms comprising primarily a doublet with four or more accessory peaks on the long wave side and several on the high frequency side. The wave-length for the principal peak is 68.12A. In addition this line when obtained from boric oxide is accompanied by satellites at 72.2, 66.0, 65.1 and 74.7. It is suggested that these lines may represent boron $K\alpha$ radiation plus or minus the quanta associated with the stimulation or ionization of atoms of other elements involved in the molecular structure. This proposition is still under consideration. Measurement of the $K\alpha$ of carbon gives 44.9A for the principal apex. The carbon line has been densitometered in three orders showing details of fine structure in the third order. The breadth of this complex line is approximately 2A.

AUTHOR INDEX

Ader, O. B.—see Collins
Allison, Samuel K.—Nos. 80, 89
Almy, G. M.—see Crawford
Astin, Allen—No. 29

Baldwin, R. S.—No. 18
Bauer, H.—see Jauncey
Bazzoni, C. B., L. Y. Faust and B. B. Weatherby—No. 135
Beams, J. W.—No. 76
Bearden, J. A.—No. 84
Becker, J. A.—No. 60
Blackwood, Oswald—No. 9
Boeckner, C.—see Mohler
Bourgin, D. G.—No. 17
Boyce, J. C.—see Compton
Bozorth, Richard M.—No. 13
Brennen, Herbert J.—Nos. 16, 128
Brice, Brooks, A.—No. 90
——— **and F. A. Jenkins**—No. 92
Brode, Robert B.—No. 5
ten Bruggencate, P.—No. 38
de Bruin, T. L.—see Meggers
Burns, Keivin and Francis M. Walters, Jr.—No. 124

Campbell, J. R., Jr.—see Race
Canfield, R. H.—No. 131
Carr, Percy H.—No. 3
Coblentz, W. W.—see Stair
——— **and R. Stair**—No. 99
Cofman, Victor—No. 26
Collins, G. D. and O. B. Ader—No. 113
Compton, K. T., J. C. Boyce and J. L. Nickerson—No. 70
Copley, M. J. and W. H. Rodebush—No. 65
Crawford, F. H. and G. M. Almy—No. 67
Crew, W. H.—see Thornton
Curtis, H. L., A. T. MacPherson and A. H. Scott—No. 50

Davey, W. P.—see Kiehl
Davis, Bergn and Harris Purks—No. 86
Dawson, L. H., L. P. Granath and E. O. Hulburt—No. 22
Duane, Wm.—No. 87
Duffendack, O. S.—see Thomas
——— see Wolfe
——— **and H. L. Smith**—No. 72
Draper, Glen H.—No. 15
Dryden, H. L. and A. M. Kuethe—No. 111

Edlefsen, N. E.—see Lawrence
Edwards, J. B.—see Null
Eglin, J. M.—No. 103

Erikson, Henry A.—No. 10

Farnsworth, H. E.—No. 4
Faust, L. Y.—see Bazzoni
Foster, Donald—No. 14
Foster, J. S.—No. 66
Frerichs, Rudolf—No. 95

Gibbs, R. C. and Alice M. Vieweg—No. 96
Granath, L. P.—No. 24
——— see Dawson
——— **and E. O. Hulburt**—No. 23
Gunn, Ross—Nos. 28, 126

Ham, W. R.—No. 64
——— see Kiehl
——— see Van Velzer
Harnwell, G. P.—No. 1
Herzfeld, Karl F.—No. 51
Hill, E. L.—see Kemble
Howe, Carl E.—No. 82
Hughes, A. L., V. Rojansky and J. H. Mc Millen—No. 6
Hulburt, E. O.—see Dawson
——— see Granath
Humphrey, C. J.—see Meggers
Hyatt, J. M.—No. 133

Ingersoll, L. R.—No. 105
Ingram, S. B.—No. 97
Ives, Herbert E.—No. 58

Jauncey, G. E. M. and H. Bauer—No. 85
Jenkins, F. A.—No. 91
——— see Brice

Karapetoff, V., H. A. Trebler and E. G. Linder—No. 52
Kemble, E. C. and E. L. Hill—No. 115
Keihl, H. R., W. R. Ham, M. W. White and W. P. Davey—No. 88
Kimball, A. L.—No. 110
Kingdon, K. H.—No. 30
Klein, Elias—No. 112
———see Langer
Koller, L. R.—No. 61
Korff, S. A.—No. 20
Kovarik, Alois F.—No. 8
Kruger, Gerald—No. 134
Kuethe, A. M.—see Dryden

Lang, R. J.—No. 117
——— see Sawyer
Langer, R. M.—Nos. 118, 127
———and Elias Klein—No. 130
Langmuir, I.—see Tonks

Langstroth, G. O.—No. 69
Lansing, W. D.—see Paton
Lawrence, Ernest O. and N. E. Edlefsen—No. 77
Linder, E. G.—see Karapetoff
Lindsay, R. B. and R. J. Seeger—No. 43
Lowry, W. Norwood—No. 55

Mack, J. E.—No. 121
Mackay, G. M. J.—No. 53
MacPherson, A. T.—see Curtis
Margenau, Henry—No. 42
Maris, H. B.—No.132
Martin, R. E.—see Sette
Maxwell, L. R.—No. 74
McMillen, J. H.—see Hughes
Meggers, W. F., T. L. de Bruin and C. J. Humphrey—No. 120
Mitchell, Allan C. G.—No. 2
Mitchell, Paul C. and W. W. Stifler—No. 109
Mohler, F. L. and C. Boeckner—Nos. 78, 129
Morris, B. D.—see Ramsey
Morse, Philip M.—No. 93

Nickerson, J. L.—see Compton
Niessen, K. F.—No. 46
Nottingham, W. B.—56
Null, F. E. and J. B. Edwards—No. 35
Nusbaum, R. E.—see Paton

O'Brien, Brian—No. 21
Olpin, A. R.—No. 57
Ovrebo, Paul J.—No. 122

Paton, R. F. and W. D. Lansing—No. 125
——— **and R. E. Nusbaum**—No. 102
Pfund, A. H.—No. 101
Pielemeier, W. H.—No. 107
Plyler, E. K.—No. 100
Purks, Harris—see Davis

Race, H. H. and J. R. Campbell, Jr.—No. 36
Ramsey, R. R. and B. D. Morris—No. 33
Randall, D. P.—No. 12
Randolph, D. W.—see Wolfe
Reynolds, N. B.—No. 63
Richtmyer, F. K.—No. 83
Rodebush, W. H.—see Copley
Rojansky, V.—No. 68
——— see Hughes
Ruark, Arthur E.—No. 41

Salant, E. O. and A. Sandow—No. 114
Samson, E. W.—see Turner
Sandow, A.—see Salant
Sawyer, C. B. and C. H. Tower—No. 34
Sawyer, R. A. and R. J. Lang—No. 119
Scott, A. H.—see Curtis
Seeger, R. J.—No. 45
——— see Lindsay
Seeman, Herman E.—No. 106
Sette, W. J. and R. E. Martin—No. 31
Silberstein, Ludwik—No. 27
Slack, F. G.—No. 71
Smith, H. L.—see Duffendack
Smith, Lloyd P.—No. 59
Smyth, C. P.—No. 54
Stair, R. and W. W. Coblentz—No. 98
——— see Coblentz
Steadman, Luville T.—No. 7
Stewart, G. W.—No. 81
Stewart, John Q.—No. 25
Stifler, W. W.—see Mitchell
Stueckelberg, E. C. G.—No. 94

Thomas, C. H. and O. S. Duffendack—No. 104
Thornton, W. N. and W. H. Crew—No. 19
Tonks, L.—No. 49
——— **and I. Langmuir**—No. 11
Tower, C. H.—see Sawyer
Trebler, H. A.—see Karapetoff
Turner, L. A. and E. W. Samson—No. 73
Tykocinski-Tykociner, J.—No. 108

Vallarta, M. S.—No. 40
——— see Wiener
Van Velzer, H. L. and W. R. Ham—No. 62
Vieweg, Alice M.—see Gibbs

Uhlenbeck, G. E. and H. C. Wolfe—No. 44

Walters, Francis M., Jr.—see Burns
Way, H. E.—see Worthing
Weatherby, B. B.—see Bazzoni
White, H. E.—No. 123
White, M. W.—see Kiehl
Whitehead, J. B.—No. 47
Wiener, Norbert and M. S. Vallarta—No. 39
Wilson, Thomas A.—No. 79
Wolfe, H. C.—see Uhlenbeck
Wolfe, R. A., O. S. Duffendack and D. W. Randolph—No. 32
Wood, R. W.—No. 116
Worthing, A. G. and H. E. Way—No. 75

Zwicky, F.—Nos. 37, 48

AUTHOR INDEX TO VOLUME 33

Reference with (A) are merely to abstracts of papers presented at meetings of the Physical Society.

Ader, Olin B. (see **Collins, Gyfford D.**)—1096(A)

Allen, A. J. (see Loomis, F. W.)—639(A)

Allen, Mildred. Compton effect produced by standing electromagnetic waves according to wave mechanics—293(A)

Allison, Samuel K. Experimental evidence for the filling of electron levels from the relative intensity of x-ray lines—1087(A)

———Separation and relative intensity of the diagram-components of the $L\beta_2$ line by means of the double x-ray spectrometer—1090(A)

Almy, G. M. (see Crawford, F. H.)—1084(A)

Anderson, Carl D. Momentum of photoelectrons in relation to the momentum of the ejecting x-rays—265(A)

Anderson, S. Herbert and William Bleakney Striking potential of aluminum arc—280(A)

Andrews, Mary R. The evaporation of thorium from tungsten—454

Armstrong, R. W. (see Tykocinski-Tykociner, J.)—634(A)

Astin, Allen. Resonance in circuits with parallel resistances—1074(A)

Babcock, Harold D. Revision of a former value of the specific charge of an electron, e/m—268(A)

Badger, Richard M. and **C. Hawley Cartwright.** Pure rotation spectrum of ammonia—692

Baldwin, Rollin Smith. The optical constants of solid Hg—1072(A)

Banta, H. E. Mobility of positive ions in flames—211

Barker, E. F. (see Scinchcomb, G. A.)—305

———Molecular spectrum of NH_3: II. Double band at 10μ—684

Barnes, James. Absorption spectrum of liquid benzene: Reply to criticism by Ellis—627

Barnes, S. W. and **F. K. Richtmyer.** A high potential electrostatic voltmeter—636(A)

Batrky, W. and **A. J. Demster.** Paths of charged particles in electric and magnetic fields—1019

Bartlett, James H., Jr. Positive ray analysis of H_2S—117(A)

———Ionization by slow electron impact of NH_3 and H_2S—169

Bateman, H. New treatment of vortex motion—270(A)

Bates, John R. (see Urey, H. C.)—279(A)

Bauer, H. (see Jauncey, G. E. M.)—1088(A)

Bazzoni, C. B., L. Y. Faust and **B. B. Weatherby.** The fine structure and satellites of the **K**α lines of the light elements—1101(A)

Beams, J. W. The electrical breakdown of liquids—632(A)

———Spectra in condensed discharges—1086(A)

———and **J. C. Street.** Time lags of spark gaps in air at various pressures—280(A)

Bearden, J. A. Absolute wave-length of the Kα and Kβ lines of Cu—1088(A)

Becker, J. A. Thermionic emission as a function of the amount of adsorbed material—1082(A)

———Book Review—263

Begeman, Hilda L. (see McDowell, Louise S.)—55

Bichowsky, F. Russell and Channing W. Wilson. Study of gaseous effusion at high temperatures—851

Bidwell, C. C. and **E. J. Lewis.** Thermal conductivity of lead and of single and poly-crystal Zn—249

Birge, Raymond T. Probable values of the general physical constants—265(A)

Bitter, Francis. Magnetic susceptibilities of several organic gases—389

Blackwood, Oswald. Apparatus for the determination of ionic mobilities—1070(A)

Bleakney, William (see Anderson, S. Herbert)—280(A)

Bless, A. A. The effect of x-rays on the rotatory power of some substances—121(A)

Bloomenthal, Sidney. Detection of the isotopes of lead by means of their oxide band spectra—285(A)

Boeckner, C. and **F. L. Mohler.** Duration of the effect of ions on a negative space charge—119(A)

———(see Mohler, F. L.)—1087(A), 1099(A)

Bourgin, D. G. Sound propagation—282(A)

———Group velocity—1072(A)

Bowen, I. S. Book Reviews—109, 628

Boyce, J. C. (see Compton, K. T.)—115(A), 145, 1085(A)

Bozorth, Richard M. The Barkhausen effect in iron, nickel and permalloy—636(A)

———Determination of the average size of the discontinuities in magnetization—1071(A)

Bramley, A. Modulation of light waves by high frequency radio waves—279(A)

———Effect of high frequency waves on the optical properties of water—640(A)
Brasefield, Charles J. Some peculiar hydrogen bands—925
Breit, G. Book Review—460
Brennen, Herbert J. Clausius' equation of state—1099(A)
———Electronic theory of light and other forms of electromagnetism—1071(A)
Brice, Brooks A. Band spectrum of silver chloride—1090(A)
———and **F. A. Jenkins.** A new band system probably due to singly ionized HCl—1090(A)
Brickwedde, F. G. and **M. F. Peters.** Temperature variations of the Raman effect in quartz—116(A)
Bridgman, P. W.—Book Reviews—261, 262
Brode, Robert B. The absorption coefficient of slow electrons in alkali vapors—1069(A)
ten Bruggencate, P. On the radial velocities of globular clusters—1077(A)
de Bruin, T. L. (see Meggers, William F.)—1097(A)
Buchta, J. W.—Book Reviews—459
Buckley, O. E. (see McKeehan, L. W.)—636(A)
Burns, Keivin and **Francis M. Walters, Jr.** Atomic levels and wave-lengths in the spectrum of the vacuum iron arc—1098(A)

Cady, W. G.—Book Review—109
———Some electromechanical properties of Rochelle salt crystals—278(A)
Cameron, G. H. (see Millikan, R. A.)—266(A)
Campbell, J. R., Jr. (see Race, H. H.)—1076(A)
Canfield, R. H. Internal friction in metals—277(A)
———Lattice energetics of thermal vibrations in solids—294(A)
———Lattice energetics of plastic flow in metals—1100(A)
Carr, Percy H. New method of recording electrons—1068(A)
Cartwright, C. Hawley (see Badger, Richard M.)—692
Carwile, Preston B. Double-valued characteristics of a resistance-coupled feed-back amplifying circuit—284(A)
Cassen, Benedict. Shot fluctuations in wave mechanics—270(A)
———Protonic spin—270(A)
———Spectral intensities of non-harmonic and aperiodic systems—271(A)
Charlton, E. E. (see Kingdon, K. H.)—998
Christy, Andrew. Quantum analysis of the blue-green bands of TiO—701
Coblentz, W. W. and **R. Stair.** The infra-red absorption spectrum of CCl_4 as related to the Raman spectrum of scattered radiation—1092(A)
———(see Stair, R.)—1092(A)
Cofman, Victor. Classification of physical laws: periodicity of physical concepts—1073(A)
Collins, Gyfford D. and **Olin B. Ader.** The extension, period, and modulus of rigidity of a spring wound in the form of a truncated cone—1096(A)
Colwell, R. C. Weather forcasting by the intensity of radio signals—283(A)
Compton, K. T. and **J. C. Boyce.** Arc spectrum of N in extreme ultra-violet—115(A), 145
———**J. C. Boyce** and **J. L. Nickerson.** Extreme ultra-violet spectra of Ne and A excited by electrodeless ring discharge—1085(A)
Condon, E. U.—Book Reviews—107, 108
———Nuclear motions associated with electron transitions in diatomic molecules—122(A)
———(see Gurney, Ronald W.)—122(A), 127
Cook, S. G. Surface tension of mercury in the presence of gases under varying pressures—277(A)
Cooper, D. and **G. O. Langstroth.** The specific heat of Mo from 250°C to −40°C—243
Copley, M. J. and **W. H. Rodebush.** Molecular rays of HCl in an electric field—1083(A)
Cornish, R. E. and **E. D. Eastman.** Tube-correction in measurements of the velocity of sound in gases—90, further note, 258
Cottrell, C. L. Effect of chemical combination on the absorption of x-rays at wave-lengths on each side of the *K* discontinuity—879
Cravath, Austin M. Rate of formation of negative ions by electron attachment—266(A), 605
Crawford, F. H. The Zeeman effect in the angstrom CO bands. II—341
———and **G. M. Almy.** Zeeman effect in MgH—1084(A)
Crew, W. H. (see Thornton, W. N.)—1072(A)
Curtis, H. L., A. T. MacPherson and **A. H. Scott.** The effect of temperature, pressure and frequency on the electrical properties of rubber—1080(A)

Davey, Wheeler P. and **F. A. Steele.** Crystal structure of tricalcium aluminate—291(A)
———(see Kiehl, H. R.)—1089(A)
Davis, Bergen and **Harris Purks.** Fine structure in the Compton effect—1089(A)
———(see Mitchell, Dana)—292(A)
Davis, Harold T. (see Hufford, Mason E.)—115(A), 589
Davisson, C. J. and **L. H. Germer.** A test of the state of polarization of reflected electron waves—118(A)
———and **L. H. Germer.** "Anomalous dispersion" of electron waves by nickel—292(A)
———and **L. H. Germer.** Test for polarization of electron waves by reflection—760

Dawson, L. H., L. P. Granath and **E. O. Hulburt.** The attenuation of ultra-violet light by the lower atmosphere—1073(A)
Demster, A. J. (see Bartky, W.)—1019
Dershem, Elmer. X-ray anomalous dispersion in the region of the L series of Pt—120(A)
———Dispersion of soft x-rays in glass and platinum —291(A)
———Refractive indices and anomalous dispersion of soft x-rays in Pt, Ag, calcite and glass—659
Dillinger, Joy (see Smith, Alpheus W.)—398
Dow, R. B. Influence of surface conditions on the friction of metals—252
Draper, Glen H. A theory of light—(A)1071
Dryden, H. L. and **A. M. Kuethe.** Quantitative measurements of wind tunnel turbulence—1095(A)
Duane, William. On the polarization of x-radiation from Hg vapor—1089(A)
———and **J. C. Hudson.** Intensities of general x-radiation proceeding from an atom in different directions—635(A)
Duffendack, O. S. and **H. L. Smith.** Simultaneous ionization and excitation by positive ions and excited atoms—1085(A)
———(see Thomas, C. H.)—1093(A)
———(see Wolfe, R. A.)—1075(A)
Dufford, R. T. Becquerel effect in cells containing Grignard compounds—119(A)
———and **H. E. Hammond.** A promising method of measuring x-ray intensities—124(A)
DuMond, Jesse W. M. Compton modified line structure and its relation to the electron theory of solid bodies—123(A), 643
Dunham, E. M. Capacity in the aluminum cell 819
Dushman, S. (see Gordon, N. T.)—632(A)
Dyk, Karl. (see Loeb, Leonard B.)—267(A)

Eastman, E. D. (see Cornish, R. E.)—90, further note, 258
Edlefsen, N. (see Lawrence, Ernest O.)—265(A)
———(see Lawrence, Ernest O.)—1086(A)
Edwards, Hiram W. Total reflection of x-rays from thin Ni films. Part II—272(A), 463
Edwards, J. B. (see Null, F. E.)—1076(A)
Eglin, J. M. Direct current amplifier for measuring very small currents—113(A)
———The equilibrium between surface and volume concentrations of dissolved substances—1093(A)
Eldridge, John A. Radiation by accelerated electron in classical electron theory—123(A)
Ellett, A. Polarization of Cd resonance radiation $1^1s_0-2^3P_1$, 3261A—124(A)
———and **H. F. Olson.** Velocity of Cd atoms specularly reflected from rock-salt crystals—118(A)
———and **H. A. Zahl.** Reflection of atoms from crystals—124(A)
———and **H. A. Zahl.** Repeated reflection of atoms from crystals—635(A)
Ellis, Jospeh W. Heats of linkage of C-H and N-H bonds from vibration spectra—27
———Absorption spectrum of liquid benzene: a criticism of a paper bearing this title by Barnes and Fulweiler—625
Elo, A. E. (see Monk, G. S.)—114(A)
Engwicht, Harry (see Harrison, George R.)—271(A)
Epstein, Paul S. Settling of gases and constitution of the atmosphere—269(A)
———What is the moon made of?—269(A)
Erikson, Henry A. The effect of H_2O on the final positive air ion—118(A)
———On the nature of the ions in air—403
———Factors affecting the nature of the ions in the air—1070(A)
Evjen, H. M. and **F. Zwicky.** Internal pressure of strong electrolytes—860
Eyring, Henry. The straggling of alpha-particles from polonium in passing through gases—386

Farnsworth, H. E. The diffraction of electrons by a copper crystal—1068(A)
Faust, L. Y. (see Bazzoni, C. B.)—1101(A)
Firestone, F. A. and **D. L. Rich.** Measurement of amplitude ratio and phase difference at the ears due to a source of pure tone—634(A)
Foote, Paul D. (see Smith, W. O.)—637(A)
Foster, Donald. Magnetic properties of iron crystals—1071(A)
Foster, J. S. Effect of crossed electric and magnetic fields on the He spectrum—1084(A)
Franklin, Wm. S. A rational proposal for the control of a hurricane—294(A)
Frayne, John G. and **Carol G. Montgomery.** Variation in the intersities of mercury spectrum lines with pressure of the vapor—549
Frazer, J. H. An optical study of adsorbed films—97
Frerichs, Rudolf. New terms of the oxygen arc spectrum—1091(A)
Friesen, A. P. (see Pietenpol, W. B.)—277(A)

Gale, H. G. and **G. S. Monk.** The band spectrum of F_2—114(A)
Gartelin, C. W. (see Vieweg, Alice M.)—287(A)
Gaviola, E. Efficiency of quenching collisions and the radius of the excited Hg atom—309
———On time-lags in flourescence and in the Kerr and Faraday effects—1023
Gehman, S. D. Reflection of soft x-rays—141

Germer, L. H. (see Davisson, C. J.)—118(A), 292 (A), 760
Gibbs, R. C. (see Vieweg, Alice M.)—287(A)
———and **Alice M. Vieweg.** Some multiplets in the spectrum of doubly ionized copper, Cu III —1092(A)
———and **H. E. White.** Relations between doublets of stripped atoms in five periods of the periodic table—157
———and **H. E. White.** The hyper-fine structure of singly ionized Pr—286(A)
Glockler, George. Scattering of light by electrons —116(A)
———Efficiency of electron impact leading to resonance in He—175
Goeder, Frank Peat. The space group and crystal structure of potassium sulphate—120(A)
Goetz, Alexander. Photoelectric effect of liquid tin and two of its allotropic modifications—265(A), 373
Gordon, N. T. and **S. Dushman.** Conditions for initiation of electrodeless discharges in gases—632(A)
Gortner, Ross Aiken. Book Review—105
Goudsmit, S. (see Uhlenbeck, G. E.)—290(A)
Granath, L. P. (see Dawson, L. H.)—1073(A)
———Absorption of ultra-violet light by oxygen, water vapor and quartz—1073(A)
———and **E. O. Hulburt.** The absorption of light by fog—1073(A)
Gray, J. A. and **A. J. O'Leary.** Gamma and cosmic rays—292(A)
Green, J. B. and **R. A. Loring.** An exception of Pauli's *g*-sum rule—286(A)
Greibach, E. H. Vaporization under influence of electric fields—844
Gunn, Ross. The sun's radial magnetic gradient and atmosphere—283(A), 614
———Electromagnetic effect of importance in solar and terrestrial magnetism—832
———A new electromagnetic effect and its application to a theory of the permanent magnetic field of the sun and earth—1074(A)
———A theory of the magnetic field associated with sun-spots—1099(A)
Gurney, Ronald W. and **Edward U. Condon.** Quantum mechanics and radioactive disintegration—122(A), 127
———and **P. M. Morse.** Space charge sheaths in positive ray analysis—789

Ham, W. R. (see Kiehl, H. R.)—1089(A)
———(see Van Velzer, H.L.)—1083(A)
———The use of the Schottky relation in the determination of the thermionic work function of tungsten—1083(A)
Hammond, H. E. (see Dufford, R. T.)—124(A)
Hanawalt, J. D. X-ray study of the system palladium-hydrogen—444
Hansen, W. W. (see Webster, D. L.)—635(A)
Harnwell, Gaylord P. Angular scattering of electrons in He, Ne, H_2 and N_2—293(A), 559
———Angular distribution of secondary electrons in He—632(A)
———Electron scattering in H—1067(A)
Harrison, George R. Intensity formulas and the strong multiplets of Ti—271(A)
———and **Harry Engwicht.** Relative intensities of multiplets in triads of Ti—271(A)
Hartley, R. V. L. Wave mechanism of quantum phenomena—289(A)
Haverstick, E. J. (see Slepian, J.)—52, 280(A)
Hayeer, Lucy J. and **A. W. Hull.** Shot effect of secondary electrons—281(A)
Henderson, Jos. E. and **Elizabeth R. Laird.** Reflection of soft x-rays—291(A)
Herzfeld, Karl F. Influence of surfaces and space charges on the apparent conductivity of dielectrics—1081(A)
Hill, E. L. (see Kemble, E. C.)—1096(A)
Holmes, R. M. and **N. L. Walbridge.** Photo-e.m.f. in single crystals of Se—281(A)
Holroyd, H. B. (see Zaikowsky, W. M.)—264(A)
Houston, William V. Some relationships between singlets and triplets in the spectra of two-electron systems—297, 268(A)
———The temperature dependence of electron emission under high fields—361
Howe, Carl E. Wave-length measurements of *L* lines (Zn to Ca)—1088(A)
Hoyem, A. G. and **E. P. T. Tyndall.** Experimental study of the growth of Zn crystals by the Czochralski-Gomperz method—81
Hudson, J. C. (see Duane, William)—635(A)
Hufford, Mason E. and **Harold T. Davis.** The diffraction of light by a circular opening and the Lommel wave theory—115(A), 589
Hughes, A. L. and **G. E. M. Jauncey.** Collisions and coalescence of light quanta—290(A)
———**V. Rojansky,** and **J. H. McMillen.** Refocussing of electron paths in a radial electrostatic field—1069(A)
Hulbert, E. O. (see Maris, H. B.)—269 (A), 283(A),
———412, 1046(see Dawson, L. H.)—1073(A)
———(see Granath, L. P.)—1073(A)
———Book Review—628
Hull, Albert W. The resistance of Hg arcs—119(A)

———(see Hayner, Lucy J.)—281(A)
Humphrey, C. J. (see Meggers, William F.)—1097(A)
Hund, August. Book Review—460
Huxford, W. S. (see Williams, N. H.)—118(A), 773
Hyatt, J. M. The distribution of electrons between the plate and grid of a three electrode tube as determined by positive caesium ions—1100(A)

Ingersoll, L. R. The gas content of sputtered films —1094(A)
Ingram, S. B. The infra-red arc spectra of C and N—1092(A)
———Second spark spectrum of sulphur, S III—907
Ives, Herbert E. The preparation of photoelectric cells with thin films of Li as the photoactive material—1081(A)
———and **A. R. Olpin.** Maximum excursion of the photoelectric long wave limit of the alkali metals—281(A)

Jauncey, G. E. M. (see Hughes, A. L.)—290(A)
———and **H. Bauer.** Temperature and the Compton effect—1088(A)
Jenkins, F. A. (see Rosenthal, Jenny E.)—163, 285(A)
———(see Brice, Brooks A.)—1090(A)
———Fine structure of the beryllium flouride bands —1090(A)
Johnson, Arthur J. M. The *M*-series x-ray absorption spectra of metallic Pt and Au—120(A)
Johnson, Thomas H. Reflection of hydrogen atoms from crystals—293(A)

Kaplan, Joseph. Excitation of the aurora green line in active nitrogen—154
———Existence of metastable molecules in active nitrogen—189
———Heat of dissociation of nitrogen—267(A)
———Continuous spectrum of hydrogen—638(A)
———Active nitrogen—638(A)
———Spectrum of the aurora borealis—638(A)
———and **E. L. Kinsey.** Excitation of band spectra—114(A)
Karapetoff, V., H. A. Trebler and **E. G. Linder.** Electron bombardment of hydrocarbons—1080(A)
Karman, Th. von. Heat conduction in crystals from the point of view of wave mechanics—272(A)
Kemble, E. C. and **E. L. Hill.** Note on the Raman effect in gases—1096(A)
———and **C. Zener.** The two quantum excited states of the hydrogen molecule—512
———and **C. Zener.** Computation of properties of certain excited states of H_2—286(A)
Kennard, E. H. Classical theory of the Raman effect—289(A)
Kernaghan, Marie (see Poindexter, Franklin E.) —837
Kiehl, H. R., W. R. Ham, M. W. White and W. P. Davey Reflection of electrons and its application to the design of Mo target water-cooled Coolidge tubes—1089(A)
Killian, T. J. The positive column of the mercury arc—632(A)
Kimball, A. L. Solution of elastic vibration problems with solid damping—1095(A)
Kimball, W. S. Entropy and probability—113(A)
Kingdon, K. H. and **E. E. Charlton.** The rectification of radio signals by a thermionic tube containing alkali metal vapor—998
———Rectification by oscillation of positive ions about the potential minimum of a thermionic triode—1075(A)
Kinsey, E. L. (see Kaplan, Joseph)—114(A)
Kirkpatrick, Paul and **Iwao Miyake.** Polarization of the $L\beta_1$ radiation of tungsten—268(A)
Kleeman, R. D. Radiation and the electron—288(A)
Klein, Elias. The velocity of sound in Rochelle salt crystals—1095(A)
———(see Langer, R. M.)—1100(A)
Knipp, Chas. T. and **Wesley S. Stein.** Radiometer effect of positive ions—124(A)
———Lenard ray tube having a glass window and adjustable gas pressure in the ray chamber—125(A)
Koller, L. R. Thermionic and photoelectric emission from caesium at low temperatures—1082(A)
Korff, S. A. Refractive index of Na vapor and width of D_1 in absorption—584, 1072(A)
Kovarik, Alois F. Basis for computing the age of a mineral—1069(A)
———Book Review—628
Kruger, Gerald. An extension of the spark spectrum of copper—1101(A)
Kuethe, A. M. (see Dryden, H. L.)—1095(A)
Kunz, Jakob and **J. T. Tykociner.** Electrodeless ring discharge and the production of atomic rays of H—117(A)

Laird, Elizabeth R. (see Henderson, Jos. E.)—291(A)
Lang, R. J. On the spectrum of Ni II—547
———Further combinations in the spark spectrum of Ni—638(A)
———Singlet spectrum of Ge III—1097(A)
———(see Sawyer, R. A.)—1097(A)
Langer, R. M. Quantum resonance and chemical reaction rate—290(A)

Langer, R. M. Quantum mechanics of chemical reactions—1099(A)
———The theory of incoherent scattering—1097(A)
———and **Elias Klein.** Incoherent scattering in Rochelle salt—1100(A)
———and **W. F. Meggers.** Combination scattering in liquids—115(A)
———(see Meggers, W. F.)—287(A)
Langmuir, Irving. The interaction of electron and positive ion space charges in cathode sheaths—954
———(see Tonks, L.)—195, 990, 1080(A)
Langstroth, G. O. (see Cooper, D.)—243
———Relative intensities of Stark components in H—1084(A)
Lansing, W. D. (see Paton, R. F.)—1099(A).
Lark-Horovitz, Karl. The crystal structure of solid Hg—121(A)
Lauritsen, Charles C. (see Millikan, Robert A.) 598, 633(A)
Lawrence, Ernest O. and **N. Edlefsen.** Ionization of Cs vapor by light of frequency greater than the series limit—265(A)
———and **N. E. Edlefsen.** The photoionization of the vapors of Cs, Rb and K—1086(A)
Lewis, E. J. (see Bidwell, C. C.)—249
———Specific resistance of Be—284(A)
Liebowitz, Benjamin. Proposed interpretation of the fundamental quantum law—288(A)
Lind, S. C. Book Review—629
Linder, E. G. (see Karapetoff, V.)—1080(A)
Lindsay, R. B. and **R. J. Seeger.** Solution of problems in quantum mechanics by operator analysis—1078(A)
Loeb, Lora Lane and **Leonard B. Loeb.** The existence of radioactive recoil ions of high mobility in air—272(A)
Loeb, Leonard B. (see Loeb, Lora Lane)—272(A)
———and **Karl Dyk.** Effects of an homologous series of amines on the mobilities of ions in hydrogen gas—267(A)
Loomis, F. W. and **A. J. Allen.** Ultra-violet fluorescence of IBr and I_2—639(A)
Loring, R. A. (see Green, J. B.)—286(A)
Lowry, W. Norwood. Location of the electromotive force in a photo-voltaic cell—1081(A)

Macalpine, William W. Resistance of bismuth in alternating magnetic fields—284(A)
Mack, Julian E. Vector coupling in the Ni-, Pd-, and Pt-like spectra—1098(A)
Mackay, G. M. J. Electrical insulation from the engineering viewpoint—1080(A)
Mackeown, S. S. Cathode drop in a mercury arc—273(A)
Mahoney, J. J. Ion mobilities using the Erikson method on gases of controlled purity—217, 266(A)
MacPherson, A. T. (see Curtis, H. L.)—1080(A)
Malter, Louis (see Wolff, Irving)—282(A), 1061
Margenau, Henry. Dependence of ultra-violet reflection of Ag on plastic deformation—639(A),1035
———Interpretation of deviations from Ohm's law on Fermi statistics—1078(A)
Maris, H. B. The formation of spiral nebulae—1100(A)
———and **E. O. Hulburt.** Theory of auroras and magnetic storms—269(A), 412
———and **E. O. Hulburt.** Comets and terrestrial magnetic storms—283(A),1046
Marshall, Lauriston C. A direct measurement of recombinations of ions and of ions and electrons by a modified alternating field method—266(A)
Martin, John R. Magnetic losses of iron in high frequency alternating current fields—621
Martin, Miles J. Photoelectric and thermionic properties of Mo—991
Martin, R. E. (see Sette, W. J.)—1075(A)
Marvin, H. H. Combination bands in the infrared spectra of CCl_4 and $SiCl_4$—952
Maxwell, L. R. Mean life for the spark spectrum of Hg—1086(A)
McDowell, Louise S. and **Hilda L. Begeman.** The behavior of glass as a dielectric in alternating current circuits: II. The effect of frequency and of temperature upon the power loss—55
McKeehan, L. W. Book Reviews—106, 260, 261, 1066
———and **O. E. Buckley.** Atomic order in ferromagnetism—636(A)
McMillen, J. H. (see Hughes, A. L.)—1069(A)
Meggers, W. F. and **R. M. Langer.** Regularity in frequency shifts of scattered light—287(A)
———(see Langer, R. M.)—115(A)
——— **T. L. de Bruin,** and **C. J. Humphrey.** The first spectrum of krypton—1097(A)
Mendenhall, C. E. Book Review—106
Messenger, Helen A. (see Webb, Harold W.)—319, 282(A)
Michles, W. C. Intensity measurements in the line spectrum of He—267(A)
Miley, H. A. (see Pietenpol, W. B.)—294(A)
Miller, L. F. Heat transmission of air space by hot plate method—295(A)
Millikan, Robert A. and **Charles C. Lauritsen.** Dependence of electron emission from metals upon field strengths and temperatures—598, 633(A)
——— and **G. H. Cameron.** Another attempt to find directional effects in cosmic rays—266(A)

Mitchell, Allan C. G. Directional distribution of the relative velocity of the decomposition products in the optical dissociation of NaI—279(A)
——— On the theory of electron scattering in gases —1068(A)
Mitchell, Dana P. Change of frequency of x-rays scattered by bound electrons—871
——— and **Bergen Davis.** Fine structure of scattered x-rays—292(A)
Mitchell, Paul C. and **W. W. Stifler.** Some experiments on rubber at various temperatures—1095(A)
Miyake, Iwao (see Kirkpatrick, Paul)—268(A)
Mohler, F. L. and **C. Boeckner** Photo-ionization of alkali vapors—1087(A)
——— and **C. Boeckner.** Ionization of caesium vapor by line absorption—1099(A)
——— (see Boeckner, C.)—119(A)
Monk, G. S. (see Gale, H. G.)—114(A)
——— and **A. E. Elo.** New bands in the secondary spectrum of H_2—114(A)
Montgomery, Carol G. (see Frayne, John G.)—549
Morris, B. D. (see Ramsey, R. R.)—1076(A)
Morse, Philip M. Vibrational levels and potential energies of diatomic molecules—1091(A)
——— and **E. C. G. Stueckelberg.** The hydrogen molecular ion as a wave-mechanical perturbation of the helium ion—290(A)
——— and **E. C. G. Stueckelberg.** Diatamic molecules according to the wave mechanics I. Electronic levels of the H molecular ion—932
——— (see Gurney, R. W.)—789
Mortimore, Roy H. Measurement of the intensity of high frequency magnetic fields—113(A)
Mulder, Peter J. and **Joseph Razek.** High amplification by making use of grid currents—284(A)
——— (see Razek, Joseph)—284(A)
Mulliken, Robert S. Formation of MH molecules; effects of H atom on M atom—285(A)
——— Electronic states and band spectrum structure in diatomic molecules. VIII. Some empirical relations in σ-type doubling—507
——— Assignment of quantum numbers for electrons in molecules: III. Diatomic hydrides—730

Nickerson, J. L. (see Compton, K. T.)—1085(A)
Nicholson, Seth B. (see Pettit, Edison)—273(A)
Niessen, K. F. Saturation of electric and magnetic polarization of gases on the basis of quantum mechanics—1079(A)
Nottingham, W. B. Probe and radiation measurements in the normal copper arc—280(A)
——— Non-linearity of photoelectric response near long wavelength limit—633(A)
——— Departure from Einstein's photoelectric equation with certain alkali metal films—1081(A)
Null, F. E. and **J. B. Edwards.** Mechanism of dielectric breakdown in thin layers—1076(A)
Nusbaum, R. E. (see Paton, R. F.)—1093(A)

O'Brien, Brian. Photographic spectral energy measurements with a spiral aperture disk—640(A)
——— Energy distribution in the solar ultraviolet spectrum—1072(A)
O'Bryan, H. M. (see Smith, K. K.)—66
O'Leary, A. J. (see Gray, J. A.)—292(A)
Olpin, A. R. Use of dielectrics to sensitize alkali metal photoelectric cells to red and infra-red light—1081(A)
———(see Ives, Herbert E.)—281(A)
Olshevsky, Dmitry E. Orientation of crystals in magnetic fields—278(A)
Olson, H. F. (see Ellet, A.)—118(A)
Ovrebo, Paul J. Spectral terms of Pt and classification—1098(A)

Page, Leigh. Book Review—108
——— Motion of ions in constant fields—553, 633(A)
——— Relativity precession—572
——— Effect of the earth's magnetic and electric fields on ion paths in the upper atmosphere—823
Parlin, W. A. and **A. H. Pfund.** The effect of temperature on the absorption bands of fused quartz in the infra-red—639(A)
Parsons, Samuel R. The effect of corona current on the cooling of a hot wire—75
——— Surface friction in tubes not of circular cross section—112(A)
Paton, R. F. and **W. D. Lansing.** New terms in the spectrum of Al I—1099(A)
——— and **R. E. Nusbaum.** Series relationships in Be I—1093(A)
——— and **G. M. Rassweiler.** Furnace spectrum of beryllium—16
Paulin, Eugene A. Some polarization phenomena of very short radio waves—432
Pauling, Linus. Quantum defects for non-penetrating orbits—270(A)
Peters, M. F. (see Brickwedde, F. G.)—116(A)
Pettit, Edison and **Seth B. Nicholson.** Lunar radiation and temperatures during an eclipse—273(A)
Pfund, A. H. Resonance radiometry—639(A)
——— Transmission-reflection grating for the infra-red—1093(A)
——— (see Parlin, W. A.)—639(A)

Pielemeier, W. H. Pierce acoustic interferometer as an instrument for the determination of velocity and absorption—1094(A)
Pietenpol, W. B. and **A. P. Friesen.** New theory of the rectifying action of the aluminum cell—277(A)
——— and **H. A. Miley.** Temperature coefficients of resistance of low melting point metals in the solid and liquid states—294(A))
Plyler, E. K. Combination frequencies of the infra-red bands of quartz—48
——— The near infra-red absorption spectra of calcite and strontianite—948
——— The near infra-red absorption bands of organic compounds—1092(A)
Podolsky, Boris. On the assumptions of matrix mechanics—270(A)
Poindexter, Franklin E. and **Marie Kernaghan.** Surface tension of Na—837
Pool, M. L. Measurement of the life of metastable Hg atom—22, 117(A)
Purks, Harris (see Davis, Bergen)—1089(A)

Race, H. H. and **J. R. Campbell, Jr.** Dielectric polarization potential and the law of superposition for hard rubber—1076(A)
Rainich, G. Y. Book Reviews—461
Ramsey, R. R. and **B. D. Morris.** Resistance of air condensers—1076(A)
Randall, D. P. Influence of shape on the efficiency and stability of permanent magnets—1070(A)
Randolph, D. W. (see Wolfe, R. A.)—1075(A)
Rashevsky, N. Equilibria in systems with surface phases—278(A)
——— Compressibility of crystals and atomic fields —636(A)
——— On hysteresis in physico-chemical systems—641(A)
Rassweiler, G. M. (see Paton, R. F.)—16
Razek, Joseph and **Peter J. Mulder.** Photoelectric spectro-photometer—284(A)
——— (see Mulder, Peter J.)—284(A)
Reynolds, N. B. Schottky effect and contact potentials of thoriated tungsten filaments—1083(A)
Rice O. K. Theory of diffuse band spectra—271(A)
——— Perturbations in molecules and theory of predissociation and diffuse spectra—748
Rich, D. L. (see Firestone, F. A.)—634(A)
Richtmyer, F. K. Satellites of certain x-ray lines—291(A)
——— On the determination of the wave-length of x-ray satellites—1088(A)
——— (see Barnes, S. W.)—636(A)
Riffolt, N. (see Thompson, L.)—277(A)
Rodebush, W. H. (see Copley, M. J.)—1083(A)
Rojansky, Vladimir. On the theory of the Stark effect in hydrogenic atoms—1
——— Interaction of the Stark effect and electronic spin in alkalis—1084(A)
——— (see Hughes, A. L.)—1069(A)
Rosenthal, Jenny E. and **F. A. Jenkins.** Quantum analysis of the BeO bands—163
——— and **F. A. Jenkins.** Perturbations in band spectra—285(A)
Ruark, Arthur E. New system of dynamics—637(A)
——— Generalizations of Planck's formula—640(A)
——— Indetermination principles—1078(A)
Russell, H. N., A. G. Shenstone and **Louis A. Turner.** Report on notation for atomic spectra—900

Sabine, Paul E. Measurement of sound absorption coefficients—634(A)
Sagui, Cornelio L. The atomic electric charges in the electromagnetic quantum theory —123(A)
—— Weiss, Planck and Rydberg constants in the theory of the electromagnetic quantum—288(A)
Salant, E. O. and **A. Sandow.** Raman effect for HCl liquid—1096(A)
——— and **W. West.** Infra-red absorption of formaldehyde vapor, I—640(A)
Samson, E. W. (see Turner, Louis A.)—1085(A)
Sandow, A. (see Salant, E. O.)—1096(A)
Sappenfield, James W. The absorption spectra of certain organic liquids in the near infra-red —37
Sawyer, C. B. and **C. H. Tower.** Properties of Rochelle salt as a dielectric with Braun tube oscillograms—1076(A)
Sawyer, R. A. and **R. J. Lang.** The first spark spectrum of Ga—1097(A)
Scott, A. H. (see Curtis, H. L.)—1080(A)
Seeger, R. J. Some critical points in a study of recent quantum theories—1079(A)
——— (see Lindsay, R. B.)—1078(A)
Seemann, Herman E. Thermal conductivity of Pyrex glass as a function of temperature—1094(A)
Sette, W. J. and **R. E. Martin.** Forced electric oscillations in three circuits with electromagnetic coupling—1075(A)
Sheldon, D, C. O and N spectra in the extreme ultra-violet—267(A)
Shenstone, A. G. (see Russell, H. N.)—900
Silberstein, Ludwik. The curvature radius of space-time derived from 24 Cepheid variables and 35 O-stars—1074(A)
Slack, F. G. Low voltage electron impacts in H—1085(A)
Slater, J. C. Book Review—869
Slepian, J. and **E. J. Haverstick.** Arcs with small cathode current density—52, 280(A)
Smith, Alpheus W. and **Joy Dillinger.** Effect of tension and a longitudinal magnetic field on the thermoelectromotive forces in permalloy—398

Smith, H. L. (see Duffendack, O. S.)—1085(A)
Smith, K. K. and **H. M. O'Bryan.** A comparison of the Corbino and Hall effects in silver and brass —66
Smith, Lloyd P. Emission of positive ions from tungsten at high temperatures—279(A)
——— On the emission of positive ions from hot tungsten—1082(A)
Smith, W. O. and **Paul D. Foote.** Capillary phenomena in non-circular capillaries—637(A)
Smyth, C. P. Dependence of dielectric polarization upon molecular condition—1080(A)
Sneed, M. C. Book Review—460
Snyder, Rufus H. Some studies in the Stark effect for the diffuse lines of Ag and Li—354
Sokoloff, V. M. (see Zaikowsky, W. M.)—264(A)
Stair, R. and **W. W. Coblentz.** Infra-red absorption spectrum of chlorophyll and xanthophyll—1092(A)
——— (see Coblentz, W. W.)—1092(A)
Steadman, L. T. Wave-length measurement of γ-rays from radium and its products—120(A), 1069(A)
Steele, F. A. (see Davey, Wheeler P.)—291(A)
Stein, Wesley S. (see Knipp, Chas. T.)—124(A)
Stewart, G. W. Diffraction of x-rays in liquids: benzene, cyclohexane and certain of the derivatives—121(A), 889
——— Diffraction of x-rays in liquids: isomers of n-octyl alcohol—1087(A)
Stewart, John Q. Essay toward a new logic in physics—637(A)
——— The development of "thermodynamic symbolism"—641(A), 1073(A)
Stifler, W. W. (see Mitchell, Paul C.)—1095(A)
Stinchcomb, G. A. and **E. F. Barker.** Molecular spectrum of ammonia. I. Two types of infra-red vibration bands —305
Street, J. C. (see Beams, J. W.)—280(A)
Stueckelberg, E. C. G. The explanation of a critical potential of oxygen ($O_2 \rightarrow O^+ + O$) and the intensities of the ultra-violet O_2^+—bands—1091(A)
——— (see Morse, P. M.)—290(A), 932
Stuhlman, Jr., Otto and **M. W. Trawick.** Mercury spectrum by high voltage electrodeless discharge —287(A)
Sutton, Richard M. Ionization of Ne and A by positive ion bombardment—264(A), 364
Swann, W. F. G. Significance of measurements of ionization in closed vessels in relation to cosmic radiation—292(A)

Talbott, F. L. Dielectric constant of air at various radio frequencies—641(A)
Tate, John T. Book Reviews—105, 106, 260, 462, 629, 630
Thomas, C. H. and **O. S. Duffendack.** Anode spots and their relation to the absorption and emission of gases by the electrodes of a Geissler discharge—1093(A)
Thomassen, L. Transmutation of elements—229
Thompson, L. and **N. Riffolt.** Photographic observations of ballistic phenomena—277(A)
Thornton, W. N. and **W. H. Crew.** On the continuous spectrum of Hg—1072(A)
Tonks, Lewi. Two energy types in wave motion and their relation to group and wave velocity—239
———Electrical convection phenomena in oil—1080(A)
———and **Irving Langmuir.** Oscillations in ionized gases—195, Note, 990
———and **Irving Langmuir.** Motion of positive ions in a plasma—1070(A)
Tower, C. H. (see Sawyer, C. B.)—1076(A)
Trawick, M. W. (see Stuhlman, Otto, Jr.—287(A)
Trebler, H. A. (see Karapetoff, V.)—(A)
Turner, Louis A. and **E. W. Samson.** The excitation of *N* lines by controlled electron impact—1085(A)
———(see Russell, H. N.)—900
Tykocinski-Tykociner, J. Application of microphotometers for the analysis of photographic sound records—1094(A)
———and **R. W. Armstrong.** Determination of frequency and decrement by means of plate current variation of thermionic oscillator tubes—634(A)
———(see Kunz, Jakob)—117(A)
Tyndall, E. P. T. (see Hoyem, A. G.)—81

Uhlenbeck, G. E. and **S. Goudsmit.** A problem of Brownian motion—290(A)
———and **H. C. Wolfe.** On the principle of microscopic reversibility—1079(A)
Unsöld, Albrecht. On the influence of collisions on the structure of Fraunhofer lines—268(A)
Urey, H. C. and **John R. Bates.** Recombination spectra of the halogens—279(A)

Vallarta, M. S. Note on the statistical interpretation of Maxwell's equations—1077(A)
———(see Wiener, Norbert)—1077(A)
Van Velzer, H. L. and **W. R. Ham.** Thermionic emission from tungsten and the Schottky equation—1083(A)
Van Vleck, J. H. A mechanical analog to the hydrogen wave equation—122(A)
———On σ-type doubling and electron spin in the spectra of diatomic molecules—467

Vieweg, Alice M., C. W. Gartlein and **R. C. Gibbs.** The use of series inductance in vacuum spark spectra—287(A)
———(see Gibbs, R. C.)—1092(A)

Walbridge, N. L. (see Holmes, R. M.)—281(A)
Walerstein, I. Effect of external fields on the polarization of light in hydrogen canal rays—116 (A), 800
Walters, Francis M., Jr. (see Burns, Keivin)—1098(A)
Wang, S. C. On the separability of Schroedinger's equation for the asymmetrical top—123(A)
———Sigma-type doubling in the asymmetrical top—289(A)
———(see Webb, Harold W.)—288(A), 329
Warner, A. H. Variation of photoelectric effect with temperature and determination of long wavelength limit of tungsten—815
Waterman, A. T. Application of the Fermi-Dirac statistics to specific heats of solids—637(A)
Watson, F. R. Conditions for securing ideal acoustics in auditoriums—283(A)
Way, H. E. (see Worthing, A. G.)—1086(A)
Weatherby, B. B. (see Bazzoni, C. B.)—1101(A)
Webb, Harold W. and **Helen A. Messenger.** Persistence of λ2537 in Hg at low pressures—319, 282(A)
———and **S. C. Wang.** Excitation of sodium by ionized Hg vapor 288(A), 329
Webster, D. L. Book Review—262
———and **W. W. Hansen.** The relation between the continuous and line spectra of x-rays from thin targets—635(A)
West, W. (see Salant, E. O.)—640(A)
Wheeler, Harold A. Amplification of photoelectric currents—114(A)
———Measurement of electrical fluctuation phenomena—124(A)
White, H. E. Spectral relations between certain iso-electronic systems and sequences, Part I., Ca I, Sc II, Ti III, V IV and Cr V—538
———Part II. Sc I, Ti II, V III, Cr IV, Mn V—672
———Part III; Ti I, V II, Cr III, Mn IV, and Fe V— 914
———Spectra of trebly ionized vanadium, V IV and quadruply ionized chromium, Cr V—286(A)
———Spectral relations between certain iso-electronic systems and sequences in the "iron group" —1098(A)
———(see Gibbs, R. C.)—157, 286(A)
White, M. W. (see Kiehl, H. R.)—1089(A)
Whitehead, J. B. Dielectrics and insulation—1080(A)
Whitney, John D. Inelastic collisions of electrons with Hg atoms—117(A)
Wiener, Norbert and **M. S. Vallarta.** On the spherically symmetrical statical field in Einstein's unified theory of electricity and gravitation—1077(A)
Wilber, D. T. Fatigue in the cathodo-luminescence of zirconia—282(A)
Williams, N. H. and **W. S. Huxford.** Shot effect in thermionic emission from oxide coated electrodes—118(A)
———and **W. S. Huxford.** Determination of the charge of positive thermions from measurements of the shot effect—773
Wilson, Channing W. (see Bichowsky, F. Russell)—851
Wilson, E. D. (see Zworykin, V.)—633(A)
Wilson, Thomas A. Determination of the orientation of metallic single crystal specimens by high voltage x-rays—635(A)
———Determination of the orientation of single crystal specimens of metals of the hexagonal system—1087(A)
Wolfe, H. C. (see Uhlenbeck, G. E.)—1079(A)
Wolfe, R. A., O. S. Duffendack and **D. W. Randolph.** Some characteristics of electric sparks excited by an ignition coil—1075(A)
Wolff, Irving and **Louis Malter.** Sound radiation from a system of vibrating circular diaphragms—282(A), 1061
Wood, R. W. Improved methods of exciting Raman spectra of scattered radiation—294(A)
———Raman effect in gases and liquids—1097(A)
Woodrow, Jay W. The photographic activity of cod liver oil—119(A)
Worthing, A. G. and **H. E. Way.** Decay of the spectrum of the afterglow of N mixed with A—1086(A)

Zahl, H. A. (see Ellett, A.)—124(A), 635(A)
Zaikowski, W. M., H. B. Holroyd and **B. M. Sokoloff.** Analysis of the gradual oxidation prior to ignition of fuels in internal combustion engine and the relation of such oxidation to detonation —264(A)
Zeleny, John. Distribution of ionic mobilities in moist air—281(A)
Zener, C. (see Kemble, E. C.)—286(A), 512
Zimmerman, E. E. Effect of temperature treatment on the establishment of a stable condition of the electrodes in a polarization cell—277(A)
Zwicky, F. On the mechanical and electrical strength of dielectric crystals—1080(A)
———On the red shift of spectral lines through interstellar space—1077(A)
———(see Evjen, H. M.)—860
Zworykin, V. and **E. D. Wilson.** The caesium-magnesium photo-cell—633(A)

ANALYTIC SUBJECT INDEX TO VOLUME 33

References with (A) are merely to abstracts of papers presented at meetings of the Physical Society.

Absorption coefficient
Of light in Hg, R. S. Baldwin—1072(A)
Of slow electrons in alkali vapors, B. Brode—1069(A)
Of sound, measurement, P. E. Sabine—634(A)

Absorption of light (see also Spectra)
By Ag, effect of plastic deformation, H. Margenau—639(A), 1035
By calcite and strontianite, infra-red, E. K. —Plyler—948
By CCl_4, infra-red, relation to Raman spectrum, W. W. Coblentz, R. Stair—1092(A)
By chlorophyll and xanthophyll, infra-red, R. Stair, W. W. Coblentz—1092(A)
By fog, L. P. Granath, E. O. Hulburt—1073(A)
By formaldehyde vapor, E. O. Salant, W. West—640(A)
By Hg vapor, R. S. Baldwin—1072(A)
By liquid benzene, criticism of paper by Barnes and Fulweiler, Joseph W. Ellis—625; Reply, J. Barnes—627.
By lower atmosphere, ultra-violet, L. H. Dawson, L. P. Granath, E. O. Hulburt—1073(A)
By Na vapor, width of D_1, S. A. Korff—584, 1072(A)
By O_3, H_2O vapor and quartz in ultra-violet, L. P. Granath—1073(A)
By organic compounds, infra-red, E. K. Plyler—1092(A)
By organic liquids, infra-red, J. W. Sappenfield—37
By quartz, infra-red, bands, E. K. Plyler—48
By quartz, infra-red, effect of temperature, W. A. Parlin, A. H. Pfund—639(A)
Fraunhofer lines, effect of collision, Albrecht Unsöld—268(A)

Acoustics
Absorption coefficients, P. E. Sabine—634(A)
Amplitude ratio and phase difference at ears due to pure tone, F. A. Firestone, D. L. Rich—634(A)
Auditoriums, F. R. Watson—283(A)
Pierce interferometer for measuring velocity and absorption of sound, W. H. Pielemeier—1094(A)
Propagation of sound, D. G. Bourgin—282(A)

Acoustics—cont.
Sound radiation from circular diaphragms, I. Wolff, L. Malter—282(A), 1061
Sound records, photographic, microphotometric analysis, J. Tykocinski-Tykociner—1094(A)
Velocity measurements, tube-correction, R. E. Cornish, E. D. Eastman—90, further note, 258
Velocity of sound in Rochelle salt, E. Klein—1095(A)

Activated gases
Active nitrogen, energy states, K. T. Compton, J. C. Boyce—115(A), 145
Active nitrogen, excitation of aurora green line, J. Kaplan—154
Active nitrogen, existence of metastable molecules, J. Kaplan—189
H_2, properties of excited states, E. C. Kemble, C. Zener—286(A)
N_2, afterglow, J. Kaplan—638(A)
N_2, decay of afterglow as affected by A, A. G. Worthing, H. E. Way—1086(A)

Activity, photographic
Of cod liver oil, J. W. Woodrow—119(A)

Adsorption of gases
By electrodes in Geissler tube, C. H. Thomas, O. S. Duffendack—1093(A)
By sputtered films, L. R. Ingersoll—1094(A)
On glass, optical study, J. H. Frazer—97

Alpha-particles (see also Radioactivity)
From Po, straggling in gases, Henry Eyring—386

Amplifier
For photoelectric currents, H. A. Wheeler—114(A)
For small direct currents, J. M. Eglin—113(A)
Using grid currents, P. J. Mulder, J. Razek—284(A)

Arcs (see also Discharge of electricity in gases)
Al, striking potential, S. H. Anderson, W. Bleakney—280(A)
Cu, probe and radiation measurements, W. B. Nottingham—280(A)
Hg, cathode drop, S. S. Mackeown—273(A)
Hg, random electron and positive ion currents, electron temperatures, space potentials in positive column, T. J. Killian—632(A)

Arcs (see also Discharge of electricity in gases)—cont.
Hg, resistance, positive volt-ampere characteristic, A. W. Hull—119(A)
Of low current density, mechanism, J. Slepian, E. J. Haverstick—52, 280(A)

Astrophysics
Constitution of moon, P. S. Epstein—269(A)
Curvature of space-time from 24 Cepheid variables and 35 O-stars, L. Silberstein—1074(A)
Effect of thermal motion of ions on sun's magnetic field, R. Gunn—614
Formation of spiral nebulae, H. B. Maris—1100(A)
Lunar radiation and temperature during eclipse, E. Pettit, S. B. Nicholson—273(A)
Magnetic field of sun-spots, theory, R. Gunn—1099(A)
Radial velocities of globular clusters, P. ten Bruggencate—1077(A)
Red shift of spectral lines, theory, F. Zwicky—1077(A)
Sun's radial magnetic gradient and atmosphere, R. Gunn—283(A), 614

Atomic rays (see also Molecular rays)
In hydrogen, method of production, J. Kunz, J. T. Tykociner—117(A)
Of Cd, velocity when reflected from rock-salt crystals, A. Ellett, H. F. Olson—118(A)
Of Cd and As atoms, reflection from crystals, A. Ellett, H. A. Zahl—124 (A)
Of H, reflection from crystals, T. H. Johnson—293(A)
Repeated reflection from crystals, A. Ellett, H. A. Zahl—635(A)

Atomic structure (see also Energy levels, Spectra)
Electron distribution from x-ray intensities, S. K. Allison—1087(A)
Radius of Hg, E. Gaviola—309

Aurora
Green line excitation in active N_2, J. Kaplan—154
Origin, theory, H. B. Maris, E. O. Hulburt—269(A)
Spectrum, origin, J. Kaplan—638(A)

Ballistics
Photographic observation, L. Thompson, N. Riffolt—277(A)

Barkhausen effect (see also Magnetic properties)
Average size of discontinuities in magnetization, R. M. Bozorth—1071(A)
In Fe, Ni and permalloy, R. M. Bozorth—636(A)

Becquerel effect (see Photo-sensitivity)

Book Reviews
Berliner, Arnold. Lehrbuch der Physik—105
Birtwistle, G. The New Quantum Mechanics—869
Bloch, Eugene. Thermionic Phenomena—459
Boll, M., C. Salomon. Introduction a la Theorie des Quanta—108
Grotrian, W. Struktur der Materie, Band VII, Graphische Darstellung der Spektren von Atomen und Ionen mit Ein, Zwei und Drei Valenzelektronen. Part I—109
Caswell, Albert Edward. An Outline of Physics—109
Debye, P. Probleme der Modernen Physik—630
Eisenhart, L. P. Non-Riemannian Geometry—461
Fry, Thornton C. Probability and Its Engineering Uses—107
Kirsch, Gerhard. Geologie und Radioaktivität—629
Klein, Felix. Vorlesungen über Nichteuklidische Geometrie—461
Lagally, Max. Vorlesungen über Vektor-Rechnung—108
Larner, E.T. Practical Television—459
Longley, William Raymond and Ralph Gibbs Van Name. The Collected Works of J. Willard Gibbs—262
Lyman, Theodore. Spectroscopy of the Extreme Ultra-Violet—628
Millikan, R. A., H. G. Gale, and C. W. Edwards. A First Course in Physics for Colleges—106
Morse, Jared Kirtland. Bibliography of Crystal Structure—260
Müller-Pouillets, Lehrbuch der Physik—628
Page, Leigh. Introduction to Theoretical physics—629
Preston, Thomas. The Theory of Light—459
Richtmyer, F. K. Introduction to Modern Physics—262
Roberts, J. K. Heat and Thermodynamics—261
Scheminsky, Ferdinand. Handbuch der Biologischen Arbeitsmethoden, Teil A, Heft 6, Elektronen und Ionenrohren—460
Seidell, Atherton. Solubilities of Inorganic and Organic Compounds, Volume II—460
Sommerfeld, Arnold. Atombau und Spektrallinien—869
Svedberg, The. Colloid Chemistry—105
Voigt, Woldemar. Lehrbuch der Kristallphysik—261
Weyl, Hermann. Gruppentheorie und Quantenmechanik—460

Book Reviews—cont.
Wien-Harms, Handbuch der Experimentalphysik, Band VII, Teil 1, Krystallographische und Strukturtheoretische Grundbegriffe, P. Niggli —106
Wien-Harms, Handbuch der Experimentalphysik, Band VII, Teil 2, Strukturbestimmung mit Röntgeninterferenzen. H. Ott. Gitter-Theorie der festen Körper, K. F. Herfeld—1066
Wien-Harms, Handbuch der Experimentalphysik, Band XIII, Teil 2, Part I, Physik der Glühelektroden by W. Schottky and H. Rothe. Part II, Herstellung der Glühelektroden by H. Simon, Part III. Technische Elektronenrohren und Ihre Verwendung by H. Rothe. —263
Wien-Harms,, Handbuch der Experimentalphysik Band XV, Radioaktivität, K. W. F. Kohlrausch—628
Wilson, H. A. Modern Physics—260

Brownian motion
Of small suspended mirror, G. E. Uhlenbeck, S. Goudsmit—290(A)

Canal rays
Of hydrogen, polarization of light as affected by electric and magnetic fields, I. Walterstein—166(A), 800

Capacitance
In Al cell, E. M. Dunham—819
Of glasses in alternating current circuits, temperature variation, L. S. McDowell, H. L. Begeman—55

Capillarity (see Surface tension)

Chemical reaction
Oxidation of fuels, relation to detonation, W. M. Zaikowsky, H. B. Holroyd, V. M.. Sokoloff—264(A)
Quantum mechanics, R. M. Langer—1099(A)
Rate, quantum theory, R. M. Langer—290(A)

Collisions of second kind
Hg^+, excitation with Na, spectrum, H. W. Webb, S. C. Wang—288(A), 329
In gas mixtures He-CO, Ne-CO, O. S. Duffendack, H. L. Smith—1085(A)
Hg in gases, E. Gaviola—309

Comets
And terrestrial magnetic storms, H. B. Maris, E. O. Hulburt—283(A), 1046

Compton effect
Breadth of shifted line, relation to Fermi statistics, J. DuMond—123(A), 643

Compton effect—cont.
Effect of temperature, G. E. M. Jauncey, H. Bauer—1088(A)
Fine structure, for C, Al and Be, D. P. Mitchell 871
Fine structure of shifted lines, B. Davis, H. Purks—1089(A)
In standing electromagnetic waves, M. Allen—293(A)

Conductivity, electrical (see Electrical conductivity and resistance)

Constants, physical
Values, R. T. Birge—265(A)

Corbino effect
In silver and brass, K. K. Smith, H. M. O'Bryan —66

Corona discharge
Effect on cooling a hot wire, S. R. Parsons—75

Cosmic rays
Characteristics, from study of gamma rays, J. A. Gray, A. J. O'Leary—292(A)
Directional effect, negative result, R. A. Millikan, G. H. Cameron—266(A)
Significance of measurements of ionization, W. F. G. Swann—292(A)

Crystals and crystal structure
Atomic order in ferromagnetism, L. W. McKeehan, O. E. Buckley—636(A)
Compressibility and atomic fields, theory, N. Rashevsky—636(A)
Determination of orientation of single crystals by x-rays, T. A. Wilson—635(A)
Lattice energetics, R. H. Canfield—294(A)
Metals, lattice energetics of plastic flow, R. H. Canfield—1100(A)
Of $9CaO \cdot 3Al_2O_3$, lattice spaces, W. P. Davey, F. A. Steele—291(A)
Of K_2SO_4, lattice constants, F. P. Goeder—120(A)
Of PdH systems, J. D. Hanawalt—444
Of Se, photo-e.m.f., R. M. Holmes, N. L. Walbridge–281(A)
Of solid Hg, K. Lark-Horovitz—121(A)
Of Zn, method of growing , A. G. Hoyem, E. P. T. Tyndall—81
Orientation in magnetic fields, D. E. Olshevsky —278(A)
Orientation in metals of hexagonal system, T. A. Wilson—1087(A)

Cybotactic state
In benzene, cyclohexane and derivatives, G. W. Stewart—121(A), 889
In isomers of n-octyl alcohol, G. W. Stewart—1087(A)

Dielectrics and Dielectric properties
Air, at radio frequencies, F. L. Talbott—641(A)
Breakdown in thin layers, mechanism, F. E. Null, J. B. Edwards—1076(A)
Conductivity, influence of surfaces and space charges, K. F. Herzfeld—1081(A)
Crystals, mechanical and electrical strength, F. Zwicky—1080(A)
Dielectrics and insulation, J. B. Whitehead—1080(A)
Liquids, breakdown, time lag, J. W. Beams—632(A)
Rochelle salt, C. B. Sawyer, C. H. Tower—1076(A)
Rubber, effect of temperature, H. L. Curtis, A. T. MacPherson, A. H. Scott—1080(A)
Polarization, effect of molecular condition, C. P. Smyth—1080(A)
Polarization of gases, quantum mechanics, K. F. Niessen—1079(A)
Polarization phenomena and superposition in hard rubber, H. H. Race, J. R. Campbell, Jr.—1076(A)

Diffraction of electrons (see Electrons)

Diffraction of light
By circular opening, theory and experiment, M. E. Hufford, H. T. Davis—115(A),589

Discharge of electricity in gases (see also Arc, Spark discharge)
Anode spots, relation to gas content of electrodes, C. H. Thomas, O. S. Duffendack—1093(A)
Distribution of electrons between grid and plate as determined by Cs^+ ions, J. M. Hyatt—1100(A)
Electrodeless discharge, conditions for initiation, N. T. Gordon, S. Dushman—632(A)
Electrodeless ring discharge in H_2 to produce atomic hydrogen, J. Kunz, J. T. Tykociner—117(A)
Interaction of electron and positive ion space charges, I. Langmuir—954
Motion of positive ions in a plasma, L. Tonks, I. Langmuir—1070(A)
Oscillations in ionized gas, L. Tonks, I. Langmuir—195, Note, 990

Discharge of electricity in high vacua (see also thermionic emission)
Electron emission in high fields as function of field strength and temperature, R. A. Millikan, C. C. Lauritsen—598, 633(A)
Electron emission in high fields, temperature dependence, W. V. Houston—361

Dispersion
Anomalous, for soft x-rays in Pt, Ag, calcite and glass, E. Dershem—659
Anomalous, for electrons, by Ni, C. J. Davisson, L. H. Germer—292(A)

Dissociation (see also Heat of dissociation)
Of NaI, by light, direction and velocity of products, A. C. G. Mitchell—279(A)

Dynamics (see also Mechanics)
New system. A. E. Ruark— 637(A)

Effusion
Of gases, at high temperatures, F. R. Bichowsky, C. W. Wilson—851

Elasticity
Of springs, G. D. Collins, O. B. Ader—1096(A)
Of rubber, temperature variation, P. C. Mitchell, W. W. Stifler—1095(A)
Vibration problems with solid damping, A. L. Kimball—1095(A)

Electrical conductivity and resistance
Of air condensers, R. R. Ramsey, B. D. Morris—1076(A)
Of Be, from—180°C to 700°C, E. J. Lewis—284(A)
Of Bi, in alternating magnetic fields, W. W. Macalpine—284(A)
Of dielectrics, effect of surfaces and space charges, K. F. Herzfeld—1081(A)
Of metals, temperature coefficient, W. B. Pietenpol, H. A. Miley—294(A)

Electrical oscillations and waves (see also Radio)
Determination of frequency and decrement, oscillator tubes, J. T. Tykociner, R. W. Armstrong—634
Effect on light waves, when impressed on Kerr cell, A. Bramley—279(A)
Effect on optical properties of water, A. Bramley—640(A)
In three circuits with electromagnetic coupling, W. J. Sette, R. E. Martin—1075(A)
Polarization phenomena, E. A. Paulin—432
Resonance in circuits with parallel resistances, A. Astin—1074(A)

Electrolytes
Internal pressure, H. M. Evjen, F. Zwicky—860
Photoactive, location of e.m.f., W. N. Lowry—1081(A)

Electrolytic cells
Al cell, capacity, E. M. Dunham—819
Al cell, theory of rectifying action, W. B. Pietenpol, A. P. Friessen—277(A)

Electrolytic cells—cont.
Effect of temperature on polarization cell, E. E. Zimmerman—277(A)
Photo-active, location of e.m.f., W. N. Lowry—1081(A)

Electromagnetic theory
And gravitation, the spherically symmetrical static field, N. Weiner, M. S. Vallarta—1077(A)
Paths of charged particles in electric and magnetic fields, W. Bartky, A. J. Dempster—1019
Radiation by accelerated electron, John A. Eldridge—123(A)

Electromechanical properties (see also Piezo-electric effect)
Of Rochelle salt crystals, W. G. Cady—278(A)

Electrons (see also Electrons in gases; Electrons in metals; Electrons, secondary)
Absorption coefficients in alkali vapors, R. B. Brode—1069(A)
And radiation, R. D. Kleeman—288(A)
Anomalous dispersion by Ni, C. J. Davisson, L. H. Germer—292(A)
Charge, from x-ray measurements, J. A. Bearden —1088(A)
Diffraction by Cu crystal, H. E. Farnsworth—1068(A)
Effects of impacts on metallic surfaces, P. H. Carr—1068(A)
Paths in electric and magnetic fields, W. Bartky, A. J. Dempster—1019
Paths in radial electric field, re-focusing, A. L. Hughes,V. Rojansky, J. H. McMillen—1069(A)
Penetration through glass, C. T. Knipp—125(A)
Polarization of electron waves by reflection from Ni crystal, test, C. J. Davisson, L. H. Germer—118(A), 760
Quantum numbers in diatomic hydrides, R. S. Mulliken—730
Ratio of charge to mass, revision of value, from spectra, H. D. Babcock—268(A)
Scattering of light, G. Glockler—116(A)
Stark effect and electron spin, V. Rojansky—1084(A)

Electrons in gases (see also Arcs, Discharge of electricity in gases; Potentials, critical)
Angular scattering in He, G. P. Harnwell—632(A)
Angular scattering in He, Ne, H_2 and N_2, G. P. Harnwell—293(A), 559
Attachment to molecules of air and O_2 A. M. Cravath—266(A), 605
Impacts in hydrocarbons, chemical effects, V. Karapetoff, H. A. Trebler, E. C. Linder—1080(A)

Electrons in gases (see also Arcs) Discharge of electricity in gases; Potentials, critical)—cont.
In H_2, angular scattering, G. P. Harnwell—1067(A)
In H_2, critical potentials and spectrum, F. G. Slack—1085(A)
In He efficiency of inelastic impact at 19.77 volts, G. Glockler—175
In Hg vapor, efficiency of inelastic collisions at 4.9, 6.7 and 8.8 volts, J. D. Whitney—117(A)
In N_2, critical potentials and spectrum of N, L. A. Turner, E. W. Samson—1085(A)
Oscillations in ionized gases, L. Tonks, I. Langmuir—195, Note, 990
Recombination with ions, L. C. Marshall—266(A)
Scattering, theory, A. C. G. Mitchell—1068(A)

Electrons in metals
Confirmatory evidence for applicability of Pauli's exclusion principle, J. Du Mond—123(A), 643
Deviations from Ohm's law on Fermi statistics, H. Margenau—1078(A)
Emission under high fields as function of field strength and temperature, R. A. Millikan, C. C. Lauritsen—598, 633(A)
Emission under high fields, temperature dependence, W. V. Houston—361

Electrons, secondary
From target of x-ray tube, H. R. Kiehl, W. R. Ham, M. W. White, W. P. Davey—1089(A)
Shot effect, L. J. Hayner, A. W. Hull—281(A)

e/m
Revision of value, from spectra, H. D. Babcock—268(A)

Energy states in atoms and molecules (see also Atomic structure; Metastable states, Molecular structure)
Electron occupancy, from x-ray intensities, S. K. Allison—1087(A)
In diatomic molecules, vibration levels and potential energies, P. M. Morse—1091(A)
Of diatomic molecules, electron levels, theory, P. M. Morse, E. C. G. Stueckelberg—932
Of electrons in diatomic hydrides, assignment of quantum numbers, R. S. Mulliken—730
Of electrons in diatomic molecules, sigma type doubling, R. S. Mulliken—507
Of Hg atoms, persistence, H. W. Webb, H. A. Messenger—319, 282(A)
Of Hg^+, mean life, L. R. Maxwell—1086(A)
Of Hg, two-quantum excited states, E. C. Kemble, C. Zener—512

Entropy
Relation to probability, W. S. Kimball—113(A)

Evaporation
Effect of electric fields, E. H. Greibach—844
Of Th from W, rate, as function of temperature, M. R. Andrews—454

Faraday effect
Time lags, critique of measurements, E. Gaviola—1023

Fermi-Dirac statistics (see Statistics)

Ferromagnetism (see Magnetic properties)

Field currents (see Discharge of electricity in high vacua)

Fine structure (see spectra)

Fluorescence
Of IBr and I_2, ultra-violet, analysis, F. W. Loomis, A. J. Allen—639(A)
Time lags, critique of measurements, E. Gaviola—1023

Fraunhofer lines
Effect of collisions, A. Unsöld—268(A)

Friction
Internal, in metals, R. H. Canfield—277(A)
Internal, vibration problems, A. L. Kimball—1095(A)
Of metals, influence of surface condition, R. B. Dow—252
Surface friction in tubes, S. R. Parsons—112(A)

Galvano-magnetic effects
Corbino and Hall effects in silver and brass, K. K. Smith, H. M. O'Bryan—68

Gamma rays (see also Radioactivity)
Characteristics, relation to cosmic rays, J. A. Gray, A. J. O'Leary—292(A)
From radon products, wave-length, L. T. Steadman—120(A), 1069(A)

Gases (see also Thermodynamics)
Clausius' equation of state, H. J. Brennen—1099(A)

Geophysics
Control of hurricanes, W. S. Franklin—294(A)
Dynamics and constitution of atmosphere, P. S. Epstein—269(A)
Effect of thermal motion of ions on earth's magnetic field, R. Gunn—832
Gravitation and electricity, theory, N. Wiener, M. S. Vallarta—(A)1077

Geophysics—cont.
Ion paths in upper atmosphere, L. Page—823
Magnetic field of earth, theory, R. Gunn—1074(A)
Magnetic storms and comets, H. B. Maris, E. O. Hulburt—283(A),1046

Grating
Transmission-reflection grating for infra-red, A. H. Pfund—1093(A)

Gravitation
And electricity, the spherically symmetrical static field, Norbert Wiener, M. S. Vallarta—1077(A)

Hall effect
In silver and brass, K. K. Smith, H. M. O'Bryan—66

Heat conductivity (see Thermal conductivity)

Heat of dissociation
Of N_2, calculation, J. Kaplan—267(A)

Heat of evaporation
Of Th from W, M. R. Andrews—454

Heats of linkage
Of C-H and N-H bonds, from vibration spectra, J. W. Ellis—27

Hydrodynamics
Surface friction in tubes, S. R. Parsons—112(A)
Vortex motion, new treatment, H. Bateman—270(A)
Wind tunnel turbulence quantitative measurements, H. L. Dryden, A. M. Kuethe—1095(A)

Hysteresis
In physico-chemical systems, N. Rashevsky—641(A)

Indetermination principles (see Mechanics, quantum)

Instruments (see Methods and Instruments)

Insulation, electrical
From engineering viewpoint, G. M. J. Mackay—1080(A)

Intensities in spectra (see also Spectra)
Energy distribution in solar ultra-violet spectrum, B. O'Brien—1072(A)
Of He, effect of pressure and potential, W. C. Michels—267(A)
Of Hg, variation with pressure and mode of discharge, J. G. Frayne, C. G. Montgomery—549
Of Ti I and Ti II, formulas, G. R. Harrison—271(A)

Intensities in spectra (see also Spectra)—cont.
Of Ti I, relative intensities in multiplets, G. R. Harrison, H. Engwicht—271(A)
Quantum mechanical theory, B. Cassen—271(A)

Ionization (see also Photo-ionization)
By K^+ ion impact, in Ne, A, R. M. Sutton—264(A), 364
By positive ions and excited atoms, O. S. Duffendack, H. L. Smith—1085(A)

Ionization, residual (see Cosmic rays)

Ions (see also Positive ray analysis)
Hg^+, excitation of Na vapor, H. W. Webb, S. C. Wang—288(A), 329
In air, nature, H. A. Erikson—403
K^+, emission from hot W, L. P. Smith—1082(A)
K^+, ionization in Ne, A, by impact, R. M. Sutton—264(A), 364
Thermions, charge, from shot effect, N. H. Williams, W. S. Huxford—773
Motion in earth's magnetic field, R. Gunn—1074(A)
Motion in constant fields, L. Page—553, 633(A)
Negative, rate of formation by electron attachment, A. M. Cravath—266(A), 605
Oscillations in ionized gases, L. Tonks, I. Langmuir—195, Note, 990
Paths in electric and magnetic fields, W. Bartky, A. J. Dempster—1019
Paths in upper atmosphere, effect of earth's electric and magnetic fields, L. Page—823
Positive, duration of effect on space charge, C Boeckner, F. L. Mohler—119(A)
Positive, emitted by hot W filaments, L. P. Smith—279(A)
Positive, in triode, as rectifier, K. H. Kingdon—1075(A)
Positive, motion in a plasma, L. Tonks, I. Langmuir—1070(A)
Positive, radiometer effect, C. T. Knipp, W. S. Stein—124(A)
Recombination with electrons in gases, L. C. Marshall—266(A)
Thermal motion in inhomogeneous magnetic field, effect on solar and terrestrial magnetism, R. Gunn—832

Ions, mobility
Apparatus for determining, O. Blackwood—1070(A)
Effect of H_2O vapor on positive air ions, H. A. Erikson—118(A)
In air, nature of ions, H. A. Erikson—403, 1070(A)
In H_2, effect of amines, L. B. Loeb, K. Dyk—267(A)

Ions, mobility—cont.
In moist air, distribution of mobilities, J. Zeleny—281(A)
Of air ions in gases by Erikson method, J. J. Mahoney—217, 266(A)
Of K^+, Rb^+, CO^+ in flames, H. E. Banta—211
Of radioactive recoil ions, L. L. Loeb, L. B. Loeb—272(A)

Isotopes
Of Pb, from PbO band spectrum, S. Bloomenthal—285(A)

Kerr effect
Time lags, critique of measurements, E. Gaviola—1023
In water, as affected by high frequency waves, A. Bramley—640(A)

Latent heat
Of evaporation of Th from W, M. R. Andrews—454

Lenard ray tube
With glass window, C. T. Knipp—125(A)

Light
Electronic theory, H. J. Brennen—1071(A)
Theory, G. H. Draper—1071(A)

Light waves
Modulation produced by high frequency oscillations in Kerr cell, A. Bramley—279(A)

Logic in physics
New formulation, J. Q. Stewart—637(A)

Luminescence
Of zirconia, by cathode rays, fatigue, D. T. Wilber—282(A)

Magnetic fields
High frequency, method of measurement, R. H. Mortimore—113(A)
In sun spots, theory, R. Gunn—1099(A)
Of earth, theory, R. Gunn—1074(A)
Solar and terrestrial, effect of thermal motion of ions, R. Gunn—832(A)

Magnetic properties
Atomic order in ferromagnetism, L. W. McKeehan, O. E. Buckley—636(A)
Barkhausen effect in Fe, Ni and permalloy, R. M. Bozorth—636(A)
Eddy current and hysteresis in Fe in high frequency alternating fields, J. R. Martin—621
Of Bi, effect of alternating magnetic field on resistance, W. W. Macalpine—284(A)
Of Fe crystals, D. Foster—1071(A)

Magnetic properties—cont.
Orientation of small crystals, D. E. Olshevsky—278(A)
Polarization of gases on quantum mechanics, K. F. Niessen—1079(A)
Susceptibilities of organic gases, F. Bitter—389

Magnetic storms
Theory of origin, H. B. Maris, E. O. Hulburt—283(A), 269(A), 1046

Magnetism
Average size of discontinuities, R. M. Bozorth—1071(A)

Magnets
Permanent, efficiency and stability as affected by shape, D. P. Randall—1070(A)

Measurements (see Methods and instruments)

Mechanics, quantum
Assumptions of matrix theory, B. Podolsky—270(A)
Critique of recent theories, R. J. Seeger—1079(A)
Indetermination principles, A. E. Ruark—1078(A)
Interpretation of frequency relation, B. Liebowitz—288(A)
Mechanical analog of hydrogen wave equation, J. H. Van Vleck—122(A)
Of asymmetrical top, separability of wave equation, S. C. Wang—123(A)
Of chemical reaction, R. M. Langer—1099(A)
Of two quantum excited states of H_2, E. C. Kemble, C. Zener—512
Of diatomic molecules, P. M. Morse, E. C. G. Stueckelberg—932
Of diffuse band spectra, O. K. Rice—271(A)
Of electric and magnetic polarization of gases, saturation, K. F. Niessen—1079(A)
Of Compton effect of standing waves, M. Allen—293(A)
Of electron scattering in gases, A. C. G. Mitchell—1068(A)
Of H_2, E. C. Kemble, C. Zener—286(A)
Of H_2^+, as perterbed He^+, P. M. Morse, E. C. G. Stueckelberg—290(A)
Of heat conduction in crystals, Th. von Karman—272(A)
Of nuclear motions associated with electron transitions in diatomic molecules, E. U. Condon—122(A)
Of intensites in spectra, B. Cassen—271(A)
Of radioactivity, R. W. Gurney, E. U. Condon—122(A), 127
Of Raman effect, E. C. Kemble, E. L. Hill—1096(A)

Mechanics, quantum, cont.
Of shot effects, B. Cassen—270(A)
Of vibrational levels and potential energies of diatomic molecules, P. M. Morse—1091(A)
Perterbations in molecules, predissociation and diffuse spectra, O. K. Rice—748
Protonic spin and specific heats, B. Cassen—270(A)
Quantum defects, L. Pauling—270(A)
Relationships between singlets and triplets in two-electron spectra, W. V. Houston—297, 268(A)
Resonance and chemical reaction rate, R. M. Langer—290(A)
Sigma-type doubling and electron spin in diatomic molecules, J. H. Van Vleck—467
Sigma-type doubling in asymmetrical top, S. C. Wang—289(A)
Solution of problems by operator analysis, R. B. Lindsay, R. J. Seeger—1078(A)
Stark effect and electron spin, V. Rojansky—1084(A)
Stark effect in hydrogenic atoms, V. Rojansky—1
Wave mechanism of quantum phenomena, R. V. L. Hartley—289(A)

Mechanics, statistical
Entropy and probability, W. S. Kimball—113(A)
Evidence for Fermi-Dirac statistics, J. DuMond—123(A), 643
Interpretation of Maxwell's equations, M. S. Vallarta—1077(A)
Of electrons in metals, deviation from Ohm's law, H. Margenau—1078(A)
Principle of microscopic reversibility, G. E. Uhlenbeck, H. C. Wolfe—1079(A)

Metastable states (see also Activated gases)
Of Hg, life, E. Gaviola—309
Of Hg, life of 2^3P_0 state in presence of N_2, M. L. Pool—22, 117(A)
Of N, from spectrum, K. T. Compton, J. C. Boyce—115(A), 145

Meteorology (see also Geophysics)
Dynamics and constitution of atmosphere, P. S. Epstein—269(A)
Weather forcasting by radio signal strength, R. C. Colwell—283(A)

Methods and instruments
Amplifier for photoelectric currents, H. A. Wheeler—114(A)
Design of Mo x-ray tube, H. R. Kiehl, W. R. Ham, M. W. White, W. P. Davey—1089(A)
Direct current amplifier for measuring very small currents, J. M. Eglin—113(A)

Methods and instruments—cont.
For analysis of photographic sound records, microphotometer, J. T. Tykociner—1094(A)
For measuring ionic mobilities, O. Blackwood—1070(A)
For exciting Raman spectra, R. W. Wood—294(A), 1097(A)
For frequency and decrement by oscillator tubes, J. T. Tykociner, R. W. Armstrong—634 (A)
For growing Zn crystals, A. G. Hoyem, E. P. T. Tyndall—81
For measuring high frequency magnetic fields, R. H. Mortimore—113(A)
For measuring resistance of air condensers, R. R. Ramsey, B. D. Morris—1076(A)
For measuring x-ray intensities, R. T. Dufford, H. E. Hammond—124(A)
For producing atomic rays of hydrogen, J. Kunz, J. T. Tykociner—117(A)
For refocussing electron beam in radial electric field, A. L. Hughes, V. Rojansky, J. H. McMillen—1069(A)
For registration of electron impacts on a surface, P. H. Carr—1068(A)
Furnace, high temperature, vacuum, for furnace spectra, R. F. Paton, G. M. Rassweiler—16
Lenard ray tube with glass window, C. T. Knipp—125(A)
Optical method of studying adsorption of gases on glass, J. H. Frazer—97
Photo-cell, Cs-Mg, V. Zworykin, E. D. Wilson—633(A)
Photo-cells, of alkali metals, use of dielectrics to sensitize to red, A. R. Olpin—1081(A)
Photo-cells of Li, preparation, H. E. Ives—1081(A)
Photoelectric spectro-photometer, J. Razek, P. J. Mulder—284(A)
Pierce acoustic interferometer for measuring velocity and absorption of sound, W. H. Pielemeier—1094(A)
Radiometry, resonance, A. H. Pfund—639(A)
Spectro-photometric measurements with spiral aperture disc, B. O'Brien—640(A)
Transmission-reflection grating for infra-red, A. H. Pfund—1093(A)
Use of series induction in vacuum spark spectra, Alice M. Vieweg, C. W. Gartlein, R. C. Gibbs—287(A)
Voltmeter, high potential electrostatic, S. W. Barnes, F. K. Richtmyer—636(A)

Mobility of ions (see Ions, mobility)

Molecular rays (see also Atomic rays)
Of HCl, deflection in non-homogeneous electric field, M. J. Copley, W. H. Rodebush—1083(A)

Molecular structure (see also Energy states; Spectra, molecular)
Of BeO constants, from spectrum, J. E. Rosenthal, F. A. Jenkins—163
Of F_2, constants, H. G. Gale, G. S. Monk—114(A)
Of formaldehyde from absorption spectrum, E. O. Salant, W. West—640(A)
Of N, from phenomena of active nitrogen, J. Kaplan—189
Of NH_3, wave-lengths and analysis, G. A. Stinchcomb, E. F. Barker—305
Of NH_3, from spectrum, R. M. Badger, C. Hawley Cartwright—692
Of NH_3, from spectrum, E. F. Barker—684
Of TiO_2, from spectrum, A. Christy—701
Perterbations in molecules, O. K. Rice—748

Optical constants and properties
Of Ag, effect of plastic deformation, H. Margenau—639(A), 1035
Of Hg, absorption and refractive index, R. S. Baldwin—1072(A)
Of water, effect of high frequency waves, A. Bramely—640(A)

Oxidation of fuels
Prior to ignition in internal combustion engine, relation to detonation, W. M. Zaikowsky, H. B. Holroyd, V. M. Sokoloff—264(A)

Penetrating radiation (see Cosmic rays)

Photoelectric effect
Cs-Mg photo-cell, V. Zworykin, E. D. Wilson—633(A)
Non-linearity of response near threshold, W. B. Nottingham—633(A)
Of alkali metal films, departure from Einstein's law, W. B. Nottingham—(A)1081
Of alkali metals, use of dielectric to sensitize, A. R. Olpin—1081(A)
Of alkalis, long wave limit, H. E. Ives, A. R. Olpin—281(A)
Of Cs at low temperature, L. R. Koller—1082(A)
Of Li films, preparation of cells, H. E. Ives—1081(A)
Of liquid tin and allotropic modifications, thresholds, A. Goetz—265(A), 373
Of Mo, work function, and sensitivity, variation with heat treatment and temperature, M. J. Martin—991
Of x-rays, relation of momentums of photo-electron and x-ray, C. D. Anderson—265(A)
Temperature effect, A. H. Warner—815
Use in spectro-photometer, J. Razek, P. J. Mulder—284(A)

Photo-ionization of gases
Of Cs, Rb, K vapor, effect of wave-length, F. L. Mohler, C. Boeckner—1087(A)
Of Cs vapor, F. L. Mohler, C. Boeckner—1099(A)
Of Cs vapor, E. O. Lawrence, N. Edlefsen—265(A)

Photometer
Photoelectric spectro-photometer, J. Razek, P. J. Mulder—284(A)

Photons
Collision and coalescence, A. L. Hughes, G. E. M. Jauncey—290(A)

Photo-sensitivity
Of single crystal Se, R. M. Holmes, N. L. Walbridge—281(A)
Of voltage in cells containing Grignard compounds, R. T. Dufford—119(A)

Physical laws
Periodicity of concepts, V. Cofman—1073(A)

Piezo-electric effect
Of Rochelle salt crystals, W. G. Cady—278(A)
Of Rochelle salt, dielectric properties, C. B. Sawyer, C. H. Tower—1076(A)

Polarization of electron waves
By reflection from Ni crystal, test, C. J. Davisson, L. H. Germer—760

Polarization of light
Effect of x-rays on rotary power, A. A. Bless—121(A)
From hydrogen canal rays in electric and magnetic fields, I. Walerstein—116(A), 800
Of resonance radiation in Cd, A. Ellett—124(A)

Positive ray analysis
Effect of space charge sheaths on interpretation of results, R. W. Gurney, P. M. Morse—789
Method, W. Bartky, A. J. Dempster—1019
Of NH_3 and H_2S, nature of ions and critical potentials, J. H. Bartlett, Jr.—169
Of H_2S, nature of ions and critical potentials, J. H. Bartlett, Jr.—117(A)

Potentials, critical
In H_2, electron impacts, F. G. Slack—1085(A)
In H_2S, nature of ions, J. H. Bartlett, Jr.—117(A)
In Ne, A, ionization by K^+ ion impact, R. M. Sutton—264(A), 361
Of NH_3 and H_2S, ionization, J. H. Bartlett, Jr.—169
Of He, efficiency at 19.77 volts, G. Glockler—175
Of N by controlled electron impact, L. A. Turner, E. W. Samson—1085(A)

Potentials, critical—cont.
Of N, ionization, from spectrum, K. T. Compton, J. C. Boyce—115(A), 145
Of O_2, explanation of $O_2 \rightarrow O^+ + O$, E. C. G. Stueckelberg—1091(A)
Of Sc I, Ti II, V III, Cr IV, Mn V, ionization, from spectra, H. E. White—672

Power factor and power loss
Of glasses as dielectric in alternating current circuits, temperature variation, L. S. McDowell, H. L. Begeman—55

Proceedings of American Physical Society
Minneapolis Meeting, November 30 and December 1, 1928–111
Pasadena Meeting, December 8, 1928–264
New York Meeting, December 27–31, 1928–275
New York Meeting, February 22–23, 1929–631
Washington Meeting, April 18–20, 1929–1067

Quanta (see Photons)

Quantum theory (see Mechanics, quantum)

Radiation
And electrons, R. D. Kleeman—288(A)
Black body, generalization of Planck's formula, A. E. Ruark—640(A)

Radio (see also Electrical oscillation and waves)
Amplification by use of grid currents, P. J. Mulder, J. Razek—284(A)
Characteristics of amplifying circuit, P. B. Carwile—284(A)
Determination of frequency and decrement by oscillator tubes, J. T. Tykociner, R. W. Armstrong—634
Polarization of radio waves, E. A. Paulin—432
Rectification of signals by tubes containing alkali vapor, K. H. Kingdon, E. E. Charlton—998

Radioactivity
Basis for computing age of a mineral, A. F. Kovarik—1069(A)
Quantum mechanics, R. W. Gurney, E. U. Condon—122(A), 127
Straggling of alpha particles from Po in gases, Henry Eyring—386
Wave-length of x-rays from Ra and products, L. T. Steadman—120(A), 1069(A)

Radiometer
Effect of positive ions, C. T. Knipp, W S. Stein—124(A)
New design, A. H. Pfund—639(A)

Raman effect
Classical theory, E. H. Kennard—289(A)
For HCl, E. O. Salant, A. Sandow—1096(A)
Improved method of exciting, R. W. Wood—294(A)
In CCl_4, relation to infra-red absorption, W. W. Coblentz, R. Stair—1092(A)
In CCl_4 and $SiCl_4$, H. H. Marvin—952
In HCl and NH_3 gases, measurements and technique, R. W. Wood—1097(A)
In quartz, temperature effect, F. G. Brickwedde, M. F. Peters—116(A)
In Rochelle salt, R. M. Langer, E. Klein—1100(A)
Quantum mechanics, theory, E. C. Kemble, E. L. Hill—1096(A)
Regularity in frequency shifts of scattered light, W. F. Meggers, R. M. Langer—287(A)
Theory, R. M. Langer—1097(A)
With 21 ft. grating, nature of Raman lines, R. M. Langer, W. F. Meggers—115(A)

Rectification
By positive ions in triode, K. H. Kingdon—1075(A)

Reflection of light
By Ag, effect of plastic deformation, H. Margenau—639(A), 1035

Refractive index
Of Hg, R. S. Baldwin—1072(A)
Of Na vapor, width of D_1 in absorption, S. A. Korff—584, 1072(A)
Of Pt, Ag, calcite and glass, for soft x-rays, E. Dershem—659

Relativity
Curvature of space-time from 24 Cepheid variables and 35 O- stars, L. Silberstein—1074(A)
Precession, Leigh Page—572

Resistance, electrical (see Electrical Conductivity and resistance)

Resonance radiation
In Cd, polarization, A. Ellett—124(A)
Of Hg, persistence, H. W. Webb, H. A. Messenger—319, 282(A)

Scattering of electrons (see Electrons in gases)

Scattering of light (see also Raman effect)
By electrons, G. Glockler—116(A)
Molecular, by lower atmosphere, L. H. Dawson, L. P. Granath, E. O. Hulburt—1073(A)

Shot effect (see also Thermionic emission)
For K^+ thermions, charge, N. H. Williams, W. S. Huxford—773
In wave mechanics, B. Cassen—270(A)
Method of measuring, H. A. Wheeler—124(A)
Of secondary electrons, L. J. Hayner, A. W. Hull—281(A)

Solutions
Surface and volume concentrations of solute, J. M. Eglin—1093(A)

Sound (see Acoustics)

Space charge (see also Thermionic emission)
Duration of effect of ions, C. Boeckner, F. L. Mohler—119(A)
Sheaths, influence on positive ray analysis, R. W. Gurney, P. M. Morse—789

Spark discharge
From ignition coil, characteristics, R. A. Wolfe, O. S. Duffendack, D. W. Randolph—1075(A)
In air, time lag, J. W. Beams, J. C. Street—280(A)
In liquids, time lag, J. W. Beams—632(A)
Spectra, time characteristics, J. W. Beams—1086(A)

Specific heat
Of Mo, 250°C to −40°C, D. Cooper, G. O. Langstroth—243
Of solids, Fermi statistics, A. T. Waterman—637(A)
Of solids, from lattice energetics, R. H. Canfield—294(A)

Spectra, atomic
Fraunhofer lines, effect of collisons, A. Unsöld—268(A)
From metal sparks, time effect, J. W. Beams—1086(A)
In aurora, J. Kaplan—638(A)
Notation, H. N. Russell, A. G. Shenstone, Louis A. Turner—900
Of Ag and Li, Stark effect, R. H. Snyder—354
Of Al I, new terms, R. F. Paton, W. D. Lansing—1099(A)
Of Be, absorption and emission, in furnace, classification, R. F. Paton, G. M. Rassweiler—16
Of Be I, series relationships, R. F. Paton, R. E. Nusbaum—1093(A)
Of C and N, infra-red, wave-lengths and terms, S. B. Ingram—1092(A)
Of Ca I, Sc II, Ti III, V IV, Cr V relations, H. E. White—538
Of Cu, extension, G. Kruger—1101(A)

Spectra, atomic—cont.
Of Cu III, multiplets, R. C. Gibbs, A. M. Vieweg —1092(A)
Of Fe group, relations, H. E. White—1098(A)
Of Fe, vacuum arc, terms and wave-lengths, K. Burns, F. M. Walters, Jr.—1098(A)
Of Ga II, R. A. Sawyer, R. J. Lang—1097(A)
Of Ge III, analysis of triplets, R. J. Lang—1097(A)
Of H by controlled electron impact, F. G. Slack —1085(A)
Of He, in crossed electric and magnetic fields, J. S. Foster—1084(A)
Of He, intensities of Stark components, G. O. Langstroth—1084(A)
Of He, intensities, W. C. Michels—267(A)
Of Hg, comparison of electrodeless discharge and arc, O. Stuhlman, Jr., M. W. Trawick —287(A)
Of Hg, effect of pressure and mode of discharge on intensity, J. G. Frayne, C. G. Montgomery —549
Of Hg^+, mean life, L. R. Maxwell—1086(A)
Of hydrogenic atoms, Stark effect of fine structure, V. Rojansky—1
Of Kr, wave-lengths and intensities, W. F. Meggers, T. L. de Bruin, C. J. Humphrey—1097(A)
Of Mg, under liquids, time lag, J. W. Beams—632(A)
Of Na, excited by Hg^+, H. W. Webb, S. C. Wang—288(A), 329
Of Ne and A, extreme ultra-violet, in ring discharge, K. T. Compton, J. C. Boyce, J. L. Nickerson—1085(A)
Of N by controlled electron impact, L. A. Turner, E. W. Samson—1085(A)
Of N, in extreme ultra-violet, analysis and classification, K. T. Compton, J. C. Boyce—115(A), 145
Of Ni II, classification, R. J. Lang—547
Of Ni II, new combinations, R. J. Lang—638(A)
Of Ni, Pd, Pt-like elements, vector coupling, J. E. Mack—1098(A)
Of O and N, extreme ultra-violet, D. C. Sheldon —267(A)
Of O, aurora green line, J. Kaplan—154
Of O, new terms, R. Frerichs—1091(A)
Of Pr I, hyper-fine structure, R. C. Gibbs, H. E. White—286(A)
Of Pt, terms and classification, P. J. Ovrebo—1098(A)
Of S III, analysis, S. B. Ingram—907
Of Sb, exception to g-sum rule, J. B. Green, R. A. Loring—286(A)

Spectra, atomic—cont.
Of Sc I, Ti II, V III, Cr IV, Mn V, relations, H. E. White—672
Of stripped atoms Li I to O VI, Na I to Cl VII, K I to Mn VII, Rb I to Zr IV, Cs I to Pr V, principal and diffuse doublets, R. C Gibbs, H. E. White—157
Of Ti I, relative intensities of multiplets, G. R. Harrison, H. Engwicht—271(A)
Of Ti I Ti, II, intensity formulas and strong multiplets, George R. Harrison—271(A)
Of Ti I, V II, Cr III, Mn IV, Fe V, relations, H. E. White—914
Of two electron systems, theory, William V. Houston—297, 268(A)
Of V IV, Cr V, analysis, H. E. White—286(A)
Quantum defects, theory, L. Pauling—270(A)

Spectra, continuous
Of Hg, origin, W. N. Thornton, W. H. Crew—1072(A)

Spectra, molecular
In aurora, J. Kaplan—638(A)
Of AgCl, analysis, B. A. Brice—1090(A)
Of BeF, fine structure, F. A. Jenkins—1090(A)
Of BeO, quantum analysis, J. E. Rosenthal, F. A. Jenkins—163
Of calcite and strontianite, near infra-red, absorption, E. K. Plyler—948
Of CCl_4 and $SiCl_4$, combination bands in infra-red, H. H. Marvin—952
Of CCl_4 relation to infra-red absorption, W. W. Coblentz, R. Stair—1092(A)
Of C-H and N-H bonds, vibration, J. W. Ellis—27
Of chlorophyll and xanthophyll, infra-red absorption, R. Stair, W. W. Coblentz—1092(A)
Of CN, perterbations, J. E. Rosenthal, F. A. Jenkins—285(A)
Of CO, excited by ionized and excited atoms of He and Ne, O. S. Duffendack, H. L. Smith—1095(A)
Of CO, Zeeman effect of angstrom bands, F. H. Crawford—341
Of diatomic hydrides, assignment of electron quantum numbers, R. S. Mulliken—730
Of diatomic molecules, sigma doubling, theory, S. C. Wang—289(A)
Of diatomic molecules, sigma-type doubling and electron spin, theory, J. H. Van Vleck—467
Of diatomic molecules, sigma-type doubling, empirical relations, R. S. Mulliken—507
Of diatomic molecules, theory, P. M. Morse—1091(A)

Spectra, molecular—cont.
Of diatomic molecules, theory, P. M. Morse, E. C. G. Stueckelberg—932
Of F_2, molecular constants, H. G. Gale, G. S. Monk—114(A)
Of formaldehyde vapor, wave-lengths, E. O. Salant, W. West—640(A)
Of halogens, H. C. Urey, J. R. Bates—279(A)
Of H_2, by controlled electron impact, F. G. Slack —1085(A)
Of H_2, theory, P. M. Morse, E. C. G. Stueckelberg—290(A)
Of HCl^+, analysis, B. A. Brice, F. A. Jenkins—1090(A)
Of Hg, 2476–2482, interpretation, Edward U. Condon—122(A)
Of H_2, properties of excited states, E. C. Kemble, C. Zener—286(A)
Of IBr and I_2, fluorescence, analysis, F. W. Loomis, A. J. Allen—639(A)
Of H_2, and H_2 new bands in secondary spectrum, G. S. Monk, A. E. Elo—114(A)
Of H_2, origin, J. Kaplan—638(A)
Of H_2, secondary, peculiarities, C. J. Brasefield —925
Of H_2, two quantum excited states, theory, E. C. Kemble, C. Zener—512
Of MgH, Zeeman effect, F. H. Crawford, G. M. Almy—1084(A)
Of MH molecules, R. S. Mulliken—285(A)
Of NH_3, double band at 10μ, structure, E. F. Barker—684
Of NH_3, pure rotation, analysis, R. M. Badger, C. H. Cartwright—692
Of NH_3, wave-lengths and analysis of 3.0 and 1.9μ bands, G. A. Stinchcomb, E. F. Barker —305
Of NO, mechanism of excitation, J. Kaplan, E. L. Kinsey—114(A)
Of O_2^+, intensities, E. C. G. Stueckelberg—1091(A)
Of organic liquids, absorption, infra-red, E. K. Plyler—1092(A)
Of organic liquids, infra-red, J. W. Sappenfield —37
Of PbO, isotope effect, S. Bloomenthal—285(A)
Of quartz, infra-red bands, E. K. Plyler—48
Of Ti O_2, analysis of blue-green bands, A. Christy —701
Perterbations, predissociation and diffuse spectra, O. K. Rice—748

Spectra, Raman (see Raman effect)

Spectra, solar
Intensities in ultra-violet, B. O'Brien—1072(A)

Spectra, technique
Use of inductance in vacuum spark, A. M. Vieweg, C. W. Gartlein, R. C. Gibbs—287(A)

Spectro-photometer
With spiral aperture disc, B. O'Brien—640(A)

Sputtering
Gas content of sputtered films, L. R. Ingersoll 1094—(A)

Stark effect
In He, crossed electric and magnetic fields, J. S. Foster—1084(A)
In He, relative intensities, G. O. Langstroth 1084—(A)
Interaction with electron spin, V. Rojansky—1084(A)
Of Ag and Li lines, R. H. Snyder—354
In hydrogenic atoms, V. Rojansky—1

Statistical mechanics (see Mechanics, statistical)

Sun (see Astrophysics)

Surface tension
Capillary phenomena in non-circular capillaries, W. O. Smith, Paul D. Foote—637(A)
Of Hg, in presence of gases, S. G. Cook—277(A)
Of liquid Na, values and temperature variation, F. E. Poindexter, Marie Kernaghan—837

Susceptibility, magnetic (see Magnetic properties)

Thermal conductivity
Of air, L. F. Miller—295(A)
Of crystals, wave mechanical theory, Th. von Karman—272(A)
Of Pyrex glass, variation with temperature, H. E. Seemann—1094(A)
Of Pb and single and polycrystal Zn, C. C. Bidwell, E. J. Lewis—249

Thermionic emission of electrons
As function of adsorbed material, J. A. Becker —1082(A)
Distribution of electrons between grid and plate as determined by Cs^+ ions, J. M. Hyatt—1100(A)
From Cs at low temperature, L. R. Koller—1082(A)
From Mo, work function and sensitivity, variation with heat treatment and temperature, M. J. Martin—991
From oxide coated filaments, shot effect, N. H. Williams, W. S. Huxford—118(A)
From thoriated W, variation of work function with applied fields, N. B. Reynolds—1083(A)

Thermionic emission of electrons—cont.
From W, variation of work function with applied field, H. L. Van Velzer, W. R. Ham—1083(A)
From W, work function from Schottky effect, W. R. Ham—1083(A)

Thermionic emission of positives
From W, L. P. Smith—279(A)
K^+, from tungsten, work function, L. P. Smith —1082(A)
K^+, shot effect, determination of charge, N. H. Williams, W. S. Huxford—773

Thermodynamics
Development of symbolism, J. Q. Stewart—641(A), 1073(A)
Of systems with surface phases, equilibria, N. Rashevsky—278(A)

Thermoelectric effects
In permalloy, effect of tension and magnetic field, A. W. Smith, J. Dillinger—398

Transmutation of elements
By electron impact and in arcs, negative results, L. Thomassen—229

Turbulence
In wind tunnels, quantitative measurements, H. L. Dryden, A. M. Kuethe—1095(A)

Vaporization (see Evaporation)

Velocity of sound (see Acoustics)

Voltaic cells (see Electrolytic cells)

Vortex motion
In fluids, new treatment, H. Bateman—270(A)

Wave mechanics (see Mechanics, quantum)

Wave motion
Group velocity, D. G. Bourgin—1072(A)
Two energy types, relation to group and wave velocity, L. Tonks—239

Weather (see Meteorology)

Wind tunnels
Quantitative measurements of turbulence, H. L. Dryden, A. M. Kuethe—1095(A)

Work function (see Thermionic emission)

X-rays, absorption
Effect of chemical combination, C. L. Cottrell—879
In Pd-H systems, J. D. Hanawalt—444
M edges in Pt and Au, A. J. M. Johnson—120(A)

X-rays, diffraction
In benzene, cyclohexane and derivatives, G. W. Stewart—121(A), 889
In isomers of n-octyl alcohol, G. W. Stewart—1087(A)

X-rays, dispersion
In glass and Pt, soft rays, E. Dershem—291(A)

X-rays, general
Effect on rotary power of some substances, A. A. Bless—121(A)
From Hg vapor, polarization, W. Duane—1089(A)
Intensities, as function of direction, W. Duane, J. C. Hudson—635(A)
Method of measuring intensities, R. T. Dufford, H. E. Hammond—124(A)

X-rays, photoelectric effect
Relation of momentums of x-ray and electron, C. D. Anderson—265(A)

X-rays, polarization
Of $L\beta_1$ line of W, P. Kirkpatrick, I. Miyake—268(A)

X-rays, reflection
By glass, for soft Ni rays, J. E. Henderson, E. R. Laird—291(A)
Reflecting power of Al, C, Pt for soft x-rays (40–500) volts, S. D. Gehman—141
Total, from thin Ni films on Pt variation of critical angle with thickness, H. W. Edwards—272(A), 463

X-ray, refraction
Anomalous dispersion in Pt near L-series absorption limit, E. Dershem—120(A)
In Pt, Ag, calcite and glass, E. Dershem—659

X-rays, scattering (see also Compton effect)
By bound electrons in C, Al, Be, D. P. Mitchell —871
Fine structure, D. Mitchell, B. Davis—292(A)

X-rays, spectra
Fine structure and satellites of $K\alpha$ lines, C. B. Bazzoni, L. Y. Faust, B. B. Weatherby—1101(A)
Intensity measurements, relation to electron distribution in levels, S. K. Allison—1087(A)
Cu, $K\alpha$ and $K\beta$, absolute wave-length, J. A. Bearden—1088(A)
M-series absorption of Pt and Au, A. J. M. Johnson—120(A)
Of Ir, Tl, U, separation and intensity of components of $L\beta_2$, S. K. Allison—1090(A)

X-rays, spectra—cont.
Relation between continuous and line spectra from thin targets, D. L. Webster, W. W. Hansen—635(A)
Satellites of certain lines, F. K. Richtmyer—291(A)
Wave-lengths of satellites, F. K. Richtmyer—1088(A)
Zn to Ca, *L* wave-length, C. E. Howe—(A)1088

X-rays, technique
Design of Mo tube, H. R. Kiehl, W. R. Ham, M. W. White, W. P. Davey—1089(A)

Zeeman effect
Anomalous, in Sb, exception to *g*-sum rule, J. B. Green, R. A. Loring—286(A)
In CO angstrom bands, F. H. Crawford—341
In spectrum of MgH, F. H. Crawford, G. M. Almy—1084(A)

Fused Pure Quartz

Vitreosil

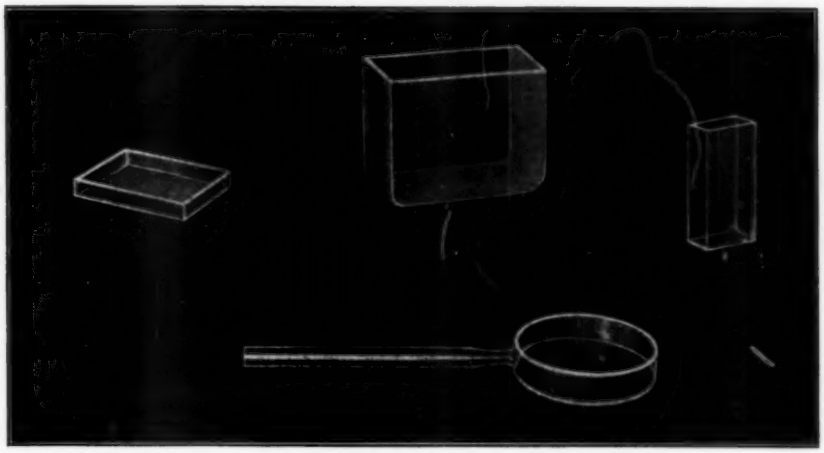

FILTER CELLS

assure the greatest possible transparency to ultra-violet rays and freedom from contamination of neutral or acid liquids. They also maintain their efficiency, as continued exposure to ultra-violet light from any source has no deteriorating effect. Those who desire transparency in the infra-red region of the spectrum will also find these cells entirely suitable.

Where it is not essential to have transparency throughout, a considerable saving can be made by using transparent Vitreosil for the faces only and the translucent quality for the sides and bottom as indicated by the large rectangular cell shown in the center of the illustration.

Let us quote on cells to your specifications
Lenses and prisms also available

THE THERMAL SYNDICATE, LTD.

1726 Atlantic Avenue Brooklyn, New York

The Stabilized Oscilloscope

A Visual Oscillograph

SIMPLE TO OPERATE: An instrument no more difficult to operate than a high grade radio receiving set.

PORTABLE: Weighing but 40 pounds in its beautiful walnut cabinet, it is easily taken from research room to lecture room or to a distant substation.

LINEAR TIME AXIS: By the use of a unique scheme, a linear time axis is obtained which is synchronized with the circuit under study, so that a perfectly stationary visual wave is obtained which may be examined with great care, traced or photographed.

HIGH FREQUENCIES: As there is no damping and the inertia of the electron beam is only 10^{-18} grams, the response to all frequencies and harmonics is true and accurate.

SMALL CURRENT: One micro-ampere is sufficient to accuate this small moving element.

IMMEDIATE RESULTS: Because it is visual, a class in Electrical Engineering or Radio can watch the effect of changing the constants in any circuit while it is happening. A power engineer can observe the effect on wave form of various loads, field excitations, etc., making a photographic record of the results which it is deemed should be permanent.

POWERFUL RESEARCH TOOL: Wherever vibrational phenomena are involved.

THE PRICE IS REASONABLE.

Described by Prof. F. Bedell, A.I.E.E. Journal, June, 1927.

Write for Reprint and Circular No. 273.

THE BURT-CELL: A Photo-electric cell without fatigue, previously advertised is described in Bulletin No. 271. Write for a copy. We also manufacture quartz photo-cells of remarkable constancy.

DR. R. C. BURT
327 South Michigan Ave.
PASADENA, CALIFORNIA
Cable address: *"Burt Pasadena"*

Scientific Instruments

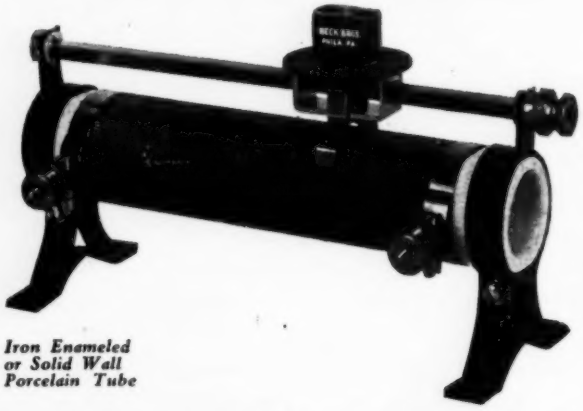

Iron Enameled or Solid Wall Porcelain Tube

"BECBRO" LABORATORY RHEOSTATS

Becbro Laboratory Rheostats made of both iron enameled and solid wall porcelain tubes.

The above illustration shows one of the numerous types of "BECBRO" tubular, slide contact, rheostats manufactured and carried in stock by us.

The various types are made in several lengths of 8", 16", and 20", respectively, with resistance values of from 0.25 ohm and 25 amperes, to 30,000 ohms and current capacity of 0.1 ampere.

"BECBRO" Rheostats are high in quality and low in price, and, due to the fact that they are giving excellent service, will be found in many of the Colleges, Universities, Research Laboratories and Commercial stations throughout the country and world.

"BECBRO" Stone Rheostats are made in the following types: Single, Double, Universal, and Crossed Sections. These rheostats, with the porcelain tubular types, find their many uses in high frequency and radio work.

Our Catalogue P-20 Sent You Upon Request

BECK BROTHERS, *Makers*

421 SEDGLEY AVENUE **PHILADELPHIA, PA.**

CENTRIPETAL FORCE APPARATUS

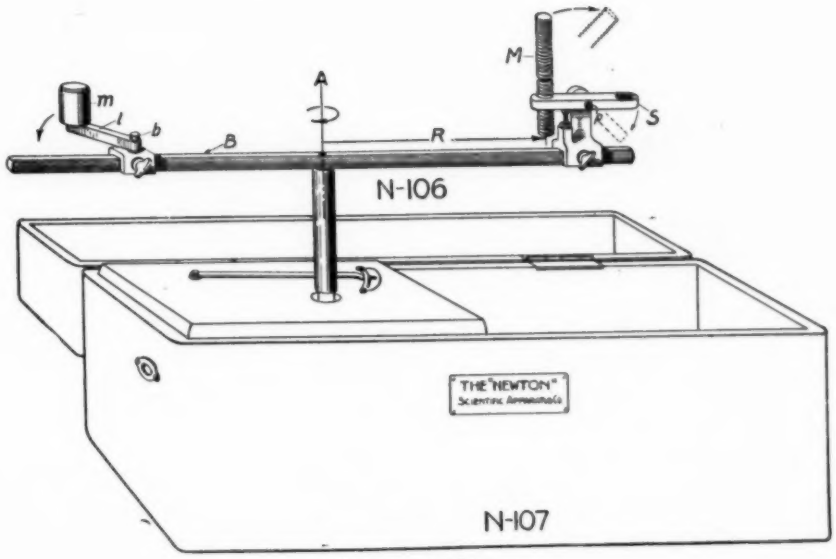

Patent applied for

N-106 Centripetal Apparatus.....$12.00
N-106 and N-107, complete.....$50.00

Write for quantity discounts.

Note—The N-106 was designed as an attachment to the Free Fall Apparatus N-100 and N-105.

All the properties of centripetal force studied by experiment with N-106. The action is visible and audible at a distance.

1. **For uniform rotation, the mass *m* takes position furthest from the axis *A*, no matter where *m* is placed at start.**
2. **For angular acceleration ± (starting or stopping) *m* lags or leads.**
3. **The radius *R* can be varied.**
4. **The speed is minutely and quickly varied between 25 and 100 R.P.M.; speed *cannot* run high.**
5. **Mass *M* is available for weighing.**

S, of aluminum, is balanced like the levers of a scale, on pin *p*, for both gravity and centripetal force, hence will not tilt by itself. Mass *M* is acted on at its c.g. by gravity and the centripetal force. The height of the c.g. of *M* is minutely variable. When adjusted so that the centripetal force barely tilts *M*, the rotation is stopped and the tilting force is measured by means of a spring balance.

Accuracy to within 1% is attainable with N-106

SCIENTIFIC APPARATUS CO.

4 LANDSCAPE AVE., YONKERS, N.Y.

Western Electric

Vacuum Thermocouples

Interior View of Container Showing a Vacuum Thermocouple

WESTERN ELECTRIC Vacuum Thermocouples provide an accurate means for measuring the values of feeble alternating currents. This new apparatus is of great value to research organizations and scientific laboratories. It is essentially a hot wire instrument enclosed in an evacuated container.

Vacuum Thermocouples are made in three standard types with various characteristics. With the proper type and a suitable galvanometer any current from .0005 ampere to 1.0 ampere may be measured with an accuracy of plus or minus 1%.

For further information write for Bulletin T-761.

GraybaR
ELECTRIC COMPANY

Distributors of Western Electric Products

Scientific Equipment Division

30 North Michigan Boulevard - - - - - - - Chicago, Ill.
420 Lexington Avenue - - - - - - - - New York, N.Y.
1700 Walnut Street - - - - - - - - - Philadelphia, Pa.

L220 Wavelength Spectrometer

OUR LATEST FORM OF WAVELENGTH SPECTROMETER incorporates a number of important improvements which we feel make the instrument superior to any of its kind and will be readily appreciated by experienced users.

The principal new feature is the use of a flat SPIRAL DIAL in place of the wavelength drum. This form of scale permits a greater uniformity in spacing of the wavelength graduations and is extremely easy and convenient to read. The dial is entirely enclosed and a small electric lamp is provided for illumination. The slit is bilateral of improved design fitted with stainless steel jaws.

Further details on request.

NOTE: Patent applications have been filed to cover the use of the FLAT SPIRAL DIAL on this and other instruments.

The

GAERTNER SCIENTIFIC CORPORATION

SUCCESSORS TO WM. GAERTNER & CO.

ESTABLISHED 1896 INCORPORATED 1930

1201 WRIGHTWOOD AVENUE, CHICAGO

Representative for India

SCIENTIFIC INSTRUMENT CO., LTD., 6, JOHNSTONGANJ, ALLAHABAD, INDIA

A new electrical study

THE AUDIBILITY METER